Activation and Reaction Volumes in Solution. 3

A. Drljaca,[†] C. D. Hubbard,[†] R. van Eldik,*[,†] T. Asano,*[,‡] M. V. Basilevsky,[§] and W. J. le Noble*[,⊥]

Institute for Inorganic Chemistry, University of Erlangen—Nürnberg, Egerlandstr. 1, 91058 Erlangen, Germany, Institute for Fundamental Research of Organic Chemistry, Kyushu University, 6-10-1 Hakozaki, Higashi-ku, Fukuoka, Japan, Karpov Institute of Physical Chemistry, 10, Vorontsovo Pole, 103064 Moscow, Russia, and Department of Chemistry, State University of New York, Stony Brook, New York 11794-3400

Received March 2, 1998 (Revised Manuscript Received May 28, 1998)

Contents

1. Introduction

A. Scope of the Review

Three of the present authors reviewed the activation and reaction volumes of chemical reactions in solution for the 10-year period January 1977 to December 1986.[1] Increased interest, activity, and developments in the field have prompted us to include additional authors in an effort to cover the next 10 years of literature, from January 1987 to December 1996, in a timely fashion. Of particular note are the developments in the theoretical treatment and interpretation of experimental volume data, and the application of high-pressure techniques to reactions of biochemical significance and to reactions in supercritical fluids, which have added new dimensions to the work over the past 10 years. In addition, some important data that became available during 1997 have also been included.

The presentation, except for the new topics, follows the outline of the earlier reviews in this series.[1,2] The current version is presented as a direct continuation of our earlier review,[1] with as little duplication as possible, and readers are therefore urged to consult ref 1 in order to bridge the presentations. The organization of data is similar to that of the earlier reviews,[1,2] i.e., the data are organized in tabular form according to the type of reaction studied. In addition, a section on the viscosity dependence of reaction rates (3.F) is included. In the accompanying text the mechanistic implications of the data are discussed and in selected cases detailed analyses are presented. Several monographs have appeared since 1986 covering the following topics: inorganic high-pressure chemistry;[3] organic high-pressure chemistry;[4] high-pressure chemical synthesis;[5] high-pressure chemistry and biochemistry;[6] high-pressure chemistry, biochemistry and materials science;[7] chemistry under extreme or nonclassical conditions;[8] high-pressure NMR;[9] experimental techniques in high-pressure research;[10] high-pressure techniques in chemistry and physics;[11] and high-pressure liquids and solutions.[12] These monographs include review chapters dealing with specific aspects of the determination and interpretation of activation and reaction volume data for particular types of chemical processes. In addition, several reviews have appeared in journals since 1986. These reviews are more limited in scope than the present one (although perhaps also more critical); among these there are accounts dealing with inorganic and organometallic reactions,[13−22] high-pressure NMR spectroscopy,[23] organic reactions,[24−28] biochemical systems,[29] and photochemical and photophysical aspects.[30−34]

[†] University of Erlangen—Nürnberg.
[‡] Kyushu University. Present and permanent address: Department of Applied Chemistry, Faculty of Engineering, Oita University, 700 Dannoharu, Oita 870-1192, Japan.
[§] Karpov Institute of Physical Chemistry.
[⊥] State University of New York, Stony Brook.

S0009-2665(97)00461-5 CCC: $30.00
Published on Web 09/24/1998

Alexander Drljaca was born in Düren, Germany, in 1970 and grew up in Australia. He was educated at Mazenod College (1982–1987) and later received his B.Sc.(Hons.) degree (1991) from Monash University. This was followed by a Ph.D. (1995) at the same institute working with Leone Spiccia. Recently he has completed one year as an Alexander von Humboldt Fellow (1997) with Rudi van Eldik at the University of Erlangen—Nürnberg working on solvent exchange reactions of metal complexes at high pressures using NMR techniques. His research interests include, besides high-pressure inorganic chemistry, the synthesis and characterization of new mesoporous materials and sol–gel/microwave chemistry.

Colin D. Hubbard was born in Ipswich, England, and grew up in Norfolk and Sussex. He read Chemistry at the University of Sheffield, and received a B.Sc. (Hons) degree in 1961 and a Ph.D. degree in 1964, also from Sheffield working with Ralph G. Wilkins. Postdoctoral education followed at Massachusetts Institute of Technology and Cornell University (Gordon G. Hammes) and at the University of California in Berkeley (Jack F. Kirsch). He was appointed as Assistant Professor (1967), Associate Professor (1972), and Professor (1979) in the Department of Chemistry at the University of New Hampshire, Durham, NH. In 1994 he accepted a position as a senior research scientist in the Institute for Inorganic Chemistry at the University of Erlangen—Nürnberg, Germany. His interest in high-pressure chemistry originated from research projects with Edward Caldin (University of Kent, Canterbury, England), and with John Burgess (University of Leicester, England). His other research interests include electron-transfer reactions, proton tunneling, and enzyme catalysis.

Rudi van Eldik was born in Amsterdam, Holland, in 1945 and grew up in Johannesburg, South Africa. He received his Ph.D. degree (1971) from the Potchefstroom University. He spent two years (1972 and 1978) with Gordon M. Harris at SUNY at Buffalo, NY, and one year as an Alexander von Humboldt Fellow with Hartwig Kelm at the University of Frankfurt, Germany. He was group leader at the Institute for Physical Chemistry, University of Frankfurt (1980–1987), and Professor of Inorganic Chemistry at the University of Witten/Herdecke (1987–1994). He is presently Professor of Inorganic and Analytical Chemistry at the University of Erlangen—Nürnberg. In 1997 he received an honorary doctorate from the Potchefstroom University. His research interests are in mechanistic studies of inorganic, organometallic, and bioinorganic reactions, with special emphasis on the application of fast kinetic and high-pressure techniques.

Tsutomu Asano was born in Osaka, Japan, in 1941. He obtained an undergraduate degree in chemistry at Kyoto University, followed by an M.A. and Ph.D. at the same institute, graduating in 1969. After postdoctoral work with Professor William J. le Noble, he returned to Kyoto and worked for the late Professor Jiro Osugi. He joined the faculty of Oita University in 1975, where he is now a Professor of Chemistry. He serves as an Associate Editor of *Bulletin of the Chemical Society of Japan* and also as a member of the editorial board of *The Review of High Pressure Science and Technology* published by Japan Society of High Pressure Science and Technology. His prime interest has been in studies of organic reaction mechanism by kinetic measurements including the ones under high pressure. He recently developed interest in dynamic solvent effects and his efforts are concentrated on kinetics in highly viscous conditions.

B. Basic Concepts

A detailed account of the basic principles and fundamental concepts relevant to the determination and interpretation of activation and reaction volumes has been given in the previous review.[1] These remain pertinent as there have been no new fundamental developments. Reaction and activation volumes for reactions in solution are still interpreted in terms of intrinsic (due to changes in bond lengths and bond angles) and solvational (due to changes in electrostriction) contributions. By way of comparison with earlier work in this area, fewer investigators have tried to measure the pressure dependence of $\Delta V^{\ddagger}$ to report data on the compressibility of activation. The accuracy of kinetic and thermodynamic measurements has improved significantly such that in principle it should be easier to study the pressure dependence of $\Delta V^{\ddagger}$. In many cases no significant pressure dependence was discerned by the original authors in the lower pressure range (up to 150 MPa). However, linear dependence of the logarithm of the

Mikhael Basilevsky was born in Moscow, Russia, in 1935. He graduated from Moscow State University in 1957 and received his Ph.D. (1964) and Doctor (1973) degrees at Karpov Institute of Physical Chemistry, Moscow. Since 1982 he has been appointed as Professor of Chemical Physics and a head of laboratory of quantum chemistry and statistical physics at Karpov Institute. He has been a member of International Academy of Quantum Molecular Science since 1991. His research interests include the theory of chemical reactions and are recently focused on reaction kinetics and mechanisms in condensed phase.

Bill le Noble is a native of Rotterdam, The Netherlands. He did undergraduate work in chemical engineering in Dordrecht and then moved to the United States in 1949. After a stint in the U.S. Army, which included wartime service in Korea, he attended the University of Chicago and received a Ph.D. degree in organic chemistry with Professor G. Wheland. Postdoctoral work at Purdue University was followed in 1959 by an appointment at the State University of New York at Stony Brook, where he has stayed ever since. He has held visiting Professorship at the Free University of Amsterdam and the University of Groningen, received Humboldt Senior Scientist and Mombusho Special Professorship Awards, and has served as senior editor of *The Journal of the Organic Chemistry* and *Recueil* as well as in the Chair's position of his Department.

rate constant upon pressure is not general or expected over wider ranges. Related to this point are the empirical equations used to fit the data, a topic we have discussed in our earlier reviews.[1,2] A recent paper[35] has examined this issue critically.

Improvements in instrumentation and development of new techniques (see section 1.C) in the study of chemical reactions at elevated pressure have opened new areas of research and volume data have been generated for systems that could not be studied before. In this respect the more widespread application of volume profile analysis has contributed toward a better understanding of reaction mechanisms for chemical reactions in solution. The location of the transition state along the reaction coordinate can then be discussed in terms of partial molar volume changes associated with the chemical process, and in cases where the partial molar volumes of reactants and products are experimentally accessible the actual partial molar volume of the transition state can be determined. The partial molar volume of the transition state can also be estimated on a computational basis, and this has been accomplished for a few organic reactions (see section 3) and has been suggested to be potentially possible for certain inorganic reactions (see section 2.M). An advantage is that the interpretation of volume changes in terms of intrinsic and solvational components as they relate to the mechanism is more direct, straightforward, and therefore more reliable than is the interpretation of thermal activation parameters, allowing molecular and solvent reorganization to be visualized, modeled, and predicted for other reactions. In this way such analyses contribute to our fundamental understanding of the detailed reaction mechanisms. In addition, such studies have more recently also been extended to reactions in supercritical fluids. More information on these advances is given in the subsequent sections.

Most of the activation volume data for inorganic, organometallic, and organic reactions reported in this review can be analyzed in terms of the transition-state theory. The interpretation of volume data for fast chemical processes where the transition-state theory is no longer valid has attracted the attention of a number of investigators, and will therefore be dealt with separately in section 3.

C. Experimental Techniques

Further development of NMR techniques to study chemical reactions under extreme conditions of temperature and pressure has been reported.[36,37] The development of a high-pressure NMR probe for a standard narrow-bore 400-MHz magnet is a remarkable achievement,[38] since in the past a considerably more expensive wide-bore magnet was usually employed. Instrumentation has also been developed to perform routinely pulse-radiolysis experiments at pressures up to 200 MPa (i.e., 2 kbar)[39] using a transportable high-pressure system.[40] Further modifications of high-pressure stopped-flow instruments constructed earlier were undertaken to enable measurements using fluorescence detection to be made, and to permit the use of low temperatures for reactions in organic solvents.[41,42] A special optical cell was constructed to carry out flash photolysis experiments on organometallic compounds at elevated pressure in supercritical fluids.[43] Noteworthy progress has also been achieved in employing electrochemical techniques at elevated pressures, and therefore more diverse applications can be pursued and a wider range of measurements obtained.[44−47]

D. Volume Data from Other than High-Pressure Experiments

Time-resolved laser-induced photoacoustic methods can be employed to obtain information on molecular volume changes. In particular these techniques have been applied to biological systems and the subject has been reviewed in recent years.[48,49] Volume changes

that occur in a photoinduced chemical reaction consist of the volume difference between the reactants and products, and the contraction or expansion of the medium through cooling or heating. These contributions can be separated by means of photothermal measurements as a function of one of the thermoelastic parameters of the medium.[48] The direct volume change originating from the molecular process other than heating or cooling can be calculated from measurements of the acoustic signal as a function of temperature. The conformational volume change associated with the photodissociation of CO from sperm whale myoglobin has been determined using this method.[50] Detailed accounts of the volume effects measured on reactions of proteins have been reported using this technique.[48,49] More recent work not covered by these reviews include volume changes that for instance occur during the bacteriorhodopsin photocycle,[51,52] photoisomerization of carbocyanines,[53] intramolecular electron transfer during MLCT (metal-to-ligand charge transfer) excitation of ruthenium cyano complexes,[54] electron-transfer quenching of excited $Ru(bpy)_3^{2+}$,[55] exciplex formation in a semiflexible donor−bridge−acceptor compound,[56] phototransformation of phytochrome A,[57] and triplet formation of water-soluble porphyrins.[58]

2. Volume Data for Inorganic Reactions

The data in Table 1 (1552 entries from 328 references) are arranged according to the different types of reactions and the atomic number of the central metal atom. Reaction volume data (ΔV) are included in the table where available, and the methods employed to determine ΔV are (a) from the pressure dependence of the equilibrium constant, (b) from dilatometric or partial molar volume (density) measurements, and (c) from theoretical extrapolations. There are other general remarks with regard to the table: $\Delta V^{\ddagger}$ data are quoted at ambient pressure; the maximum applied pressure is quoted in the fourth column; the number of data refers to the number of pressures at which measurements (usually three to five kinetic runs) were performed; concentration is given in mol L^{-1} (M) or mol kg^{-1} (m); salts quoted under remarks were used to adjust the ionic strength (μ). A list of abbreviations follows the tabulated data. Reactions for which no reaction products are specified in detail are indicated in this way since the original papers did not specify a definite product or set of products.

A. Solvent/Ligand Exchange Reactions

In this section exchange of a ligand molecule coordinated to a metal ion with an identical but uncoordinated molecule of the bulk solvent is considered. Thus there is no net reaction and the reaction volume is zero. The classification system for solvent exchange is the familiar one:[383] D for dissociative activation, in which an intermediate of lower coordination number is proposed since the departing solvent molecule is completely dissociated before the entering one is adjacent or present (the intermediate is rarely detected); A (associative) for a reaction in which the entering solvent molecule increases the coordination number since it is present in the coordination sphere before the leaving molecule departs; and I for an interchange process. The latter category, in which no intermediate of higher or lower coordination number occurs, may be further subclassified as I_a or I_d which indicate interchange with associative and dissociative characters, respectively. These can be paired with S_N2 limiting (A), S_N2 (I_a), S_N1 (I_d), and S_N1 limiting (D), the nomenclature commonly in use for organic reactions. The interchange may be regarded as "pure" if in a volume sense the extent to which the entering solvent molecule is entering is exactly matched by the extent to which the leaving molecule is departing.

In considering solvent exchange processes, it has been customary[14] to assume that any change in electrostriction during the activation process is negligible, and there is no change in volume due to possible coordinate bond length changes or rearrangements of the coordinated solvent molecules or other not exchanging ligands. It has been recognized that indeed there may be bond length changes;[14] however, it is difficult to project how this property could be readily accessible experimentally. Recent calculations on water exchange on first row transition metal ions in oxidation state two led to the conclusion[384−387] that the coordinated but nonexchanging water molecules are drawn closer to the metal ion during activation and therefore there is a volume change contribution to the measured volume of activation from this source. Yet other calculations reveal the shortcomings of this approach.[388,389] Therefore, in highlighting many solvent exchange processes, it will be assumed that $\Delta V^{\ddagger}$ is a parameter that registers pure interchange when its value is zero. Negative values denote associative activation proceeding from I_a to A with increasing compactness and increasing negative magnitude. Transition states arising from mechanisms, ranging from I_d to D, are indicated by increasing positive values of $\Delta V^{\ddagger}$. There is general agreement among experimentalists over this classification.

Of the almost 100 entries of this type of system, the large majority are ionic systems and the central metal ion is a transition metal. Water is the most common solvent reported and therefore the most common exchanging molecule, but a variety of other unidentate molecules also function as solvents. In a few cases the exchange of bidentate solvent molecules has been monitored. There is a rich variety of systems that have nonexchanging ligands some of which are of multidentate character, beside those sytems which comprise a central metal ion coordinated only by ligands of which the solvent is composed. Some of the stimulus to study the former reaction type arises from the investigation of the gadolinium ion in concert with selected ligands as suitable complexes to serve as magnetic resonance imaging agents. Indeed NMR spectroscopy remains the instrumental method used in almost all studies. However, due to the technical difficulties and nonavailability of commercial NMR high-pressure accessories, the studies reported emerge from quite a

Table 1. Activation and Reaction Volumes of Inorganic Reactions[a]

no.	reaction	solvent	T, °C	P, MPa	no. of data	$\Delta V^{\ddagger}$, $cm^3\ mol^{-1}$	$\Delta \bar{V}$, $cm^3\ mol^{-1}$ (method)	ref(s)	remarks
	Solvent/Ligand Exchange Reactions								
1	$Be(H_2O)_4^{2+} + H_2O$	H_2O	57	200	9	-13.6 ± 0.5		59	diluent CD_3NO_2
2	$Be(DMSO)_4^{2+} + DMSO$	DMSO	27	200	8	-2.5 ± 0.2		59	diluent CD_3NO_2
3	$Be(TMP)_4^{2+} + TMP$	TMP	91	200	8	-4.1 ± 0.2		59	diluent CD_3NO_2
4	$Be(DMF)_4^{2+} + DMF$	DMF	53	200	8	-3.1 ± 0.4		59	diluent CD_3NO_2
5	$Be(TMU)_4^{2+} + TMU$	TMU	73	200	8	$+10.5 \pm 0.7$		59	diluent CD_3NO_2
6	$Be(DMPU)_4^{2+} + DMPU$	DMPU	85	200	8	-10.3 ± 0.8		59	diluent CD_3NO_2
7	$Sc(TMP)^{3+} + TMP$	TMP	25	200	8−13	-20.1 ± 1.0		60	
8	$Ti(H_2O)_6^{3+} + H_2O$	H_2O	0−25	230	10	-12.1 ± 0.4		61	2.0 m triflic acid
9	$TiO(e\text{-}DMSO)_4(a\text{-}DMSO)^{2+} + DMSO$ (exchange of axially bonded a-DMSO)	CD_3NO_2	−16	200	9	$+1.6 \pm 0.1$		62	
10	$TiO(e\text{-}DMSO)_4(a\text{-}DMSO)^{2+} + DMSO$ (exchange of equatorially bonded e-DMSO)	CD_3NO_2	21	200	9	$+4.8 \pm 0.1$		62	
11	$Ti(DMF)_6^{3+} + DMF$	DMF	−3	200	9	-5.7 ± 0.6		63	
12	$Ti(DMF)_6^{3+} + DMF$	DMF	−31	200	9	-6.8 ± 0.4		63	
13	*cis*-$TiCl_4(Me_2S)_2 + Me_2S$	CH_2Cl_2	−55	220	8−12	$+24.4 \pm 1.0$		64	
14	*cis*-$TiCl_4(Me_2Se)_2 + Me_2Se$	CH_2Cl_2	−45	220	8−12	$+26.1 \pm 1.2$		64	
15	*cis*-$TiCl_4$·2TMPA + TMPA	$CHCl_3$	12	220	8−12	$+17.5 \pm 1.0$		64	
16	$V(DMSO)_6^{3+} + DMSO$	CD_3NO_2	25	200	7	-10.1 ± 0.6		65	
17	$Cr(CH_3NH_2)_5H_2O^{3+} + H_2O$	H_2O	60	200	9	-3.8 ± 0.3		66	$\mu = 0.7$ M
18	$Mn(DMF)_6^{2+} + DMF$	DMF	36	300	7	$+1.6 \pm 0.5$		67	
19	$Mn(DMF)_6^{2+} + DMF$	DMF	25	200	9	$+2.4 \pm 0.2$		68	
20	$Mn(DMF)_6^{2+} + DMF$	DMF	45	200	10	$+4.2$		69	
21	$Mn(DMTF)_6^{2+} + DMTF$	DMTF	29	200	10	$+11.5$		69	
22	$Mn(HOAc)_6^{2+} + AcOH$	AcOH	25	180	>12	$+0.4 \pm 0.7$		70	0.02 M $HClO_4$ (diluent d_2-DCM)
23	$Mn(OAc)_2(HOAc)_4 + AcOH$	AcOH	25	180	>12	$+6.7 \pm 0.6$		70	0.0 M $HClO_4$ (diluent d_2-DCM)
24	$Mn(en)_3^{2+} + en$	en	5	200	10	$+0.9 \pm 0.9$		71	
25	$Fe(en)_3^{2+} + en$	en	52	200	15	-1.2 ± 0.8		71	
26	$Fe(H_2O)(phdta)^- + H_2O$	H_2O	25	150	8	$+4.6 \pm 0.2$		72	$\mu = 1.0$ M
27	$Fe(DMF)(phdta)^- + DMF$	DMF	25	150	8	$+10 \pm 2$		72,73	
28	$Fe(DMF)_6^{2+} + DMF$	DMF	25	200	9	$+8.5 \pm 0.4$		68	
29	$Co(CH_3NH_2)_5(H_2O)^{3+} + H_2O$	H_2O	16	200	7	$+5.7 \pm 0.2$		66	$\mu = 1.3$ M
30	$Co(en)_3^{2+} + en$	en	60	200	14	$+0.9 \pm 0.9$		71	
31	$Co(tn)_3^{2+} + tn$	tn	29	200	13	$+6.6 \pm 0.3$		74	
32	$Co(CN)_5(H_2O)^{2-} + H_2O$	H_2O	18	400	4	$+7.1 \pm 0.4$		75	pH = 3, $\mu = 0.35$ M (CF_3SO_3H)
33	$Ni(DMTF)_6^{2+} + DMTF$	DMTF	−22	200	10	$+20.6$		69	
34			9	200	10	$+21.8$			
35	$Ni(Ma)(DMF)^{2+} + DMF$	DMF	50	200	>10	$+10.6 \pm 0.8$		76	
36	$Ni(Ma)(MeCN)^{2+} + MeCN$	MeCN	50	200	>10	-3.5 ± 0.9		76	
37	$Ni(MeCN)_6^{2+} + MeCN$	MeCN	59	>200	>12	$+12.0 \pm 0.4$		77	
38	$Ni(EtCN)_6^{2+} + EtCN$	EtCN	57	>200	>12	$+13.7 \pm 0.5$		77	
39	$Ni(PrCN)_6^{2+} + PrCN$	PrCN	56	>200	>12	$+13.1 \pm 0.5$		77	
40	$Ni(Pr^iCN)_6^{2+} + Pr^iCN$	Pr^iCN	55	>200	>12	$+12.4 \pm 0.6$		77	
41	$Ni(BuCN)_6^{2+} + BuCN$	BuCN	56	>200	>12	$+14.4 \pm 0.4$		77	
42	$Ni(PhCN)_6^{2+} + PhCN$	PhCN	59	>200	>12	$+13.1 \pm 0.6$		77	
43	$Ni(en)_3^{2+} + en$	en	25	270	8	$+11.4 \pm 2.0$		78	
44	$Cu(DMF)_6^{2+} + DMF$	DMF	27	200	9	$+8.4 \pm 0.4$		79	
45	$Cu(tren)H_2O^{2+} + H_2O$	H_2O	25	200	9	-4.7 ± 0.2		80	$\mu = 1.0$ M ($NaClO_4$)
46	$Ga(H_2O)_6^{3+} + H_2O$	H_2O	25	220	9−12	$+5.0 \pm 0.5$		81	$[HClO_4] = 3$, 0.4 and 0.25 M
47	$Ga(H_2O)_5(OH)^{2+} + H_2O$	H_2O	25	220	9−12	$+7.7 \pm 1.4$		81	$[HClO_4] = 3$, 0.4 and 0.25 M
48	*trans*-$ZrCl_4$·2TMPA + TMPA	$CHCl_3$	6	200	10	-11.1 ± 0.8		82,83	
49	$Mo(O)_2(acac)_2 + Hacac$	Hacac	5	90	3	0		84	
50	$Ru(NH_3)_5H_2O^{3+} + H_2O$	H_2O	25	400	5	-4.04 ± 0.14		85	0.01 m triflic acid
51	$Ru(H_2O)_6^{2+} + H_2O$	H_2O	−5 to 0	190	5−6	-0.4 ± 0.7		86	1.5 m triflic acid
52	$Ru(H_2O)_6^{3+} + H_2O$	H_2O	5	190	4	-8.3 ± 2.1		86	[Htos] = 0.1, 0.5 and 3.0 M
53	$Ru(H_2O)_5(OH)^{2+} + H_2O$	H_2O	15	190	4	-2.1 ± 1.4		86	
54	$Ru(CH_3CN)_6^{2+} + CH_3CN$	CH_3CN	100	>200	5	$+0.4 \pm 0.6$		86	
55	$Ru(\eta\text{-}C_6H_6)(H_2O)_3^{2+} + H_2O$	H_2O	83	200	9	$+1.5 \pm 0.4$		87	
56	$Ru(\eta\text{-}C_6H_6)(CH_3CN)_3^{2+} + CD_3CN$	CD_3CN	25	200	5	$+2.4 \pm 0.8$		88	
57	$Ru(\eta\text{-}C_5H_5)(CH_3CN)_3^{+} + CD_3CN$	CD_3CN	25	200	11	$+11.1 \pm 0.5$		88	
58	$Rh(CH_3NH_2)_5H_2O^{3+} + H_2O$	H_2O	45	200	8	$+1.2 \pm 1.1$		66	$\mu = 0.7$ M
59	$Rh(H_2O)_6^{3+} + H_2O$	H_2O	50	210	4	-4.2 ± 0.6		89	$\mu = 5.6$ M ($NaClO_4$), see text
60	$Rh(H_2O)_5OH^{2+} + H_2O$	H_2O	50	210	4	$+1.5$		89	$\mu = 5.6$ M ($NaClO_4$), see text
61	$Cp^*Rh(H_2O)_3^{2+} + H_2O$	H_2O	−2	200	9	$+0.6 \pm 0.6$		90	
62	$Rh_2(CH_3CN)_{10}^{4+} + CH_3CN$	CH_3CN	41	200	6	-4.9 ± 0.2		91	
63	$Pd(H_5dien)H_2O^{2+} + H_2O$	H_2O	23	200	7	-2.8 ± 0.4		92	
64	$Pd(Me_5dien)H_2O^{2+} + H_2O$	H_2O	25	200	7	-7.2 ± 0.6		93	
65	$Pd(Et_5dien)H_2O^{2+} + H_2O$	H_2O	25	200	7	-7.7 ± 1.3		93	
66	$Pd(1,4\text{-dithiane})_2^{2+} + 1,4\text{-dithiane}$	CD_3NO_2	9	200	9	-9.8 ± 0.4		94	
67	$Pd(Et_2S)_4^{2+} + Et_2S$	Et_2S	85	200	>10	-11.6 ± 0.4		95	
68	$Pd(H_2O)_4^{2+} + H_2O$	H_2O	51	200	>10	-2.2 ± 0.2		95	
69	$Pd(dma)_4^{2+} + dma$	dma	30	200	>10	-2.8 ± 0.2		95	
70	$Pd(MeCN)_4^{2+} + MeCN$	MeCN	63	200	>10	-0.1 ± 0.4		95	
71	$Pd(DMF)_4^{2+} + DMF$	DMF	32	200	>10	-0.2 ± 0.6		95	
72	$Pd(Me_2S)_4^{2+} + Me_2S$	Me_2S	30	200	>10	-9.4 ± 0.3		95	
73	$Pd(MeNC)_4^{2+} + MeNC$	MeNC	−9	200	>10	-3.1 ± 0.1		95	
74	$bisoxa(Gd(DO3A)H_2O) + H_2O$	H_2O	−1	200	9	$+2.3 \pm 0.2$		96	
75	$Gd(DTPA)(H_2O)^{2-} + H_2O$	H_2O	13, 64	200	9	$+12.5 \pm 0.2$		97	
76	$Gd(DOTA)(H_2O)^{-} + H_2O$	H_2O	12, 67	200	9	$+10.5 \pm 0.2$		97	
77	$(N(CS)N\text{-}bz\text{-}Gd(DO3A)(H_2O))_{23} + H_2O$	H_2O	5	200	8	$+3.1 \pm 0.2$		98	
78	$Gd(DO3A\text{-}bz\text{-}NO_2)(H_2O) + H_2O$	H_2O	15	200	10	$+7.7 \pm 0.5$		98	
79	$BO\text{-}(Gd(DO3A)(H_2O))_2 + H_2O$	H_2O	4	200	10	$+0.5 \pm 0.2$		99	

Table 1. (Continued)

no.	reaction	solvent	T, °C	P, MPa	no. of data	$\Delta V^{\ddagger}$, cm^3 mol^{-1}	$\Delta\bar{V}$, cm^3 mol^{-1} (method)	ref(s)	remarks
	Solvent/Ligand Exchange Reactions (Continued)								
80	$Tb(H_2O)_9^{3+} + H_2O$	H_2O	−5	250	9−12	−5.7 ± 0.5		100,101	$[HClO_4] = 2.0$ M
81	$Tb(PDTA)(H_2O)_2^- + H_2O$	H_2O	18	200	9	−7.6 ± 0.3		102	pH = 4.0 ($HClO_4$)
82	$Dy(H_2O)_9^{3+} + H_2O$	H_2O	−5	250	9−12	−6.0 ± 0.4		100,101	$[HClO_4] = 2.0$ M
83	$Dy(PDTA)(H_2O)_2^- + H_2O$	H_2O	18	200	9	−5.5 ± 0.3		102	pH = 4.1 ($HClO_4$)
84	$Ho(H_2O)_9^{3+} + H_2O$	H_2O	−5	250	9−12	−6.6 ± 0.4		100,101	$[HClO_4] = 2.0$ M
85	$Er(H_2O)_9^{3+} + H_2O$	H_2O	−5	250	9−12	−6.9 ± 0.4		100,101	$[HClO_4] = 2.0$ M
86	$Er(PDTA)(H_2O)_2^- + H_2O$	H_2O	−1	200	9	−6.5 ± 0.3		102	pH = 4.1 ($HClO_4$)
87	$Tm(H_2O)_9^{3+} + H_2O$	H_2O	−5	250	9−12	−6.0 ± 0.8		100,101	$[HClO_4] = 2.0$ M
88	$Tm(PDTA)(H_2O)_2^- + H_2O$	H_2O	−1	200	9	−1.2 ± 0.5		102	pH = 4.1 ($HClO_4$)
89	$Yb(PDTA)(H_2O)_2^- + H_2O$	H_2O	19	200	9	+7.4 ± 0.8		102	pH = 4.0 ($HClO_4$)
90	$Os(\eta\text{-}C_6H_6)(H_2O)_3^{2+} + H_2O$	H_2O	87	200	9	+2.9 ± 0.6		87	
91	*trans*-$Os(en)_2(\eta^2\text{-}H_2)(H_2O)^{2+} + H_2O$	H_2O	11	200	10	−1.5 ± 0.5		103	
92	*trans*-$Os(en)_2(\eta^2\text{-}H_2)(CH_3CN)^{2+} + CH_3CN$	CH_3CN	25	200	4	−0.5 ± 0.2		103	
93	$Cp^*Ir(H_2O)_3^{2+} + H_2O$	H_2O	8	200	9	+2.4 ± 0.5		90	
94	$Ir(H_2O)_6^{3+} + H_2O$	H_2O	85	200	4	−5.7 ± 0.5		104	$\mu = 5.1$ M ($NaCF_3SO_3$)
95	$Ir(H_2O)_5(OH)^{2+} + H_2O$	H_2O	85	200	4	−0.2 ± 0.8		104	$\mu = 5.1$ M ($NaCF_3SO_3$)
96	$Pt(H_2O)_4^{2+} + H_2O$	H_2O	24	200	>10	−4.6 ± 0.2		95	
97	$Pt(MeNC)_4^{2+} + MeNC$	MeNC	−9	200	>10	−3.7 ± 0.1		95	
98	$Pt(1,4\text{-dithiane})_2^{2+} + 1,4\text{-dithiane}$	CD_3NO_2	57	200	9	−12.6 ± 1.2		94	
99	$Pt(Me_2S)_4^{2+} + Me_2S$	CD_3NO_2	39	200	9	−22.0 ± 1.3		94	
100	$Pt(DMSO)_2(DMSO)_2^{2+} + DMSO$	CD_3NO_2	−9	180	5	−2.5 ± 0.3		105	
101			87	180	5	−5 ± 3		105	
102	*cis*-$PtPh_2(Me_2S)_2 + Me_2S$	C_6H_6	69, 75	200	8	+4.7 ± 0.5		106	
103	*cis*-$PtPh_2(DMSO)_2 + DMSO$	$CDCl_3$	58	200	9	+5.5 ± 0.8		106	pH = 5.1
104	*cis*-$PtMe_2(DMSO)_2 + DMSO$	C_6H_6	60	200	11	+4.9 ± 0.5		106	pH = 5.0
105	$UO_2(HMPA)_4^{2+} + HMPA$	HMPA	7	200	9	−11.3 ± 1.4		107	
106	$UO_2(TMPA)_5^{2+} + TMPA$	TMPA	7	200	9	+2.1 ± 1.5		107	$\mu = 3.0$ M ($NaClO_4$)
	Ligand Substitution Reactions								
107	$Be(H_2O)_4^{2+} + hipt \rightleftarrows Be(ipt)(OH_2)_2^+ + H^+$	H_2O	25	200	8	−7.1 ± 0.2	+5.3 ± 0.2 (a)	108	$\mu = 0.1$ M ($NaClO_4$/$HClO_4$)
108	$B(OH)_3 + hipt \rightleftarrows B(OH)_2(ipt) + H_2O$	H_2O	25	200	6	−9.9 ± 0.3	−2.8 (c)	109	$\mu = 0.1$ M ($NaClO_4$)
109	$B(OH)_3 + H_2cht^{2-} \rightleftarrows B(OH)_2(cht)^{3-} + H_3O^+$	H_2O	25	200	6	−15.3 ± 1.9	−9.0 (c)	109	$\mu = 0.1$ M ($NaClO_4$)
110	$B(OH)_3 + H_2res^{2-} \rightleftarrows B(OH)(res)^{2-} + H_2O$	H_2O	25	200	6	+3.9 ± 0.4		109	$\mu = 0.1$ M ($NaClO_4$)
	$Mg^{2+} + 8\text{-hydroxyQui} \rightarrow Mg(8\text{-oxyQui})^+ + H^+$	H_2O	5	100	9			42	$\mu = 0.2$ M (KCl), pH = 8.0
111						−3.1 ± 0.4	−6.7 ± 2.6 (b)		absorbance
112						−3.6 ± 0.5	−7.6 ± 3.2 (b)		fluorescence
113						−3.4 ± 0.3	−7.2 ± 2.2 (b)		global
	$Mg(8\text{-oxyQui})^+ + H^+ \rightarrow Mg^{2+} + 8\text{-hydroxyQui}$	H_2O	5	100	9			42	$\mu = 0.2$ M (KCl), pH = 8.0
114						+3.6 ± 2.2			absorbance
115						+4.0 ± 2.7			fluorescence
116						+3.8 ± 1.9			global
	hydrolysis of	H_2O	40	500	6			110	pH = 1 (HCl)
117	P_{6m}					−5.67			
118	P_6					−3.81			
119	P_{8m}					−5.35			
120	P_8					−3.87			
121	$V(H_2O)_6^{3+} + SCN^- \rightarrow V(H_2O)_5NCS^{2+} + H_2O$	H_2O	25	200	9	−9.4 ± 0.6	+8.5 ± 1.2 (a,c)	111	$\mu = 0.6$ M, 0.014 < pH < 1.7
122	$V(H_2O)_5NCS^{2+} + H_2O \rightarrow V(H_2O)_6^{3+} + SCN^-$	H_2O	25	200	9	−17.9 ± 0.7		111	$\mu = 0.6$ M, 0.014 < pH < 1.7
123	$VO(H_2O)_5^{2+} + D_2O \rightarrow VO(H_2O)_4D_2O^{2+} + H_2O$	D_2O	65	200	6	+1.9 ± 0.2		112	
124	$V(DMSO)_6^{3+} + NCS^- \rightarrow V(DMSO)_5NCS^{2+} + DMSO$	DMSO	40	180	7	−1.1 ± 1.1	+10.5 ± 2.7 (a)	65	
125	$V(DMSO)_5NCS^{2+} + DMSO \rightarrow V(DMSO)_6^{3+} + NCS^-$	DMSO	40	180	7	−11.6 ± 1.6		65	
	$Cr(NH_3)_5(DMF)^{3+} + H_2O \rightarrow Cr(NH_3)_5(H_2O)^{3+} + DMF$	H_2O		150				113	
126			40			−2.8			
127			45			−3.1			
128			50			−3.7			
129	$Cr(Hedta)OH_2 + NCS^- \rightarrow$ products	H_2O	25	200	7	−7.8 ± 0.9	+3 ± 2 (a)	114	$\mu = 1.0$ M ($HClO_4$/$NaClO_4$)
130	$Cr(edta)^- + NCS^- \rightarrow$ products	H_2O	25	200	7	−13.6 ± 0.6		114	$\mu = 1.0$ M ($HClO_4$/$NaClO_4$)
131	$Cr(bpy)_3^{3+} + OH^- \rightarrow$ products	H_2O	50	300	7	−0.9 ± 0.5	+32 ± 5 (a)	115	$\mu = 1.0$ M (NaCl)
132	$Cr(phen)_3^{3+} + OH^- \rightarrow$ products	H_2O	50	300	7	+5.2 ± 0.4	+21 ± 4 (a)	115	$\mu = 1.0$ M (NaCl)
	$Cr(CO)_5(FB)pip \rightarrow Cr(CO)_5pip + FB$	FB	25	150				116	[FB]; [hep] (M)
133					4	+9.7 ± 0.5			0.89; 6.0
134					3	+9.5 ± 0.9			1.3; 5.6
135					4	+7.5 ± 0.1			2.0; 5.3
136					4	+9.6 ± 1.0			2.6; 5.0
137					4	+7.9 ± 0.5			4.4; 3.8
138					4	+5.4 ± 0.5			5.5; 3.0
139					4	+6.1 ± 0.3			10.1; 0
140	*trans*-$Cr(tacpa)Cl^{2+} + OH^- \rightarrow$ products	H_2O	10	140		+31.1 ± 0.1		117	
	$CrCl(N_5)^{2+} + OH^- \rightarrow Cr(N_5)(OH)^{2+} + Cl^-$	H_2O	25	100				118	
141	N_5 = *sfac*-(en)(dien)				5	+23.3 ± 1.9			$\mu = 0.05$ M
142	N_5 = *mer*-(en)(Medpt)				6	+30.3 ± 1.6			$\mu = 0.1$ M
143	N_5 = *mer*-(en)(dpt)				5	+25.3 ± 1.0			$\mu = 0.5$ M
144	N_5 = *mer*-(ibn)(dpt)				6	+24.0 ± 1.9			$\mu = 0.1$ M
145	N_5 = *mer*-(tn)(dpt)				5	+25.5 ± 1.0			$\mu = 0.5$ M
146	$Cr(CO)_5thf + pip \rightarrow Cr(CO)_5pip + thf$	thf	25	100	9	−2.2 ± 0.6		119	
147	$Cr(CO)_5thf + PPh_3 \rightarrow Cr(CO)_5PPh_3 + thf$	thf	25	100	8	−1.9 ± 1.0		119	
148	$Cr(CO)_5thf + P(OEt)_3 \rightarrow Cr(CO)_5P(OEt)_3 + thf$	thf	25	100	5	−3.6 ± 0.7		119	
149	$Cr(NH_3)_5X^{3+} + H_2O \rightarrow Cr(NH_3)_5(H_2O)^{3+} + X$	H_2O					+10 (b)	120a	$\mu = 0.01$ M ($HClO_4$)
150	X = DMSO		45	100	3	−3.2 ± 0.1			

Table 1. (Continued)

no.	reaction	solvent	T, °C	P, MPa	no. of data	$\Delta V^{\ddagger}$, cm^3 mol^{-1}	$\Delta\bar{V}$, cm^3 mol^{-1} (method)	ref(s)	remarks
	Ligand Substitution Reactions (Continued)								
151	X = $HCONH_2$		45	150	4	-4.8 ± 0.3			
152	X = $OC(NH_2)_2$		51	140	5	-8.2 ± 0.5			
153	X = $OC(NHMe)_2$		49	170	4	-3.8 ± 0.2			
154	X = $MeCONMe_2$		45	100	3	-6.2 ± 0.4			
155	X = DMF		45	100	3	-7.4 ± 0.1			
156	X = $(MeO)_3PO$		45	100	3	-8.7 ± 0.1			
157	$Cr(MeNH_2)_5Me_2SO^{3+} + H_2O \rightarrow Cr(MeNH_2)_5H_2O^{3+} + Me_2SO$	H_2O	25			-0.8 ± 1.1		120b	
158	$Cr(MeNH_2)_5HCONMe_2^{3+} + H_2O \rightarrow Cr(Me_2NH_2)_5H_2O^{3+} + HCONMe_2$	H_2O	25			-0.5 ± 0.3		120b	
159	$Cr(Me_2NH_2)_5MeCONMe_2^{3+} + H_2O \rightarrow Cr(MeNH_2)_5H_2O^{3+} + MeCONMe_2$	H_2O	25			-0.1 ± 1.2		120b	
160	$Cr(NH_3)_5Cl^{2+} + H_2O \rightarrow Cr(NH_3)_5(H_2O)^{3+} + Cl^-$	H_2O	33.5	100	5	$+17.0 \pm 0.9$		121	$[OH^-] = 0.2$ M, $\mu = 1.0$ M(ClO_4^-)
161	$Cr(NH_2CH_3)_5Cl^{2+} + H_2O \rightarrow Cr(NH_2CH_3)_5(H_2O)^{3+} + Cl^-$	H_2O	25	100	5	$+34.8 \pm 1.7$		121	$[OH^-] = 0.5$ M, $\mu = 1.0$ M(ClO_4^-)
162	$Cr(NH_3)_5I^{2+} + H_2O \rightarrow Cr(NH_3)_5(H_2O)^{3+} + I^-$	H_2O	17	100	5	$+22.2 \pm 0.6$		121	$[OH^-] = 0.1$ M, $\mu = 1.0$ M(ClO_4^-)
163	$Cr(NH_3)_5(OC(CH_3)N(CH_3)_2)^{2+} + H_2O \rightarrow Cr(NH_3)_5(H_2O)^{3+} + CH_3CON(CH_3)_2$	H_2O	29	100	5	$+25.0 \pm 0.7$		121	$[OH^-] = 0.1$ M, $\mu = 1.0$ M(ClO_4^-)
	$Cr(TPP)(Cl)L^{2+} \rightleftarrows Cr(TPP)(Cl)^{2+} + L$; k_1, k_2	toluene	25	100	5			122	
	$Cr(TPP)(Cl)^{2+} + MeIm \rightarrow Cr(TPP)(Cl)MeIm^{2+}$; k_3								
164	L = py, k_1					$+25.7 \pm 0.5$			
165	L = py, k_2/k_3					$+1.3 \pm 1.1$			
166	L = Qui, k_1					$+23.8 \pm 0.6$			
167	L = Qui, k_2/k_3					-1.9 ± 1.6			
168	L = PPh_3, k_1					$+19.6 \pm 0.2$			
169	L = PPh_3, k_2/k_3					$+2.0 \pm 0.6$			
170	*trans*-$Cr(tmd)_2F_2^+ + H_2O \rightarrow$ *trans*-$Cr(tmd)_2(H_2O)F^{2+} + F^-$	H_2O	35−50	150	4	−3.4 to −2.3		123	acidic solution
171	*trans*-$Cr(tmd)_2(F)Cl^+ + H_2O \rightarrow$ *trans*-$Cr(tmd)_2(H_2O)F^{2+} + Cl^-$	H_2O	20−35	150	4	−8.8 to −7.7		123	acidic solution
	$Cr(CO)_4(DTH) + 2L \rightarrow Cr(CO)_4L_2 + DTH$								
172	L = $P(OMe)_3$	DCE	60	100	5	$+10.1 \pm 0.8$		124	
173	L = $P(OMe)_3$	CB	50	100	5	$+8.8 \pm 0.4$		124	
174	L = $P(OPr^i)_3$	DCE	60	125	5	$+10.4 \pm 0.4$		124	
175	L = $P(OPh)_3$	DCE	55.5	100	5	$+9.3 \pm 0.5$		124	
	$Cr(NH_3)_5(OSO_2CF_3)^{2+} + S \rightarrow Cr(NH_3)_5S^{3+} + CF_3OSO_2^-$			150	4			125	S = solvent
176		CH_3CN	25			-8.9 ± 0.5			
177		MeOH	20			-10.5 ± 0.7			
	$(bz)Cr(CO)_5 \rightleftarrows Cr(CO)_5 + bz$; k_1, k_{-1}								
	$Cr(CO)_5 + pip \rightarrow (pip)Cr(CO)_5$; k_2								
178	k_1k_2/k_{-1}	C_6H_6	25	100	5	$+4.2 \pm 0.3$		126	
179	k_{-1}	C_6H_6	25	100	5	$+12.3 \pm 1.4$		126	
	$Cr(phen)(CO)_4 + P(OMe)_3 \rightleftarrows$ *fac*-$Cr(phen)(CO)_3(P(OMe)_3) + CO$; k_1, k_{-1}								
180	k_1	DCE	50	100	5	$+13.8 \pm 0.5$	-4 ± 1 (b)	127	
181	k_{-1}	DCE	35	100	5	$+19.2 \pm 0.5$		127	
	trans-$Cr(tn)_2Cl_2^+ + H_2O \rightarrow$ *trans*-$Cr(tn)_2Cl(H_2O)^{2+} + Cl^-$	H_2O		150	4			128	
182			35			−2.02			
183			40			−1.93			
184			45			−1.78			
185			50			−1.7			
	trans-$Cr(tn)(en)Cl_2^+ + H_2O \rightarrow$ *trans*-$Cr(tn)(en)Cl(H_2O)^{2+} + Cl^-$	H_2O		150	4			128	
186			35			−2.99			
187			40			−2.75			
188			45			−2.69			
189			50			−2.53			
	$Mn(CO)_5Br + bpy \rightarrow Mn(CO)_3(bpy)Br + CO$		25.5	100	3			129	
190		MeOH				+22			
191		MeOH−H_2O				−20			
192	$Mn(CO)_5Cl + dab \rightarrow Mn(CO)_3(dab)Cl + CO$	toluene	30	150	4	$+20.6 \pm 0.4$		130	
193	$Mn(CO)_5Cl + [9]aneS_3 \rightarrow ([9]aneS_3)Mn(CO)_3Cl + CO$	acetone	29.5	140	5	$+20.6 \pm 2.6$		31	
194	$Mn(DMF)_6^{2+} + Et_2DTC^- \rightarrow Mn(DMF)_4(Et_2DTC)^+ + 2DMF$	DMF	−45	120	7	$+9.5 \pm 0.5$		132	
195	$Fe^{3+} + Hipt \rightarrow Fe(ipt)^{2+} + H^+$	H_2O	25	250	6	6	$+7.8 \pm 0.1$ (a)	133	$\mu = 1.0$ M, $[H^+] = 1.0$ M
196	$Fe(ipt)^{2+} + H^+ \rightarrow Fe^{3+} + Hipt$	H_2O	25	250	6	6	-16.5 ± 0.9 (a)	133	$\mu = 1.0$ M, $[H^+] = 1.0$ M
197	$Fe^{3+} + ClO_2^- \rightleftarrows FeClO_2^{2+}$	H_2O	5	150	5	5	$+16.5 \pm 2.7$ (a)	134	
198	$Fe(OH)^{2+} + HClO_2 \rightarrow FeClO_2^{2+} + H_2O$	H_2O	5	150	5	$+6.9 \pm 2.3$		134	
199	$Fe(bpy)_3^{2+} + CN^- \rightarrow$ products	H_2O	25	100	4	+12.2		135	$\mu = 0.33$ M (NaCl)
200	$Fe(phen)_3^{2+} + CN^- \rightarrow$ products	H_2O	25	100	4	+10.5		135	$\mu = 0.33$ M (NaCl)
201	$Fe(4,4'\text{-}Me_2bpy)_3^{2+} + CN^- \rightarrow$ products	H_2O	25	100	4	+12.3		135	$\mu = 0.33$ M (NaCl)
202	$Fe(4,4'\text{-}Me_2bpy)_3^{2+} + OH^- \rightarrow$ products	H_2O	25	100	4	+11.7		135	$\mu = 0.01$ M (NaCl)
203	$Fe(H_2O)_6^{3+} + SCN^- \rightleftarrows Fe(SCN)(H_2O)_5^{2+} + H_2O$	H_2O	25	150	4		$+8.9 \pm 0.2$ (b)	136	$[HClO_4] = 1.0$ M
204	$Fe(DMSO)_6^{3+} + SCN^- \rightleftarrows Fe(SCN)(DMSO)_5^{2+} + DMSO$	DMSO	25	150	4		$+12.4 \pm 0.7$ (b)	136	$[NaClO_4] = 0.2$ M

Table 1. (Continued)

no.	reaction	solvent	T, °C	P, MPa	no. of data	$\Delta V^{\ddagger}$, $cm^3\ mol^{-1}$	$\Delta \bar{V}$, $cm^3\ mol^{-1}$ (method)	ref(s)	remarks
	Ligand Substitution Reactions (Continued)								
205	$Fe(DMF)_6^{3+} + SCN^- \rightleftarrows Fe(SCN)(DMF)_5^{2+} + DMF$	DMF	25	150	4		+25.1 ± 0.3 (b)	136	$[NaClO_4] = 0.2$ M
	$Fe(CN)_5L^{3-} + CN^- \rightarrow Fe(CN)_6^{4-} + L$		25	100	5			137	
206	L = 4-(1-butylpentyl)pyridine	H_2O−MeOH				+16			
207	L = 4-phenylpyridine	H_2O				+10			
208	L = *N*-(*n*-pentyl)pyrazinium (Na_2 salt)	H_2O				+10			
209	L = pyrazine	H_2O				+13			
	$Fe(CN)_5L^{3-} + CN^- \rightleftarrows Fe(CN)_6^{4-} + L$	H_2O	25		4			138	
210	L = 4-CNpy			100		+19.0 ± 0.5	(+8.0 ± 1.5)		μ = 0.1 M (CN^-) + 5.0 M (NaCl)
211	L = 4,4′-bpy			100		+13.5 ± 0.7	(+15.6 ± 1.5)		μ = 0.1 M (CN^-)
212	L = 4-^{t}Bupy			130		+11.4 ± 1.0	(+9.1 ± 1.5)		μ = 0.1 M (CN^-)
	$Fe(CN)_5(NO_2)^{3-} + H_2O \rightarrow Fe(CN)_5(H_2O)^{2-} + NO_2^-$	H_2O	25	100	5			139	μ = 0.5 M ($LiClO_4$)
213						+2.2 ± 0.1			$[H^+]$ = 0.2 M (HCl)
214						+1.9 ± 0.1			$[H^+]$ = 0.5 M (HCl)
215	$Fe(CN)_5(NO_2)^{3-} + DMF \rightarrow Fe(CN)_5(DMF)^{2-} + NO_2^-$	DMF	25	100	5	+26.9 ± 1.5		140	0.5% H_2O
216	$Fe(CN)_5(NO_2)^{3-} + DMSO \rightarrow Fe(CN)_5(DMSO)^{2-} + NO_2^-$	DMSO	25	75	4	+25.9 ± 1.1		140	
217	$Fe(CN)_5(NO_2)^{3-} + MeOH \rightarrow Fe(CN)_5(MeOH)^{2-} + NO_2^-$	MeOH	45	100	5	+19.6 ± 1.8		140	0.5% H_2O
218	$Fe(CN)_5(NO)_2^{4-} + H_2O \rightarrow Fe(CN)_5(H_2O)^{3-} + NO_2^-$	H_2O	25	125	5	+20.1 ± 1.0		139	$[OH^-]$ = 0.1 M
	$Fe(CN)_5(L)^{3-} + CN^- \rightarrow Fe(CN)_6^{4-} + L$	H_2O	25	150	4−5			141	
219	L = *p*-$(CH_3CH_2CH_2)_2CHC_5H_4N$	20% MeOH				+16.3 ± 1.4			
220	L = *p*-$(C_5H_4N)_2$	H_2O				+13.6 ± 0.5			
221	L = *p*-$(C_6H_5)(C_5H_4N)$	H_2O				+10.4 ± 0.5			
222		40% MeOH				+11.2 ± 1.5			
223	L = *p*-$CH_3(CH_2)_5NC_4H_4N^+$	H_2O				+9.6 ± 0.8			
224		40% MeOH				+2.3 ± 0.9			
225		80% MeOH				+13.2 ± 0.9			
226		40% isopropyl alcohol				−3.1 ± 0.6			
227	L = *p*-$C_6H_4N_2C_2H_2$	H_2O				+17.9 ± 0.4			
228		40% MeOH				+19.2 ± 0.5			
229	L = *p*-$(CH_3)_3CC_5H_4N$	H_2O				+11.4 ± 1.0			
230		40% MeOH				+20.1 ± 0.9			
231		17% *tert*-butyl alcohol				+12.0 ± 0.8			
232		40% Me_2CO				+19.5 ± 1.2			
233	L = *p*-NCC_5H_4N	H_2O				+19.0 ± 1.0			
234		40% MeOH				+11.8 ± 0.7			
235	L = *p*-$CH_3C_4H_4N_2^+$	H_2O				+0.9 ± 0.5			
236		40% MeOH				−6.1 ± 0.9			
237		80% MeOH				−2.4 ± 0.6			
238		40% isopropyl alcohol				+8.0 ± 0.8			
239	L = $C_4H_4N_2$	H_2O				+12.5 ± 1.2			
240		40% MeOH				+14.4 ± 1.5			
241	L = *p*-$CH_3C_4H_4N_2^+$	H_2O				+20.9 ± 0.5			
242	$Fe(CN)_5(4\text{-}CNpy)^{3-} + CN^- \rightarrow Fe(CN)_6^{4-} + 4CNpy$	H_2O	25	100	4	+19.0 ± 1.0		142	$[CN^-]$ = 0.10 M
243	$Fe(CN)_5(4,4'\text{-}bpy)^{3-} + CN^- \rightarrow Fe(CN)_6^{4-} + 4,4'\text{-}bpy$	H_2O	25	100	4	+13.5 ± 0.7		143	$[CN^-]$ = 0.10 M
244	$Fe(CN)_5(4\text{-}t\text{-}bupy)^{3-} + CN^- \rightarrow Fe(CN)_6^{4-} + 4\text{-}t\text{-}bupy$	H_2O	25	125	4	+11.4 ± 1.0		143	$[CN^-]$ = 0.10 M
	$Fe(CN)_5(NH_2R)^{3-} + py \rightarrow Fe(CN)_5(py)^{3-} + NH_2R$	H_2O		100	5			144	
245	R = H		40			+16.4 ± 0.6			
246	R = CH_3		40			+24.0 ± 1.0			
247	R = C_2H_5		40			+16.3 ± 1.5			
248	R = $PhCH_2$		40			+17.4 ± 1.4			
249	R = ^{i}Pr		25			+18.5 ± 0.6			
	$Fe(CN)_5H_2O^{3-} + L^{n-} \rightarrow Fe(CN)_5L^{(3+n)-} + H_2O$	H_2O	25	100	4			145	μ = 0.1 M
250	L^{n-} = imidazole					+15.5 ± 0.7			pH = 7.0
251	L^{n-} = histidine					+17.0 ± 0.4			pH = 7.5
252	L^{n-} = methionine					+17.9 ± 0.6			pH = 6.5
253	L^{n-} = glutathione					+14.1 ± 0.4			pH = 6.0
254	L^{n-} = glycine					+16.4 ± 0.6			pH = 11.7
255	L^{n-} = β-alanine					+16.8 ± 0.2			pH = 11.7
	$Fe(CN)_5H_2O^{2-} + L \rightarrow Fe(CN)_5L^{2-} + H_2O$	H_2O	40	150	4			146	pH = 6.0
256	L = cytosine					+2.5 ± 0.5			
257	L = cytidine					+9.5 ± 1.2			
258	L = CMP					+12.8 ± 1.1			
259	$Fe(5\text{-}Brphen)_3^{2+} + H_2O \rightarrow$ 5-Brphen + $Fe(5\text{-}Brphen)(H_2O)_2^{2+}$	H_2O	25	100	7	+23.0		147	
260	$Fe(DMF)_6^{2+} + Et_2DTC^- \rightarrow Fe(DMF)_4(Et_2DTC)^+ + 2DMF$	DMF	−35	160	9	+12.3 ± 0.8		132	μ = 0.10 M ($NaClO_4$)
261	$Fe(DMF)_6^{2+} + Paa \rightarrow Fe(DMF)_4(Pada)^{2+} + 2DMF$	DMF	−35	160	9	+7.5 ± 1.0	−2.0 ± 0.3 (a)	132	μ = 0.10 M ($NaClO_4$)
262	$Fe(DMF)_4(Pada)^{2+} + 2DMF \rightarrow Fe(DMF)_6^{2+} + Pada$	DMF	−35	160	9	+9.5 ± 1.3		132	μ = 0.10 M ($NaClO_4$)
263	$Fe(Ah)_3 + H^+ + 2H_2O \rightarrow Fe(H_2O)_2(Ah)_2^+ + HAh$	H_2O	−0.5	100	5	−5.4 ± 0.5	−3.2 ± 0.7 (a)	148	μ = 2.0 M ($NaClO_4$)
264	$Fe(H_2O)_2(Ah)_2^+ + H^+ + 2H_2O \rightarrow Fe(H_2O)_4Ah^{2+} + HAh$	H_2O	3	100	5	−9.1 ± 0.6	−6.9 ± 0.5 (a)	148	μ = 2.0 M ($NaClO_4$)
265	$Fe(H_2O)_4(Ah)^{2+} + H^+ + 2H_2O \rightarrow Fe(H_2O)_6^{3+} + HAh$	H_2O	25	100	5	−15.6 ± 1.5	−9.3 ± 0.1 (a)	148	μ = 2.0 M ($NaClO_4$)
266	$Fe(H_2O)_4Ah^{2+} + 2H_2O \rightarrow Fe(H_2O)_5(OH)^{2+} + HAh$	H_2O	25	100	5	−3.3 ± 0.6		148	μ = 2.0 M ($NaClO_4$)
267	$Fe(H_2O)_5(OH)^{2+} + HAh \rightarrow Fe(H_2O)_4Ah^{2+} + 2H_2O$	H_2O	25	100	5	+5.2 ± 0.5		148	μ = 2.0 M ($NaClO_4$)
268	$Fe(H_2O)_6^{3+} + HAh \rightarrow Fe(H_2O)_4(Ah)^{2+} + H^+ + 2H_2O$	H_2O	25	100	5	−6.3 ± 1.4		148	μ = 2.0 M ($NaClO_4$)
269	$Fe(H_2O)_4Ah^{2+} + HAh \rightarrow Fe(H_2O)_2(Ah)_2^+ + H^+ + 2H_2O$	H_2O	25	100	5	−2.2 ± 0.5		148	μ = 2.0 M ($NaClO_4$)
270	$Fe(H_2O)_2Ah_2^+ + HAh \rightarrow Fe(Ah)_3^+ + H^+ + 2H_2O$	H_2O	25	100	5	−2.2 ± 0.9		148	μ = 2.0 M ($NaClO_4$)
271	$Fe(H_2O)_5(OH)^{2+} + H_4dfb^+ \rightarrow Fe(H_2O)_4(H_3dfb)^{3+} + 2H_2O$	H_2O	25	100	5	+4.3 ± 0.5		148	μ = 2.0 M ($NaClO_4$)
272	$Fe(H_2O)_6^{3+} + H_4dfb^+ \rightarrow Fe(H_2O)_4(H_3dfb)^{3+} + H^+ + 2H_2O$	H_2O	25	100	5	−4.7 ± 1.6		148	μ = 2.0 M ($NaClO_4$)
	$FeL_3^{2+} + NaOH \rightarrow$ products	H_2O	25					149	

Table 1. (Continued)

no.	reaction	solvent	T, °C	P, MPa	no. of data	$\Delta V^{\ddagger}$, $cm^3\,mol^{-1}$	$\Delta \bar{V}$, $cm^3\,mol^{-1}$ (method)	ref(s)	remarks
	Ligand Substitution Reactions (Continued)								
273	L = bpy			140	6	+12.8 ± 0.4			μ = 0.01 M
274	L = phen			140	6	+14.2 ± 0.8			μ = 0.005 M
275	L = 3-Mebsb			120	3	+13.6 ± 1.8			μ = 0.33 M (KOH)
276	L = 4-MeObsb			100	4	+12.0 ± 2.1			μ = 0.33 M (KOH)
	$FeL_3^{2+} + H_2O \rightarrow$ products	H_2O	25					149	(edta)
277	L = 5-Brphen				6	+22.3 ± 1.0			μ = 0.030 M
278	L = 5-NO_2phen				5	+21.7 ± 1.0			μ = 0.030 M
279	$Fe(gmi)_3^{2+} + OH^- \rightarrow Fe(OH)^+ + 3gmi$	H_2O	25	100	3	+16.7		150	
280		20% CH_3OH	25	100	3	+16.2			
281		40% CH_3OH	25	140	5	+15.5			
282		50% CH_3OH	25	100	3	+12.6			
283		60% CH_3OH	25	100	3	+8.1			
284		80% CH_3OH	25	100	3	+4.9			
285		20% C_2H_5OH	25	100	3	+15.0			
286		30% C_2H_5OH	25	100	3	+15.0			
287		40% C_2H_5OH	25	100	3	+10.0			
288		50% C_2H_5OH	25	100	3	+3.3			
289		20% i-C_3H_7OH	25	100	3	+15.3			
290		30% i-C_3H_7OH	25	100	3	+13.7			
291		40% i-C_3H_7OH	25	100	3	+9.7			
292		50% i-C_3H_7OH	25	100	3	+7.6			
293		60% i-C_3H_7OH	25	100	3	+5.8			
294		10% t-C_4H_9OH	25	100	3	+14.9			
295		17% t-C_4H_9OH	25	100	3	+12.2			
296		30% t-C_4H_9OH	25	100	3	+7.4			
297		50% t-C_4H_9OH	25	100	3	+4.0			
298		20% $(H_3C)_2CO$	25	100	3	+11.0			
	$Fe(gmi)_3^{2+} + OH^- \rightarrow Fe(OH)^+ + 3gmi$	H_2O	25	100	3			151	μ = 0.33 M (NaCl)
299		20% egly				+14.1			
300		30% egly				+15.7			
301		40% egly				+17.7			
	$Fe^{3+} + X^{n-}$	H_2O	25	200	7			152	
302	$Fe(H_2O)_6^{3+} + NCS^- \rightarrow Fe(H_2O)_5(NCS)^{2+} + H_2O$					−5.7 ± 0.3	+11.8 ± 0.3 (a)		
303	$Fe(H_2O)_5(OH)^{2+} + NCS^- \rightarrow Fe(H_2O)_5(NCS)^+ + H_2O$					+9.0 ± 0.4			
304	$Fe(H_2O)_6^{3+} + HN_3 \rightarrow Fe(H_2O)_5N_3^{2+} + H_2O + H^+$						+3.8 ± 0.8 (a)		
305	$Fe(H_2O)_5(OH)^{2+} + HN_3 \rightarrow Fe(H_2O)_5N_3^{2+} + H_2O$					+6.8 ± 0.5			
306	$Fe(H_2O)_6^{3+} + N_3^- \rightarrow Fe(H_2O)_5N_3^{2+} + H_2O$					+16.5 ± 0.5			
307	$Fe(H_2O)_5(OH)^{2+} + N_3^- \rightarrow Fe(H_2O)_5N_3^{2+} + OH^-$					+12.9 ± 1.5			
	$Fe(hxsb)^{2+} + OH^- \rightarrow Fe(OH)^+ + hxsb$		25					153	
308		H_2O		130	5	+13.3 ± 1.9			$[OH^-]$ = 0.33 M
309		50% MeOH		130	5	+14.0			$[OH^-]$ = 0.33 M
310		75% MeOH		130	5	+6.2 ± 0.6			$[OH^-]$ = 0.33 M
311		75% MeOH		130	4	+5.5 ± 1.2			$[OH^-]$ = 0.10 M
312		85% MeOH		130	4	+6.8			$[OH^-]$ = 0.33 M
313		35% Pr^iOH		100	3	+9			$[OH^-]$ = 0.10 M
314		67% Pr^iOH		100	3	−2.5			$[OH^-]$ = 0.10 M
315		17% Bu^tOH		130	4	+14.1 ± 1.1			$[OH^-]$ = 0.33 M
316		38% Bu^tOH		130	2	+12			$[OH^-]$ = 0.10 M
317		50% Bu^tOH		120	3	−4.2			$[OH^-]$ = 0.10 M
318	$Co(DMF)_6^{2+} + Et_2DTC^- \rightarrow Co(DMF)_4Et_2DTC^+ +$ 2DMF	DMF	−35	160	9	+12.1 ± 0.6		132	μ = 0.10 M ($NaClO_4$)
319	$Co(H_2O)_6^{2+} +$ Cl-phen $\rightarrow Co(Cl\text{-}phen)(H_2O)_4^{2+} + 2H_2O$	H_2O	25	150	7	+6.6 ± 0.3	+6.4 ± 0.8 (a)	154	
320	$Co(Cl\text{-}phen)(H_2O)_4^{2+} + 2H_2O \rightarrow Co(H_2O)_6^{2+} +$ Cl-phen	H_2O	25	150	7	+0.2 ± 0.4		154	
321	*trans*-$Co(tacpa)Cl^{2+} + OH^- \rightarrow$ products	H_2O	12	140		+27.1 ± 0.4		117	
322	$Co(edta)^- + H^+ + H_2O \rightarrow Co(hedta)OH_2$	H_2O	85	230	7	+3.5 ± 0.7		155	
323	$Co(hedta)OH_2 \rightarrow Co(edta)^- + H^+ + H_2O$	H_2O	85	230	7	+6.7 ± 0.7		155	
324	α-$Co(tetren)Cl^{2+} + H_2O \rightarrow \alpha$-$Co(tetren)OH_2^{3+} + Cl^-$	H_2O	80	100	5	−3.6 ± 0.9		156	μ = 1.0 M ($HClO_4$)
325	α-$Co(tetren)Cl^{2+} + OH^- \rightarrow \alpha$-$Co(tetren)OH^{2+} + Cl^-$	H_2O	80	100	5	+42 ± 1.3		156	μ = 1.0 M ($HClO_4$)
326	β-$Co(tetren)Cl^{2+} + H_2O \rightarrow \beta$-$Co(tetren)OH_2^{3+} + Cl^-$	H_2O	80	100	5	−1.7 ± 1.0		156	μ = 1.0 M ($HClO_4$)
327	β-$Co(tetren)Cl^{2+} + OH^- \rightarrow \beta$-$Co(tetren)OH^{2+} + Cl^-$	H_2O	60	100	5	+35 ± 1.0		156	μ = 0.01 M ($HClO_4$)
328	$Co(NH_3)_5Cl^{2+} + H_2O \rightarrow$ products	H_2O	65	100	5	−7.4 ± 0.6		156	μ = 0.01 M ($HClO_4$)
329	$Co(tmen)_3^{3+} + OH^- \rightarrow$ products	H_2O	25	100	5	+57.6 ± 0.9		157	μ = 0.1 M ($NaClO_4$)
330						+59.1 ± 0.3		157	μ = 1.0 M ($NaClO_4$)
331	$Co(TAPP)(H_2O)_2^{5+} + NCS^- \rightarrow$ $Co(TAPP)(H_2O)(NCS)^{4+} + H_2O$	H_2O	25	150	5	+18.8 ± 0.8		158	pH = 1, μ = 1.0 M ($NaNO_3$)
	dmbzim-Co-H_2O + L → dmbzim-Co-L + H_2O	H_2O	25	100	5			159	
332	L = N_3^-					+6.4 ± 0.1	−9.9 (b)		
333	L = NH_3					+5.5 ± 0.3			
334	*trans*-$[Co(NH_3)_4Cl_2]^+ + H_2O \rightarrow$	H_2O	16	200	5		−12.0 (b) (*trans*)	160	
335	45% *t*, 55% *c*-$[Co(NH_3)_4(H_2O)Cl]^{2+} + Cl^-$						−14.0 (b) (*cis*)		
336	*trans*-$[Co(en)_2Cl_2]^+ + H_2O \rightarrow$ 74% *t*, 26% *c*-$[Co(en)_2(H_2O)Cl]^{2+} + Cl^-$	H_2O	40	200	5	+1.8	−9.1 (b)	160	$[HClO_4]$ = 1 mM $[HNO_3]$ = 7.6 mM
337	*cis*-$[Co(en)_2Cl_2]^+ + H_2O \rightarrow$ *cis*-$[Co(en)_2(H_2O)Cl]^{2+} + Cl^-$	H_2O	30	200	6	−0.3	−18.6 (b)	160	$[HClO_4]$ = 1.1 mM $[HNO_3]$ = 0.6 mM
338	*trans*-$[Co(trien)Cl_2]^+ + H_2O \rightarrow$ *cis*-β-$[Co(trien)(H_2O)Cl]^{2+} + Cl^-$	H_2O	10	200	6	+1.1	−8.8 (b)	160	$[HClO_4]$ = 1.0 mM
339	*cis*-α-$[Co(trien)Cl_2]^+ + H_2O \rightarrow$ *cis*-α-$[Co(trien)(H_2O)Cl]^{2+} + Cl^-$	H_2O	32	200	6	−1.9	−10.0 (b)	160	$[HClO_4]$ = 10 mM
340	*cis*-β-$[Co(trien)Cl_2]^+ + H_2O \rightarrow$ *cis*-β-$[Co(trien)(H_2O)Cl]^{2+} + Cl^-$	H_2O	15	200	6	−0.1	+1.9 ± 0.8 (b)	160	$[HClO_4]$ = 1.0 mM
341	*cis*-α-$[Co(edda)Cl_2]^- + H_2O \rightarrow$ *cis*-α-$[Co(edda)(H_2O)Cl] + Cl^-$	H_2O	31	200	6	+3.2	−7.4 (b)	160	$[HClO_4]$ = 9.6 mM

Table 1. (Continued)

no.	reaction	solvent	T, °C	P, MPa	no. of data	$\Delta V^{\ddagger}$, cm^3 mol^{-1}	$\Delta\bar{V}$, cm^3 mol^{-1} (method)	ref(s)	remarks
	Ligand Substitution Reactions (Continued)								
342	*cis*-α-[Co(edda)(H_2O)Cl] + H_2O → *cis*-α-[Co(edda)(H_2O)$_2$]$^+$ + Cl^-	H_2O	47	200	6	+0.8		160	[$HClO_4$] = 1.0 mM
343	*trans*-[Co(en)$_2$$Br_2$]$^+$ + H_2O → 85% *t*, 15% *c*-[Co(en)$_2$(H_2O)Br]$^{2+}$ + Br^-	H_2O	25	200	6	+1.0		160	[$HClO_4$] = 10 mM
	$Co(NH_3)_5X^{2+}$ + H_2O → $Co(NH_3)_5(H_2O)^{2+}$ + X^-	H_2O		200	5			161	[$HClO_4$] = 100 mM
344	X = Cl^-		65			−6.0			
345	X = Br^-		54			−6.4			
346	X = NO_3^-		40			−5.7			
	$Co(en)_2(NH_3)X^{2+}$ + H_2O → $Co(en)_2(NH_3)(H_2O)^{2+}$ + X^-	H_2O		200	5			161	
347	X = *trans*-Cl^-		70			−5.0	−17.3 (b)		[$HClO_4$] = 100 mM
348	X = *trans*-Br^-		60			−3.1	−14.7 (b)		[$HClO_4$] = 1 mM
349	X = *cis*-Br^-		60			−5.6	−16.1 (b)		[$HClO_4$] = 100 mM
350	X = *cis*-NO_3^-		45			−6.1	−13.2 (b)		[$HClO_4$] = 100 mM
	cis-$Co(en)_2(OH_2)_2^{3+}$ + XO_4^{2-}/HXO_4^- → H_2O + *cis*-$Co(en)_2(OH_2)(XO_4)^+$	H_2O	55	140	3			162	pH = 2.0, μ = 1.0 M ($NaClO_4$)
351	X = S					+8.3 ± 0.5			
352	X = Se					+8.5 ± 0.4			
	cis-$Co(en)_2(OH)(XO_4)^+$ + H_2O → XO_4^{2-} + *cis*-$Co(en)_2(OH_2)_2^{3+}$	H_2O	55	140	3			162	pH = 2.0, μ = 1.0 M ($NaClO_4$)
353	X = S					+2.2 ± 0.4			
354	X = Se					+3.3 ± 0.7			
	cobalt(III) ammine base hydrolysis	H_2O		100	5			163	
355	$Co(NH_3)_5OC(Me)N(Me)_2^{3+}$ + OH^- → $Co(NH_3)_5OH^{2+}$ + $MeCONMe_2$		15			+43.2 ± 1.7			[OH^-] = 25 mM, μ = 34 mM
356	$Co(NH_2Me)_5Cl^{2+}$ + OH^- → $Co(NH_2Me)_5OH^+$ + Cl^-		9.5			+32.8 ± 1.7			[OH^-] = 10 mM, μ = 13 mM
357	$Co(NH_2Et)_5Cl^{2+}$ + OH^- → $Co(NH_2Et)_5OH^+$ + Cl^-		12			+31.1 ± 0.5			[OH^-] = 1 mM, μ = 3 mM
358	*cis*-$Co(en)_2(NH_3)Cl^{2+}$ + OH^- → 78% *cis*-, 22% *trans*-$Co(en)_2(NH_3)OH^{2+}$ + Cl^-		25			+31.8 ± 0.6			[OH^-] = 50 mM, μ = 56 mM
359	*cis*-$Co(en)_2(NH_3)Br^{2+}$ + OH^- → 77% *cis*-, 23% *trans*-$Co(en)_2(NH_3)OH^{2+}$ + Br^-		25			+30.8 ± 1.0			[OH^-] = 50 mM, μ = 56 mM
360	*trans*-$Co(en)_2Cl_2^+$ + OH^- → 5% *cis*-, 95% *trans*-$Co(en)_2(Cl)OH^+$ + Cl^-		14.5			+24.3 ± 1.1			[OH^-] = 15 mM, μ = 16 mM
361	*cis*-$Co(en)_2Cl_2^+$ + OH^- → 37% *cis*-, 63% *trans*-$Co(en)_2(Cl)OH^+$ + Cl^-		14.5			+27.9 ± 0.7			[OH^-] = 50 mM, μ = 51 mM
362	*trans*-$Co(en)_2(N_3)Cl^+$ + OH^- → 23% *cis*-, 77% *trans*-$Co(en)_2(N_3)OH^+$ + Cl^-		15			+26.7 ± 0.4			[OH^-] = 50 mM, μ = 50 mM
363	*cis*-β-$Co(trien)Cl_2^+$ + OH^- → *cis*-$Co(trien)(Cl)OH^+$ + Cl^-		4			+35.7 ± 1.2			[OH^-] = 0.005 mM, μ = 100 mM
364	*trans*-$Co(RSSR\text{-}cyclam)Cl_2^+$ + OH^- → *trans*-$Co(RSSR\text{-}cyclam)(Cl)OH^+$ + Cl^-		9.5			+18.7 ± 1.5			[OH^-] = 1 mM, μ = 1 mM
365	*cis*-$Co(en)_2(NO_2)Cl^+$ + OH^- → *cis*-$Co(en)_2(NO_2)OH^+$ + Cl^-		24			+20.8 ± 0.3			[OH^-] = 50 mM, μ = 50 mM
366	*cis*-$Co(tet)Cl_2^+$ + OH^- → *cis*-$Co(tet)(Cl)OH^+$ + Cl^-		12			+23.1 ± 0.8			[OH^-] = 1 mM, μ = 3 mM
367	*cis*-$Co(tet)(Cl)OH^+$ + OH^- → *cis*-$Co(tet)(OH)_2^+$ + Cl^-		12			+25.9 ± 2.1			[OH^-] = 1 mM, μ = 3 mM
368	*trans*-RS-$Co(tet)(Cl)_2^+$ + OH^- →		12			+22.1 ± 0.7			[OH^-] = 1 mM, μ = 3 mM
369	*trans*-RS-$Co(tet)(Cl)OH^+$ + Cl^-		5			+20.4 ± 0.7			[OH^-] = 2 mM, μ = 6 mM
370	*trans*-RR(SS)-$Co(tet)Cl_2^+$ + OH^- → *trans*-RS-$Co(tet)(Cl)OH^+$ + Cl^-		6			+24.4 ± 1.2			[OH^-] = 2 mM, μ = 6 mM
371	*trans*-RS-$Co(tet)(Cl)OH^+$ + OH^- → *trans*-RS-$Co(tet)(OH)_2^+$ + Cl^-		12			+23.8 ± 0.9			[OH^-] = 1 mM, μ = 3 mM
	$Co(NH_3)_5(OSO_2CF_3)^{2+}$ + CH_3CN → $Co(NH_3)_5(CH_3CN)^{3+}$ + $CF_3OSO_2^-$			150	4			125	μ not adjusted
372		CH_3CN	25			−3.1 ± 0.1			
373		MeOH	17			−3.2 ± 0.1			
	trans-$Co(N\text{-}eten)_2Cl_2^+$ + H_2O → *trans*-$Co(N\text{-}eten)_2Cl(H_2O)^+$ + Cl^-	H_2O/ Bu^tOH wt % ROH	25	150	4			164	[HCl] = 0.01 M, μ = 0.5 M (NaCl)
374		0				+5.83			
375		5				+5.61			
376		10				+5.61			
377		20				+5.00			
378		30				+3.95			
379		40				+2.55			
	s-cis-$Co(eee)X_2^+$ + H_2O → X^- + *s-cis*-$Co(eee)(H_2O)X^{2+}$	H_2O	40	150	4			165	[$HClO_4$] = 0.1 M
380	X = Cl^-					−4.6			
371	X = Br^-					−4.2			
	$Co(NH_3)_5(RCOO)^{2+}$ + H_2O → $Co(NH_3)_5(H_2O)^{3+}$ + $RCOO^-$ $k_{obs} = k_o + k_1[H^+]$	H_2O		200	5			166	[$HClO_4$] = 0.4 M
	R = H		64.5						
382	k_o					+0.9			
383	k_1					−5.8 ± 0.3	−3.6 (b)		
	R = CH_3		64.5						
384	k_o					+0.7			
385	k_1					−4.2 ± 0.3	−4.7 (b)		
	R = C_2H_5		64.5						
386	k_o					+0.5			
387	k_1					−4.4 ± 0.4	−5.9 (b)		
	R = CH_2Cl		74.5						
388	k_o					+0.4			
389	k_1					−4.5 ± 0.4	−6.9 (b)		
	R = CH_2Br		74.5						

Table 1. (Continued)

no.	reaction	solvent	T, °C	P, MPa	no. of data	$\Delta V^{\ddagger}$, $cm^3\ mol^{-1}$	$\Delta\bar{V}$, $cm^3\ mol^{-1}$ (method)	ref(s)	remarks
	Ligand Substitution Reactions (Continued)								
390	k_o					−1.5			
391	k_1					−6.4 ± 0.3	−4.4 (b)		
	R = $CHCl_2$		79.5						
392	k_o					−7.0 ± 0.3	−18.5 (b)		$[HClO_4]$ = 0.01 M, $[NaClO_4]$ = 0.39 M
	R = $CHBr_2$		79.5						
393	k_o					−6.4 ± 0.2	−16.3 (b)		$[HClO_4]$ = 0.01 M, $[NaClO_4]$ = 0.39 M
	R = CCl_3		74.5						
394	k_o					−5.7 ± 0.4	−18.1 (b)		$[HClO_4]$ = 0.01 M,
395	R = CF_3		74.5			−5.7 ± 0.3	−14.4 (b)		
396	$Co(TMPP)(H_2O)_2^{5+} + TU \rightleftarrows Co(TMPP)(H_2O)(TU)^{5+} + H_2O$	H_2O	22	140	5	+12.6 ± 0.6		167	$[H^+]$ = 0.1 M, μ = 1.0 M ($NaClO_4$)
397	$Co(NH_3)_5Cl^{2+} + OH^- \rightarrow Co(NH_3)_5OH^{2+} + Cl^-$	H_2O	64	150	8	−5.1 ± 0.2		168	pH = 1 ($HClO_4$)
398	$Co(tacn)(en)Cl^{2+} + OH^- \rightarrow Co(tacn)(en)OH^{2+} + Cl^-$	H_2O	64	150	8	−3.6 ± 0.2		168	pH = 1 ($HClO_4$)
399	$Co(tacn)(tn)Cl^{2+} + OH^- \rightarrow Co(tacn)(tn)OH^{2+} + Cl^-$	H_2O	64	150	8	−4.5 ± 0.8		168	pH = 1 ($HClO_4$)
	trans-$CoCl_2$(RSSR-cyclam)$^+ + OH^- \rightarrow$ *trans*-Co(OH)(RSSR-cyclam)$(Cl)^+ + Cl^-$	H_2O		200				169	
400			10			+17.5 ± 0.3			
401			15			+19.7 ± 0.4			
402			20			+18.3 ± 0.6			
403			25			+17.2 ± 0.5			
404			30			+17.1 ± 0.6			
405			35			+15.9 ± 0.7			
406			40			+15.6 ± 0.8			
407	*trans*(*O*)-Co(taud)Cl + $H_2O \rightarrow$ *trans*(*O*)-Co(taud)$H_2O^+ + Cl^-$	H_2O	25	160	5	−3.2 ± 0.2		170	μ = 1.0 M ($NaClO_4$), pH = 1
408	*trans*(*O*)-Co(taud)Br + $H_2O \rightarrow$ *trans*(*O*)-Co(taud)$H_2O^+ + Br^-$	H_2O	25	160	5	−2.3 ± 0.1		170	μ = 1.0 M ($NaClO_4$), pH = 1
409	*trans*(*O*)-Co(taud)Cl + $OH^- \rightarrow$ *trans*(*O*)-Co(taud)OH + Cl^-	H_2O	25	160	5	+19.1 ± 0.3		170	μ = 1.0 M ($NaClO_4$), pH = 9
410	*trans*(*O*)-Co(taud)Br + $OH^- \rightarrow$ *trans*(*O*)-Co(taud)OH + Br^-	H_2O	25	160	5	+19.7 ± 0.4		170	μ = 1.0 M ($NaClO_4$), pH = 9
411	$Ni(H_2O)_6^{2+}$ + Cl-phen → $Ni(Cl\text{-}phen)(H_2O)_4^{2+} + 2H_2O$	H_2O	25	150	7	+6.0 ± 0.1	+3.9 ± 0.6 (a)	154	
412	$Ni(Cl\text{-}phen)(H_2O)_4^{2+} + 2H_2O \rightarrow Ni(H_2O)_6^{2+}$ + Cl-phen	H_2O	25	150	7	+2.1 ± 0.2		154	
413	$Ni(H_2O)_6^{2+} + OAc^- \rightleftarrows Ni(H_2O)_5(OAc)^+ + H_2O$	H_2O	25	160	9		+8.0 ± 1.5 (b)	171	μ = 0.10 M ($NaClO_4$)
414	$Ni(H_2O)_6^{2+} + gly^- \rightleftarrows Ni(H_2O)_4(gly)^+ + 2H_2O$	H_2O	25	160	9		+11.2 ± 0.2 (b)	171	μ = 0.10 M ($NaClO_4$)
415	$Ni(H_2O)_4(gly)^+ + gly^- \rightleftarrows Ni(H_2O)_2(gly)_2 + 2H_2O$	H_2O	25	160	9		+12.0 ± 0.5 (b)	171	μ = 0.10 M ($NaClO_4$)
416	$Ni(H_2O)_6^{2+} + sar^- \rightleftarrows Ni(H_2O)_4(sar)^+ + 2H_2O$	H_2O	25	160	9		+11.7 ± 0.5 (b)	171	μ = 0.10 M ($NaClO_4$)
417	$Ni(H_2O)_4(sar)^+ + sar^- \rightleftarrows Ni(H_2O)_2(sar)_2 + 2H_2O$	H_2O	25	160	9		+9.9 ± 0.8 (b)	171	μ = 0.10 M ($NaClO_4$)
418	$Ni(H_2O)_6^{2+} + en \rightleftarrows Ni(H_2O)_4(en)^{2+} + 2H_2O$	H_2O	25	160	9		+5.2 ± 0.5 (b)	171	μ = 0.10 M ($NaClO_4$)
419	$Ni(H_2O)_4(en)^{2+} + en \rightleftarrows Ni(H_2O)_2(en)_2^{2+} + 2H_2O$	H_2O	25	160	9		+5.6 ± 0.9 (b)	171	μ = 0.10 M ($NaClO_4$)
420	$Ni(H_2O)_6^{2+} + edda^{2-} \rightleftarrows Ni(H_2O)_2(edda) + 4H_2O$	H_2O	25	160	9		+28.6 ± 0.2 (b)	171	μ = 0.10 M ($NaClO_4$)
421	$Ni(H_2O)_6^{2+} + NH_3 \rightleftarrows Ni(H_2O)_5(NH_3)^{2+} + H_2O$	H_2O	25				−0.1 ± 0.5 (b)	136	μ = 1.0 M ($NaClO_4$)
422	$Ni(CH_3OH)_6^{2+} + isoq \rightleftarrows Ni(CH_3OH)_5(isoq) + CH_3OH$	CH_3OH	25				+3.2 ± 0.1 (b)	136	μ = 1.0 M ($NaClO_4$)
423	$Ni(C_2H_5OH)_6^{2+} + isoq \rightleftarrows Ni(C_2H_5OH)_5(isoq)^{2+} + C_2H_5OH$	C_2H_5OH	25				+1.1 ± 0.1 (b)	136	μ = 1.0 M ($NaClO_4$)
424	$Cu(tren)H_2O^{2+}$ + 4-Clpy → $Cu(tren)4\text{-}Clpy^{2+} + H_2O$	H_2O	25	200	6	−10.0 ± 2.0	−5.3 (a)	80	μ = 1.0 M ($NaClO_4$)
425	$Cu(tren)H_2O^{2+}$ + py → $Cu(tren)py^{2+} + H_2O$	H_2O	25	200	6	−7.1 ± 1.0	+1.6 (a)	80	μ = 1.0 M ($NaClO_4$)
426	$Cu(tren)H_2O^{2+}$ + 4-Mepy → $Cu(tren)(4\text{-}Mepy)^{2+} + H_2O$	H_2O	25	200	8	−8.7 ± 1.1	−1.2 (a)	80	μ = 1.0 M ($NaClO_4$)
427	$Cu(tren)(4\text{-}Clpy)^{2+} + H_2O \rightarrow Cu(tren)H_2O^{2+}$ + 4-Clpy	H_2O	25	200	6	−4.7 ± 1.0		80	μ = 1.0 M ($NaClO_4$)
428	$Cu(tren)py^{2+} + H_2O \rightarrow Cu(tren)H_2O^{2+}$ + py	H_2O	25	200	6	−8.7 ± 1.0		80	μ = 1.0 M ($NaClO_4$)
429	$Cu(tren)(4\text{-}Mepy)^{2+} + H_2O \rightarrow Cu(tren)H_2O^{2+}$ +4-Mepy	H_2O	25	200	8	−7.5 ± 1.2		80	μ = 1.0 M ($NaClO_4$)
430	$Cu(H_2O)_6^{2+}$ + Cl-phen → $Cu(H_2O)_4(Cl\text{-}phen)^{2+} + 2H_2O$	H_2O	25	200	4	−7.1 ± 0.5	+1.9 ± 0.4 (a)	172	μ = 0.05 M ($NaClO_4$), 5.7 < pH < 5.9
431	$Cu(H_2O)_4(Cl\text{-}phen)^{2+} + 2H_2O \rightarrow Cu(H_2O)_6^{2+}$ + Cl-phen	H_2O	25	200	4	+5.2		172	μ = 0.05 M ($NaClO_4$), 5.7 < pH < 5.9
432	$Cu(H_2O)_6^{2+} + phen \rightarrow Cu(H_2O)_4(phen)^{2+} + 2H_2O$	H_2O	25				+10.0 (b)	173	
433	$Cu(H_2O)_4(phen)^{2+} + phen \rightarrow Cu(H_2O)_2(phen)_2^{2+} + 2H_2O$	H_2O	25				+8.8 (b)	173	
434	$Cu(H_2O)_2(phen)_2^{2+} + phen \rightarrow Cu(phen)_3^{2+} + 2H_2O$	H_2O	25				+1.6 (b)	173	
435	$Zn(H_2O)_6^{2+} + bpy \rightarrow Zn(H_2O)_4(bpy)^{2+} + 2H_2O$	H_2O	25				+11.9 (b)	173	
436	$Zn(H_2O)_4(bpy)^{2+} + bpy \rightarrow Zn(H_2O)_2(bpy)_2^{2+} + 2H_2O$	H_2O	25				+1.1 (b)	173	
437	$Zn(H_2O)_2(bpy)_2^{2+} + bpy \rightarrow Zn(bpy)_3^{2+} + 2H_2O$	H_2O	25				+1.6 (b)	173	
438	$Zn(H_2O)_6^{2+} + phen \rightarrow Zn(H_2O)_4(phen)^{2+} + 2H_2O$	H_2O	25				+19.4 (b)	173	
439	$Zn(H_2O)_4(phen)^{2+} + phen \rightarrow Zn(H_2O)_2(phen)_2^{2+} + 2H_2O$	H_2O	25				+6.0 (b)	173	
440	$Zn(H_2O)_2(phen)_2^{2+} + phen \rightarrow Zn(phen)_3^{2+} + 2H_2O$	H_2O	25				−1.7 (b)	173	
441	$Zn(H_2O)_6^{2+}$ + Cl-phen → $Zn(H_2O)_4(Cl\text{-}phen)^{2+} + 2H_2O$	H_2O	25	200	4	+5.0 ± 0.4	+0.9 (c)	172	μ = 0.05 M ($NaClO_4$), 5.7 < pH < 5.9
442	$Zn(H_2O)_4(Cl\text{-}phen)^{2+} + 2H_2O \rightarrow Zn(H_2O)_6^{2+}$ + Cl-phen	H_2O	25	200	4	+4.1 ± 0.4		172	μ = 0.05 M ($NaClO_4$), 5.7 < pH < 5.9
443	$Zn(H_2O)_6^{2+} + bpy \rightleftarrows Zn(H_2O)_4(bpy)^{2+} + 2H_2O$	H_2O	0	200	6−9	+7.1 ± 0.4	+3.5 ± 0.4 (a)	174	μ = 0.01 M ($NaClO_4$)
444	$Mo(CO)_5(4\text{-}CNpy) + bpy \rightarrow Mo(CO)_4bpy + CO$ + 4-CNpy	$C_6H_5CH_3$	25	100	4	+3		175	
445	$Mo(H_2O)_6^{3+} + NCS^- \rightleftarrows Mo(H_2O)_5(NCS)^{2+} + H_2O$	triflic acid	12	140	8	−11.4 ± 0.5		176	$[H^+]$ = 1.0 M, μ = 1.0 M (lithium triflate)
	$Mo(DTH)(CO)_4 + 2\ L \rightarrow Mo(CO)_4L_2$ + DTH	DCE		100	5			124	
446	L = $P(OMe)_3$		40.0			−11.3 ± 0.5			
447	L = $P(OPr^i)_3$		50.0			−10.2 ± 0.8			
448	L = $P(OPh)_3$		40.0			−9.3 ± 0.4			
449	$Mo(dto)(CO)_4 + 2\ P(OPr^i)_3 \rightarrow Mo(CO)_4(P(OPr^i)_3)_2$ + dto	DCE	46	150	4	−9.4 ± 0.2		124	
450	$Mo(BTE)(CO)_4 + 2\ P(OPr^i)_3 \rightarrow Mo(CO)_4(P(OPr^i)_3)_2$ + BTE	DCE	56	150	4	+3.9 ± 0.3		124	
	$Ru(medtra)(H_2O/OH^-) + SC(NH_2)_2 \rightarrow Ru(medtra)SC(NH_2)_2 + H_2O/OH^-$	H_2O	25	100	5			177	μ = 0.2 M (Na_2SO_4)
451						−6.1 ± 0.7			pH = 2.5
452						−8.9 ± 1.1			pH = 8

Table 1. (Continued)

no.	reaction	solvent	T, °C	P, MPa	no. of data	$\Delta V^{\ddagger}$, $cm^3\ mol^{-1}$	$\Delta\bar{V}$, $cm^3\ mol^{-1}$ (method)	ref(s)	remarks
	Ligand Substitution Reactions (Continued)								
453						-9.7 ± 1.2			pH = 9
	$Ru(medtra)(H_2O/OH^-) + SCN^- \rightarrow Ru(medtra)SCN^- + H_2O/OH^-$	H_2O	25	100	5			177	$\mu = 0.2$ M (Na_2SO_4)
454						-7.7 ± 0.5			pH = 2.5
455						-15.4 ± 1.5			pH = 8
456						-15.1 ± 1.5			pH = 9
	trans-$Ru(NH_3)_4(P(OEt)_3)(H_2O)^{2+} + L \rightarrow$ *trans*-$Ru(NH_3)_4(P(OEt)_3)(L)^{2+} + H_2O$	H_2O	25	100				178	
457	L = imidazole					$+4.2 \pm 0.2$			pH = 8.6
458	L = isonicotinamide					$+1.9 \pm 0.3$	-5.6 ± 0.8 (b)		pH = 5.3
459	L = pyrazine					$+2.0 \pm 0.3$	-8.4 ± 0.6 (b)		pH = 5.0
	$Ru(edta)(H_2O)^- + L^{n-} \rightarrow Ru(edta)(L)^{(1+n)-} + H_2O$	H_2O	25	100	6			179	$\mu = 0.2$ M (Na_2SO_4)
460	$L = (NH_2)_2CS$					-6.8 ± 0.6			pH = 5
461	$L = (NHMe)_2CS$					-8.8 ± 0.2			pH = 5
462	$L = (NMe_2)_2CS$					-12.2 ± 0.5			pH = 5
463	$L = N_3^-$					-9.0 ± 0.6			pH = 5
464						-9.9 ± 0.5			pH = 6
465	$L = SCN^-$					-9.6 ± 0.3			pH = 5
	$Ru(hedta)(H_2O)^- + L^{n-} \rightarrow Ru(hedta)(L)^{(1+n)-} + H_2O$	H_2O	25	100	5			180	$\mu = 0.2$ M (Na_2SO_4)
466	$L = SCN^-$					-7.3 ± 0.6			pH = 3
467						-10.8 ± 0.7			pH = 8.3
468	$L = N_3^-$					-14.2 ± 1.2			pH = 8.3
469	$L = (NH_2)_2CS$					-4.1 ± 0.7			pH = 3
470						-7.1 ± 0.5			pH = 8.3
471	$L = (NHMe)_2CS$					-6.2 ± 0.5			pH = 3
472	$L = (NMe_2)_2CS$					-10.4 ± 1.0			pH = 3
473	$HRu_3(CO)_{11}^- + PPh_3 \rightarrow HRu_3(CO)_{10}(PPh_3)^-$	THF	25	100	5	$+21.2 \pm 1.4$		181	
474	$Ru_3(CO)_{11}(CO_2CH_3)^- + P(OMe)_3 \rightarrow Ru_3(CO)_{10}(CO_2CH_3)P(OMe)_3^- + CO$	90% THF, 10% MeOH	25	100	4	$+16 \pm 2$		181	
475	$Ru_3(CO)_{10}(CO_2CH_3)P(OMe)_3^- + P(OMe)_3 \rightarrow Ru_3(CO)_{10}(P(OMe)_3)_2 + CH_3O^- + CO$	90% THF, 10% MeOH	25	100	5	$+24.5 \pm 2.0$		181	
476	$Ru_3(CO)_{11}(CO_2CH_3)^- + P(OMe)_3 \rightarrow Ru(CO)_{10}(CO_2CH_3)P(OMe)_3^- + CO$	10% THF, 90% MeOH	25	100	5	$+2.5 \pm 2.5$		181	
477	*trans*-$Rh(tacpa)Cl^{2+} + OH^- \rightarrow$ products	H_2O	25	140		$+19.5 \pm 1.2$		117	
478	$Rh^{III}(NH_3)_5(H_2O) + CO_3^{2-} \rightarrow Rh^{III}(NH_3)_5(OCO_2) + H_2O$	H_2O	50	150	4	-1.8 ± 0.6		182	$\mu = 1.0$ M, pH = 12
479	$Rh^{III}(NH_3)_5(OCO_2) + H_2O \rightarrow Rh^{III}(NH_3)_5(H_2O) + CO_3^{2-}$	H_2O	50	150	4	-2.4 ± 0.5		182	$\mu = 1.0$ M, pH = 12
	$Rh(NH_3)_5(OSO_2CF_3)^{2+} + S \rightarrow Rh(NH_3)_5(S)^{3+} + CF_3OSO_2^-$			150	4			125	S = solvent
480		CH_3CN	35			-7.8 ± 0.5			
481		MeOH	25			-6.6 ± 0.1			
482	$Rh(NH_3)_5Me_2SO^{3+} + H_2O \rightarrow Rh(NH_3)_5H_2O^{3+} + Me_2SO$	H_2O	25			$+1.5 \pm 1.2$		120b	
483	$Rh(NH_3)_5HCONMe_2^{3+} + H_2O \rightarrow Rh(NH_3)_5H_2O^{3+} + HCONMe_2$	H_2O	25			-2.9 ± 0.3		120b	
484	$Rh(MeNH_2)_5Me_2SO^{3+} + H_2O \rightarrow Rh(MeNH_2)_5H_2O^{3+} + Me_2SO$	H_2O	25			$+1.5 \pm 0.6$		120b	
485	$Rh(MeNH_2)_5HCONMe_2^{3+} + H_2O \rightarrow Rh(MeNH_2)_5H_2O^{3+} + HCONMe_2$	H_2O	25			$+1.7 \pm 0.4$		120b	
486	*trans*-$Rh(Hdmg)_2(CH_3)H_2O + I^- \rightarrow$ *trans*-$Rh(Hdmg)_2(CH_3)I^- + H_2O$	H_2O	9	150	4	$+2.1 \pm 0.4$		183	$\mu = 1.0$ M ($NaClO_4$)
487	*trans*-$Rh(Hdmg)_2(CH_3)H_2O + py \rightarrow$ *trans*-$Rh(Hdmg)_2(CH_3)py + H_2O$	H_2O	20	150	4	$+7.16 \pm 0.01$		183	$\mu = 1.0$ M ($NaClO_4$)
488	*trans*-$Rh(Hdmg)_2(CH_3)H_2O + TMTU \rightarrow$ *trans*-$Rh(Hdmg)_2(CH_3)TMTU + H_2O$	H_2O	20	150	4	$+4.30 \pm 0.04$		183	$\mu = 1.0$ M ($NaClO_4$)
489	*trans*-$Rh(Hdmg)_2(CH_3)I + H_2O \rightarrow$ *trans*-$Rh(Hdmg)_2(CH_3)H_2O + I^-$	H_2O	9	150	4	$+6.3 \pm 0.3$		183	$\mu = 1.0$ M ($NaClO_4$)
490	$Rh(acac)(cod) + phen \rightarrow Rh(cod)(phen)^+ + acac^-$	MeOH	25	100	5	-6.9 ± 0.2		176	
491	$Rh(tfac)(cod) + phen \rightarrow Rh(cod)(phen)^+ + tfac^-$	MeOH	25	100	5	-6.0 ± 0.1		176	
492	$Rh(TPPS)(H_2O)_2^{3-} + TU \rightarrow Rh(TPPS)(H_2O)(TU)^{3-} + H_2O$	H_2O	22	140	4	-11.1 ± 0.5		167	$[H^+] = 0.1$ M, $\mu = 1.0$ M ($NaNO_3$)
493	$(\eta^5\text{-}C_5H_5)Rh(CO)_2 + PPh_3 \rightarrow$ products	$C_6H_5CH_3$	40	150	4	-14.4 ± 1.5		184	
494	$(\eta^5\text{-}C_5H_5)Rh(CO)_2 + P(n\text{-}Bu)_3 \rightarrow$ products	$C_6H_5CH_3$	40	150	4	-17.0 ± 0.7		184	
	$Pd(pp_3)X^+ + P(OCH_3)_3 \rightarrow Pd(pp_3)(P(OCH_3)_3)^{2+} + X^-$	CH_3Cl	30					185	
495	$X^- = Cl^-$					-25.5 ± 0.5			
496	$X^- = Br^-$					-24.5 ± 0.7			
497	$X^- = I^-$					-22.6 ± 0.8			
498	$Pd(H_2O)_4^{2+} + Me_2S \rightarrow PdMe_2S(H_2O)_3^{2+} + H_2O$	H_2O	25	200	9	-4.0 ± 0.2		186	$\mu = 1.0$ M ($HClO_4$)
499	$Pd(H_2O)_4^{2+} + Et_2S \rightarrow PdEt_2S(H_2O)_3^{2+} + H_2O$	H_2O	25	200	9	-8.7 ± 0.1		186	$\mu = 1.0$ M ($HClO_4$)
500	$Pd(H_2O)_4^{2+} + S(CH_2)_4O \rightarrow Pd\,S(CH_2)_4O(H_2O)_3^{2+} + H_2O$	H_2O	25	200	9	-6.6 ± 0.2		186	$\mu = 1.0$ M ($HClO_4$)
501	$Pd(H_2O)_4^{2+} + S(CH_2)_4S \rightarrow Pd\,S(CH_2)_4S(H_2O)_3^{2+} + H_2O$	H_2O	25	200	9	-10.1 ± 0.3		186	$\mu = 1.0$ M ($HClO_4$)
	$Pd(H_2O)_4^{2+} + L \rightarrow Pd(H_2O)_3L^{2+} + H_2O$	H_2O	25	200				187	$[HClO_4] = 1.0$ M
502	$L = S(CH_2CH_2COOH)_2$					-7.6 ± 0.3			
503	$L = EtSCH_2COOH$					-7.9 ± 0.5			
504	$L = S(CH_2COOH)_2$	H_2O				-8.1 ± 0.4			
505	$Pd(met)Ino(H_2O)^{2+} + Ino \rightarrow Pd(met)(Ino)_2^{2+} + H_2O$	H_2O	25	130	6	-15 ± 3	-1 ± 3 (a)	188	$\mu = 0.5$ M, pH = 4.0
506	$Pd(met)IMP(H_2O)^{2+} + IMP \rightarrow Pd(met)(IMP)_2^{2+} + H_2O$	H_2O	25	130	6		-9 ± 2 (a)	188	$\mu = 0.5$ M, pH = 4.0
507	$Pd(met)(Cl)Ino^+ + H_2O \rightarrow Pd(met)(Ino)(H_2O)^{2+} + Cl^-$	H_2O	25	130	6	-1 ± 4		188	$\mu = 0.5$ M, pH = 4.0
508	$Pd(met)(Ino)(H_2O)^{2+} + Cl^- \rightarrow Pd(met)(Cl)Ino^+ + H_2O$	H_2O	25	130	6	$+1 \pm 2$		188	$\mu = 0.5$ M, pH = 4.0
	$Pd(R_4en)(H_2O)_2^{2+} + Nu \rightarrow Pd(R_4en)(H_2O)(Nu)^{2+} + H_2O$	H_2O	25	100	5				
509	R = H, Nu = adenosine					-9.6 to -7.1			pH = 4.1
510	R = H, Nu = adenosine					-6.74 ± 0.01			pH = 2.9
511	R = H, Nu = inosine					-9.7 ± 1.5			

Table 1. (Continued)

no.	reaction	solvent	T, °C	P, MPa	no. of data	$\Delta V^{\ddagger}$, cm^3 mol^{-1}	$\Delta \bar{V}$, cm^3 mol^{-1} (method)	ref(s)	remarks
	Ligand Substitution Reactions (Continued)								
512	R = Et, Nu = adenosine					−10.6 ± 0.8			
513	R = Et, Nu = inosine					−6.1 ± 0.1			
514	$Pd(Et_4en)(H_2O)(adenosine)^{2+} + H_2O \rightarrow Pd(Et_4en)(H_2O)_2^{2+} + adenosine$	H_2O	25	100	5	−6.3 ± 2.5		189	
515	$Pd(Et_4en)(H_2O)_2^{2+} + inosine \rightarrow Pd(Et_4en)(H_2O)(inosine)^{2+} + H_2O$	H_2O	25	100	5	−4.3 ± 0.6		189	
516	$Pd(H_2O)_4^{2+} + MeCN \rightleftarrows Pd(H_2O)_3(MeCN)^{2+} + H_2O$	H_2O	5	200	4−7	−4.0 ± 0.8	−2.5 ± 0.4 (a)	189	1.00 M $HClO_4$
517	$Pd(H_2O)_3(MeCN)^{2+} + H_2O \rightleftarrows Pd(H_2O)_4^{2+} + MeCN$	H_2O	5	200	4−7	−1.5 ± 0.5		190	1.00 M $HClO_4$
	$Pd(R_5dien)H_2O^{2+} + L \rightarrow Pd(R_5dien)L^{2+} + H_2O$	H_2O		100				93	pH < 5, μ = 0.1 M ($NaClO_4$)
	R = Me								
518	L = $SC(NH_2)_2$		15		5	−9.3 ± 0.4			
519	L = $SC(NHMe)_2$		25		5	−9.1 ± 0.6			
520	L = $SC(NMe_2)_2$		25		5	−13.4 ± 0.7			
	R = Et								
521	L = $SC(NH_2)_2$		15		6	−8.3 ± 0.3			
522	L = $SC(NHMe)_2$		25		6	−10.2 ± 0.6			
523	L = $SC(NMe_2)_2$		25		6	−12.7 ± 0.6			
	$Pd(H_2O)_4^{2+} + RCOOH \rightarrow Pd(H_2O)_3OOCR^+ + H^+$	H_2O	25	150	7			191	μ = 1.0 M ($HClO_4$)
524	R = CH_3					−8.1 ± 0.3			
525	R = CH_3CH_2					−8.9 ± 0.8			
526	R = $HOCH_2$					−3.4 ± 0.2			
	$Pd(H_2O)_3OOCR^+ + H^+ \rightarrow Pd(H_2O)_4^{2+} + RCOOH$	H_2O	25	150	7			191	μ = 1.0 M ($HClO_4$)
527	R = CH_3					−1.7 ± 0.2			
528	R = CH_3CH_2					−1.7 ± 0.2			
529	R = $HOCH_2$					−2.3 ± 0.2			
530	$Pd(Et_4en)(H_2O)_2^{2+} + d(GpG) \rightarrow Pd(Et_4en)(d(GpG))H_2O^{2+} + H_2O$	H_2O	25	140	4	−3.8 ± 0.2		192	μ = 0.1 M ($HClO_4$)
531	$Pd(Et_4en)(d(GpG))H_2O^{2+} \rightarrow Pd(Et_4en)(d(GpG))^{2+} + H_2O$	H_2O	25	140	4	+1 ± 2		192	μ = 0.1 M ($HClO_4$)
	$Pd(Me_5dien)py^{2+} + S \rightarrow Pd(Me_5dien)S^{2+} + py$							193	
532	(S = solvent)	H_2O	25	150	7	−3.1 ± 0.1			[OH] = 0.01 M
533		MeOH	25	150	7	−6 ± 1			0.1 M ptsa
534		EtOH	25	100	5	−4.1			0.1 M ptsa
535		DMSO	30	80	5	0			0.1 M ptsa
536		DMF	30	100	5	−3.4 ± 0.3			0.1 M ptsa
537		MeCN	30	100	5	−2.4 ± 0.6			0.1 M ptsa
538	$Pd(H_2O)_4^{2+} + DMSO \rightarrow Pd(H_2O)_3(DMSO)^{2+} + H_2O$	H_2O	25	180	9	−9.2 ± 0.6	−7.5 ± 0.3 (a)	194	μ = 1.0 M ($HClO_4$)
	$Pd(dien)(OH_2)^{2+} + L \rightarrow Pd(dien)(L)^{2+} + H_2O$	H_2O	12	100	5			195	μ = 0.1 M ($NaClO_4$)
539	L = adenosine					−2.0 ± 0.4			pH = 5 (NaOH)
540	L = cytidine					+1.5 ± 0.7			5 < pH < 7
541	L = thymidine					−0.6 ± 2.2			5 < pH < 7
542	L = uridine					−0.8 ± 2.2			5 < pH < 7
	$Pd(Et_4dien)(OH_2)^{2+} + HSO_3^-/SO_3^{2-} \rightarrow Pd(Et_4dien)(SO_3) + H_2O$	H_2O	25	100	5			196	μ = 0.5 M
543						−10.4 ± 0.5			pH = 3.3, [total sulfur] = 0.001 M
544						−12.4 ± 0.6			pH = 3.3, [total sulfur] = 0.01 M
545						−11.5 ± 0.4			pH = 5.2, [total sulfur] = 0.001 M
546						−16.6 ± 0.9			pH = 5.2, [total sulfur] = 0.01 M
	$Pd(R_5dien)X^{(2-n)+} + H_2O \rightarrow Pd(R_5dien)H_2O^{2+} + X^{n-}$	H_2O		100	5			197	[OH^-] = 0.01 M, μ = 0.1 M ($NaClO_4$)
	R = Me								
547	X = Br^-		25			−11.4 ± 0.7	−4.1 ± 1.1 (c)		
548	X = I^-		25			−9.7 ± 0.3	+0.2 ± 1.5 (c)		
549	X = N_3^-		25			−11.7 ± 0.7	−1.3 ± 1.0 (c)		
550	X = $C_2O_4^{2-}$		25			−10.4 ± 0.6	−4.5 ± 1.0 (c)		
	R = Et								
551	X = Br^-		34			−11.6 ± 0.5			
552	X = I^-		34			−6.8 ± 0.9	+0.2 ± 1.5 (c)		
553	X = N_3^-		34			−11.3 ± 0.4	−0.3 ± 0.8 (c)		
554	X = $C_2O_4^{2-}$		25			−7.6 ± 0.8	−3.7 ± 1.0 (c)		
555	$Cd(H_2O)_6^{2+} + bpy \rightarrow Cd(H_2O)_4(bpy)^{2+} + 2H_2O$	H_2O	0	200	6	−5.5 ± 1.0	+1.4 (c)	166	μ = 0.01 M ($NaClO_4$)
556	$La(H_2O)_n^{3+} + Hdcp^{2-} \rightarrow La(H_2O)_{n-3}(Hdcp)^+ + 3H_2O$	H_2O	25	200	8	−4.9 ± 0.3	+12.1 ± 1.5 (a)	198	
557	$La(H_2O)_{n-3}(Hdcp)^+ + 3H_2O \rightarrow La(H_2O)_n^{3+} + Hdcp^{2-}$	H_2O	25	200	8	+7		198	
558	$Ce(H_2O)_9^{3+} \rightleftarrows Ce(H_2O)_8^{3+} + H_2O$	H_2O	25	200	6		+10.9 ± 0.3 (a)	199	
559	$Eu(edta)(H_2O)_3 \rightleftarrows Eu(edta)(H_2O)_2 + H_2O$	H_2O	87.5	200	4		+13.2 ± 0.2 (a)	102	pH = 6.5 ($NaClO_4$)
560	$Eu(CyDTA)(H_2O)_3 \rightleftarrows Eu(CyDTA)(H_2O)_2 + H_2O$	H_2O	115	200	4		+3.0 ± 0.3 (a)	102	pH = 6.0 ($NaClO_4$)
	$Eu^{III}(ar)_2(H_2O) + H^+ + dtpa \rightarrow Eu^{III}(ar)dtpa(H_2O) + Har$	H_2O	25	100	5			200	pH = 4.8
561	fast step					−19.3 ± 0.4			
562	slow step					−1.0 ± 1.4			
563	$Gd^{III}(ar)(H_2O)_x + dtpa^{5-} + H^+ \rightarrow Gd^{III}(dtpa)(H_2O)^{2-} + Har$	H_2O	25	100	4	−24.0 ± 1.8		201	μ = 0.3 M, pH = 3.4
564						−13.9 ± 0.8			μ = 0.3 M, pH = 5.7
565	$Gd^{III}(ar)_2(H_2O) + dtpa^{5-} + H^+ \rightarrow Gd^{III}(dtpa)(H_2O)^{2-} + Har + ar$	H_2O	25	100	4	+1.4 ± 2.8		201	μ = 0.3 M, pH = 3.4
566						+69.6 ± 3.7			μ = 0.3 M, pH = 5.7
567	*cis*-$(C_6H_5Cl)(PPh_3)W(CO)_4 + pip \rightarrow$ *cis*-$(pip)(PPh_3)W(CO)_4 + C_6H_5Cl$	C_6H_5Cl	24.5	150	4	−11.3 ± 0.4		124	
568	*cis*-$W(CO)_4(4\text{-Mepy})_2 + phen \rightarrow$ *cis*-$W(CO)_4(phen) + 2(4\text{-Mepy})$	$C_6H_5CH_3$	25	70	2	+8		202	
569	$CH_3ReO_3 + OH^- \rightarrow CH_4 + ReO_4^-$	H_2O	25	200	2	−2.4 ± 0.4		203	
	$PtMe_4(phen) + HA \rightarrow PtMe_3(A)(phen) + CH_4$		25	150	4			204	

Table 1. (Continued)

no.	reaction	solvent	T, °C	P, MPa	no. of data	$\Delta V^{\ddagger}$, cm^3 mol^{-1}	$\Delta \bar{V}$, cm^3 mol^{-1} (method)	ref(s)	remarks
	Ligand Substitution Reactions (Continued)								
570	HA = salicylic acid	H_2O				-8.5 ± 0.5			
571	HA = formic acid	H_2O				-6.6 ± 1.0			
572	HA = benzoic acid	MeOH				-8.2 ± 0.3			
573	HA = benzoic acid	H_2O				-15.1 ± 1.6			
574	HA= acetic acid	H_2O				-10.5 ± 0.5			
	$PtMe_4(bpy) + HA \rightarrow PtMe_3(A)(bpy) + CH_4$		25	150	4			204	
575	HA = formic acid					-12.2 ± 0.4			
576	HA = acetic acid	H_2O				-11.6 ± 1.0			
577	$Pt(H_2O)_4^{2+} + Me_2S \rightarrow PtMe_2S(H_2O)_3^{2+} + H_2O$	H_2O	25	200	8	-15.3 ± 0.4		186	$\mu = 0.01$ M ($HClO_4$)
578	$Pt(H_2O)_4^{2+} + Et_2S \rightarrow PtEt_2S(H_2O)_3^{2+} + H_2O$	H_2O	25	200	8	-17.0 ± 0.3		186	$\mu = 0.01$ M ($HClO_4$)
579	$Pt(H_2O)_4^{2+} + S(CH_2)_4O \rightarrow PtS(CH_2)_4O(H_2O)_3^{2+} + H_2O$	H_2O	25	200	8	-13.9 ± 0.3		186	$\mu = 0.01$ M ($HClO_4$)
580	$Pt(H_2O)_4^{2+} + S(CH_2)_4S \rightarrow PtS(CH_2)_4S(H_2O)_3^{2+} + H_2O$	H_2O	25	200	8	-20.1 ± 0.2		186	$\mu = 0.01$ M ($HClO_4$)
581	*rac*-$Pt(R_1\text{-en})Cl_2 + H_2O \rightarrow$ *rac*-$Pt(R_1\text{-en})(H_2O)Cl^+ + Cl^-$	H_2O	38	200	5	-9.4 ± 0.7	-5.3 ± 1.1 (a)	205	
582	*rac*-$Pt(R_1\text{-en})(H_2O)Cl^+ + Cl^- \rightarrow$ *rac*-$Pt(R_1\text{-en})Cl_2 + H_2O$	H_2O	38	200	5	-4.0 ± 0.4		205	
583	*rac*-$Pt(R_1\text{-en})(H_2O)Cl^+ + H_2O \rightarrow$ *rac*-$Pt(R_1\text{-en})(H_2O)_2^{2+} + Cl^-$	H_2O	6	200	5	-6.6 ± 1.7	-2.2 ± 2.0 (a)	205	
584	*rac*-$Pt(R_1\text{-en})(H_2O)_2^{2+} + Cl^- \rightarrow$ *rac*-$Pt(R_1\text{-en})(H_2O)Cl^+ + H_2O$	H_2O	6	200	5	-4.4 ± 0.5		205	
585	*cis*-$Pt(NH_3)_2(1\text{-MeU})H_2O^+ + I^- \rightarrow$ *cis*-$Pt(NH_3)_2(1\text{-MeU})I + H_2O$	H_2O	15	100	5	-7.7 ± 0.1		206	
586	*cis*-$Pt(NH_3)_2(1\text{-MeU})_2 + I^- \rightarrow$ *cis*-$Pt(NH_3)_2(1\text{-MeU})I + 1\text{-MeUH}$	H_2O	60	100	5	-5.6 ± 0.6		206	
587	$Pt(CN)_4ClOH^{2-} + HSO_3^- \rightleftarrows (O_2SO)Pt(CN)_4Cl^{3-} + H_2O$	H_2O	25	150	9	-9.4 ± 0.4		207	$\mu = 1.0$ M, $[H^+] = 0.03$ M
588	$Pt(N\text{-}C\text{-}N)H_2O^+ + tmtu \rightarrow Pt(N\text{-}C\text{-}N)tmtu^+ + H_2O$	H_2O	25	125		-12.0 ± 0.5		208a	5−10% DMF
589	$Pt(N\text{-}C)(py\text{-}SO_3)H_2O + tmtu \rightarrow Pt(N\text{-}C)(py\text{-}SO_3)tmtu + H_2O$	H_2O	25	150		-10.5 ± 0.1		208b	
590	$Pt(N\text{-}C)(py\text{-}SO_3)H_2O + N_3^- \rightarrow Pt(N\text{-}C)(py\text{-}SO_3)N_3^- + H_2O$	H_2O	10	150		-10.1 ± 0.6		208b	
591	$Pt(N\text{-}C)(py\text{-}SO_3)N_3^- + H_2O \rightarrow Pt(N\text{-}C)(pySO_3)H_2O + N_3^-$	H_2O	10	150		-12.4 ± 0.9		208b	
	$CrCl(L)^{2+} + Hg^{2+} \rightarrow Cr(L)^{3+} + HgCl^+$	H_2O	25	150	5			209	
592	L = *mer*-(tn)(dpt)					$+0.3 \pm 0.3$			
593	L = *mer*-(Me_2tn)(dpt)					-0.5 ± 0.1			
594	L = *mer*-(tn)(Medpt)					$+1.8 \pm 0.2$			
595	L = *mer*-(en)(dpt)					-5.0 ± 0.2			
596	L = *mer*-(ibn)(dpt)					-0.03 ± 0.07			
597	L = *mer*-(en)(2,3-tri)					-5.7 ± 0.2			
598	L = *mer*-(en)(Medpt)					-0.8 ± 0.6			
	Photoinduced Thermal Substitution Reactions								
599	$Cr(CO)_5(en) \rightarrow Cr(CO)_4(en) + CO$	$C_6H_5CH_3$	50	150	4	-11.9 ± 1.5		210	
600	$Cr(CO)_5(R_2dab) \rightarrow Cr(CO)_4(R_2dab) + CO$	$C_6H_5CH_3$	30	150	4	$+17.2 \pm 1.0$		210	
601	$(\eta^1\text{-phen})Cr(CO)_5 \rightarrow (\eta^2\text{-phen})Cr(CO)_4 + CO$	C_6H_5F	25	150	5	$+6.2 \pm 0.5$		211	
	$Cr(CO)_5(S) + L \rightarrow Cr(CO)_5L + S$		25	100	5			212	
602	L = 1-hexene	S = *n*-heptane				$+6.2 \pm 0.2$			
603	L = piperidine					$+1.4 \pm 0.4$			
604	L = 2-picoline					-1.4 ± 0.3			
605	L = pyridine					-1.4 ± 0.5			
606	L = 1-hexene	S = C_6H_5F				$+9.4 \pm 0.7$			
607	L = piperidine					$+6.1 \pm 0.3$			
608	L = pyridine					$+8.2 \pm 0.2$			
609	L = 1-hexene	S = C_6H_5Cl				$+5.4 \pm 0.4$			
610	L = piperidine					$+0.2 \pm 0.2$			
611	L = 2-picoline					$+3.1 \pm 0.6$			
612	L = 1-hexene	S = C_6H_6				$+10.9 \pm 1.0$			
613	L = piperidine					$+4.2 \pm 0.3$			
614	L = 1-hexene	S = $C_6H_5CH_3$				$+10.8 \pm 0.7$			
615	L = piperidine					$+4.8 \pm 1.4$			
	$Mo(CO)_5(S) + L \rightarrow Mo(CO)_5L + S$		25	100	5			212	
616	L = 1-hexene	S = *n*-heptane				$+2.2 \pm 0.3$			
617	L = 1-hexene	S = C_6H_5F				$+5.8 \pm 0.8$			
618	L = pyridine					$+6.3 \pm 0.1$			
619	L = 1-hexene	S = C_6H_5Cl				$+3.2 \pm 0.3$			
620		S = $C_6H_5CH_3$				$+2.7 \pm 0.4$		213	
621	$Mo(CO)_5bpy \rightarrow Mo(CO)_4bpy + CO$	$C_6H_5CH_3$	26	150	5	-3.9 ± 0.6		213	
622	$Mo(CO)_5dmbpy \rightarrow Mo(CO)_4dmbpy + CO$	$C_6H_5CH_3$	26	150	5	-5.6 ± 0.4		213	
623	$Mo(CO)_5dpbpy \rightarrow Mo(CO)_4dpbpy + CO$	$C_6H_5CH_3$	26	150	4	-5.4 ± 0.5		210	
624	$Mo(CO)_5en \rightarrow Mo(CO)_4en + CO$	$C_6H_5CH_3$	40	150	4	-5.4 ± 0.8		210	
625	$Mo(CO)_5(R_2dab) \rightarrow Mo(CO)_4(R_2dab) + CO$	$C_6H_5CH_3$	25	150	5	-9.5 ± 0.5		211	
626	$(\eta^1\text{-phen})Mo(CO)_5 \rightarrow (\eta^2\text{-phen})Mo(CO)_4 + CO$	C_6H_5F	25	150	5	-2.9 ± 0.2			
	$Mo(OC)_5L\text{-}L \rightarrow Mo(OC)_4L\text{-}L + CO$		25	150	5			214	
627	L-L = phen	$C_6H_5CH_3$				-1.6 ± 0.1			
628	L-L = phen	C_6H_5Cl				-11.0 ± 1.6			
629	L-L = phen	THF				-18.2 ± 2.2			
630	L-L = dpp	C_6H_5Me				$+4.9 \pm 0.4$			
631	L-L = dmp	C_6H_5Me				$+9.5 \pm 0.6$			
632	L-L = 5-NO_2phen	C_6H_5Me				$+10.3 \pm 1.2$			
633	L-L = Cl-phen	C_6H_5Me				-1.2 ± 0.1			
	$Mo(OC)_5L\text{-}L \rightarrow Mo(OC)_4L\text{-}L + CO$	$C_6H_5CH_3$	25	150				215	
634	L-L = phen				4	$+0.6 \pm 0.2$			
635	L-L = 2,9-Me_2phen				4	-0.1 ± 0.4			
636	L-L = 4,7-Me_2phen				5	$+1.5 \pm 0.3$			

Table 1. (Continued)

no.	reaction	solvent	T, °C	P, MPa	no. of data	$\Delta V^{\ddagger}$, $cm^3\ mol^{-1}$	$\Delta \bar{V}$, $cm^3\ mol^{-1}$ (method)	ref(s)	remarks
	Photoinduced Thermal Substitution Reactions (Continued)								
637	L-L = 5-Clphen				5	+3.3 ± 0.5			
638	L-L = 3, 4, 7, 8-Me_4phen				5	+2.3 ± 0.4			
	$Mo(OC)_5$L-L → $Mo(OC)_4$L-L + CO							216	
639	L-L = phen	liquid CO_2	10	210	6	+16.2 ± 0.2			
640	L-L = phen		20	210	7	+23 ± 2			
641	L-L = phen		30	210	5	+36 ± 2			
642	L-L = phen	heptane	25	210	>5	−3.0 ± 0.1			
643	L-L = phen	$C_6H_5CH_3$	25	210	>5	−1.6 ± 0.1			
644	L-L = phen	C_6H_5Cl	25	210	>5	−9.8 ± 1.4			
645	$W(CO)_5$en → $W(CO)_4$en + CO	$C_6H_5CH_3$	50	150	4	−12.3 ± 1.4		210	
646	$W(CO)_5(R_2dab)$ → $W(CO)_4(R_2dab)$ + CO	$C_6H_5CH_3$	40	150	4	−13.7 ± 1.3		210	
647	(η^1-phen)$W(CO)_5$ → (η^2-phen)$W(CO)_4$ + CO	C_6H_5F	25	150	5	−8.2 ± 0.2		211	
	$W(OC)_5$L-L → $W(OC)_4$L-L + CO			210	>5			216	
648	L-L = phen	supercritical	35			+181 ± 18			150−250 bar
649	L-L = phen	fluid ethane	40			+36 ± 4			150−250 bar
650	L-L = phen		48			+33 ± 3			150−250 bar
651	L-L = phen		60			+11 ± 1			150−250 bar
652	L-L = phen		35			+6.7 L/mol			50−100 bar (near critical point)
653	L-L = phen		40			+6.2 L/mol			50−100 bar (near critical point)
654	L-L = phen		48			+3.9 L/mol			50−100 bar (near critical point)
655	L-L = phen		60			+3.0 L/mol			50−100 bar (near critical point)
656	L-L = phen	supercritical	35			+7.2 L/mol			50−100 bar (near critical point)
657	L-L = phen	fluid CO_2	42			+3.6 L/mol			50−100 bar (near critical point)
658	L-L = phen		48			+1.4 L/mol			50−100 bar (near critical point)
659	L-L = phen		60			+0.5 L/mol			50−100 bar (near critical point)
660	L-L = phen	heptane	25			−4.0 ± 0.2			
661	L-L = phen	$C_6H_5CH_3$	25			+3.6 ± 0.1			
662	L-L = phen	C_6H_5Cl	25			−5.4 ± 0.2			
663	$W(OC)_5$bpy → $W(OC)_4$bpy + CO	$C_6H_5CH_3$	25	100	5	−10.9 ± 1.1		217	
	$W(CO)_5$(S) + 1-hexene → $W(CO)_5$(1-hexene) + S		25	100	5			212	
664		S = *n*-heptane				+2.7 ± 0.4			
665		S = C_6H_5F				+2.5 ± 0.2			
666		S = C_6H_5Cl				+0.4 ± 0.3			
667	$W(CO)_5$dbubpy → $W(CO)_4$dbubpy + CO	$C_6H_5CH_3$	25	150	4	−4.5 ± 0.2		218	
668	$W(CO)_5$dpbpy → $W(CO)_4$dpbpy + CO	$C_6H_5CH_3$	25	150	4	−6.4 ± 0.6		218	
669	$W(CO)_5$dmbpy → $W(CO)_4$dmbpy + CO	$C_6H_5CH_3$	25	150	4	−8.4 ± 1.0		218	
670	*cis*-(CB)(Ph_2MeP)$W(CO)_4$ + 1-hexene → *cis*-(hexene)(Ph_2MeP)$W(CO)_4$ + CB	CB	35	150	4	+9.7 ± 0.8		219	
	cis-(CB)($PPh_2(CH_2)_nCH{=}CH_2$)$W(CO)_4$ → ring closure	CB	35	150	4			219	
671	*n* = 1					+7.7 ± 0.8			
672	*n* = 2					+5.12 ± 0.01			
673	*n* = 3					+10.7 ± 0.8			
674	*n* = 4					+10.5 ± 0.2			
	Addition Reactions								
675	$Li^+ + B(OH)_4^- \rightleftarrows LiB(OH)_4$	H_2O	25	200	16		+7.8 ± 0.7 (a)	220	μ = 0.1 M
	$B(OH)_3 + H_2O \rightleftarrows H^+ + B(OH)_4^-$	H_2O	25	200	16			221	
676							−28.9 ± 0.3 (a)		μ = 0.1 M (NaCl)
677							−31.8 ± 0.1 (a)		μ = 1.0 M (NaCl)
	$Na^+ + B(OH)_4^- \rightleftarrows NaB(OH)_4$	H_2O	25	200	16			221	
678							+5.9 ± 1.0 (a)		μ = 0.1 M (NaCl)
679							+7.0 ± 0.2 (a)		μ = 1.0 M (NaCl)
680							−17.4 ± 0.7 (a)		μ = 1.0 M (Me_4NCl)
681	$Cr(CO)_5O(C_6H_5)(C_2H_5)$ + C_4H_9N → $Cr(CO)_5O(C_6H_5)(C_2H_5)(C_4H_9N)$	CH_3CN	25	150	5	−16.6 ± 0.4		222	
682	carbene + 3,4-dihydro-2*H*-pyran carbene = $(OC)_5Cr{=}C(OMe)(C_2Me)$	3,4-dihydro-2*H*-pyran	25	100	3	−15.0 ± 0.6		223	
683	$(OC)_5Cr{=}C(OMe)(Ph)$ + Pr_2N-CN → $(OC)_5Cr{=}C(NPr_2)(N{=}C(OMe)(Ph))$	MeCy	28	150	4	−17.3 ± 0.3		224	
684	$(OC)_5Cr{=}C(OMe)(Ph)$ + Et_2N-CC-Me → $(OC)_5Cr{=}C(NEt_2)(C(Me){=}C(OMe)(Ph))$	octane	30	150	5	−20.2 ± 1.4		224	
	$(CO)_5Cr(OEt)C_2(C_6H_5)$ + $(NH_2)C_6H_4(X)$ → $(CO)_5CrC(OEt)HC_2$ $(C_6H_5)NH(C_6H_4)X$	CH_3CN		150	5			225	
685	X = CN			15		−27.9 ± 0.6			
686	X = CH_3CO			44		−26.6 ± 0.5			
687	X = Cl			34		−24.5 ± 0.4			
688	X = F			15		−24.6 ± 0.9			
689	X = H			15		−22.2 ± 0.8			
690	X = CH_3			15		−21.1 ± 1.0			
691	X = CH_3O			15		−21.1 ± 1.0			
	β-elimination of $(H_2O)_5Cr^{III}$-$CH_2CH_2OH^{2+}$	H_2O	20	150				226	
692						−4.1 ± 0.2			pH = 2.58
693						−5.4 ± 0.3			pH = 3.05
694						−3.6 ± 0.3			pH = 3.53
695						−3.1 ± 1.0			pH = 3.67
696						−5.4 ± 0.4			pH = 4.27
697	$Fe(N_4)^{2+}$ + Im → $Fe(N_4)Im^{2+}$	DMSO	30	90	10	+27.2 ± 1.5		227	μ = 0.2 M ($NaClO_4$)
698	$Fe(N_4)Im^{2+}$ + Im → $Fe(N_4)(Im)_2^{2+}$	DMSO	35	100	6	+21.8 ± 0.9		227	μ = 0.2 M ($NaClO_4$)
	$(OC)_3Fe$(1-5-η-$C_6H_7)^+$ + 4-CHOpy → 2a	CH_3CN		150	4			228	
699			14			+5.6 ± 0.4			[4-CHOpy] = 0.01 M
700			14			−2.9 ± 0.1			[4-CHOpy] = 0.05 M

Table 1. (Continued)

no.	reaction	solvent	T, °C	P, MPa	no. of data	$\Delta V^{\ddagger}$, cm^3 mol^{-1}	$\Delta \bar{V}$, cm^3 mol^{-1} (method)	ref(s)	remarks
	Addition Reactions (Continued)								
701	2a → $(OC)_3Fe(1\text{-}5\text{-}\eta\text{-}C_6H_7)^+$ + 4-CHOpy		25			+5.6 ± 0.4			
	$(OC)_3Fe(1\text{-}5\text{-}\eta\text{-}2\text{-}MeOC_6H_6)^+$ + 4-CHOpy → 2b	CH_3CN		150	4			228	
702			14			+5.9 ± 0.3			[4-CHOpy] = 0.02 M
703			14			+1.2 ± 0.1			[4-CHOpy] = 0.04 M
704			14			−2.9 ± 0.3			[4-CHOpy] = 0.08 M
705			14			−3.8 ± 0.2			[4-CHOpy] = 0.10 M
706			25			−9.8 ± 0.9			[4-CHOpy] = variable
707	2b → $(OC)_3Fe(1\text{-}5\text{-}\eta\text{-}2\text{-}MeOC_6H_6)^+$ + 4-CHOpy		25			+18.0 ± 1.9			
	$(OC)_3Fe(1\text{-}5\text{-}\eta\text{-}C_7H_9)^+$ + 4-CHOpy → 2c	CH_3CN	25	150	5				
708						+0.4 ± 1.1			[4-CHOpy] = 0.01 M
709						+0.1 ± 0.1			[4-CHOpy] = 0.10 M
710	2c → $(OC)_3Fe(1\text{-}5\text{-}\eta\text{-}C_7H_9)^+$ + 4-CHOpy					≈0			
711	$(OC)_3Fe(\eta^5\text{-}2\text{-}MeOC_6H_6)^+$ + Et-py → 3b	CH_3CN	15	150	5	−7.8 ± 0.2		229	
712	$(OC)_3Fe(\eta^5\text{-}2\text{-}C_7H_9)^+$ + Et-py → 3c	CH_3CN	25	150	5	−6.4 ± 0.2		229	
	PFeL + L → $PFeL_2$	DMF	20	180	4			230	
713	L = CN^-					−11.4 ± 2.3			
714	L = imidazole					−7.6 ± 1.3			
	$Co(hfac)L^{n+} + OH^- \rightleftarrows Co(hfac)LOH^{(n-1)+}$	H_2O						231	
715	L = $(en)_2$						+10.3 ± 0.2 (a)		
716	L = tren						+10.5 ± 0.2 (a)		
717	L = β-2,3,2-tet						+13.1 ± 0.2 (a)		
718	L = β-3,2,3-tet						+14.4 ± 0.2 (a)		
719	L = cyclen						+12.8 ± 0.2 (a)		
720	L = cyclam						+15.7 ± 0.2 (a)		
721	L = mer(N)-(gly)(en)						+2.7 ± 0.2 (a)		
722	L = mer(N)-i-dtma						+4.2 ± 0.2 (a)		
723	L = *cis*(O)-aeida						−1.8 ± 0.2 (a)		
724	L = trans(O)-aeida						−8.7 ± 0.2 (a)		
		MeOH							
725	L = $(en)_2$						+20.6 ± 0.3 (a)		
726	L = tren						+18.8 ± 0.2 (a)		
727	L = β-2,3,2-tet						+24.4 ± 0.2 (a)		
728	L = β-3,2,3-tet						+29.4 ± 0.4 (a)		
729	L = cyclen						+18.8 ± 0.2 (a)		
730	L = cyclam						+20.6 ± 0.2 (a)		
731	L = mer(N)-(gly)(en)						+10.3 ± 0.2 (a)		
732	L = mer(N)-i-dtma						+8.7 ± 0.2 (a)		
733	L = *cis*(O)-aeida						+0.1 ± 0.4 (a)		
734	L = trans(O)-aeida						−13.3 ± 0.4 (a)		
735	L = $(NH_3)_4$						+27.1 ± 0.4 (a)		
736	L = α-trien						+22.9 ± 0.4 (a)		
737	L = β-trien						+19.8 ± 0.2 (a)		
738	L = fac(N)-i-dtma						+4.0 ± 0.4 (a)		
739	L = α-edda						−13.0 ± 0.2 (a)		
740	L = β-edda						−5.0 ± 0.2 (a)		
	$CoX_2(3\text{-Mepy})_2$ + 2(3-Mepy) ⇄ $CoX_2(3\text{-Mepy})_4$	3-Mepy	17	300	7			232	
741	X = Cl^-		18.5	150	4		−18 (a)		
742	X = Br^-		20	300	7		−19 (a)		
	$CoX_2(4\text{-Mepy})_2$ + 2(4-Mepy) ⇄ $CoX_2(4\text{-Mepy})_4$	4-Mepy						233	
743	X = Cl^-						−26 (a)		
744	X = Br^-						−27 (a)		
745	$Co(aben)_4Cl$ + py ⇄ $Co(aben)_4Cl(py)$	py	19	150	5		−21.8 (a)	234	
	R,*S*,*R*,*S*-Ni(tmc)$^{2+}$ + A ⇄ *R*,*S*,*R*,*S*-Ni(tmc)A^{2+}		25	140	8			235	0.03 < μ < 0.04 M (unadjusted)
746		A = CH_3CN					−3.2 ± 0.5 (a)		
747		A = C_6H_5CN					−4.2 ± 0.5 (a)		
748		A = DMF					−0.2 ± 0.5 (a)		
749		A = H_2O					−0.5 ± 0.5 (a)		
750	$Mo(CO)_5O(C_6H_5)(C_2H_5)$ + C_4H_9N → $Mo(CO)_5O(C_6H_5)(C_2H_5)(C_4H_9N)$	CH_3CN	25	150	5	−16.4 ± 0.3		222	
751	[Rh(MPI)]PF_6 + CH_3CN → products	CH_3CN	25	400	8		−4.4 ± 0.5 (a)	236	
	$Rh^I(\beta\text{-diketone})[P(OPh)_3]_2$ + CH_3I → $Rh^{III}(\beta\text{-diketone})[P(OPh)_3]_2(CH_3)(I)$								
752	β-diketone = acac	$(CH_3)_2CO$	25	150	4	−17.3 ± 0.7		176	
753			21	140	7	−18.7 ± 1.0		237	
754	β-diketone = tfac	$(CH_3)_2CO$	25	150	4	−14.5 ± 0.8		176	
755	β-diketone = cupf	$(CH_3)_2CO$	25	150	4	−17.1 ± 0.8		176	
756	β-diketone = TFBA	$(CH_3)_2CO$	21	130	5	−19.3 ± 0.5		237	
757		DCE	21	120	4	−9.1 ± 0.3		237	
758		DCM	21	130	5	−17.7 ± 0.5		237	
759		$CHCl_3$	21	110	5	−22.7 ± 0.4		27	
760	$Rh^I(cupf)[P(OPh)_3](CO)$ + CH_3I → $Rh^{III}(cupf)[P(OPh)_3](CO)(CH_3)(I)$	CH_3OH	25	150	4	−24.9 ± 0.5		176	
	Rh(sacac)$(CO)(PPh_3)$ + CH_3I → products		25	100	5			238	
761		$CHCl_3$				−16.9 ± 1.0			
762		C_6H_5Cl				−13.6 ± 0.3			
763		CH_2Cl_2				−18.3 ± 0.9			
764		ClH_2CCH_2Cl				−13.2 ± 0.5			
765		$(CH_3)_2CO$				−15.2 ± 0.6			
766		CH_3NO_2				−15.2 ± 0.7			
767		CH_3CN				−13.9 ± 0.7			
	Rh(cupf)$(CO)(PPh_3)$ + CH_3I → products								

Table 1. (Continued)

no.	reaction	solvent	T, °C	P, MPa	no. of data	$\Delta V^{\ddagger}$, $cm^3\,mol^{-1}$	$\Delta \bar{V}$, $cm^3\,mol^{-1}$ (method)	ref(s)	remarks
				Addition Reactions (Continued)					
768		$CHCl_3$				-17.3 ± 0.8			
769		CH_2Cl_2				-17.4 ± 0.8			
770		ClH_2CCH_2Cl				-16.1 ± 0.3			
771		$(CH_3)_2CO$				-15.7 ± 0.7			
772		CH_3CN				-25.4 ± 0.7			
773	$Pd(bpy)Me_2 + MeI \rightarrow Pd(bpy)(I)Me_3$	$(CH_3)_2CO$	20	150	5	-11.9 ± 0.6		239	[MeI] = 0.04 M
774	$Pd(bpy)(I)Me_3 \rightarrow C_2H_6 + Pd(bpy)(I)Me$	$(CH_3)_2CO$	20	150	5	$+17.3 \pm 1.4$		239	[NaI] = 0.04 M
	$[Pd(C_6H_3RCH_2NMe_2)X]_2 + 2PhC_2Ph \rightarrow 2(Pd(C_6H_3RCH_2NMe_2)X(PhC_2Ph))$	$CHCl_3$	25	150	4			240	
775	R, X = F, Cl					-18.6 ± 0.9			
776	R, X = H, Cl					-15.0 ± 0.5			
777	R, X = MeO, Cl					-16.2 ± 1.4			
778	R, X = H, Cl					-14.4 ± 1.2			
	$[Pd(C_6H_3RCH_2NMe_2)X]_2 + 2EtC_2Et \rightarrow 2(Pd(C_6H_3RCH_2NMe_2)X(EtC_2Et))$	$CHCl_3$	25	150	4			240	
779	R, X = H, I					$+0.9 \pm 0.7$			
780	$H_2C{=}CHCH_2SnBu^t_3 + Cl_3CCHO \rightarrow Cl_3CCH(OSnBu^t_3)CH_2CH{=}CH_2$	$H_2C{=}CH_2SnBu^t_3$	37.5	80	5	-11.7 ± 0.3		241	
781	$Eu(fod)_3$ + adamantine → products	$CDCl_3$	21	100	6	$+8 \pm 2$		242	
	carbene + 3,4-dihydro-2*H*-pyran	3,4-dihydro-2*H*-pyran	25	100	3			223	
	carbene =								
782	$(OC)_5W{=}C(OMe)(C_2Me)$					-14.9 ± 0.5			
783	$(OC)_5W{=}C(OEt)(C_2Ph)$					-17.8 ± 0.5			
	$(CO)_5WC(OEt)C_2Ph + C_3H_3NNH \rightarrow (CO)_5WC(OEt)CHCPhC_3H_3N_2$	MeCN:$C_6H_5CH_3$ (% vol)	44	100	4			243	
784		100:0				-18.0 ± 1.4			
785		35:65				-19.0 ± 1.2			
786		15:85				-19.7 ± 0.9			
787		0:100				-22.7 ± 0.6			
788	$(OC)_5W{=}C(OMe)(Ph) + Pr_2N\text{-}CN \rightarrow (OC)_5W{=}C(NPr_2)(N{=}C(OMe)(Ph))$	MeCy	60	150	4	-20.7 ± 1.1		224	
789	$(OC)_5W{=}C(OMe)(Ph) + Et_2N\text{-}CC\text{-}Me \rightarrow (OC)_5W{=}C(NEt_2)(C(Me){=}C(OMe)(Ph))$	octane	25	150	5	-24.7 ± 1.0		224	
	$W(CO)_5O(R1)(R2) + C_4H_9N \rightarrow W(CO)_5O(R1)(R2)(C_4H_9N)$		25	150	5			222	
790	R1, R2 = C_6H_5, C_2H_5	CH_3CN				-15.0 ± 0.7			
791	R1, R2 = C_6H_5, C_2H_5	$C_6H_4Cl_2$				-16.5 ± 0.6			
792	R1, R2 = C_6H_5, C_2H_5	C_6H_5Cl				-17.0 ± 0.9			
793	R1, R2 = C_6H_5, C_2H_5	$C_6H_5CH_3$				-18.8 ± 0.8			
794	R1, R2 = C_6H_5, C_2H_5	*n*-heptane				-21.9 ± 0.7			
795	R1, R2 = CH_3, CH_3	CH_3CN				-15.3 ± 0.8			
	$H_2Os_3(CO)_{10} + L \rightarrow H_2Os_3(CO)_{10}L$	C_6H_5Cl	30	180				244	
796	L = etbp					-16.6 ± 2.4			
797	L = $P(OMe)_3$					-13.2 ± 1.6			
798	L = $P(OPh)_3$					-12.8 ± 0.7			
799	L = $P(OPr^i)_3$					-12.7 ± 0.5			
800	L = $P(Bu^n)_3$					-16.1 ± 1.1			
801	L = $PPh_2(OEt)$					-14.9 ± 1.7			
802	L = PPh_3					-20.2 ± 0.2			
803	L = $P(p\text{-}F_3CC_6H_4)_3$					-20.4 ± 0.6			
804	L = $P(p\text{-}FC_6H_4)_3$					-21.0 ± 1.0			
805	L = $P(p\text{-}MeC_6H_4)_3$					-19.3 ± 0.4			
806	L = $P(p\text{-}MeOC_6H_4)_3$					-19.0 ± 0.8			
807	L = $(m\text{-tol})_3$					-16.4 ± 0.7			
808	L = $PBzPh_2$					-20.9 ± 0.8			
809	L = $PCyPh_2$					-26.2 ± 1.0			
810	L = $(NMe_2)_3$					-31.8 ± 0.9			
811	L = PCy_2Ph					-22.9 ± 1.0			
812	L = PBz_3					-20.4 ± 0.7			
813	L = $P(o\text{-tol})_3$					-8.1 ± 1.4			
814	$Me_2Pt(bpy) + MeI \rightarrow Me_3Pt(bpy)^+ + I^-$	$(CH_3)_2CO$	25	200	5	-11.7 ± 0.3		245	
815	$Me_2Pt(bpy) + EtI \rightarrow EtMe_2Pt(bpy)^+ + I^-$	$(CH_3)_2CO$	25	200	5	-9.7 ± 0.7		25	
				Formation and Dissociation Reactions					
816	$HF \rightleftarrows H^+ + F^-$	H_2O	25	200	16		$+3.3 \pm 0.5$ (b)	246	μ = 0.1 M
817	$Na^+(C222) +$ en → products	en	30	200	12	$+8.9 \pm 0.4$		247	
818	$NaF \rightleftarrows Na^+ + F^-$	H_2O	25	200	16		-9.6 ± 0.1 (b)	246	μ = 0.1 M
	$CryNa^+ \rightarrow Cry + Na^+$			200	5−7			248	
819		DMSO	40			$+2.1 \pm 0.7$			
820		DMF	25			$+2.0 \pm 0.2$			
	$CryNa^+ + Hdca \rightarrow CryH^+ + Na^+ + dca^-$		25	200	5−7			248	
821		DMF				-8.0 ± 1.0			
822		MeCN				-16.0 ± 0.8	$+3.3 \pm 0.4$ (b)	248	
823	$Cry + Na^+ \rightarrow CryNa^+$	DMSO	25	200	5−7	$+5.4 \pm 1.1$		248	
824	$Cry + Hdca \rightarrow CryH^+ + dca^-$	DMSO	25	200	5−7	-11.1 ± 2.6		136	μ = 1.06 M (KCl)
825	18-crown-6 + $K^+ \rightarrow K(18\text{-crown-6})^+$	H_2O	25	200	5−7	$+10.9 \pm 0.2$		249	μ = 3.00 M ($NaClO_4/HClO_4$)
	$VO_2^+ + H_2O_2 \rightleftarrows VO(O_2)^+ + H_2O$	H_2O	20	160	8				
826	$[H^+]$-independent path					$+2.8 \pm 1.0$			
827	$1/[H^+]$-dependent path					$+9.9 \pm 1.7$			
828	$[H^+]$-dependent path					$+14.2 \pm 3.2$			

Table 1. (Continued)

no.	reaction	solvent	T, °C	P, MPa	no. of data	$\Delta V^{\ddagger}$, cm^3 mol^{-1}	$\Delta \bar{V}$, cm^3 mol^{-1} (method)	ref(s)	remarks
	Formation and Dissociation Reactions (Continued)								
829	$VO(O_2)_2^+ + H_2O_2 \rightleftarrows VO(O_2)_2^- + 2H^+$	H_2O	20	200	8	0.0 ± 0.2		249	
830	$H^+ + ClO_2^- \rightleftarrows HClO_2$	H_2O	5	150	5		+10.7 ± 1.5 (a)	134	μ = 1.0 M ($NaClO_4$)
831	Cu^{2+} + C221 → $Cu(C221)^{2+}$	DMSO	35	80	8	−1.6 ± 1.5		250	
832	$Cu(C221)^{2+} \rightarrow Cu^{2+}$ + C221	DMSO	39.5	100	6	+1.6 ± 0.5		250	
833	Cu^{2+} + C221 → $Cu(C221)^{2+}$	DMF	25	200	9	−0.4 ± 0.6		250	
834	$(C_6H_4CH_2PdN(CH_3)_2I)_2$ + (2)2,6-Me_2py → 2($C_6H_4CH_2PdN(CH_3)_2$I-2,6-Me_2py)	CH_3Cl	25	100	3	−22.6 ± 2.9		251	
835	$ReMeO_3 + H_2O_2 + Br^- \rightleftarrows ReMeO_2(\eta^2\text{-}O_2)(H_2O) + Br^-$, with $ReMeO_3$	H_2O	20	150	4	−10.6 ± 1.4		252	μ = 2.0 M
836	$H_2O_2 + 2Br^- + 2H^+ \rightarrow Br_2 + 2H_2O$, without $ReMeO_3$	H_2O	20	150	4	−7.5 ± 1.1		252	μ = 2.0 M
837	$(C_6H_3(4\text{-MeO})CH_2PtN(CH_3)_2Cl)_2$ + (2)4-Mepy → 2(C_6H_3(4-MeO)$CH_2PtN(CH_3)_2$Cl-4-Mepy)	CH_3Cl	25	100	5	−14.5 ± 1.3		251	
	Isomerization Reactions								
	$(C221)_1 \rightleftarrows (C221)_2$		25	200				248	
838		Me_2SO					+40 (a)		
839		DMF					+41 (a)		
840		CH_3CN					+43 (a)		
841	*cis*-$TiCl_4$·2TMPA ⇄ *trans*-$TiCl_4$·2TMPA	$CHCl_3$	−30				−1.3 ± 0.8 (a)	253	
842	*cis*-$TiCl_4$·2TMPA ⇄ *trans*-$TiCl_4$·2TMPA	$CHCl_3$	67	230	8	+6.2 ± 1.8		64	
843	$Cr(NH_3)_5(OCHNH_2)^{3+} \rightarrow Cr(NH_3)_5(NHCHO)^{2+} + H^+$	H_2O	25	100	5	−7.6 ± 0.8		121	μ = 1.0 M ($NaClO_4$), [OH^-] = 0.1 M
844	$Cr(NH_3)_5(OC(NH_2)_2^{3+} \rightarrow Cr(NH_3)_5(NHCONH_2)^{2+} + H^+$	H_2O	23.5	100	5	−9.8 ± 0.9		121	μ = 1.0 M ($NaClO_4$), [OH^-] = 0.1 M
845	$Fe(CO)_2$(1,3-cyclooctadiene)(PPh_3), fluxionality	$C_6H_5CH_3$	−73	200	9	+0.5 ± 0.2		254	
846	*trans*-$Co(en)_2(OH_2)(OSeO_2H)^{2+}$ ⇄ *cis*-$Co(en)_2(OH_2)(OSeO_2H)^{2+}$	H_2O	41	140	5	+7.2 ± 0.4		162	pH = 1
	trans-$Co^{III}(en)_2(H_2O)X^{n+} \rightarrow$ *cis*-$Co^{III}(en)_2(H_2O)X^{n+}$	H_2O		200	5−6			255	$HClO_4$ solution
847	X = H_2O		45			+4.9 ± 1.3	−1.0 ± 1.2 (b)		μ = 1.05 M
848	X = OH^-		13			+6.1 ± 0.4	−5.5 ± 0.4 (b)	255	μ = 0.03 M
849	X = NCS^-		63			+7.5 ± 0.3	−0.8 ± 0.0 (b)		μ = 0.03 M
850	X = NH_3		73			+7.4 ± 0.7	+0.4 ± 0.2 (b)		μ = 0.26 M
851	X = NO_2^-		65			+11.4 ± 1.0	+1.5 ± 0.5 (b)		μ = 0.01 M
852	X = Br^-		30			+2.1 ± 0.7	−2.8 ± 0.0 (b)		μ = 0.02 M
853	X = N_3^-		30			+7.5 ± 0.3	−2.3 ± 0.2 (b)		μ = 0.01 M
854	X = OH^-		45			+11.4 ± 0.5	−3.7 ± 0.5 (b)		μ = 0.07 M
855	X = NH_3		45			+18.6 ± 0.6	−1.5 (b)		μ = 0.03 M
	cis-$Co^{III}(en)_2(H_2O)X^{n+} \rightarrow$ *trans*-$Co^{III}(en)_2(H_2O)X^{n+}$	H_2O		200	5−6				$HClO_4$ solution
856	X = H_2O		45			+5.8 ± 1.2			μ = 1.05 M
857	X = OH^-		13			+11.6 ± 0.4			μ = 0.03 M
858	X = NCS^-		63			+8.3 ± 0.3			μ = 0.03 M
859	X = NH_3		73			+7.0 ± 0.9			μ = 0.26 M
860	X = NO_2^-		65			+10.1 ± 1.0			μ = 0.01 M
861	X = Br^-		30			+4.9 ± 0.7			μ = 0.02 M
862	X = N_3^-		30			+9.8 ± 0.3			μ = 0.01 M
863	X = OH^-		45			+15.1 ± 0.5			μ = 0.07 M
864	X = NH_3		45			+19.5 ± 1.1			μ = 0.03 M
865	*trans*-$Co(en)_2(H_2O)_2^{3+} \rightarrow$ *cis*-$Co(en)_2(H_2O)(OH)^{2+} + H^+$	H_2O	19.5	200	5−6		+3.0 ± 0.1 (b)	255	
866	*trans*-$Co(en)_2(H_2O)(OH)^{2+} \rightarrow$ *trans*-$Co(en)_2(OH)_2^{2+} + H^+$	H_2O	19.5	200	5−6		+5.9 ± 0.0 (b)	255	
867	*cis*-$ZrCl_4$·2TMPA → *trans*-$ZrCl_4$·2TMPA	$CHCl_3$	−12.5	150	9	−1.6 ± 0.6		82,83	
868	$(\mu\text{-}H)_3Ru_3(\mu_3\text{-}CCO_2\text{-}Me)(CO)_9 \rightarrow (\mu\text{-}H)_2Ru_3(\mu_3\text{-}\eta^2\text{-}CHCO_2\text{-}Me)(CO)_9$	decane	57	200	5	−0.3 ± 0.7		256	
869	$(\mu\text{-}H)_3Ru_3(\mu_3\text{-}CSEt)(CO)_9 \rightarrow (\mu\text{-}H)Ru_3(\mu_3\text{-}\eta^2\text{-}CH_2SEt)(CO)_9$	decane	57	200	5	+22.0 ± 1.4		256	
870	$HRu_3(\mu_3\text{-}\eta^3\text{-}EtSCCMeCMe)(CO)_9 \rightarrow Ru_3(\mu\text{-}SEt)(\mu_3\text{-}\eta^3\text{-}CCMeCHMe)(CO)_9$	decane	48	210	5	+12.7 ± 1.1		257	
871	*ttt*-$RuCl_2(CO)_2(Ph_2MeP)_2 \rightarrow$ *ccc*-$RuCl_2(CO)_2(Ph_2MeP)_2$	$CHCl_3$	63	140		+19 ± 2		258	
872	*ttt*-$RuCl_2(CO)_2(PhMe_2P)_2 \rightarrow$ *ccc*-$RuCl_2(CO)_2(PhMe_2P)_2$	CB	70	140		−19 ± 2		258	
873	*t*-$RuCl_2(CO)_2(Ph_2MeP)_2 \rightarrow$ *c*-$RuCl_2(CO)_2(Ph_2MeP)_2$	$CHCl_3$	34	140		+15 ± 2		258	
874	*t*-$RuCl_2(CO)_2(PhMe_2P)_2 \rightarrow$ *c*-$RuCl_2(CO)_2(PhMe_2P)_2$	TCE	64	140		+16 ± 2		258	
875	$(\mu\text{-}H)_2Ru_3(\mu_3\text{-}CHCO_2Me)(CO)_9$	$CD_3C_6D_5$	36	200	9	+4.1 ± 0.3		259	
	hydride exchange (bridging, terminal)								
	$C_6H_4XP(p\text{-}XC_6H_4)_2Rh_2(\mu\text{-}O_2CHCH_3)_2(O_2CHCH_3)\text{-}(p\text{-}YC_6H_4)_3PCH_3 \rightarrow (C_6H_4XP(p\text{-}XC_6H_4)_2\text{-}(p\text{-}YC_6H_4)_2)_2(CH_3)_2Rh_2(\mu\text{-}O_2CHCH_3)_2$		25	150	5			260	
	spontaneous process	$C_6H_5CH_3$				−22.7 ± 0.2			
876	X = H, Y = H					−21.5 ± 0.5			
877	X = H, Y = Me					−23.1 ± 1.1			
878	X = Me, Y = H					−21.4 ± 0.7			
879	X = Me, Y = Me								
	acid-assisted process	CH_3COOH				−15.3 ± 0.2			
880	X = H, Y = H					−13.8 ± 0.2			
881	X = H, Y = Me					−14.8 ± 0.2			
882	X = Me, Y = H					−13.7 ± 0.3			
883	X = Me, Y = Me								
	trans-(NZ)$W(CO)_2(F)$ + L → *cis*-(NZ)W(CO)(L)(F)							261	
884	no CO (L = 0)		60	100	5	+15.6 ± 0.4			
885	L = CO		60	100	5	+3.9 ± 0.2			
886	L = $P(OMe)_3$		25	150	4	+15.7 ± 0.6			
887	$H(\mu\text{-}H)Os_3(CO)_{10}(PPh_3)$	CD_2Cl_2	−19.5	200	9	−0.8 ± 0.4		259	
	hydride exchange (bridging, terminal)								

Table 1. (Continued)

no.	reaction	solvent	T, °C	P, MPa	no. of data	$\Delta V^{\ddagger}$, cm^3 mol^{-1}	$\Delta \bar{V}$, cm^3 mol^{-1} (method)	ref(s)	remarks
	Isomerization Reactions (Continued)								
	$Ir_4(CO)_9(SCH_3)_3$		1.3	200	7			262	
888	bridged $\rightleftarrows$ unbridged						+15.4 ± 0.4 (b)		
889	intramolecular CO exchange					+8.3 ± 0.8			
890	$Ir_2Rh_2(CO)_{11}PPh_3$ (fluxional PPh_3 migration)	CD_2Cl	51	180	7	+10.1 ± 1.5		263	
891	$(O_2SO)Pt(CN)_4Cl^{3-} \rightarrow (O_3S)Pt(CN)_4Cl^{3-}$	H_2O	25	150	10	+5.3 ± 0.4		208	μ = 1.0 M, $[H^+]$ = 0.03M
	Electron-Transfer Reactions								
892	V^V + acetoin $\rightleftarrows$ MeCOCOMe + $2V^{IV}$ + $2H^+$					−3.5 ± 0.4		264	
893	V^V + hydroxyacetone $\rightleftarrows$ MeCOCHO + $2V^{IV}$ + $2H^+$					−1.3 ± 0.7		264	
	$Cr(H_2O)_6^{2+}$ + −R → products	H_2O	20	150	5			265	
894	−R = CH_3					+6.3 ± 1.0			
895	−R = CH_2CH_2OH					+4.0 ± 1.0			
896	−R = $CH(CH_3)OH$					+3.5 ± 1.0			
897	−R = $C(CH_3)_2OH$					+5.7 ± 1.0			
898	−R = $CH(CH_3)CH_2OH$					+3.9 ± 1.0			
899	−R = $CH_2C(CH_3)_2OH$					+3.4 ± 1.0			
900	−R = $CH_2C(CH_3)_2NH_2$					+3.6 ± 1.0			
901	−R = $CH(OH)CH_2OH$					+4.8 ± 1.0			
902	−R = $CH(CH_3)OCH_2CH_3$					+4.3 ± 1.0			
903	−R = $CH(CH_3)CH(CH_3)OH$					+3.9 ± 1.0			
	$Cr(H_2O)_6^{2+}$ + H_2O_2 + reactant → products	H_2O	25	200	4			266	μ = 0.5 M, pH = 3
	reactant					+3.5 ± 0.2			
904	0.01 M CF_3COO^-					+5.4 ± 0.5			
905	0.1 M CF_3COO^-					+2.3 ± 0.6			
906	0.01 M CH_3COO^-					−6.0 ± 0.2			
907	0.32 M CH_3COO^-					−1.1 ± 1.3			
908	H_2O								
909	Cr(II) reactants → $Cr(H_2O)_5(CMe_2OH)^{2+}$	H_2O	25	150	4		−38 ± 3 (a)	267	μ = 0.5 M, pH = 5.3
910			20			+5.7			pH = 4.1, $[MeCO_2]$ = 0
911			20			+6.0			pH = 5.2, $[MeCO_2]$ = 0.009 M
912			20			−3.9			pH = 5.2, $[MeCO_2]$ = 0.050 M
913			20			−7.4			pH = 5.2, $[MeCO_2]$ = 0.27 M
914	$Cr(bpy)_3^{3+/2+}$ (redox couple)	H_2O	25	130	8		+21.1 (B)	268	μ = 0.1 M (KNO_3)
915	$Cr(CNdipp)_6^{2+}$ + $Co(nox)_3(BBu)_2$ → $Cr(CNdipp)_6^{+}$ + $Co(nox)_3(BBu)_2^{+}$	CH_3CN	25	150	11	+2.2 ± 2		269	Bu_4NBF_4 electrolyte
	$Cr(CNdipp)_6^{2+}$ + $Co(nox)_3(BPh)_2$ → $Cr(CNdipp)_6^{+}$ + $Co(nox)_3(BPh)_2^{+}$	CH_3CN		150	11			269	
916			20			+5.6 ± 2			
917			16			+10.8 ± 1			
918			19			+11.0 ± 1			
919			19			+10.8 ± 1			$[Bu_4N(BF_4)]$ = 4×10^{-5} M
920			19			+9.7 ± 2			$[Bu_4N(BF_4)]$ = 5×10^{-5} M
921			19			+7.3 ± 2			$[Bu_4N(BF_4)]$ = 10×10^{-5} M
922			19			+8.2 ± 2			$[Bu_4N(BF_4)]$ = 25×10^{-5} M
923			19			+8.5 ± 2			$[Bu_4N(BF_4)]$ = 50×10^{-5} M
924			19			+11.0 ± 2			$[Bu_4N(BF_4)]$ = 0.120 M
925			19			+15.0 ± 2			$[Bu_4N(BF_4)]$ = 0.204 M
926	$Mn^{III}(cydta)^-$ + $HONH(SO_3)^-$ → products	H_2O	25	100	5	−10 ± 1		270	μ = 0.25 M
	$MnO_4^{1-/2-}$ (self-exchange)	75% H_2O−25% D_2O	45	180	10			271	$[OH^-]$ = 0.2 M, μ = 1.1 M
	$k_{obs} = k_0 + k_M[M^+]$								
927	k_0					−22.8 ± 1.2			
928	$M^+ = Na^+$, k_M					+3.3 ± 1.0			
929	$M^+ = K^+$, k_M					−1.1 ± 0.3			
	$Mn(CNC(CH_3)_3)_6^{+/2+}$ (OS self-exchange)			200				272	
930		CH_3CN	6		10	−12 ± 1			μ = 0.69 M
931		CH_3OH	6		6	−20 ± 2			μ = 0.17 M
932		C_6H_5CN	12		9	−9 ± 2			μ = 0.52 M
933		EtOH	7		9	−16 ± 2			μ = 0.16 M
934		$(CH_3)_2CO$	6		10	−20 ± 2			μ = 0.16 M
935		$(CH_3O)_3PO$	6		6	−10 ± 2			μ = 0.16 M
936		Et_2CO	7		7	−22 ± 2			μ = 0.18 M
937		DCM	0		11	−18 ± 2			μ = 0.11 M
		CH_3CN/CH_2Cl_2		200					
938		9:1	1		10	−12 ± 2			
939		4:1	0		14	−14 ± 2			μ = 0.17 M
940		7:3	1		23	−15 ± 2			μ = 0.18 M
941		3:2	0		13	−15 ± 2			μ = 0.16 M
942		1:1	1		14	−14 ± 2			μ = 0.14 M
943		2:3	2		19	−19 ± 3			μ = 0.12 M
944		3:7	1		13	−15 ± 3			μ = 0.12 M

Table 1. (Continued)

no.	reaction	solvent	T, °C	P, MPa	no. of data	$\Delta V^{\ddagger}$, $cm^3\ mol^{-1}$	$\Delta \bar{V}$, $cm^3\ mol^{-1}$ (method)	ref(s)	remarks
	Electron-Transfer Reactions (Continued)								
945		1:4	2		14	-13 ± 3			$\mu = 0.12$ M
946		1:9	2		8	-15 ± 2			$\mu = 0.11$ M
		CH_3CN/BrC_6H_5		200					
947		4:1	2		10	-12 ± 4			$\mu = 0.15$ M
948		1:1	2		18	-15 ± 3			$\mu = 0.15$ M
949		1:4	2		14	-13 ± 3			$\mu = 0.11$ M
		DCM/BrC_6H_5					-22.6 ± 0.8 (a)		
950		4:1	1	100	14	-17 ± 2			$\mu = 0.08$ M
951		1:1	1	100	19	-21 ± 3			$\mu = 0.11$ M
952		3:7	3	300	18	-16 ± 2			$\mu = 0.14$ M
	$Mn(CNC_6H_{11})_6^{+/2+}$ (OS self-exchange)							272	
953		CH_3CN	2	200	11	-17 ± 1			$\mu = 0.20$ M
954		CH_3OH	2	200	18	-16 ± 2			$\mu = 0.18$ M
955		$(CH_3)_2CO$	3	300	17	-20 ± 2			$\mu = 0.19$ M
956		DCM	3	300	15	-21 ± 4			$\mu = 0.12$ M
957		BrC_6H_5	2	200	10	-9 ± 2			$\mu = 0.17$ M
		DCM/BrC_6H_5							
958		7:3	3	300	21	-17 ± 2			$\mu = 0.09$ M
959		1:1	3	300	18	-18 ± 2			$\mu = 0.10$ M
960		3:7	3	300	18	-10 ± 4			$\mu = 0.10$ M
961	$(Fe^{II})_2O(O_2Ph)(N(CH_2CEtN_2C_6H_4)_2)_2 + O_2 \rightarrow (Fe^{III})_2O(O_2)(O_2Ph)(N(CH_2CEtN_2C_6H_4)_2)_2$	propionitrile	20	140	11	-12.8 ± 0.9		273	
	$Fe^{II}(edta)/O_2 \rightarrow Fe^{III}(edta)$	H_2O	25					274	pH = 5, $\mu = 0.5$ M
962	[Fe(edta)] = 0.0025 M			100	6	-16.9 ± 1.2			
963	[Fe(edta)] = 0.02 M			95	5	-12.7 ± 0.9			
	$Fe^{II}(hedtra)/O_2 \rightarrow Fe^{III}(hedtra)$	H_2O	25					274	pH = 5, $\mu = 0.5$ M
964	[Fe(hedtra)] = 0.0025 M			95	5	-11.6 ± 1.2			
	$Fe^{II}(dtpa)/O_2 \rightarrow Fe^{III}(dtpa)$	H_2O	25					274	pH = 5, $\mu = 0.5$ M
965	[Fe(dtpa)] = 0.02 M			100	5	-7.1 ± 0.4			
966	$Fe(H_2O)_6^{3+} + Co([9]aneS_3)_2^{2+} \rightarrow Fe(H_2O)_6^{2+} + Co([9]aneS_3)_2^{3+}$	H_2O	25	200	7	-15.9 ± 0.3	-17.1 ± 0.4 (a)	275	$\mu = 0.1$ M ($CF_3SO_3^-$)
967	$Fe(H_2O)_6^{3+} + Co(sep)^{2+} \rightarrow Fe(H_2O)_6^{2+} + Co(sep)^{3+}$	H_2O	2	210	7	-5.0		275	$\mu = 0.3$ M ($CF_3SO_3^-$)
968	$(CN)_5Fe(CN)Pt(NH_3)_4(CN)Fe(CN)_5^{4-}$, intramolecular one-electron-transfer event	H_2O	25	150	10	-5.7 ± 0.2		276	
969	$H_2Asc + Fe(CN)_6^{3-} \rightleftarrows H_2Asc^{\bullet+} + Fe(CN)_6^{4-}$	H_2O	25	60	5	-40 ± 68		277	$\mu = 0.1$ M ($NaClO_4$)
970	$HAsc^- + Fe(CN)_6^{3-} \rightleftarrows HAsc^{\bullet} + Fe(CN)_6^{4-}$	H_2O	25	60	5	-14 ± 3		277	$\mu = 0.1$ M ($NaClO_4$)
	$H_2Asc + 2Fe(CN)_6^{3-} \rightarrow Asc + 2H^+ + 2Fe(CN)_6^{4-}$	H_2O	25		5			278	
971				95		-16.6 ± 0.5			pH = 0.30, $\mu = 1.0$ M
972				95		-15.0 ± 1.0			pH = 5.00, $\mu = 1.0$ M
973				96		-16.3 ± 0.4			
974	$H_2Asc + 2Fe(H_2O)_6^{3+} \rightarrow Asc + 2H^+ + 2Fe(H_2O)_6^{2+}$	H_2O	25	90	5	$+14 \pm 2$		279	$\mu = 1.0$ M
975	$H_2Asc + 2Fe(H_2O)_5(OH)^{2+} \rightarrow Asc + 2Fe(H_2O)_6^{2+}$	H_2O	25	90	5	$+4.6 \pm 0.7$		279	$\mu = 1.0$ M
976	$K_3Fe(CN)_6$ + L-ascorbic acid	H_2O	35	190		-16 ± 1.5		280	
	$2[Fe(CN)_4(bpy)^- + QH_2 \rightarrow 2[Fe(CN)_4(bpy)^{2-} + Q + 2H^+$	H_2O	25	100	5			281	
	QH_2 = catechol								$\mu = 1.0$ M
977	[catechol] = 0.017 M					-18.3 ± 0.8			
978	[catechol] = 0.005 M					-18.3 ± 2.5			
979	QH_2 = Bu^t-catechol					-18.0 ± 1.3			
980	QH_2 = Me-1,4-hydroquinone					-16.7 ± 1.1			
	$Fe(phen)_3^{2+}/Fe(phen)_3^{3+}$ (self-exchange)							282	
981	as bisulfate salt	D_2O/D_2SO_4	3	210	8−10	-2.2 ± 0.1			0.3 mol kg^{-1} (bisulfate)
982	as perchlorate salt	CD_3CN	4	210	8−10	-5.9 ± 0.5			0.2 mol kg^{-1} (perchlorate)
983	$Fe(CN)_6^{3-/4-}$ (OS self-exchange)	H_2O	25	150	4		-1.0 ± 0.2 (a)	283	
984	$Fe(cp)_2/Fe(cp)_2^+$ (self-exchange)	CD_3CN	−8.5 to 10	200	9	-7 ± 1		284	$\mu = [Fe(cp)_2$
	peroxodisulfate oxidation of		25		3			285	
985	$Fe^{II}(CN)_4(ein)^{2-}$	H_2O		100		$+4.6$			
986	$Fe^{II}(CN)_4(phen)^{2-}$	H_2O		140		-2.1			
987		H_2O/DMSO		140		-3.6			
988	$Fe^{II}(CN)_4(Me_2bsb)^{2-}$	H_2O		100		-10.2			
989	$Fe^{II}(CN)_2(bpy)_2$	H_2O		100		-7.7			
990		H_2O/DMSO		100		-8.3			
991	$Fe(CN)_6^{3-/4-}$ (redox couple)	H_2O	25	200	5−6		-38.3 ± 1.0 (a)	286	$\mu = 1.00$ M (KCl)
992							-36.6 ± 0.7 (a)		$\mu = 0.51$ M (KCl)
993							-36.2 ± 0.8 (a)		$\mu = 0.28$ M (KCl)
994							-37.1 ± 1.3 (a)		$\mu = 0.28$ M (LiCl)
995							-34.4 ± 0.6 (a)		$\mu = 0.28$ M (K_2SO_4)
996	$Fe(H_2O)_6^{3+/2+}$ (redox couple)	H_2O	25	200	5−6		$+5.0 \pm 0.3$ (a)	286	$\mu = 0.28$ M (CF_3SO_3H)
997	$Fe(phen)_3^{3+/2+}$ (redox couple)	H_2O	25	200	5−6		$+6.2 \pm 0.5$ (a)	286	$\mu = 1.00$ M (KNO_3)
998							$+14.2 \pm 0.5$ (a)		$\mu = 0.25$ M (KNO_3)
999							$+16.3 \pm 0.2$ (a)		$\mu = 0.27$ M ($NaHSO_4$)
1000	$Fe(CN)_6^{3-/4-}$ (redox couple)	H_2O	25	130	8		-38.7 ± 0.5 (a)	47	$\mu = 1.0$ M (KNO_3)
1001	$Fe(phen)(CN)_4^{1-/2-}$ (redox couple)	H_2O	25	130	8		-25.5 ± 0.8 (a)	47	$\mu = 1.0$ M (KNO_3)
1002	$Fe(bpy)(CN_4)^{1-/2-}$ (redox couple)	H_2O	25	130	8		-25.7 ± 0.6 (a)	47	$\mu = 1.0$ M (KNO_3)
1003	$Fe(bpy)_2(CN)_2^{1+/0}$ (redox couple)	H_2O	25	130	8		-6.6 ± 0.5 (a)	47	$\mu = 1.0$ M (KNO_3)
1004	$Fe(phen)_3^{3+/2+}$ (redox couple)	H_2O	25	130	8		$+6.7 \pm 1.0$ (a)	47	$\mu = 1.0$ M (KNO_3)
1005	$Fe(bpy)_3^{3+/2+}$ (redox couple)	H_2O	25	130	8		$+8.0 \pm 0.3$ (a)	47	$\mu = 1.0$ M (KNO_3)
1006	$Fe(H_2O)_6^{3+}/ Fe(H_2O)_6^{2+}$ (self-exchange)	H_2O	25	130	8	-11.1 ± 0.4		287	$\mu = 0.5$ M ($HClO_4/NaClO_4$)

Table 1. (Continued)

no.	reaction	solvent	T, °C	P, MPa	no. of data	$\Delta V^{\ddagger}$, $cm^3\ mol^{-1}$	$\Delta\bar{V}$, $cm^3\ mol^{-1}$ (method)	ref(s)	remarks
	Electron-Transfer Reactions (Continued)								
1007	$Fe(H_2O)_5OH^{2+}/Fe(H_2O)_6^{2+}$ (self-exchange)	H_2O	25	130	8	-0.8 ± 0.9		287	$\mu = 0.5$ M ($HClO_4/NaClO_4$)
	$Fe(CN)_6^{3-/4-}$ (self-exchange)	H_2O	25	100	6			288	
1008						$+22 \pm 2$			$\mu = 0.5$ M
1009						$+8 \pm 2$			at a Pt electrode
	$Co(RNH_2)_5X^{n+} + Fe(CN)_6^{4-} \rightarrow$ products	H_2O		130	5			289	$\mu = 1.0$ M ($LiClO_4$)
1010	R = Me, X = H_2O		25			$+29.4 \pm 1.6$			pH = 3.9
1011	R = Me, X = OH^-		25			$+32.9 \pm 1.3$			pH = 7.3
1012	R = Et, X = H_2O		25			$+33.1 \pm 2.0$			pH = 3.9
1013	R = Et, X = OH^-		35			$+30.6 \pm 2.8$			pH = 7.3
1014	$Co(nta)(H_2O)_2^- + {}^{\bullet}CH_3 \rightarrow Co(nta)(H_2O)(CH_3)^- + H_2O$	H_2O	17	150	4	k_b: $+19 \pm 2$		290,291	
1015						k_f: $+6 \pm 2.5$			
1016	$Co(nta)(H_2O)_2^- + {}^{\bullet}O_2CH_3 \rightarrow Co(nta)(H_2O)(O_2CH_3)^- + H_2O$	H_2O	17	150	4	$+6.0 \pm 1.0$		290,291	
1017	$(HCY)Co(H_2O)_2^{2+} + O_2 \rightarrow (H_2O)Co(HCY)(O_2)^{2+} + H_2O$	H_2O	25	200	5	-4.7 ± 0.3	-22.6 ± 0.8 (a)	292	
1018	$(H_2O)Co(HCY)(O_2)^{2+} + H_2O \rightarrow (HCY)Co(H_2O)_2^{2+} + O_2$	H_2O	25	200	5	$+17.9 \pm 0.5$		292	
1019	$Co(NH_3)_5(HP_2O_7) + Fe(CN)_6^{4-} \rightarrow$ products	H_2O	35	150	5	$+36 \pm 3$		293	$\mu = 1.0$ M, pH = 4.3
1020	$Co(NH_3)_5(P_2O_7)^- + Fe(CN)_6^{4-} \rightarrow$ products	H_2O	44	150	5	$+13 \pm 1$		293	$\mu = 1.0$ M, pH = 9.6
1021	β-$Co(NH_3)_5(P_3O_{10})^{2-} + Fe(CN)_6^{4-} \rightarrow$ products	H_2O	35	150	5	$+13 \pm 2$		293	$\mu = 1.0$ M, pH = 8.8
1022	χ-$Co(NH_3)_5(P_3O_{10})^{2-} + Fe(CN)_6^{4-} \rightarrow$ products	H_2O	44	150	5	$+32 \pm 2$		293	$\mu = 1.0$ M, pH = 9.0
1023	$Co(NH_3)_5(HPO_3)^+ + Fe(CN)_6^{4-} \rightarrow$ products	H_2O	41	150	5	$+22 \pm 2$		293	$\mu = 1.0$ M, pH = 9.0
1024	$Co(NH_3)_5(H_2PO_2)^{2+} + Fe(CN)_6^{4-} \rightarrow$ products	H_2O	41	150	5	$+30 \pm 1$		293	$\mu = 1.0$ M, pH = 4.3
1025	$Co(NH_3)_4(pzc)^{2+} + Fe(CN)_5H_2O^{3-} \rightleftarrows (NH_3)_4Co(\mu\text{-pzc})Fe(CN)_5^- + H_2O$	H_2O	24	100	5	$+23.1 \pm 1.6$		294	$\mu = 0.10$ M ($NaClO_4$)
1026	$Co(en)_2(pzc)^{2+} + Fe(CN)_5H_2O^{3-} \rightleftarrows (en)_2Co(\mu\text{-pzc})Fe(CN)_5^- + H_2O$	H_2O	24	100	5	$+27.8 \pm 0.9$		294	$\mu = 0.10$ M ($NaClO_4$)
1027	$Co(NH_3)_5(HPO_4)^+ + Fe(CN)_6^{4-}$	H_2O	25	150	4	$+37 \pm 4$		295	$\mu = 1.0$ M ($LiClO_4$)
1028	$Co(NH_3)_5(H_2PO_4)^{2+} + Fe(CN)_6^{4-}$	H_2O	25	150	4	$+17 \pm 1$		295	$\mu = 1.0$ M ($LiClO_4$)
1029	$Co(NH_3)_5(PO_4) + Fe(CN)_6^{4-}$	H_2O	25	150	4	$+44 \pm 5$		295	$\mu = 1.0$ M ($LiClO_4$)
1030	$Co(NH_2Me)_5(PO_4) + Fe(CN)_6^{4-}$	H_2O	25	150	4	$+32 \pm 1$		295	$\mu = 1.0$ M ($LiClO_4$)
1031	$Co(AT)(HPO_4)^+ + Fe(CN)_6^{4-}$	H_2O	25	150	4	$+36 \pm 2$		295	$\mu = 1.0$ M ($LiClO_4$)
1032	$Co(NH_3)_5(H_2O)^{3+} + Fe(CN)_6^{4-}$	glyc/H_2O	30	100	6	$+27.9 \pm 0.1$		296	
1033	$Co(CyDTA)^{2-} + Fe(CN)_6^{3-} \rightarrow Co(CyDTA)^- + Fe(CN)_6^{4-}$	H_2O	25	120	4	$+6.5$		297	pH < 10.8, $\mu = 0.5$ M ($NaClO_4$)
	$Co(NH_3)_4(NH_2R)X^{(3-n)+} + Fe(CN)_6^{4-} \rightarrow Co^{2+} + 4NH_3 + NH_2R + X^{n-} + Fe(CN)_6^{3-}$	H_2O	35	100	5			298	$\mu = 1.0$ M
1034	R = H, $X^{n-} = N_3^-$					$+18.8 \pm 1.1$	-16 ± 2 (c)		
1035	R = H, $X^{n-} = Cl^-$					$+25.9 \pm 3.1$	-3 ± 8 (c)		
1036	R = CH_3, $X^{n-} = Cl^-$					$+25.1 \pm 1.5$	$+3 \pm 2$ (c)		
1037	R = ^{i}Bu, $X^{n-} = Cl^-$					$+31.3 \pm 0.9$	-6 ± 1 (c)		
1038	$Co(phen)_3^{3+/2+}$ (redox couple)	H_2O	25	130	8		$+21.1$ (a)	268	$\mu = 0.1$ M (KNO_3)
1039	$Co(bpy)_3^{3+/2+}$ (redox couple)	H_2O	25	130	8		$+34.4$ (a)	268	$\mu = 0.1$ M (KNO_3)
1040	$Co(en)_3^{3+/2+}$ (redox couple)	H_2O	25	130	8		$+34.0$ (a)	268	$\mu = 0.1$ M (KNO_3)
1041	$Co(sep)^{3+/2+}$ (redox couple)	H_2O	25	200	6		$+13.5 \pm 0.4$ (a)	286	$\mu = 1.0$ M (KCl)
1042	$Co(sep)^{3+/2+}$ (redox couple)	H_2O	25	200	6		$+13.9 \pm 0.5$ (a)	286	$\mu = 0.28$ M (KCl)
1043	$Co(diamsar)^{3+/2+}$ (redox couple)	H_2O	25	160	5	-10.4 ± 0.5	$+17.4 \pm 0.5$ (a)	299	$\mu = 0.14$ M
1044	$Co(diamsarH_2)^{5+/4+}$ (redox couple)	H_2O	25	160	5	-9.6 ± 0.8	$+19.5 \pm 0.8$ (a)	299	$\mu = 0.39$ M
1045	$Co(en)_3^{3+/2+}$ (self-exchange)	H_2O	65	210	5	-15.9 ± 1.0		300	$\mu = 0.5$ M
1046	$Co([9]aneS_3)_2^{2+/3+}$ (self-exchange)	H_2O	25	200	11	-4.8 ± 0.2		301	$\mu = 0.5$ M
1047	$Co(sep)^{3+/2+}$ (self-exchange)	H_2O	10	200	11	-6.4 ± 0.2		301	$\mu = 0.5$ M
	$Co(phen)_3^{3+/2+}$ (self-exchange)	H_2O	25	160	5			302	$\mu = 0.1$ M ($NaCl/NaNO_3$)
1048	anion = Cl^-					-20.4 ± 0.5			
1049	anion = NO_3^-					-19.7 ± 1.1			
1050	$Co(terpy)_2^{3+} + V(H_2O)_6^{2+} \rightarrow Co(terpy)_2^{2+} + V(H_2O)_6^{3+}$	H_2O	25	100	3	-1.8 ± 0.7		303	$\mu = 1.0$ M ($NaClO_4$)
	$(N_x)Co^{III}(\mu\text{-L})Fe^{II}(CN)_5 \rightarrow Co^{2+} + xN + Fe^{III}(CN)_5L$	H_2O	24	100	5			294	$\mu = 0.1$ M ($NaClO_4$)
1051	$N_x = (NH_3)_4$, L = pzc					-4.8 ± 0.2			
1052						-6.4 ± 0.2			photoinduced
1053	$N_x = (en)_2$, L = pzc					-4.8 ± 0.2			
1054	$N_x = (NH_3)_5$, L = pz					-6.4 ± 0.2			
1055						-4.8 ± 0.2			photoinduced
1056	$Co(nox)_3(BF)_2^+ + FeCp_2 \rightleftarrows Co(nox)_3(BF)_2 + FeCp_2^+$	CH_3CN	25	150	15−20	-6 ± 1		304	
1057						-14 ± 2			0.1 M Bu_4NBF_4
1058	$Co(dmg)_3(BF)_2^+ + FeCp_2 \rightleftarrows Co(dmg)_3(BF)_2 + FeCp_2^+$	CH_3CN	25	150	15−20	-9 ± 1		304	
1059						-15 ± 2			0.1 M Bu_4NBF_4
1060		$C_6H_5NO_2$				-9 ± 1			
1061		Me_2CO				-12 ± 1			
1062	$Co(dmg)_3(BF)_2^+ + FeCp_2 \rightleftarrows Co(dmg)_3(BF)_2 + FeCp_2^+$	CH_3CN	25	150	15−20	-10 ± 1		304	
1063						-15 ± 2			0.1 M Bu_4NBF_4
1064	$Co(dmg)_3(BF)_2^+ + Fe(CH_3Cp)_2 \rightleftarrows Co(dmg)_3(BC_6H_5)_2 + Fe(CH_3Cp)_2^+$	CH_3CN	25	150	15−20	-11 ± 1		304	
1065	$Co(dmg)_3(BC_4H_9)_2^+ + Fe(CH_3Cp)_2 \rightleftarrows Co(dmg)_3(BC_4H_9)_2 + Fe(CH_3Cp)_2^+$	CH_3CN	25	150	15−20	-11 ± 1		304	
	$Co(dmg)_3(BC_6H_5)_2^+ + Fe(CH_3Cp)_2 \rightleftarrows Co(dmg)_3(BC_6H_5)_2 + Fe(CH_3Cp)_2^+$		25	150	15−20			304	
1066		CH_3CN				-4 ± 1			
1067		$C_6H_5NO_2$				-5 ± 2			
1068		Me_2CO				-12 ± 1			
1069		CH_2Cl_2				-14 ± 1			

Table 1. (Continued)

no.	reaction	solvent	T, °C	P, MPa	no. of data	$\Delta V^{\ddagger}$, $cm^3\ mol^{-1}$	$\Delta \bar{V}$, $cm^3\ mol^{-1}$ (method)	ref(s)	remarks
	Electron-Transfer Reactions (Continued)								
1070	$Co(nox)_3(BC_6H_5)_2^+ + Fe(CH_3Cp)_2 \rightleftarrows Co(nox)_3(BC_6H_5)_2 + Fe(CH_3Cp)_2^+$	CH_3CN	25	150	15−20	−9 ± 1		304	
1071	$Co(dpg)_3(BC_6H_5)_2^+ + Fe(CH_3Cp)_2 \rightleftarrows Co(dpg)_3(BC_6H_5)_2 + Fe(CH_3Cp)_2^+$	CH_3CN	25	150	15−20	−14 ± 1		304	
1072	$Co(dmg)_3(BF)_2^+ + FeCp_2 \rightleftarrows Co(dmg)_3(BF)_2 + FeCp_2^+$	CH_3CN	25	150	15−20	−13 ± 2		304	
1073	$(en)_2Co^{III}(\mu\text{-}NH_2,O_2^{(-)})Co^{III}(en)_2^{4+} + TMPNO \rightarrow (en)_2Co^{III}(\mu\text{-}NH_2,O_2^{(2-)})Co^{III}(en)_2^{3+} + TMPNO^+$	H_2O	15	200	9	+0.2 ± 0.5		305	μ = 0.1 M ($NaClO_4$)
1074					5	−1.4 ± 1.3			μ = 0.5 M ($NaClO_4$)
1075	$(en)_2Co^{III}(pzc)Fe^{II}(CN)_5^- \rightarrow Co^{2+} + 2en + Fe^{III}(CN)_5(pzc)^{3-}$	H_2O	25	70	3	+24		306	
1076		60% MeOH	25	70	3	+7			
1077	$Co^{III}(NH_3)_5pz^{3+} + Fe^{II}(CN)_5(H_2O)^{3-} \rightleftarrows$	H_2O	25	70	10	+38 ± 1		307	pH = 5, μ = 0.10 M ($NaClO_4$)
1078	$(NH_3)_5Co^{III}(\mu\text{-}pz)Fe^{II}(CN)_5 \rightarrow$					+36 ± 1			pH = 5, μ = 0.10 M (NaCl)
1079	$Co^{2+} + 5NH_3 + Fe^{III}(CN)_5(pz)^{2-}$					+37 ± 1			pH = 5, μ = 0.10 M ($(C_2H_5)_4NClO_4$)
1080	$^{60}Co^{III}(edta)^- + Co^{II}(Hedta)OH_2^- \rightleftarrows {}^{60}Co^{II}(Hedta)OH_2^- + Co^{II}(edta)^-$	H_2O	85	230	7	−3.2 ± 0.3		155	pH = 2.0, μ = 0.5 M
	$Ni^{II}L(ClO_4)_2 + 2X^- + HO_2^{\bullet} \rightarrow Ni^{III}LX_2$	H_2O	25	150	4			308	
1081	X = SO_4^{2-}					−0.3			[X] = 0.02 M
1082	X = SO_4^{2-}					−1.3			[X] = 0.05 M
1083	X = SO_4^{2-}					−5.9			[X] = 0.70 M
1084	X = SO_4^{2-}					−6.2			[X] = 1.50 M
1085	X = $H_2PO_4^-$					−12.4			[X] = 0.05 M
1086	X = $H_2PO_4^-$					−10.7			[X] = 0.70 M
1087	X = $H_2PO_4^-$					−9.6			[X] = 2.0 M
1088	$Ni(cyclam)^{2+} + {}^{\bullet}CH_3 \rightleftarrows (cyclam)(H_2O)Ni^{III}\text{-}CH_3^{2+}$	H_2O	25	150	4	+24.4 ± 1.0	+20 ± 1.0 (a, c)	309	
1089	$(phen)_2Cu^I + O_2 \rightarrow (phen)_2Cu^{II} + O_2^-$	H_2O	17	150	3	−22 ± 2		310	
1090	$(Cu^I(C_6H_4(CH)_2N_2)NH((CH_2)_2)_2)_2 + O_2 \rightarrow (Cu^{II})_2(O_2)(C_6H_4(CH)_2N_2)NH((CH_2)_2)_2$	MeOH	25	150		−21 ± 1		311	
1091	$Cu(H_2O)_m^{2+} + {}^{\bullet}OH \rightarrow Cu(III)_{aq} + OH^-$	H_2O	25	150	3	+0.7 ± 0.2		312	
	$Cu(dmp)_2^{+/2+}$ (self-exchange)							313	
1092		CD_3CN	38	200		−3.4 ± 0.6			μ = 0.094 mol kg^{-1} (CF_3SO_3K)
1093		$(CD_3)_2CO$	29.5	200		−7.8 ± 0.6			μ = 0.121 mol kg^{-1} (CF_3SO_3K)
1094	Cu^{III}(GlyGlyHis), formation	H_2O	25	150		−5.1 ± 1		314	
1095	Cu^{III}(GlyGlyHis), decomposition	H_2O	25	150		+8 to +14		314	
1096	Ld Ru^{II}-Ru^{III}	D_2O	24	150	6	−7.5 ± 0.2		315	
1097	$Ru(en)_3^{3+/2+}$ (redox couple)	H_2O	25	130	8		+27.0 (b)	268	μ = 0.1 M (KNO_3)
1098	$Ru(NH_3)_6^{3+/2+}$ (redox couple)	H_2O	25	130	8		+30.3 (b)	268	μ = 0.1 M (KNO_3)
1099	$Ru(NH_3)_6^{3+/2+}$ (redox couple)	H_2O	25	130	8		+29.8 (b)	268	μ = 0.1 M ($HClO_4$)
1100	$Ru(H_2O)_6^{3+/2+}$ (redox couple)	H_2O	25	130	8		+12.5 (b)	268	μ = 0.1 M (KNO_3)
1101	$Ru(H_2O)_6^{3+/2+}$ (redox couple)	H_2O	25	130	8		+13.0 (b)	268	μ = 0.1 M ($HClO_4$)
1102	$Ru^0(cp)_2 + Ru^{II}(cp)_2Br$ (IS self-exchange)	CD_3CN	34−55	200	10	−3.0 ± 0.2		316	
	$Ru(hfac)_3^- + Ru(hfac)_3^0 \rightleftarrows Ru(hfac)_3^0 + Ru(hfac)_3^-$			200	8			317	
1103		$(CD_3)_2C$	25			−6.1 ± 0.3			
1104		CD_3CN	26			−5.5 ± 0.1			
1105		$CDCl_3$	26			−8.1 ± 0.2			
1106		CD_3OD	25			−5.8 ± 0.3			
	$Ru(cp)_2/Ru(cp)_2I(CF_3SO_3)$			200				318	
1107		CD_3CN	−2		11	−7.7 ± 1.1			
1108		CD_3CN	−14		12	−4.8 ± 1.0			
1109		CD_3NO_2	5		11	−4.0 ± 0.9			
1110		CD_3NO_2	8		12	−3.5 ± 1.0			
	$Ru(cp)_2/Ru(cp)_2Br(PF_6)$							318	
1111		CD_3CN	33	200	10	−2.9 ± 0.1			
1112		CD_3CN	41	200	8	−2.7 ± 0.4			
1113		CD_3CN	42	200	9	−2.9 ± 0.1			
1114		CD_3CN	44	200	9	−3.1 ± 0.2			
1115		CD_3CN	55	200	11	−3.3 ± 0.2			
1116		$C_6D_5NO_2$	34	200	9	−2.3 ± 0.7			
1117		$C_6D_5NO_2$	33	200	9	−3.1 ± 0.6			
1118		$C_6D_5NO_2$	40	150	7	−2.8 ± 0.4			
1119		CD_3NO_2	42	200	9	−3.9 ± 0.5			
1120	$H_2Asc + Ru(CN)_6^{3-} \rightleftarrows H_2Asc^{\bullet+} + Ru(CN)_6^{4-}$	H_2O	25	60	7	−26 ± 18		277	μ = 0.1 M ($NaClO_4$)
1121	$HAsc^- + Ru(CN)_6^{3-} \rightleftarrows HAsc^{\bullet} + Ru(CN)_6^{4-}$	H_2O	25	60	7	−9 ± 3		277	μ = 0.1 M ($NaClO_4$)
1122	$H_2Asc + Os(CN)_6^{3-} \rightleftarrows H_2Asc^{\bullet+} + Os(CN)_6^{4-}$	H_2O	25	60	7	−90 ± 75		277	μ = 0.1 M ($NaClO_4$)
1123	$HAsc^- + Os(CN)_6^{3-} \rightleftarrows HAsc^{\bullet} + Os(CN)_6^{4-}$	H_2O	25	60	7	−10 ± 3		277	μ = 0.1 M ($NaClO_4$)
	$Os(cp)_2/Os(cp)_2I(CF_3SO_3^-)$							318	
1124		CD_3CN	10	200	19	−7.6 ± 0.9			
1125		CD_3NO_2	−5	200	14	−4.7 ± 1.0			
1126		$(CD_3)_2CO$	10	150	13	+9.7 ± 0.8			
1127		$(CD_3)_2CO$	20	150	7	+11.0 ± 1.0			
1128		$CDCl_3$	20	170	16	−2.7 ± 0.7			
1129		$CDCl_3$	30	170	11	−7.0 ± 0.8			
1130		$CDCl_3$	41	170	12	−5.0 ± 1.0			
1131		$(CD_3)_2SO$	42	170	22	+0.07 ± 0.2			
	$IrCl_6^{2-} + QH_2 \rightarrow IrCl_6^{3-} + QH_2^+$	H_2O		100	5			319	
1132	QH_2 = catechol		25			−30.9 ± 1.3			pH = 0, μ = 1.0 M
1133	QH_2 = catechol		25			−24.5 ± 0.9			pH = 2, μ = 1.0 M

Table 1. (Continued)

no.	reaction	solvent	T, °C	P, MPa	no. of data	$\Delta V^{\ddagger}$, $cm^3\,mol^{-1}$	$\Delta \bar{V}$, $cm^3\,mol^{-1}$ (method)	ref(s)	remarks
	Electron-Transfer Reactions (Continued)								
1134	QH_2 = 4-*tert*-butylcatechol		25			−28.0 ± 3.6			pH = 0, μ = 1.0 M
1135	QH_2 = 3,4-dihydroxybenzoic acid		25			−30.3 ± 1.3			pH = 0, μ = 1.0 M
1136	QH_2 = 2,3-dihydroxybenzoic acid		25			−26.0 ± 0.2			pH = 0, μ = 1.0 M
1137	QH_2 = adrenalin		25			−29.2 ± 3.6			pH = 0, μ = 1.0 M
1138	QH_2 = 4-*tert*-butylcatechol		10			−24.9 ± 1.1			pH = 0, μ = 1.0 M
1139	QH_2 = 4-*tert*-butylcatechol		10			−21.2 ± 0.7			pH = 2, μ = 1.0 M
1140	QH_2 = 4-*tert*-butylcatechol		10			−23.5 ± 1.2			pH = 0, μ = 1.0 M
1141	QH_2 = 4-*tert*-butylcatechol		10			−23.6 ± 0.7			pH = 2, μ = 0.10 M
1142	QH_2 = adrenalin		10			−25.9 ± 1.3			pH = 0, μ = 0.10 M
1143	QH_2 = L-dopa		10			−25.1 ± 1.6			pH = 0, μ = 0.10 M
1144	QH_2 = 4-*tert*-butylcatechol		2			−20.0 ± 0.6			pH = 2, μ = 0.10 M
	Electrodeposition/Electrochemical Reactions								
	0.5 M $CoSO_4$ + 0.1 M K_2SO_4	H_2O	23	170				320	
1145	+ 0.01 M $NaClO_4$					+12.3 ± 0.2			
1146	+ 0.01 M KCl					+12.4 ± 0.3			
1147	+ 0.1 M KCl					+6.0 ± 0.2			
1148	+ 1 M KCl					+5.9 ± 0.2			
1149	+ 2 M KCl					+6.0 ± 0.4			
1150	+ 3.5 M KCl					+6.0 ± 0.3			
1151	+ 0.01 M KCl, 10^{-5} M KSCN					+12.0 ± 0.2			
1152	+ 0.01 M KCl, 0.01 M KSCN					0			
	0.5 M $NiSO_4$ + 0.1 M K_2SO_4	H_2O	23	170				320	
1153	+ 0.01 M KCl					+13.3 ± 0.5			
1154	+ 0.01 M KCl, 0.01 M 2-propane sulfonate					+14.6 ± 0.2			
1155	+ 0.01 M KCl, 0.05 M 2-propane sulfonate					+13.8 ± 0.2			
1156	+ 0.01 M KCl, 0.1 M 2-propane sulfonate					+13.6 ± 0.4			
1157	+ 0.01 M KCl, 0.01 M 2-naphthalene sulfonate					+5.3 ± 0.2			
1158	+ 0.01 M KCl, 0.05 M 2-naphthalene sulfonate					+5.0 ± 0.2			
1159	+ 0.01 M KCl, 0.02M 1,5-naphthalene sulfonate					+7.4 ± 0.1			
1160	+ 0.01 M KCl, 0.1 M 1,5-naphthalene sulfonate					+6.9 ± 0.3			
	0.5 M $NiSO_4$ + 0.1 M K_2SO_4	H_2O	25	170				321	
1161	+ 0.01 M KCl					+13.4 ± 0.4			
1162	+ 0.01 M KCl, KSCN additive					0			
	0.01 M $AgNO_3$ + 0.1 M KNO_3	H_2O	23	170				320	
1163	+ 0.5 M KCN					0			
1164	+ 5 M NH_3					+20.3 ± 0.4			
1165	+ 10 M NH_3					+20.9 ± 0.5			
1166	+ 5 M NH_3, 0.05 M KSCN					+21.1 ± 0.4			
1167	+ 5 M NH_3, 0.1 M KSCN					+20.0 ± 0.5			
	Heterolysis, Homolysis, and Homolytic Fission								
	heterolysis reactions:								
1168	$(H_2O)_5Cr(i\text{-}PrOH) + H_2O \rightarrow$ products	H_2O	25	200		+11.5 ± 0.8		322	μ = 0.5 M ($NaClO_4$)
1169	$(H_2O)_5Cr(MeOH) + H_2O \rightarrow$ products	H_2O	25	200		+9.3 ± 0.7		322	μ = 0.5 M ($NaClO_4$)
1170	$([15]aneN_4)(H_2O)Cr(MeOH) + H_2O \rightarrow$ products	H_2O	25	200		+6.9 ± 0.4		322	μ = 0.5 M ($NaClO_4$)
1171	$([15]aneN_4)(H_2O)Cr(i\text{-}PrOH) + H_2O \rightarrow$ products	H_2O	25	200		+10.4 ± 0.3		322	μ = 0.5 M ($NaClO_4$)
1172	*cis*-(nta)$(H_2O)Cr(i\text{-}PrOH) + H_2O \rightarrow$ products	H_2O	25	200		+10.2 ± 1.0		322	μ = 0.5 M ($NaClO_4$)
	$(H_2O)_5CrC(CH_3)_2OH^{2+} + H_2O \rightarrow$ products	H_2O	25	200				323	μ = 0.5 M ($NaClO_4$)
	anion:								
1173	CF_3COO^-					+14.2 ± 0.4			pH = 3.0
1174	SO_4^{2-}					+11.2 ± 0.4			pH = 3.0
1175	$ClCH_2COO^-$					+19.5 ± 1.1			pH = 3.8
1176	$CH_3CH(OH)COO^-$					+9.1 ± 0.3			pH = 3.5
1177	$HCOO^-$					+10.8 ± 0.3			pH = 4.5
1178	$HOCH_2COO^-$					+13.5 ± 0.5			pH = 4.5
1179	CH_3COO^-					+15.1 ± 0.8			pH = 5.3
1180	$CH_3CH_2COO^-$					+14.1 ± 0.6			pH = 5.4
1181	$H_2PO_4^-$					+15.5 ± 0.3			pH = 3.2
	$LCr\text{-}R^{2+} + H_2O \rightarrow LCr\text{-}OH_2^{3+} + RH$	H_2O	25	50				324	$[CH_3COO^-]$ =
	L = H_2O, R = CMe_2OH								
1182						+15.1 ± 0.8			0.015 M
1183						+11.3 ± 0.6			0.31 M
1184						+14.2 ± 0.5			0.0032 M
1185						+13.2 ± 0.9			0.0085 M
1186						+15.9 ± 0.3			0.0069 M
1187						+14.7 ± 0.3			0.0063 M
1188						+12.5 ± 0.8			0.027 M
1189						+9.2 ± 0.2			0.16 M
	L = H_2O, R = CH_2OH								
1190						+10.7 ± 0.5			0.015 M
1191						+6.1 ± 0.4			0.31 M
1192						+11.2 ± 0.2			0.038 M
1193						+10.0 ± 0.6			0.076 M
1194						+8.9 ± 0.4			0.17 M
1195						+6.4 ± 0.3			0.26 M
1196	L = nta, R = CMe_2OH					+4.6 ± 0.3			0.017 M
1197						+4.8 ± 0.5			0.27 M
1198	L = nta, R = CH_2OH					+7.2 ± 0.7			0.024 M
1199						+7.4 ± 0.7			0.27 M
1200	L = $[15]aneN_4$, R = CMe_2OH					+14.1 ± 1.4			0.028 M
1201	L = $[15]aneN_4$, R = CH_2OH					+14.0 ± 0.7			0.014 M

Table 1. (Continued)

no.	reaction	solvent	T, °C	P, MPa	no. of data	$\Delta V^{\ddagger}$, $cm^3\,mol^{-1}$	$\Delta\bar{V}$, $cm^3\,mol^{-1}$ (method)	ref(s)	remarks
	Heterolysis, Homolysis, and Homolytic Fission (Continued)								
	homolysis reactions:								
	$R\text{-}B_{12}$							325	
1202	R = ado	egly	100	150	6	$+18.5 \pm 1.5$			
1203	R = ado	H_2O	100	150	5	-2.0 ± 0.5			
1204	R = neopentyl	egly	40	150	5	$+7.9 \pm 1.2$			
1205	R = methyl	egly	110	100	4	$+17.0 \pm 2.2$			
	$R\text{-}B_{12}$			150				325	
1206	$R = Pr^i$	70% egly	37	150	5	$+0.2 \pm 0.3$			
1207	$R = Pr^i$	95% egly	37	150	3	-1.2 ± 0.3			
1208	R = ado	70% egly	100	150		+14			
	$AdoB_{12}$	H_2O		150	6			326	
1209			107			$+19.0 \pm 0.2$			
1210		20% 1-propanol	107			$+17.7 \pm 0.2$			
1211		50% 1-propanol	101			$+16.7 \pm 0.4$			
1212		80% 1-propanol	107			$+17.7 \pm 0.5$			
	NpB_{12}	H_2O	41	150	6			326	
1213						$+16.4 \pm 0.1$			
1214		20% 1-propanol				$+18.8 \pm 0.1$			
1215		35% 1-propanol				$+21.4 \pm 0.1$			
1216		50% 1-propanol				$+23.1 \pm 0.1$		328	
1217		65% 1-propanol				$+28.0 \pm 0.1$			
1218		80% 1-propanol				$+29.9 \pm 0.1$			
1219	MeB_{12}	H_2O	15	150	6	$+18.2 \pm 0.2$		326	
1220	$[AdoCbi]^+OH^-$	H_2O	15	150	6	$+18.5 \pm 0.2$		326	
	$^iPrB_{12}$	H_2O	30	150	6			326	
1221						$+1.2 \pm 0.8$			
1222		20% 1-propanol				$+1.3 \pm 1.3$			
1223		40% 1-propanol				$+0.1 \pm 0.1$			
1224		50% 1-propanol				-0.6 ± 1.0			
1225		60% 1-propanol				-0.1 ± 0.7			
1226		80% 1-propanol				-0.2 ± 0.9			
1227		90% 1-propanol				0.0 ± 0.3			
	homolytic fission reactions:								
		wt %							
1228	$PhCH_2Co(Hdmg)_2PCy_3$	H_2O/1-propanol	55	150	5−7	$+24.4 \pm 1.7$		327	
1229		10:90				$+14.8 \pm 1.2$			
1230		40:60				$+12.0 \pm 1.3$			
1231		50:50				$+9.7 \pm 0.6$			
1232		60:40							
	$C_6H_5CH_2Co(Hdmg)_2L$			150				328	
1233	$L = PMe_3$	$C_6H_5CH_3$	108			$+32.6 \pm 0.6$			
1234	$L = PEt_3$	$C_6H_5CH_3$	93			$+23.1 \pm 0.3$			
1235	$L = PBu_3$	$C_6H_5CH_3$	56			$+22.5 \pm 0.2$			
1236	$L = PBu_3$	$C_6H_5CH_3$	83			$+21.8 \pm 1.2$			
1237	$L = PBu_3$	CH_3OH	80			$+12.4 \pm 0.6$			
1238	$L = PPh_3$	$C_6H_5CH_3$	49			$+21.4 \pm 0.5$			
1239	$L = PPh_3$	$C_6H_5CH_3$	68			$+20.2 \pm 0.4$			
1240	$L = PCy_3$	$C_6H_5CH_3$	49			$+24.7 \pm 0.8$			
1241	L = pyridine	$C_6H_5CH_3$	92			$+32.2 \pm 1.1$			
1242	L = CNpy	$C_6H_5CH_3$	79			$+29.6 \pm 0.3$			
	$C_4H_9Co(salen)L$			150				328	
1243	L = CNpy	acetone	48			$+23.1 \pm 0.4$			
1244	L = CNpy	iodoethane	48			$+17.0 \pm 0.7$			
1245	L = CNpy	$C_6H_5CH_3$	48			$+20.8 \pm 1.3$			
1246	L = CNpy	$C_6H_5CH_3$	69			$+20.0 \pm 3.3$			
1247	L = pyridine	$C_6H_5CH_3$	69			$+34.3 \pm 3.2$			
1248	$L = PCy_3$	$C_6H_5CH_3$	48			$+25.5 \pm 1.8$			
1249	$L = PCy_3$	$C_6H_5CH_3$	56			$+25.1 \pm 1.5$			
	Photochemical and Photophysical Processes								
	photochemical reactions:								
	$Cr(CO)_4(phen) + PMe_3 \rightarrow Cr(CO)_3(phen)(PMe_3) + CO$	$C_6H_5CH_3$	25	160	4			329	
1250						$+6.8 \pm 1.3$			$\lambda_{irr} = 366$ nm
1251						$+4.7 \pm 1.0$			$\lambda_{irr} = 403$ nm
1252						-0.2 ± 0.8			$\lambda_{irr} = 436$ nm
1253						$+1.3 \pm 0.6$			$\lambda_{irr} = 486$ nm
1254						$+1.9 \pm 0.7$			$\lambda_{irr} = 546$ nm
	$Cr(CO)_4(phen) + PPh_3 \rightarrow Cr(CO)_3(phen)(PPh_3) + CO$	$C_6H_5CH_3$	25	160	4			329	
1255						$+6.4 \pm 0.3$			$\lambda_{irr} = 366$ nm
1256						$+5.0 \pm 0.8$			$\lambda_{irr} = 403$ nm
1257						$+2.9 \pm 0.1$			$\lambda_{irr} = 436$ nm
1258						$+2.8 \pm 0.7$			$\lambda_{irr} = 486$ nm
1259						$+2.7 \pm 0.8$			$\lambda_{irr} = 546$ nm
	cis-$Cr(cyclam)(NH_3)_2^{3+} + H_2O \rightarrow$ *cis*$Cr(cyclam)(NH_3)(H_2O)^{3+} + NH_3$	$C_6H_5CH_3$	25	160	4			329	
1260						+0.6			$\lambda_{irr} = 646$ nm, pH = 3 (HNO_3)
1261						$+0.6 \pm 0.4$			$\lambda_{irr} = 476.5$ nm, pH = 3 (HNO_3)
	$Cr(CO)_4(phen) + PEt_3 \rightarrow Cr(CO)_3(PEt_3)(phen) + CO$	$C_6H_5CH_3$	25	200	9			331	
1262	LF					$+9.6 \pm 1.6$			
1263	MLCT					$+2.7 \pm 0.3$			

Table 1. (Continued)

no.	reaction	solvent	T, °C	P, MPa	no. of data	$\Delta V^{\ddagger}$, $cm^3\,mol^{-1}$	$\Delta \bar{V}$, $cm^3\,mol^{-1}$ (method)	ref(s)	remarks
	Photochemical and Photophysical Processes (Continued)								
	$Cr(CO)_6 + pip \rightarrow Cr(CO)_5(pip) + CO$		25	200	9			332	$\lambda_{irr} = 313$ nm
1264		*n*-pentane				$+9.1 \pm 1.3$			
1265		*n*-hexane				$+7.0 \pm 0.7$			
1266		*n*-heptane				$+9.3 \pm 0.6$			
1267		*n*-octane				$+7.0 \pm 1.0$		334	
1268		*n*-decane				$+7.3 \pm 0.7$			
1269		*n*-dodecane				$+7.6 \pm 0.5$			
1270		perfluorohexane				$+9.2 \pm 0.3$			
	$Cr(CO)_6 + L \rightarrow Cr(CO)_5(L) + CO$		25	200	9			332	$\lambda_{irr} = 313$ nm
1271	L = py	*n*-heptane				$+9.5 \pm 1.0$			
1272	L = CH_3CN	*n*-heptane				$+9.3 \pm 1.0$			
1273	L = CH_3CN	CH_3CN				$+5.0 \pm 0.6$			
1274	$CpFe(CO)_2(COCH_3) + P(OMe)_3 \rightarrow CpFe(CO)_2CH_3$ (k_1)	*n*-heptane	22	80	2	-39 ± 8		333	
1275	$CpFe(CO)(COCH_3)(P(OMe)_3)$ (k_L)						-16.4 ± 1.6 (b)		
	$Mo(CO)_4(phen) + PEt_3 \rightarrow Mo(CO)_3(PEt_3)(phen) + CO$	$C_6H_5CH_3$	25	200				331	
1276	LF				4	$+5.7 \pm 0.2$			
1277	MLCT				9	-13.3 ± 1.2			
1278	$Mo(CO)_6 + py \rightarrow Mo(CO)_5(py) + CO$	*n*-heptane	25	200	9	$+14.0 \pm 1.2$		332	$\lambda_{irr} = 313$ nm
	$Ru(bpy)_3^{2+} + Cl^- + CH_3CN \rightarrow Ru(bpy)_2(CH_3CN)Cl^+ + bpy$	CH_3CN		300				334	
1279			15		2	$+12$			
1280			25		6	$+14$			
1281			60		6	$+22$			
	$[Ru(bpy)_3](PF_6)_2 + 2CH_3CN \rightarrow [Ru(bpy)_2(CH_3CN)_2](PF_6)_2 + bpy$	CH_3CN		300	6			334	
1282			25			$+8$			
1283			60			$+10$			
	$[Ru(bpy)_3]^{2+} + Cl^- + H_2O \rightarrow [Ru(bpy)_2(H_2O)]Cl^+ + bpy$	H_2O	60	300	6			334	
1284						$+9.5$			
1285						$+12$			9 M LiCl
1286	$[Ru(bpy)_3]Cl_2 + CH_2Cl_2 \rightarrow [Ru(bpy)_2(CH_2Cl_2)Cl]Cl + bpy$	CH_2Cl_2	25	300	2	$+17$		334	
	$[Ru(phen)_3]Cl_2 + CH_3CN \rightarrow [Ru(phen)_2(CH_3CN)Cl]Cl + phen$	CH_3CN		300	2			334	
1287			15			$+9$			
1288			25			$+18$			
1289			60			$+27$			
	$W(CO)_4(phen) + PEt_3 \rightarrow W(CO)_3(PEt_3)(phen) + CO$	$C_6H_5CH_3$	25	200	9			331	
1290	LF					$+8.1 \pm 0.5$			
1291	MLCT					-12.0 ± 0.7			
1292	$W(CO)_6 + py \rightarrow W(CO)_5(py) + CO$	*n*-heptane	25	200	9	$+8.8 \pm 0.4$		332	$\lambda_{irr} = 313$ nm
	$W(CO)_5(4\text{-X-py}) + P(OEt)_3 \rightarrow W(CO)_5(P(OEt)_3) + 4\text{-X-py}$	$C_6H_5CH_3$	25	200	9			335	$\lambda_{irr} = 436$ nm (LF)
1293	X = H					$+5.7 \pm 0.3$			
1294	X = NC					$+6.3$			
1295	X = OAc					$+9.9$			
	$W(CO)_4(phen) + PEt_3 \rightarrow$ *cis*-$W(CO)_3(phen)PEt_3 + CO$	$C_6H_5CH_3$	25	200	9			336	
1296	LF					$+8.1 \pm 0.5$			$\lambda_{irr} = 366$ nm
1297	MLCT					-12.0 ± 0.7			$\lambda_{irr} = 546$ nm
1298	$(CO)_5ReMn(CO)_3(\alpha\text{-diimine}) + CH_2Cl_2 \rightarrow Re(CO)_5Cl + Mn(CO)_3(\alpha\text{-diimine})Cl$	CH_2Cl_2	25	150	5	$+17.2 \pm 1.3$		337	$\lambda_{irr} = 577$ nm
1299	$(CO)_5ReMn(CO)_3(\alpha\text{-diimine}) + PPh_3 \rightarrow (CO)_5ReMn(CO)_2(PPh_3)(\alpha\text{-diimine}) + CO$	CH_2Cl_2	25	150	5	$+15.7 \pm 0.5$		337	$\lambda_{irr} = 577$ nm
	Photophysical Reactions: Spin Change			120				338	
	$^1A_1 \rightarrow {}^5T_2$								
	$Fe(pyimH)_3^{2+}$								
1300		MeOH/MeCN				0.0 ± 0.2	$+5.3 \pm 0.2$ (a)		
1301		MeCN				$+8.9 \pm 0.4$	$+14.3 \pm 0.5$ (a)		
1302		Me_2CO				$+4.9 \pm 0.3$	$+10.3 \pm 0.4$ (a)		
	$Fe(pyBimH)_3^{2+}$								
1303		MeOH/MeCN				$+0.2 \pm 0.3$	$+4.3 \pm 0..4$ (a)		
1304		MeCN				$+5.9 \pm 0.4$	$+12.4 \pm 0.5$ (a)		
1305		Me_2CO				$+4.7 \pm 0.4$	$+9.6 \pm 0.4$ (a)		
1306	$Fe(ppa)_2^{2+}$	Me_2CO				$+2.6 \pm 0.5$	$+8.7 \pm 0.5$ (a)		
	$Fe(tppn)^{2+}$								
1307		DMF				$+7 \pm 3$	$+16.1 \pm 2.0$ (a)		
1308		MeCN				$+5.1 \pm 0.7$	$+10.7 \pm 1.0$ (a)		
	$Fe(tpchxn)^{2+}$								
1309		DMF				$+21 \pm 3$	$+15.5 \pm 2.0$ (a)		
1310		MeCN				$+5.4 \pm 1.2$	$+11.5 \pm 1.0$ (a)		
	$^5T_2 \rightarrow {}^1A_1$			120				338	
	$Fe(pyimH)_3^{2+}$								
1311		MeOH/CN				-5.3 ± 0.3			
1312		MeCN				-5.4 ± 0.3			
1313		Me_2CO				-5.4 ± 0.3			
	$Fe(pyBimH)_3^{2+}$								
1314		MeOH/CN				-4.1 ± 0.3			
1315		MeCN				-6.4 ± 0.3			
1316		Me_2CO				-4.9 ± 0.4			
	$Fe(ppa)_2^{2+}$								
1317		Me_2CO				-6.1 ± 0.5			

Table 1. (Continued)

no.	reaction	solvent	T, °C	P, MPa	no. of data	$\Delta V^{\ddagger}$, $cm^3\ mol^{-1}$	$\Delta \bar{V}$, $cm^3\ mol^{-1}$ (method)	ref(s)	remarks
	Photochemical and Photophysical Processes (Continued)								
1318		H_2O				−6.5			
	$Fe(tppn)^{2+}$								
1319		DMF				−9 ± 3			
1320		MeCN				−5.6 ± 0.7			
	$Fe(tpchxn)^{2+}$								
1321		DMF				+5.7 ± 2.0			
1322		MeCN				−6.1 ± 1.2			
	$^3Pt_2(\mu\text{-}\eta^2\text{-}H_2P_2O_5)_4^{4-}$		21	300	6			339	quencher:
1323		CH_3OH				−5.4 ± 1			$PhCH_2OH$
1324		CH_3CN				−5.7 ± 1			$PhCH_2OH$
1325		CH_3OH				−2.8 ± 1			Ph_2CHOH
1326		CH_3OH				−2.6 ± 1			$PhCH(OH)C_2H_5$
1327		CH_3OH				−4.4 ± 1			$PhCH(OH)CH_3$
1328		CH_3OH				−4.7 ± 1			$PhCD(OH)CH_3$
1329		CH_3OH				−4.1 ± 1			$PhCH_2OCH_3$
1330		H_2O				−1.4 ± 1			$H_2C{=}CHCH_2OH$
1331		CH_3OH				−0.2 ± 1			$H_2C{=}CHCH_2OH$
1332		CH_3OH				+0.7 ± 1			$H_2C{=}CHCH(^iPr)OH$
1333		CH_3CN				+0.6 ± 2			$n\text{-}Bu_3SnH$
1334		CH_3OH				−2.5 ± 1			$n\text{-}Bu_3SnH$
1335		CH_3OH				+2.8 ± 1			O_2
1336		CH_3OH				−7.6 ± 3			cyclohexane
	$Pt_2(\mu\text{-}\eta^2\text{-}H_2P_2O_5)_4^{4-}$	H_2O	8−22					340	
1337	$^1A_{1g} \rightarrow {}^3A_{2u}$					+0.5 ± 0.3			
1338	$^1A_{1g}$ + 0.01 M $TlNO_3 \rightarrow {}^3A_{2u}$					−10.6 ± 0.9			
1339	quenching $Tb(dpa)_3^{3-}$ by Δ-$Ru(phen)_3^{3+}$	H_2O	25	280	9	−1.5		341	
1340	quenching $Tb(dpa)_3^{3-}$ by Δ-$Ru(phen)_3^{3+}$	MeOH	25	280	14	−2.6		341	
	Photophysical Reactions: Emission Lifetimes								
	$Cr(NH_3)_6^{3+} + L \rightarrow Cr(NH_3)_5L^{3+} + NH_3$			210				342	λ_{irr} = 437 nm
1341	L = H_2O	H_2O	25			+4.3 ± 0.3			
1342	L = DMF	DMF	25			+3.8 ± 0.2			
1343	L = DMSO	DMSO	25			+3.5 ± 0.2			
1344	L = HMPA	HMPA	30			+3.4 ± 0.2			
1345	*cis*-$Cr(cyclam)(NH_3)_2^{3+}$	DMF	11−40	210		+2.9 ± 0.4		343	λ_{irr} = 488 nm, $[HClO_4]$ = 1 mM
	trans-$Cr(cyclam)(NH_3)_2^{2+}$	DMF		210	2			344	
1346			2		2	+0.3 ± 0.1			
1347			62			+7.0 ± 0.2			
1348	$Cu(dpp)_2^+$	CH_2Cl_2	20	250		−1.6		345	
1349	$Cu(dpp)_2^+$	CH_3CN	20	250		−1.2		345	
1350	$Cu(dpp)_2^+$	$CHCl_3$	20	250		+1.2		345	
1351	$Cu(dpp)_2^+$	THF	20	250		−0.3		345	
	$Cu(dmp)_2^+$ (MLCT state)	DCM	23					346	quencher:
1352				300	4	−3.4 ± 0.2			none
1353				260	2	−4.3 ± 0.2			0.3 M CH_3CN
1354				260	2	−4.0 ± 0.2			0.3 M CH_3OH
	$Cu(dpp)_2^+$ (MLCT state)	DCM	23					346	quencher:
1355				300	5	−1.6 ± 0.2			none
1356				260	2	−1.2 ± 0.2			0.3 M CH_3CN
	$^3Cu(dpp)_2^+$ (MLCT state)	CH_2Cl_2	23	250	6			31,347	quencher:
1357						+8.0 ± 0.8			$Cr(hfac)_3$
1358						+0.8 ± 1.8			$Cr(tfbzac)_3$
1359						+2.1 ± 1.8			$Cr(tta)_3$
1360						+3.8 ± 0.4			$Cr(tc\text{-}bzac)_3$
1361						−3.5 ± 0.4			$Cr(br\text{-}dbm)_3$
1362						−8.1 ± 1.0			$Cr(tfac)_3$
1363						−3.8 ± 1.0			$Cr(n\text{-}acac)_3$
1364						−1.4 ± 0.7			$Cr(tc\text{-}acac)_3$
1365						−2.4 ± 0.5			$Cr(br\text{-}acac)_3$
1366						−0.3 ± 1.0			$Cr(dbm)_3$
1367						−0.1 ± 0.8			$Cr(acac)_3$
1368						+6.9 ± 1.3			*p*-dinitrobenzene
1369						−20.4 ± 4.8			*p*-chloronitrobenzene
1370						+1.2 ± 0.4			9,10-dichloroanthracene
1371						−2.4 ± 1.0			O_2
1372	$Ru(bpy)_3^{2+}$	EtOH/MeOH	−113	100	9	+0.47		348	
	$Ru(bpy)_3^{2+} + Q \rightarrow Ru(bpy)_3^+ + Q$		25	300	4			349	quencher:
1373		CH_3CN				+1.3			DMA
1374		CH_3CN				+1.1			DEA
1375		CH_3CN				+1.0			DMpT
1376		CH_3CN				+8.9			B
1377		CH_3CN				+7.7			TMB
1378		*n*-butyl alcohol				+1.8			DMA
1379		*n*-butyl alcohol				+4.0			DEA
1380		*n*-butyl alcohol				+6.5			DMpT
1381		*n*-butyl alcohol				+13			B
1382		*n*-butyl alcohol				+11			TMB
	$Rh_2(\mu\text{-}\eta^2\text{-}1,3\text{-diisocyanopropane})^{2+}$	CH_3CN	25	300	7			350	
1383	radiative decay					−0.5			
1384	nonradiative decay					−0.5			
	$Rh_2(\mu\text{-}\eta^2\text{-}2,5\text{-dimethyl-}2,5\text{-diisocyanohexane})^{2+}$	CH_3CN	7	250	7			350	

Table 1. (Continued)

no.	reaction	solvent	T, °C	P, MPa	no. of data	$\Delta V^{\ddagger}$, $cm^3\ mol^{-1}$	$\Delta \bar{V}$, $cm^3\ mol^{-1}$ (method)	ref(s)	remarks
	Photochemical and Photophysical Processes (Continued)								
1385	radiative decay					+2.8			
1386	nonradiative decay					+2.8			
1387	$W(CO)_5$(4-AcOpy)	$C_6H_5CH_3$		300	2	+0.1 ± 0.3		335	
1388	$W(CO)_5$(CNpy)	$C_6H_5CH_3$		300	2	+1.2 ± 0.3		335	
	$Ir_2(\mu\text{-}\eta^2\text{-pyrazolate})_2(COD)_2$		25	300	7			350	
1389	radiative deactivation	CH_3CN				+4.6			
1390	nonradiative deactivation	CH_3CN				+4.7			
1391	radiative deactivation	$C_6H_5CH_3$				+4.4			
1392	nonradiative deactivation	$C_6H_5CH_3$				+4.4			
	$Pt_2(\mu\text{-}\eta^2\text{-}H_2P_2O_5)_4^{4-}$		25	300	7			350	
1393	radiative deactivation	H_2O				−1.6			
1394	nonradiative deactivation	H_2O				−2.4			
1395	radiative deactivation	CH_3CN				−0.2			
	Bioinorganic and Biological Reactions								
1396	$B_{12}\text{-}H_2O^+ + 4\text{-Mepy} \rightleftarrows B_{12}\text{-4-Mepy}^+ + H_2O$	H_2O	25	150	6		+1.7 ± 0.7 (a)	351	μ = 1.5 M, pH = 7
1397	$B_{12}\text{-}H_2O^+ + 3\text{-Acpy} \rightleftarrows B_{12}\text{-3-Acpy}^+ + H_2O$	H_2O	25	150	6		+5.7 ± 1.3 (a)	351	μ = 1.5 M, pH = 7
1398	$B_{12}\text{-}H_2O^+ + TU \rightarrow B_{12}\text{-}TU^+ + H_2O$	H_2O	20	150	4	+9.1 ± 0.9		352	μ = 0.1 M, pH = 4
1399	$B_{12}\text{-}TU^+ + H_2O \rightarrow B_{12}\text{-}H_2O^+ + TU$	H_2O	20	150	4	+6.7 ± 0.3		352	μ = 0.1 M, pH = 4
	$B_{12a}\text{-}H_2O^+ + L^{n-} \rightarrow B_{12a}\text{-}L^{(n-1)+} + H_2O$	H_2O	25	500	5			353	
1400	$L^{n-} = Fe(CN)_6^{4-}$					+16.2 ± 1.2			μ = 0.13 M ($NaClO_4$), pH = 6.0
1401	$L^{n-} = Fe(CN)_5NO^{2-}$					+8.9 ± 0.5			μ = 0.1 M ($NaClO_4$), pH = 6.0
1402	$L^{n-} = Fe(CN)_5H_2O^{2-}$					+8.2 ± 0.8			μ = 0.1 M ($NaClO_4$), pH = 6.0
1403	$L^{n-} = N_3^-$					+6.9 ± 0.2			μ = 0.5 M ($NaClO_4$), pH = 6.4
1404	$B_{12}\text{-}H_2O^+ + py \rightarrow B_{12}\text{-}py^+ + H_2O$	H_2O	25	100	5	+8.7 ± 1.2	−8.2 ± 2.0 (c)	354	μ = 0.5 M
1405	$B_{12}\text{-}py^+ + H_2O \rightarrow B_{12}\text{-}H_2O^+ + py$	H_2O	25	100	5	+16.9 ± 0.8	−12.0 ± 2.0 (a)	354	μ = 0.5 M
1406	$B_{12}\text{-}H_2O^+ + NH_3 \rightarrow B_{12}\text{-}NH_3^+ + H_2O$	H_2O	25	130	6	+9.4 ± 0.8		355	μ = 1.0 M ($NaClO_4$), pH = 2.0
1407	$B_{12}\text{-}H_2O^+ + NH_3 \rightarrow B_{12}\text{-}NH_3^+ + H_2O$	H_2O	25	130	5	+8.6 ± 0.4		355	μ = 1.0 M ($NaClO_4$), pH = 2.5
1408	$B_{12}\text{-}H_2O^+ + NH_3 \rightarrow B_{12}\text{-}NH_3^+ + H_2O$	H_2O	25	130	5	+8.3 ± 0.4		355	μ = 1.0 M ($NaClO_4$), pH = 3.0
1409	$B_{12}\text{-}H_2O^+ + N_3^- \rightarrow B_{12}\text{-}N_3 + H_2O$	H_2O	25	130	6	+4.9 ± 0.3		355	μ = 1.0 M ($NaClO_4$)
1410	$B_{12}\text{-}H_2O^+ + N_3^- \rightarrow B_{12}\text{-}N_3^+ + H_2O$	H_2O	25	130	6	+6.9 ± 0.3		355	μ = 0.1 M ($NaClO_4$)
1411	$B_{12}\text{-}NH_3^+ + H_2O \rightarrow B_{12}\text{-}H_2O^+ + NH_3$	H_2O	25	130	6	+8.3 ± 1.6		355	μ = 1.0 M ($NaClO_4$), pH = 2.0
1412	$Hr + O_2 \rightarrow HrO_2$	H_2O	23	150	5	+13.3 ± 1.1	−39 ± 2 (b)	356	
1413	$HrO_2 \rightarrow Hr + O_2$	H_2O	23	150	5	+52.2 ± 0.7		356	
1414	$Mhr + O_2 \rightarrow MhrO_2$	H_2O	22	100	5	+8.4 ± 0.3		357	
1415	$MhrO_2 \rightarrow Mhr + O_2$	H_2O	25	100	5	+28 ± 3		357	
1416	$Mb + O_2 \rightarrow MbO_2$	H_2O	25	150	5	+5.2 ± 0.5	−19.3 ± 1.5 (a)	358	μ = 0.1 M (NaCl), pH = 8.5
1417	$MbO_2 \rightarrow Mb + O_2$	H_2O	25	150	5	+23.3 ± 1.8		359	μ = 0.1 M (NaCl), pH = 8.5
	$Mb + L \rightarrow Mb\text{-}L$	H_2O	25	150				359	μ = 0.1 M NaCl
1418	L = CO				4	−10.0 ± 0.8			
1419	$L = O_2$				4	+5.2 ± 0.5			
1420	L = MeNC				8	+8.8 ± 1.0			
1421	L = ^{t}BuNC				6	+9.3 ± 0.3			
	$Mb\text{-}L \rightarrow Mb + L$	H_2O	25	200	4			359	
1422	L = CO					+11.7 ± 1.1			
1423	$L = O_2$					+12.6 ± 1.7			
1424	L = MeNC					+9.1 ± 3.5			
1425	$Mb + CO \rightarrow Mb\text{-}CO$	H_2O	25	150	4	−3.8 ± 1.6	−4.1 ± 0.8 (c)	360	
1426	$Mb\text{-}CO \rightarrow Mb + CO$	H_2O	25	150	4		−3.0 ± 0.6 (a)	360	
		H_2O	20	200	7			361	pH = .8
1427	$(Mb_s\cdots O_2) \rightarrow Mb_sO_2$					+3.5			
1428	$(Mb_s\cdots O_2) \rightarrow Mb_s + O_2$					+16.7			
1429	$Mb_s + O_2 \rightarrow (Mb_s\cdots O_2)$					+10.4	−6.3 (c)		
1430	$Mb_s + O_2 \rightarrow Mb_sO_2$					+4.6			
1431	$Mb_s + CO \rightarrow (Mb_s\cdots CO)$					−9.2			
1432	$Mb_H\cdots O_2 \rightarrow Mb_HO_2$					−8.4			
1433	$Mb_H\cdots O_2 \rightarrow Mb_H + O_2$					+11.2			
1434	$Mb_H + O_2 \rightarrow (Mb_H\cdots O_2)$					+12.3	+1.1 (c)		
1435	$Mb_H + O_2 \rightarrow Mb_HO_2$					+3.8			
1436	$Mb_H + CO \rightarrow (Mb_H\cdots CO)$					−12.7			
1437	$(Mb_D\cdots O_2) \rightarrow Mb_DO_2$					−17.8			
1438	$(Mb_D\cdots O_2) \rightarrow Mb_D + O_2$					−2.1			
1439	$Mb_D + O_2 \rightarrow (Mb_D\cdots O_2)$					+8.6	+10.7 (c)		
1440	$Mb_D + O_2 \rightarrow Mb_DO_2$					0.0			
1441	$Mb_D + CO \rightarrow (Mb_D\cdots CO)$					−18.8			
1442	CO + α-Hb ⇄ α-Hb-CO	H_2O	20	150	4	−18.4 ± 0.5		362	
1443	CO + β-Hb ⇄ β-Hb-CO	H_2O	20	150	4	−22.4 ± 1.7		362	
1444	R-Hb + CO → R-Hb-CO	H_2O	20	150	15	−9.0 ± 0.7		363	pH = 7, 50 mM Tris/HCl
1445	T-Hb + CO → T-Hb-CO	H_2O	10	150	15	−31.7 ± 2.4		363	pH = 7, 50 mM Tris/HCl
1446	MCPH + CO	H_2O	25	150	6	−19.3 ± 0.4		359	
1447	MCPH + O_2	H_2O	25	150	6	−11.3 ± 1.0		359	
1448	PHDME + MeNC	H_2O	25	150	6	+11.6 ± 0.8		359	
1449	PHDME + ^{t}BuNC	H_2O	25	150	6	−9.9 ± 1.0		359	
1450	PHDME + 1Melm	H_2O	25	150	6	+10.9 ± 3.1		359	
1451	PCO → P•CO (α chain)	H_2O	20	150	4	−21.8 ± 0.9		362	see abbvn
1452	PCO → P•CO (β chain)	H_2O	20	150	4	−15.4 ± 0.8		362	see abbvn
1453	P•CO → P + CO (α chain)	H_2O	20	150	4	+11.1 ± 0.8		362	see abbvn
1454	P•CO → P + CO (β chain)	H_2O	20	150	4	+7.4 ± 0.7		362	see abbvn
1455	P + CO → P•CO (α chain)	H_2O	20	150	4	+16.0 ± 0.6		362	see abbvn
1456	P + CO → P•CO (β chain)	H_2O	20	150	4	+12.1 ± 0.6		362	see abbvn

Table 1. (Continued)

no.	reaction	solvent	T, °C	P, MPa	no. of data	$\Delta V^{\ddagger}$, $cm^3\ mol^{-1}$	$\Delta\bar{V}$, $cm^3\ mol^{-1}$ (method)	ref(s)	remarks
	Bioinorganic and Biological Reactions (Continued)								
1457	Bhm + CO → products	$C_6H_5CH_3$	25	300	6	−13.7 ± 1.4		364	
	HRP + CO → HRP-CO			120	4			365	
1458		H_2O	34			−23.6 ± 1			
1459		H_2O	20			−23.7 ± 1			
1460		H_2O	4			−26.9 ± 1			
1461		H_2O/40% egly	20			−6.98 ± 0.02			
1462		H_2O/40% egly	0.5			−10.5 ± 0.6			
1463		H_2O/40% egly	−10			−14.6 ± 0.8			
1464		50% MeOH	20			−9.4 ± 0.2			
1465		50% MeOH	10			−6 ± 0.2			
1466		50% MeOH	4			−5.5 ± 0.2			
1467		50% MeOH	0			−5.2 ± 1			
1468		50% MeOH	−10			−2.3 ± 0.3			
1469		H_2O/glyc	−20			−1.6 ± 0.4			
	hemoprotein + CO	H_2O/glyc	25	200	6			366	
1470	enzyme = $P450_{scc}$, ligand = S^- (cis)					+2 ± 2			
1471	enzyme = P450LM2, ligand = S^- (cis)					+3 ± 2			
1472	enzyme = P450LM3, ligand = S^- (cis)					+6 ± 2			
1473	enzyme = P4507α, ligand = S^- (cis)					+2 ± 2			
1474	enzyme = CPO, ligand = S^- (cis)					+1 ± 2			
1475	enzyme = LP, ligand = N (his)					−10 ± 3			
1476	enzyme = P420, ligand = unknown					−25 ± 5			
1477	enzyme = P420, ligand = unknown					−11 ± 6			
1478	enzyme = P420, ligand = unknown					−42 ± 8			
	cytochrome $P450_{cam}$ + CO	H_2O/glyc	20					367	pH = 7.4
1479	substrate = adamantane					+7 ± 3			
1480	substrate = norcamphor					+3 ± 2			
1481	substrate-free					+4 ± 1			
1482	substrate = fenchone					+20 ± 1			
1483	substrate = TMCH					+14 ± 1			
1484	substrate = bromocamphor					−32 ± 2			
1485	substrate = camphor					−31 ± 2			
	NADH + horse liver alcohol dehydrogenase							368	
1486		H_2O/DMSO	20	100	3	+19 ± 2			
1487		H_2O	−5	150	4	+23 ± 0.5			
1488		H_2O	−21.5	100	3	+28 ± 0.3			
1489	carbonic anhydrase catalysis	H_2O	25	150	6	−9 to +14		369	details in ref
	cytochrome *c* oxidase:	H_2O	7	150				370	
1490	reduced oxidase, 445 nm ⇄ 443 nm						>0 (a)		
1491	aerobic steady state ⇄ partially reduced oxidase						−76 (a)		pH = 7
1492	porphyrin *c*−cytochrome b_5 complex formation	H_2O	5	200	>10		−50 (a)	371	μ = 1−10 mM (KCl), pH = 7
1493	Cyt c^{II} + $Co(terpy)_2^{3+}$ → Cyt c^{III} + $Co(terpy)_2^{2+}$	H_2O	25	100	5	+18.4 ± 1.3	+36 (b), +33 (c)	372	μ = 0.1 M, pH = 7.2
1494	Cyt c^{III} + $Co(terpy)_2^{2+}$ → Cyt c^{II} + $Co(terpy)_2^{3+}$	H_2O	25	130	5	+18.0 ± 1.4		372	μ = 0.1 M, pH = 7.2
1495	Ru^{2+} → $ZnP^{\bullet+}$ in $(NH_3)_5$Ru(His33)Zn-Cyt c	H_2O	25	150	4	−12 ± 1		373	
1496	Fe^{2+} → Ru^{3+} in $(bpy)_2$(im)Ru(His33)Fe-Cyt c	H_2O	25	150	4	0		373	
1497	Fe^{2+} → Ru^{3+} in $(bpy)_2$(im)Ru(His72)Fe-Cyt c	H_2O	25	150	4	−6 ± 2		373	
1498	$(NH_3)_5$(lut)Ru^{III} + $Cytc^{II}$ → $(NH_3)_5$(lut)Ru^{II} + $Cytc^{III}$	H_2O	25	150	4	+16.9 ± 1.4	+33.6 ± 1.7 (a)	374	μ = 0.1 M, pH = 7.1
1499	$(NH_3)_5$(lut)Ru^{II} + $Cytc^{III}$ → $(NH_3)_5$(lut)Ru^{III} + $Cytc^{II}$	H_2O	25	150	4	−17.8 ± 1.6	+34.7 ± 2.1 (a)	374	μ = 0.1 M, H = 7.1
1500	$(NH_3)_5$(etpy)Ru^{III} + $Cytc^{II}$ → $(NH_3)_5$(etpy)Ru^{II} + $Cytc^{III}$	H_2O	25	150	4	+14.7 ± 0.9	+26.9 ± 1.8 (a)	374	μ = 0.1 M, pH = 7.1
1501	$(NH_3)_5$(etpy)Ru^{II} + $Cytc^{III}$ → $(NH_3)_5$(etpy)Ru^{III} + $Cytc^{II}$	H_2O	25	150	4	−14.9 ± 1.1	+29.6 ± 1.4 (a)	374	μ = 0.1 M, pH = 7.1
1502	$(NH_3)_5$(py)Ru^{III} + $Cytc^{II}$ → $(NH_3)_5$(py)Ru^{II} + $Cytc^{III}$	H_2O	25	150	4	+17.4 ± 1.5	+33.4 ± 1.9 (a)	374	μ = 0.1 M, pH = 7.1
1503	$(NH_3)_5$(py)Ru^{II} + $Cytc^{III}$ → $(NH_3)_5$(py)Ru^{III} + $Cytc^{II}$	H_2O	25	150	4	−17.7 ± 0.8	+35.1 ± 1.7 (a)	374	μ = 0.1 M, pH = 7.1
1504	$Ru(NH_3)_5isn^{3+}$ + $Cytc^{II}$ → $Ru(NH_3)_5isn^{2+}$ + $Cytc^{III}$	H_2O	15	100	4	+14.2 ± 1.5		375	μ = 0.1 M, pH = 7.1
1505	$Ru(NH_3)_5isn^{2+}$ + $Cytc^{III}$ → $Ru(NH_3)_5isn^{3+}$ + $Cytc^{II}$	H_2O	25	100	4	−17.2 ± 1.5		375	μ = 0.1 M, pH = 7.1
1506	$(H_3N)_5Ru^{II}$-(His33)$Cytc^{III}$ → $(H_3N)_5Ru^{III}$-(His33)$Cytc^{II}$	H_2O	25	150	4	−17.7 ± 0.9		376	
1507	$(H_3N)_5Ru^{II}$-(His39)$Cytc^{III}$ → $(H_3N)_5Ru^{III}$-(His39)$Cytc^{II}$	H_2O	25	150	4	−18.3 ± 0.7		376	
1508	$Ru^{II}(NH_3)_6^{2+}$ + (His33)$Cytc^{III}$ → $Ru^{III}(NH_3)_6^{3+}$ + (His33)$Cytc^{II}$	H_2O	25	150	4	−15.6 ± 0.6		376	
	histone $(H2A\text{-}H''B)_2$ dissociation	H_2O	20	220	>10			377	
1509							+90 ± 4 (a)		μ = 0.2 M (NaCl)
1510							+75 ± 5 (a)		μ = 2.0 M (NaCl)
1511	tetramer−dimer equilibrium						+108 ± 4 (a)		μ = 0.2 M (NaCl)
1512	octamer−tetramer equilibrium						+168 ± 6 (a)	379	μ = 2.0 M (NaCl)
1513	octamer−dimer equilibrium						+143 ± 2 (a)		μ = 0.2 M (NaCl)
1514	octamer-dimer equilibrium						+142 ± 2 (a)		μ = 2.0 M (NaCl)
	yeast hexokinase dissociation: P2 monomer−dimer equilibrium	H_2O		280	>6			378	
1515			0				+116 to+154 (a)		pH = 7.5
1516			0				+119 (a)	380	pH = 7.5, 0.1 M Na_2SO_4
1517			30				+167 (a)		pH = 7.5
1518			20				+162 (a)		pH = 7.5
1519			20				+111 (a)		pH = 6.0
1520			20				+155 (a)		pH = 9.0
	P1 monomer-dimer equilibrium								
1521			0				+141 (a)		pH = 7.5
1522			0				+135 (a)		pH = 7.5, 0.1 M Na_2SO_4
	Rb. sphaeroides R-26			300	6−8			379	
1523	$P^+Q_A^-$ → PQ_A					−6.1 ± 0.6			
1524	$P^+Q_B^-$ → PQ_B					−6.9 ± 1.9			
1525	P^R decay (Q_A^-)					−5.7 ± 0.8			

Table 1. (Continued)

no.	reaction	solvent	T, °C	P, MPa	no. of data	$\Delta V^{\ddagger}$, $cm^3\,mol^{-1}$	$\Delta \bar{V}$, $cm^3\,mol^{-1}$ (method)	ref(s)	remarks
	Bioinorganic and Biological Reactions (Continued)								
1526	P^R decay (no Q_A^-)					-0.5 ± 1.0			
	Rps. viridis			300	6−8			379	
1527	$P^+Q_A^- \rightarrow PQ_A$					$+8.5 \pm 0.9$			
1528	P^R decay (Q_A^-)					$+0.4 \pm 0.8$			
	bacteriochlorophyll *a* (pyridine)			300	6−8			379	
1529	Triplett decay					$+2.6 \pm 0.4$			
	inactivation of proteins:								
	cyt $P_{450cam} \rightarrow$ cyt P_{420}	H_2O	20	200	10			380	pH = 7.5, 0.1 M Na_2SO_4
	wild-type protein								
1530	no camphor bound to the active site					-73 ± 1			
1531	camphor bound to the active site					-197 ± 7			
	[Tyr96 → Phe] mutant								
1532	no camphor bound to the active site					-86 ± 7			
1533	camphor bound to the active site					-87 ± 4			
	electron transfer:	H_2O						280	
1534	DCPIP + L-ascorbic acid		25	150		-4.3 ± 1			
1535	cytochrome *c* + L-ascorbic acid		10	190		-16.4 ± 0.8			
1536	HAO + cytochrome *c*		20	100		-24.3 ± 0.4			
1537	$Ru(NH_3)_5isn^{3+} + Cytc^{II} \rightleftarrows Ru(NH_3)_5isn^{2+} + Cytc^{III}$	H_2O	25	200	5		$+26.4 \pm 0.9$ (a)	381	
1538	$(NH_3)_5Ru^{III}$-$Cytc^{II} \rightleftarrows (NH_3)_5Ru^{II}$-$Cytc^{III}$	H_2O	25	200	5		$+31.7 \pm 1.2$ (a)	381	
1539	*trans*-$(NH_3)_4$(isn)Ru^{III}-$Cytc^{II} \rightleftarrows$ *trans*-$(NH_3)_4$(isn)Ru^{II}-$Cytc^{III}$	H_2O	25	200	5		$+21.1 \pm 1.0$ (a)	381	
1540	*trans*-$(NH_3)_4$(py)Ru^{III}-$Cytc^{II} \rightleftarrows$ *trans*-$(NH_3)_4$(py)Ru^{II}-$Cytc^{III}$	H_2O	25	200	5		$+23.3 \pm 0.6$ (a)	381	
1541	*trans*-$(NH_3)_4$(lut)Ru^{III}-$Cytc^{II} \rightleftarrows$ *trans*-$(NH_3)_4$(lut)Ru^{II}-$Cytc^{III}$	H_2O	25	200	5		$+18.6 \pm 0.4$ (a)	381	
	$Cytc^{III} + Ag + Cl^- \rightleftarrows Cytc^{II} + AgCl$	H_2O	25		11			382	1 M NaCl, H = 7
1542				0			−27 (a)		
1543				50			−25 (a)		
1544				100			−23 (a)		
1545				150			−20 (a)		
1546				200			−18 (a)		
1547				250			−15 (a)		
1548				300			−13 (a)		
1549				350			−10 (a)		
1550				400			−7.9 (a)		
1551				450			−5.5 (a)		
1552				500			−3.0 (a)		

[a] Abbreviations: 2a, tricarbonyl[1-4-η-5-exo(*N*-4-formylpyridinio)cyclohexa-1,3-diene]iron; 2b, tricarbonyl[1-4-η-5-exo(*N*-4-formylpyridinio)-2-methoxycyclohexa-1,3-diene]iron; 2c, tricarbonyl[1-4-η-5-exo(*N*-4-formylpyridinio)cyclohepta-1,3-diene]iron; 3a, tricarbonyl[η^5-exo(4-ethylpyridinio)-2-methoxycyclohexa-1,3-diene]iron; 3b, tricarbonyl[η^5-exo(4-ethylpyridinio)cyclohepta-1,3-diene]iron; 4-CHOpy, 4-formylpyridine; [15]aneN$_4$, *trans*-1,4,8,12-tetraazacyclopentadecane; [9]aneS$_3$, 1,4,7-trithiacyclononane; aben, 1,2-bis(*o*-iminobenzylideneamino)ethane; acac, acetylacetone; AcO^-, acetate ion; ado, 5′-deoxyadenosyl (radical); $[AdoCbi]^+OH^-$, adenosylcobinamide; ar (arsenazo III), 3,6-bis(*o*-arsonophenylazo)-4,5-dihydroxynaphthalene; Asc, ascorbate anion; AT, 10-amino-10-methyl-1,4,8,12-tetraazacyclopentadecane; ATA, *N*-acetyl-L-tryptophanamide; ATpCA, *N*-acetyl-L-tryptophan *p*-chloroanilide; ATP, adenosine triphosphate; B, benzidine; B_{12a} and B_{12}, Cob(III)alamin; B_{12}-H_2O^+, aquocobalamin; BHm, Protoheme; bisoxa(DO3A)$_2$, bis(1,4-(1-(carboxymethyl)-1,4,7,10-tetraaza-4,7,10-tris(carboxymethyl)-1-cyclododecyl))-1,10-diaza-3,6-dioxadecane; BO(DO3A)$_2$, 2,11-dihydroxy-4,9-dioxa-1,12-bis[1,4,7,10-tetraaza-4,7,10-tris(carboxymethyl)cyclododecyl]dodecane; bpy, 2,2′-bipyridine; br-acac, 3-bromo-2,4-pentanedione; br-dbm, 2-bromo-1,3-diphenyl-1,3-propanedione; BTE, *cis*-2,2,7,7-tetramethyl-3,6-dithiaoctane; Bu, *n*-butyl; Bu^t, *tert*-butyl; Bz, benzyl; bz, benzene; C222, 4,7,13,16,21,24-hexaoxa-1,10-diazabicyclo[8.8.8]hexacosane; CB, chlorobenzene; H_2cht^{2-}, chromotropic acid (1,8-dihydroxynaphthalene-3,6-disulfonate); Cl-phen, 2-chloro-1,10-phenanthroline; CMP, cytidine-5′-monophosphate; Cndipp, 2,6-diisopropylphenyl isocyanide; CNpy, 4-cyanopyridine; cod, cyclooct-1,5-diene; COD, η^4-1,4-cyclooctadiene; cp, cyclopentadienyl; 18-crown-6, 1,4,7,10,13,16-hexaoxacyclooctadecane; Cry, 4,7,13,16,21-pentaoxa-1,10-diazabicyclo[8.8.5]tricosane; cupf, cupferron (ammonium *N*-nitrosophenylhydroxylamine); cyclam, 1,4,8,11-tetraazacyclotetradecane; cyclen, 1,4,7,10-tetraazacyclododecane; CyDTA, cyclohexyldiaminetetraacetate; cyt *c*, cytochrome *c*; dab, 1,4-diisopropyl-1,4-diazabutadiene; dbm, dibenzoylmethane; dbubpy, 4,4′-di-*tert*-butyl-2,2′-bipyridine; DCA, 9,10-dicyanoanthracene; DCE, 1,2-dichloroethane; DCM, dichloromethane; DCPIP, 2,6-dichlorophenolindophenol; DEA, *N*,*N*-diethylaniline; DEMX, diethyl mesoxalate; d(GpG), dinucleotide; diamsar, $H_2NC(CH_2N(CH_2)_2NCH_2)_3CNH_2$; diamsar$H_2$, $H_3NC(CH_2N(CH_2)_2NCH_2)_3CNH_3^{2+}$; dien, diethylenetriamine; dma, *N*,*N*-dimethylacetoamide; DMA, *N*,*N*-dimethylaniline; DMAD, dimethyl acetylenedicarboxylate; DMMX, dimethyl mesoxalate; dmbpy, 4,4′-dimethyl-2,2′-bipyridine; dmbzim, 5,6-dimethylbenzimidazole; DMF, *N*,*N*-dimethylformamide; H_2dmg, dimethylglyoxime; dmp, 2,9-dimethyl-1,10-phenanthroline; DMpT, *N*,*N*-dimethyl-*p*-toluidine; DMPU, dimethylpropylene urea; DMSO, dimethyl sulfoxide; a-, e-DMSO, axially, equatorially bonded DMSO; dmtf, *N*,*N*-dimethylthioformamide; DOTA, tetraazacyclododecane-*N*,*N*′,*N*″,*N*‴-pentaacetate; dpbpy, 4,4′-diphenyl-2,2′-bipyridine; H_2dpg, diphenylglyoxime; dpp, 2,9-diphenyl-1,10-phenanthroline; dpt, $H_2N(CH_2)_3NH(CH_2)_3NH_2$; DTBN, di-*tert*-butyl nitroxide; DTH, 2,5-dithiahexane; dto, 3,6-dithiaoctane; dtpa, diethylenetriaminepentaacetate; edta, ethylenediaminetetraacetate ion; eddaH_2, ethylenediamine-*N*,*N*′-diacetic acid; edtaH_4, ethylenediaminetetraacetic acid; eee, 1,8-diamino-3,6-dithiaoctane; egly, ethylene glycol; ein, ethane-1,2-diimine; en, 1,2-diaminoethane; Et, ethyl; etbp, 4-ethyl-2,6,7-trioxa-1-phosphabicyclo[2.2.2]octane; Et$_4$dien, 1,1,7,7-tetraethyldiethylenetriamine; Et$_5$dien, 1,1,4,7,7-pentaethyldiethylenetriamine; Et$_2$DTC, diethyldithiocarbamate; etpy, 4-ethylpyridine; FB, fluorobenzene; fod, tris-6,6,7,7,8,8,8-heptafluoro-2-dimethyl-3,5-octanedionate; glyc, glycerol; GlyGlyHis, glycylglycylhistidine; glyH, glycine; gmi, *N*,*N*′-dimethylglyoxal diimine; H_2aeida, *N*-(2-aminoethyl)-*N*-(carboxymethyl)glycine; H_2dmg, 2,3-butanedione dioxime; HAh, acethydroxamic acid; HAO, hydroxylamine oxidoreductase; Hb, human adult hemoglobin; α-Hb, β-Hb, isolated chains of human hemoglobin; HCY, hexamethylcyclam; Hdca, dichloroacetic acid; $Hdcp^{2-}$, 2,6-dicarboxy-4-hydroxypyridine; H_4dfb^+, desferrioxamine B; hedta, *N*-(hydroxyethyl)ethylenediamine triacetate; hfac, hexafluoroacetylacetonate; H(i-dtma), *N*,*N*-bis(2-aminoethyl)glycine; hipt, 4-isopropyltropolone; (His33)cyt, horse heart ferricytochrome *c*; (His39)cyt, *Candida krusei* ferricytochrome *c*; HMN, 2,2,4,4,6,8,8-heptamethylnonane; HMPA, hexamethylphosphoramide; Hr, hemerythrin; Htos, *p*-toluenesulfonic acid; H_2res^{2-}, 1-((2,4-dihydroxy-1-phenyl)azo)-8-hydroxynaphthalene-3,6-disulfonate; HRP, horseradish peroxidase; hxsb, 1,8-bis((2-pyridylmethylene)amino)-3,6-diazaoctane; ibn, $H_2NC(CH_3)_2CH_2NH_2$; H_2salen, bis(salicylidene)ethylenediamine; IHP, inositol hexaphosphate; im, imidazole; IMP, inosine 5′-monophosphate; In, indicator; Ino, inosine; IS, inner sphere (electron transfer); isn, isonicotinamide; isoq, isoquinoline; L, *meso*-5,7,7,12,14,14-hexaamethyl-1,4,8,11-tetraazacyclotetradecane; $LdRu^{II}Ru^{III}$, (μ-2,6-dithiaspiro[3,3]hep-

Table 1. (Continued)

tane)decaamminediruthenium(II,III) hexafluorophosphate; LF, ligand field; Ln, a lanthanide ion; lut, 3,5-lutidine; Ma, 3,7,11-tribenzyl-3,7,11,17-tetraazabicyclo[11.3.1]heptadeca-1,(17),13,15-triene; MA^+, *N*-methylacridinium; Mb, myoglobin (subscripts S, H, D refer to sperm whale, horse, and dog myoglobin respectively); MCH, methylcyclohexane; MCPH, monochelated protoheme; Me, methyl; 3Mebsb, $(C_5H_4N)CPhN(3\text{-}MeC_6H_4)$; Me_2bsb, $(C_5H_4N)CPhN(3,4\text{-}Me_2C_6H_3)$; MeCy, methylcyclohexane; Medpt, $H_2N(CH_2)_3NMe(CH_2)_3NH_2$; Medtra, *N*-methylethylenediaminetriacetate; MeIm, 1-methylimidazole; 3-MP, 3-methylpentane; Me_5dien, 1,1,4,7,7-pentamethyl-dien; Medpt, $H_2N(CH_2)_3NCH_3(CH_2)_3NH_2$; 4-MeObsb, $(C_5H_4N)CPhN(4\text{-}CH_3OC_6H_4)$; MES, 2-morpholinoethanesulfonic acid; met, L-methionine anion; 1-MeU, 1-methyluracil; Mhr, myohemerythrin; MLCT, metal-to-ligand charge transfer; MNZ, metronidazole; MOPS, 3-morpholinopropanesulfonic acid; MPI, *p*-methylphenyl isocyanide; N_4, 2,3,9,10-tetraphenyl-1,4,8,11-tetraaza-1,3,8,10-cyclotetradecatetraene; NADH, nicotine amide adenine dinucleotide; n-acac, 3-nitro-2,4-pentanedione; N−C, $C_6H_4CH_2NMe_2$-2; N−C−N, $C_6H_3(CH_2NMe_2)_2$-2,6; N-eten, *N*-ethylethylenediamine; nox, 1,2-cyclohexanedione dioxime; Np, neopentyl; nta, nitrilotriacetate; NZ, $Me_2N(CH_2)_2NCH(C_6F_4)(CF_3)C_\beta{=}C_\alpha(CF_3)$; OS, outer sphere (electron transfer); pa, *n*-propylamine; Pada, *trans*-pyridine-2-azo(*p*-dimethylaniline); PCO, CO bond to heme iron; P•CO, geminate state after bond dissociation; PCy_3, tricyclohexylphosphine; PCy_2Ph, dicyclohexylphenylphosphine; PDTA, 1,3-propylenediamine-*N*,*N*,*N*′,*N*′-tetraacetate; PFe, ferric porphyrin; Ph, phenyl; PHDME, protoheme dimethylester; phdta,$^{4-}$ *o*-phenylendiamine-*N*,*N*,*N*′,*N*′-tetraacetate; phen, 1,10-phenanthroline; pip, piperidine; piv, pivalate ion; PMMA, poly(methyl methacrylate) polymer; P_n, linear phosphate oligomer, polymerization degree *n*; P_{nm}, cyclic phosphate oligomer, polymerization degree *n*; pp_3, tris(2-(diphenylphosphine)ethyl)phosphine; ppa, μ-1-$(NH_2NCH_2)(C_5H_4N)_2$; PPh_3, triphenylphosphine; Pr, propyl; Pr^i, isopropyl; ptsa, *p*-toluenesulfonic acid; py, pyridine; pyBimH, 1-$(CNNHC_6H_4)(C_5H_4N)$; pyimH, 1-$(CNNHC_2H_2)(C_5H_4N)$; py-SO_3, $NC_5H_4SO_3$-3; pz, pyrazine; pzc, pyrazinecarboxylate; Qui, quinoline; RB_{12}, alkylcobalamin; R_1-en, (1*R*,2*R*,4*S*)-exo-2-(aminomethyl)-2-amino-7-oxabicyclo[2.2.1]heptane; S, solvent; Sacac, thioacetylacetone; SA_1pNA, succinyl-L-alanine *p*-nitroanilide; SA_2pNA, succinyl-L-alanyl L-alanine *p*-nitroanilide; SA_3pNA, succinyl-L-alanyl L-alanyl L-alanine *p*-nitroanilide; SarH, sarcosine; sep, $N(CH_2N(CH_2)_2NCH_2)_3N$; tacpa, 10-methyl-1,4,8,12-tetraazacyclopentadecan-10-amine; TANONE, 2,2,6,6-tetramethyl-4-oxo-1-piperidinyloxyl; TAPP, *meso*-tetrakis(*N*-trimethylammoniumphenyl)porphine; taud, 3,6,9-triazaundecanedioate; TCA, 2,6,9,10-tetracyanoanthracene; tc-acac, 3-thiocyanato-2,4-pentanedione; tc-bzac, 2-thiocyanato-1-phenyl-1,3-butanedione; TCE, *sym*-tetrachloroethane; TCNE, tetracyanoethene; TEMPO, 2,2,6,6-tetramethylpiperidine 1-oxide; terpy, 2,2′:6′,2″-terpyridine; 2,3,2-tet, 1,9-diamino-3,7-diazanone; 3,2,3-tet, 4,7-diaza-1,10-decanediamine; tetren, $H_2N(CH_2)_2NH$ $(CH_2)_2NH(CH_2)_2NH(CH_2)NH_2$; tfac, 1,1,1-trifluoro-2,4-pentanedione; TFBA, trifluorobenzoylacetone; tfbzac, 4,4,4-trifluoro-1-phenyl-1,1-butanedione; TH, triflic acid; THF, tetrahydrofuran; TMB, *N*,*N*,*N*′,*N*′-tetramethylbenzidine; tmc, 1,4,8,11-tetramethyl-1,4,8,11-tetraazacyclotetradecane; TMCH, 3,3,5,5-tetramethylcyclohexanone; tmd, 1,3-propanediamine; tmen, 2,3-diamino-2,3-dimethylbutane; TMP, trimethyl phosphate; 2,2,4-TMP, 2,2,4-trimethylpentane; TMPA, $(MeO)_3PO$; TMPNO, 2,2,6,6-tetramethylpiperidinyloxyl radical; TMPP, *meso*-tetrakis(4-*N*-methylpyridyl)porphine; tmtu, tetramethylthiourea; TMS, tetramethylsilane; TMU, tetramethylurea; tn, trimethylenediamine; tpchxn, tetrakis(2-pyridylmethyl)-*trans*-1,2-cyclohexanediamine; tpmbn, μ-$CH_2(CH_3)CH(CH_3)[\mu\text{-}1\text{-}N(CH_2)_2(C_5H_4N)_2]_2$; TPP, 5,10,15,20-tetraphenylporphyrin; tppn, μ-$CH_2CH(CH_3)[\mu\text{-}1\text{-}N(CH_2)_2(C_5H_4N)_2]_2$; TPPS, *meso*-tetrakis(*p*-sulfonatophenyl)porphinato; 2,3-tri, $NH_2(CH_2)_3NH(CH_2)_3NH_2$; tren, *tris*-(2-aminoethyl)amine; trien, 1,8-diamino-3,6-diazaoctane; triflic, trifluoromethanesulfonic acid; tris, tris(hydroxymethyl)aminomethane; tta, 4,4,4-trifluoro-1-(2-thienyl)-1,3-butanedione; TU, thiourea.

limited number of laboratories. In this section the extensive variety of metal centers, noncoordinating ligands, and solvents leads naturally to a discussion of individual systems proceeding mostly in terms of an order arranged by increasing magnitude of the atomic number of the metal center rather than by mechanistic similarity.

In a study employing six different solvents coordinating to the Be(II) ion (entries 1−6), the exchange of five could be monitored by proton NMR, while exchange of H_2O was followed using ^{17}O NMR spectroscopy.[59] The kinetics were followed in the presence of a noncoordinating diluent CD_3NO_2, and a two-term rate law described the exchange process. The results could be analyzed to conclude that the series is subject to a sterically controlled mechanistic changeover from an A mechanism for the smallest solvent water to a D mechanism for the most bulky tetramethyl- and dimethylpropyleneurea, with the other three solvents exhibiting small negative $\Delta V^{\ddagger}$ values between these extremes.

Attention has been directed to solvent exchange on titanium(III) and titanium(IV) species[61−63] (entries 8−12). Water exchanges on hexaaqua titanium(III) by an A mechanism, and the volume of activation is close to that calculated on a theoretical basis for such a mechanism,[61] whereas DMF exchanges on $Ti(DMF)_6^{3+}$ less associatively and therefore by an I_a mechanism.[63] This latter result allows the observation that there is a mechanistic shift for solvent exchange on first row transition metal ions in oxidation state three, since exchange becomes progressively less associative as the radius becomes generally smaller as the atomic number of the metal increases. Both axial and equatorial exchange of DMSO from $TiO(DMSO)_5^{2+}$ occur with an expanded transition state;[62] the faster axial exchange is proposed to proceed by a D mechanism, while the loss of an equatorial DMSO is in concert with an axial to equatorial coordinated solvent migration. Exchange of solvent (S) on *cis*-$TiCl_4$·2S complexes (entries 13−15) proceeds by a D mechanism[64] (a striking contrast to similar reactions with zirconium complexes[82,83] (vide infra) in which bond making is occurring as the transition state is formed).

The exchange of DMSO on $V(DMSO)_6^{3+}$ (entry 16) proceeds by an I_a mechanism[65] as for exchange of H_2O on the same metal ion,[390] and as mentioned earlier there is a pattern of progressively less associative exchange reactions across the first row of transition trivalent metal ions (where measurable); for example, the exchange of trimethyl phosphate (TMP) on $Sc(TMP)_6^{3+}$ (entry 7) has been described as occurring by a limiting A mechanism, or by a mechanism near to a limiting A. This is related to the larger radius of the first transition metal.[60] Indeed this trend is a general observation for solvent exchange on divalent metal ions too, unless special steric effects impose differences (see also below). However, it should be emphasized that the only solvated trivalent metal ion for which a distinctly positive $\Delta V^{\ddagger}$ has been obtained is Ga(III), a main group element. The exchange of water on $Ga(H_2O)_5(OH)^{2+}$ is more dissociatively activated than is the hexaaqua Ga(III) ion (entries 46 and 47).[81] In contrast to the exchange of the

smaller H_2O, CH_3CN and CH_3OH on hexasolvated Mn(II) ions ($\Delta V^{\ddagger}$ negative)[390−393] the exchange of acetic acid has a modestly positive $\Delta V^{\ddagger}$ value in two different media (entries 22 and 23),[70] and therefore is in common with the exchange of DMF on $Mn(DMF)_6^{2+}$ (entries 18−20).[67−69] It is argued that the relative bulkiness of the latter two ligands is responsible for the less associative and even slightly dissociative interchange processes on their part. This steric feature is demonstrated markedly when the thio analogue of DMF is the exchanging solvent since the volume of activation is 8−10 $cm^3\ mol^{-1}$ more positive in value for exchange on Mn(II) and Ni(II)[69] (entries 21, 33, and 34) than for exchange of DMF on the same ions (entries 18−20).[67−69] Attempts to correlate $\Delta V^{\ddagger}$ with the partial molar volumes of the leaving groups were somewhat thwarted by the finding of an almost constant $\Delta V^{\ddagger}$ for several exchanging (on Ni(II)) nitriles (RCN) of considerable variation in magnitude of the R moiety (entries 37−42).[77] This study highlighted the lack of match between $\Delta V^{\ddagger}$ and $\Delta S^{\ddagger}$. A parallel between these two parameters could be expected on a superficial basis, and is noted in some cases. All the nitriles exchange with a $\Delta V^{\ddagger}$ that is distinctly positive, ca. 12 $cm^3\ mol^{-1}$, but the $\Delta S^{\ddagger}$ values vary between −30 and +4 $J\ mol^{-1}\ K^{-1}$. The interactions of the departing, exchanging nitriles with like molecules of the second coordination sphere are cited as the cause of the negative entropies of activation.

Volumes of activation are close to zero for exchange of ethylenediamine on the tris en complex ions of Mn(II), Fe(II), and Co(II) but a value of +11.4 $cm^3\ mol^{-1}$ was recorded for the corresponding nickel species (entries 24, 25, 30, and 43).[71,78] In the latter case the increase in volume upon reaching the transition state was proposed to be followed by the formation of an intermediate in which two en molecules are each bonded to the $Ni(en)_2^{2+}$ species in a monodentate mode. On the basis of an analysis of the rate constants, thermal activation parameters, the volumes of activation, the estimated ring opening and closure rates, and the corresponding results for the exchange of the similar ligand 1,3-diaminopropane,[74] which yields three six-membered rings on Co(II) (entry 31), it was concluded that effects termed the kinetic chelate effect and the chelate strain effect could be invoked to explain the overall findings. Efforts to explore the effect of a nonexchanging multidentate ligand on exchange of water (entries 26 and 27) on Fe(III) have been reported;[72,73] a dissociative interchange mechanism is found for both H_2O and DMF exchange.

Study of the exchange of solvent on hexasolvated Cu(II) is complicated by the consequences of Jahn−Teller distortion. It prevails that the rate of inversion is rapid compared with the rate of DMF exchange and the latter (entry 44) is a dissociative interchange process.[79] Lability of coordinated water can be drastically affected by the geometry of a copper(II) complex ion, as witnessed by the lowering by 3 orders of magnitude of the water exchange rate constant on the trigonal-bipyramidal $Cu(tren)H_2O^{2+}$ ion from that for the hexaaqua $Cu(H_2O)_6^{2+}$ ion. The water exchange on the tren complex ion (entry 45) proceeds by an associative interchange mechanism.[80]

Ligand exchange on tetrachloro zirconium complexes (entry 48) in a noncoordinating solvent is characterized by a strongly associative mechanism reflecting the accessibility to the incoming ligand with increasing radius[82,83] (cf. titanium complexes,[64] entries 13−15).

The possible compensating effects of several contributing volume changes in the exchange of acetyl acetonate on a molybdenum−oxo complex (entry 49), create difficulty in interpreting the zero volume of activation obtained.[84] Further this study points to the complexities arising in exchange studies of bidentate ligands. Clearly the analysis of any measured volume changes for kinetics of exchange of higher dentate ligands would probably be equally or more complicated.

Hexasolvated ruthenium(II) complexes of either H_2O or CH_3CN exchange solvent by an almost pure interchange mechanism (entries 51 and 54).[86] The same holds for water exchange on $Ru(H_2O)_5(OH)^{2+}$ (entry 53), whereas there is significant associative character in the exchange of water on $Ru(H_2O)_6^{3+}$ (entry 52), and moderate associative interchange of the water exchange on $Ru(NH_3)_5H_2O^{3+}$ (entry 50).[85] The structure of the nonexchanging component of the complex ion has important consequences: this is manifest in the exchange of CH_3CN on ruthenium complexes (entries 56 and 57) in which the benzene complex exchanges coordinated CH_3CN with solvent by an interchange mechanism but the latter complex (entry 57) undergoes exchange by a fully dissociative mechanism.[88] The aqueous analogue (entry 55) exchanges water by a mechanism in which bond breaking is only slightly more significant than bond making.[87]

Water exchange on aqua rhodium(III) has been determined as a function of acid concentration,[89] allowing the kinetic and activation parameters for the water exchange on both the hexaaqua- and the monohydroxopentaaquarhodium(III) species (entries 59 and 60) to be determined. The results imply an associative interchange mechanism for the former ion and an interchange mechanism with a slight dissociative character for the $Rh(H_2O)_5(OH)^{2+}$ species which is strongly labilized by the presence of the OH group. The reaction volume ($-0.2 \pm 0.5\ cm^3\ mol^{-1}$) for deprotonation of the hexaaquarhodium(III) ion, obtained potentiometrically, was also reported.

Water exchange on the $Cp^*Rh(H_2O)_3^{2+}$ complex ion (entry 61) is modestly dissociative in interchange character,[90] as is water exchange on the corresponding iridium species (entry 93).[90] The properties and reactivities of palladium and platinum complexes are frequently compared and contrasted. For a wide variety of nonexchanging ligands on the central palladium(II) ion (entries 63−66) the solvent exchange is associative.[92−94] In cases where the solvents used are common the exchange is often more markedly associative in the case of Pt complexes than for Pd complexes (entries 67−73 and 96−99),[94,95] undoubtedly resulting from a radius increase down the group.

Complexes of gadolinium(III) are prominent in the search for improved magnetic resonance imaging materials. Investigating the water exchange kinetics on such complexes is an integral component of determining their potential efficacy through measurement of properties such as the relaxivity.[96] The design of newer agents may in part be based on the extent to which steric crowding by noncoordinating ligands of the exchanging water molecule may enhance the degree of dissociative mechanistic character. The complexes studied thus far (entries 74−79), exchange water by an interchange, a dissociative interchange or a dissociative mechanism.[96−99] Water exchange on fully hydrated lanthanide ions (entries 80, 82, 84, 85, and 87) is characterized uniformly by an associative interchange mechanism.[100,101] Upon complexing the ions with propylenediamine tetraacetic acid, water exchange is dramatically decelerated across the series (entries 81, 83, 86, 88, and 89) accompanied by a change of mechanism from an associative to a dissociative one.[102]

An examination of the kinetics of exchange of H_2O or CH_3CN on a *trans*-Os complex (entries 91 and 92)[103] led to the conclusion that solvent exchange occurs by a dissociative or dissociative interchange mechanism. In this report other complementary results (references *loc. cit.* therein) were evaluated and interpreted to show that ligand substitution on such species occurs with rate-limiting loss of a coordinated solvent molecule.

Some final examples in this section illustrate the variety of solvent exchange studies reported over this period: $Ir(H_2O)_6^{3+}$ exchanges water with solvent *extremely* slowly, by an I_a mechanism,[104] while the exchange on the deprotonated analogue occurs via an I_d mechanism (entries 94 and 95). Whether DMSO is coordinated through oxygen or sulfur the exchange on $Pt(DMSO)_4^{2+}$ is associatively activated[105] (entries 100 and 101), whereas exchange of Me_2S or DMSO on the platinum complexes of entries 102−104 is dissociatively activated,[106] suggesting that the presence of platinum to carbon bonding has a significant effect in changing the activation mode. The oxo uranium complexes (entries 105 and 106) exchange the equatorial ligands with two different mechanisms, TMPA by a D mechanism and HMPA by an A mechanism.[107] The axial oxo ligands do not exchange on the NMR spectroscopy time scale.

B. Ligand Substitution Reactions

This is a subheading forming an umbrella under which many variants of ligand substitution reactions are grouped. More than 400 entries are contained in this section, reflecting an abundance of investigations from several laboratories. The substitution can be of one ligand for another where neither is the solvent (ligand for ligand substitution), it can be substitution where one or more ligands attached to a metal center is/are replaced by one or more solvent molecules (for example aquation, solvolysis, base hydrolysis; it is recognized that these reactions may also be classified as metal complex dissociation reactions), or it can be a reaction of a solvated metal ion in which one or more coordinated solvent molecules is/are replaced by one or more other ligands (complex formation or anation). Thus the products and the reactants are different unlike the case for solvent exchange reactions. Therefore, in a volume sense these reactions have an additional component of considerable interest, since the partial molar volumes of reactants and products will differ except by the (unlikely) coincidence that they would be identical. Thus, as with all other reactions from this point in the discussion, except for electron self-exchange reactions, the volume profile, if available, will consist of volumes of activation in both directions, and the reaction volume. The latter may be obtained directly or indirectly depending on the kinetic accessibility and other properties of the system. In favorable examples, the volume profile can be developed on an absolute scale rather than only on a relative volume basis, when direct measurements of densities of reactants and products can be made. This narrative section will, when appropriate, focus on some examples of particular subclasses of ligand substitution reactions but the table follows the order of the atomic number of the central metal and the reaction entries in the table are not further divided into subclassifications. When a literature report contains results that fit more than one subcategory, for example a reversible complex formation/aquation reaction then these results will be considered together in one point in the narrative. The subclassifications are base hydrolysis, aquation and solvolysis, complex formation reactions, and ligand for ligand substitution.

a. Base Hydrolysis

Hydrolysis of chromium(III) pentaammine complexes[118] in which the unhydrolyzed ligands are of higher dentate than one and the sixth, departing ligand is Cl^- and is characterized by large positive $\Delta V^{\ddagger}$ values (entries 141−145). The reaction volume for the preequilibrium step that involves the formation of the conjugate base species could be estimated to be 22 $cm^3\ mol^{-1}$, giving rise to $\Delta V^{\ddagger}$ values for the rate determining ligand substitution step ranging from −5 to +13 $cm^3\ mol^{-1}$, signifying a mechanistic changeover from I_a to I_d or D throughout the series for substitution on the conjugate base species. The outcome of the competition between the Cr−Cl bond breakage and the addition of solvent is controlled by the nature of the nonsubstituting ligands to the extent that when the ligands cause steric hindrance a more dissociative mechanism is promoted. The results[121] for base hydrolysis of some halopentaammine and related complexes of Cr(III) (entries 160−163) in some of which the nonhydrolyzing ligands are aliphatic amines also indicate an associative interchange is occurring, underlining the difference, albeit not major from similar reactions for cobalt(III) complexes.[120a]

Several studies have been reported of base hydrolysis on iron(II) tris diimine complexes and a related complex (entries 202, 273−276, 279−301, and 308−317)[136,149,150,153] in aqueous medium and in mixed solvents. The kinetics are indicative of an associative nucleophilic attack, and the positive volumes of

activation have been interpreted as a negative intrinsic component being overshadowed by a large electrostriction decrease due to the desolvating hydroxide ion.[394] The values of $\Delta V^{\ddagger}$ in water are within a small range, supporting this essentially common contribution, independent of the complex ion. The influence of the complex ion, in terms of the hydrophobic/hydrophilic balance of the periphery having contact with the solvent, on the values of $\Delta V^{\ddagger}$ obtained, has been probed by determining $\Delta V^{\ddagger}$ in mixed solvents. In addition, the transfer chemical potentials (for transfer from water to mixed solvents of the same composition), of both reactant species and for the transition state have been determined.[395−397] These potentials provide a measure of the change of solvation of species with change in the solvating medium, and therefore can be correlated with variations in $\Delta V^{\ddagger}$ with solvent composition. Changes in the latter can be quite dramatic and vary considerably with the nature of the cosolvent. For example, the value of +16.7 cm^3 mol^{-1} for hydrolysis of the Fe(II) complex containing three small gmi ligands[150] is reduced to about one-quarter of that value by the presence respectively of 80%, 50%, 60%, and 50% (vol %) methanol, ethanol, 2-propanol, and *tert*-butyl alcohol. For the iron(II) complex of the hexadentate hxsb ligand, similar but more marked trends are observed with $\Delta V^{\ddagger}$ varying from +13 cm^3 mol^{-1} to small negative values in similar solvent mixtures.[153] These trends can be understood in terms of the solvation differences in species and by consideration of the characteristics of the solvent mixtures which possess typically aqueous properties but experience water structure making and breaking at different mole fraction points depending on the alkyl moiety of the alcohol. However, the overall complexity of such systems and the need to establish carefully the rate law and products under all conditions precludes a general application of the mixed-solvent approach, although in appropriately chosen cases instructive findings can be acquired.

The kinetics and mechanism of base hydrolysis of Co(III) pentaammine complexes have fascinated for decades, and have been compared with and contrasted to those of corresponding reactions of Cr(III) complexes. The conjugate base mechanism gives rise to complications, but not insurmountable ones, in interpretation of measured $\Delta V^{\ddagger}$ values. The distinctly positive values (entries 352−368) can be explained[163] by charge neutralization and release of a solvent molecule in the preequilibrium conjugate base formation step and ligand dissociation in the rate-limiting step. Although a wide selection of the nonhydrolyzing ligands was employed the results indicated a relative insensitivity to their nature. Overall the results are compatible within the accepted S_N1CB mechanism for these reactions. Volume profiles were developed. Other examples of base hydrolysis in which the spectator ligand is a macrocycle[117,156] (entries 321, 325, and 327) illustrate mechanistic similarity between the reactions of the Cr(III) (entry 140)[117] and Co(III) complexes, whereas the corresponding rhodium(III) complex[117] (entry 477) has a less positive value of $\Delta V^{\ddagger}$ and was accordingly assigned to a limiting case of an interchange conjugate base mechanism.

b. Aquation and Solvolysis

Empirical volumes of activation have been obtained for the cyclic and linear condensed phosphate oligomers, with polymerization degrees of six and eight, undergoing hydrolysis in acidic solution (entries 117−120). Each reaction, regarded as a nucleophilic attack by a water molecule is characterized by a small decrease in volume upon reaching the transition state. This is explained by proposing that a hydrating water molecule, loosely bound in the initial state becomes more tightly bound to the phosphorus atom in the transition state.

A parallel has been pointed out between the aquation reactions of the V(III) (entry 122)[111] and Fe(III) pentaaqua thiocyanate[152] (entry 302) complex ions in that both are characterized by $\Delta V^{\ddagger}$ values of −17 cm^3 mol^{-1}, suggesting a mechanistic similarity between the two systems and difference from aquation reactions of Cr(III) and Co(III) pentaammine complexes.

The aquation in mildly acidic medium of chromium(III) pentaammine complexes (entries 149−159) containing neutral leaving groups is characterized by small negative $\Delta V^{\ddagger}$ values which do not readily relate to the size of the leaving group.[120] An I_a mechanism distinguishes the intimate mechanism from that (I_d) for analogous cobalt(III) complexes.

Solvolysis of pentacyano iron(III) nitrite[140] (entries 213−217) has been studied in several solvents, and the rate constants for replacement of nitrite correlated with the electron donor ability of the solvent. It was concluded on the basis of the values of $\Delta V^{\ddagger}$ and other considerations that the solvents interact with the cyanide ligands and increase the electron density on the metal center and contribute to inducing a dissociative mechanism.

Cobalt(III) pentaamine complexes (entries 382−395) in which the sixth position is occupied by carboxylic acids have also been the subject of an aquation (in acidic solution) kinetics study.[166] Values of $\Delta V^{\ddagger}$, not unexpectedly, vary according to whether the departing species is the neutral acid or the anionic form. In the latter case there is charge separation and enhanced electrostriction, resulting in more negative $\Delta V^{\ddagger}$ values than when the unionized acid departs. For both cases an interchange mechanism was proposed. The solvolysis of a dichlorobisethylethylenediamine Co(III) complex (entries 374−379) has been monitored in water and water/*tert*-butyl alcohol mixtures.[164] The solvolysis of the second chloro ligand can be suppressed by employing a medium of pH less than 3. The variation in $\Delta V^{\ddagger}$ with solvent composition is small; however, the nature of the variation and the fact that the rate-determining step involves the extension of the cobalt−chloro bond in the transition state (an I_d mechanism) prompted the authors to comment on the similarity to the S_N1 mechanism for the solvolysis of *tert*-butyl chloride (extension of a C−Cl bond in the transition state) in the same solvent mixtures. Aquation studies[160−162] on this and related dichloro complex ions and $Co(en)_2(NH_3)X^{2+}$ where X = Br, Cl, or NO_3

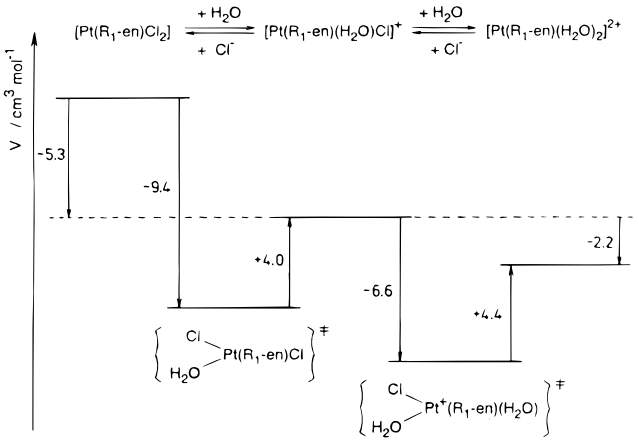

Figure 1. Volume profile for the two-step reversible aquation of [Pt-(R_1en)Cl_2]. First step is at 311.3 K, and the second step, at 279.0 K. (From ref 205.)

yield reaction volumes and activation volumes that led to the conclusion that the entering water and leaving halide ion participate almost equally in the transition state in the ligand interchange process (entries 334−350). It was also noted that among the latter group of complexes $\Delta V^{\ddagger}$ was essentially temperature independent.

Solvolysis of a palladium(II) complex of pentamethylated dien and one pyridine ligand[193] by six different solvents (entries 532−537) proceeds in each case by an associative process with no immediately obvious correlation between $\Delta V^{\ddagger}$ and any property of the solvents. The aquation and the reverse process of anation of *rac*-Pt(R_1-en)Cl_2 (entries 581−584) occur in two steps each possessing transition states of smaller volume than either reactant or product,[205] as illustrated in Figure 1, with the consequence of an I_a mechanism for both steps in the forward direction.

c. Complex Formation Reactions

The reaction under entry 107 is believed to be the first report[108] of volume of activation and reaction volume data for ligand binding and ligand dissociation from an aqua beryllium ion, and therefore is described in some detail. The keto oxygen of the bidentate ligand is thought to bind first and the subsequent (fast) chelate ring closure reaction is accompanied by release of a proton. The first step, based on a negative $\Delta V^{\ddagger}$ value, proceeds by an associative mechanism. Since the reaction volume for proton dissociation from the ligand has been determined to be -8.2 cm^3 mol^{-1}, this allows the reaction volume for the reaction of the deprotonated ligand with the Be(II) aqua ion to form the monopositively charged aqua Be(ipt)$^+$ species to be calculated as $+13.5$ cm^3 mol^{-1}. In the reverse direction the first step is the preequilibrium protonation of the latter species to form the dechelated species with only one of the ligand oxygen atoms bonded to the beryllium atom. It is argued that if this species has the same volume as the original separated reactants (for the forward reaction), then the activation volume for the rate-determining step of the reverse reaction is also negative and indicative of associative activation.

There are many interesting features[109] in the reactions of entries 108−110. The first two reactions are accompanied by a change in coordination number on boron, and therefore, the coordination geometry. The trigonal to tetrahedral conversion on B (sp^2 to sp^3 hybridization) results in an extension of the B−O bond length, but this contribution is overshadowed by the presence of the incoming ligand in an associative mode of activation. The reverse reactions are also of associative mechanistic character. The third ligand, a tridentate, is considered to bind with the final chelate ring closure as the rate-determining step.

In the process of development of a high-pressure stopped-flow fluorometer[42] the reaction of Mg^{2+} ions with 8-hydroxyquinoline (entries 111−116) was examined as a suitable standard kinetics test for the fluorescence mode and compared with the same reaction in a stopped-flow spectrophotometer (absorbance mode). In an excess of metal ion only the 1:1 complex is formed and the second-order rate constants at pH of 8.0 and 278 K are 3.81×10^3 mol^{-1} dm^3 s^{-1} (absorbance) and 3.69×10^3 mol^{-1} dm^3 s^{-1} (fluorometer) and experimental $\Delta V^{\ddagger}$ values of -3.1 ± 0.4 and -3.6 ± 0.5 cm^3 mol^{-1}, respectively were obtained. Thus this reaction system is very well suited for use as a standard reaction.

Formation of the SCN^- complex of V(III) in both water and DMSO solutions (entries 121−125) occurs by an I_a mechanism, which in the case of aqueous solution is regarded as a stronger associative activation than for the corresponding V(II) system. The reaction volumes are distinctly positive which can be understood in terms of the release of electrostricted solvent upon charge neutralization. The associative interchange mechanism is consistent with the information afforded from an earlier water exchange mechanistic study.[397] There is a mechanistic changeover from I_a to I_d as the first row of transition elements, in oxidation state three, is traversed to the representative Ga^{3+} ion.

Entry 194 and entries 260 and 318 may be grouped together.[132] Introduction of the Et_2DTC^- ligand to DMF solvated Mn(II), Fe(II), and Co(II) ions follows a dissociatively activated mechanism, by virtue of the strongly positive activation volumes. Indeed the values led to the suggestion that the DMF solvates are sterically bulky so that an associative mode of activation is not applicable even for the larger Mn cation. This is in contrast to solvent exchange on these cations for smaller solvent molecules where there is a mechanistic changeover from I_a to I_d across the first row of transition metals as noted in section 2.A. However, the trend in values here indicates a possible shift from I_d for Mn to a D mechanism for reaction of the other two cations. Formation and dissociation of the Pada complex on the DMF Fe(II) solvate (entries 261 and 262) also proceed by dissociative mechanisms.[132]

Although the kinetics at elevated pressures of formation of $Fe(H_2O)_5NCS^{2+}$ and the corresponding deprotonated species, $Fe(H_2O)_4(OH)NCS^+$ have been studied previously they were reinvestigated (entries 302 and 303) to resolve discrepancies in the literature.[152] The latest values of $\Delta V^{\ddagger}$ are -5.7 and $+9.0$ cm^3 mol^{-1} respectively for formation of the two

species and reflect I_a and I_d mechanisms. See also the discussion in the aquation section regarding the comparison of the aquation reactions of pentaaqua V(III) and Fe(III) thiocyanate complexes. In the reaction of Fe(III)aq with HN_3/N_3^- (entries 304−307) two pathways predominate: $Fe(H_2O)_5(OH)^{2+}$ reacting with N_3^- and with HN_3. The respective values of $\Delta V^{\ddagger}$ are +12.9 and +6.8 cm^3 mol^{-1},[152] both of which denoted I_d mechanisms to be operative.

The nucleophilicity of the ligand effects mechanistic control for reactions of the ClO_2^- (entry 197),[134] N_3^- (entries 304−307),[152] and NCS^- (entries 302 and 303) ions with aqua iron(III) ions. The overall reaction is described as conjugate acid/conjugate base. The first two ions react by an I_d mechanism and the last by an I_a mechanism. A reaction volume of +7.8 cm^3 mol^{-1} has been determined for the reaction shown in entry 195. As described[133] this value together with other data allowed the calculation of the activation volume for entry 196. This in turn it was argued, confirmed that the ligand reacts with aqua iron(III) by an I_a mechanism. A reaction volume (+2.8 cm^3 mol^{-1}) was reported for protonation of Hipt.

The stepwise dissociation (by aquation) and formation of Ah complexes of Fe(III) are controlled by the presence of OH^- or Ah^- in the coordination sphere (entries 263−270).[148] Analysis of the activation volumes led to the conclusion that the catalyzed hydrolysis of the tris Ah complex undergoes a mechanistic changeover from I_a to I to I_d for the successive steps, a sequence that is reversed for reaction in the reverse direction. The reaction of dfb in tetraprotonated form with the hexaaquairon(II) species is accelerated by pressure, whereas when dfb in the same form reacts with the deprotonated form of the iron species the reaction is retarded by pressure (entries 271 and 272) resulting in volumes of activation of opposite sign, suggesting that the two reactions proceed by I_a and I_d mechanisms, respectively.[149] Under the experimental conditions H_4dfb binds only as a bidentate ligand.

The complications of ion pairing and electrostriction changes were discussed in a study[162] of the anation reactions of *cis*-$Co(en)_2(H_2O)_2^{3+}$ by sulfate ions or by selenate ions (entries 351−354). However, following due consideration of these features it was possible to assign dissociative mechanisms to these reactions as well as for the reverse solvolysis reactions and furthermore for the trans to cis isomerization[162] of *trans*-$Co(en)_2(H_2O)OSeO_2H^{2+}$ (entry 846, see also section 2.F).

Reaction volumes for formation of complexes of nickel(II) with either anionic or neutral ligands have been determined (entries 413−420).[171] In general the values are more positive as the extent of charge neutralization increases. However, in addition to electrostriction changes a detailed explanation involved the difference between oxygen and nitrogen donors, contraction of donor atoms in the first coordination sphere, expansion due to metal−water bond elongation caused by the presence of bound amine(s) or carboxylate groups, and what is termed the volume chelate effect which envisages a different packing by multidentate ligands vis a vis monodentate ligands.

Expectation was fulfilled when the activation volumes for reaction of 2-chloro-1,10-phenanthroline with the hexaaqua ions of Co(II) (entries 319 and 320),[154] Ni(II) (entries 411 and 412),[154] and Cu(II) (entries 430 and 431)[172] were determined, since their anticipated positive values indicated an I_d mechanism as had previously been invoked for the corresponding reaction of hexaaqua Zn(II) ions.[172]

Reaction volumes obtained for the formation of mono, bis, and tris phen complexes of Cu(II) and for the formation of both the phen and bpy mono, bis, and tris complexes of Zn(II) (entries 432−440) show[173] the general feature of successive replacement of coordinated water giving rise to progressively smaller positive volume changes. This was explained by suggesting that the substitution of electrostricted coordinated water by neutral ligands is accompanied by a volume increase but that the solvent release proceeds only as far as the second coordination sphere. It should be noted that the volume changes for comparable systems do not exhibit a particularly systematic quantitative pattern.

The formation of the mono bpy complexes of Zn(II) and Cd(II) aqua ions (entries 443 and 555)[166,174] provides excellent straightforward examples of both size influence on mechanistic determination and of complementariness of activation volume and reaction volume measurements. An improved access to the coordinated solvent by the ligand in the outer sphere permits an I_a mechanism for formation of Cd(bpy)-$(H_2O)_4^{2+}$, a process not possible one period higher in formation of the analogous Zn(II) complex which is formed from a smaller hexaaqua ion, resulting in an I_d mechanism. Figure 2 displays the volume profiles for these two complexes. The approach used in estimating the volume change in forming the outer-sphere complex has been presented earlier. The mechanism proposed for the zinc complex formation is entirely consistent with recent calculations for water exchange on $Zn(H_2O)_6^{2+}$ reported earlier in this review.

A series of ligands has been chosen for displacing the water in both Ru(edta)$(H_2O)^-$ and in Ru(hedta)-$(H_2O)^-$ (entries 460−472):[179,180] the outcome is a markedly rapid substitution in the former case which was suggested to be due to distortion of the metal−ligand bonds and labilization of the coordinated water molecule arising from H-bonding between the free carboxylate and the coordinated water. Both sets of reactions proceed by an associatively activated substitution process based on the interpretation of the $\Delta V^{\ddagger}$ values.

An interesting illustration of the finesse of high-pressure kinetics vis a vis variable-temperature kinetics is in the substitution of bound water in *trans*-rhodoximes by various nucleophiles (entries 486−489).[183] Whether the organic moiety is varied or not for a given nucleophile all reactions studied were characterized by moderately negative entropies of activation. However, the values of $\Delta V^{\ddagger}$ for the same reactions are positive for the faster reactions when the R group is CH_3, but become negative for slower

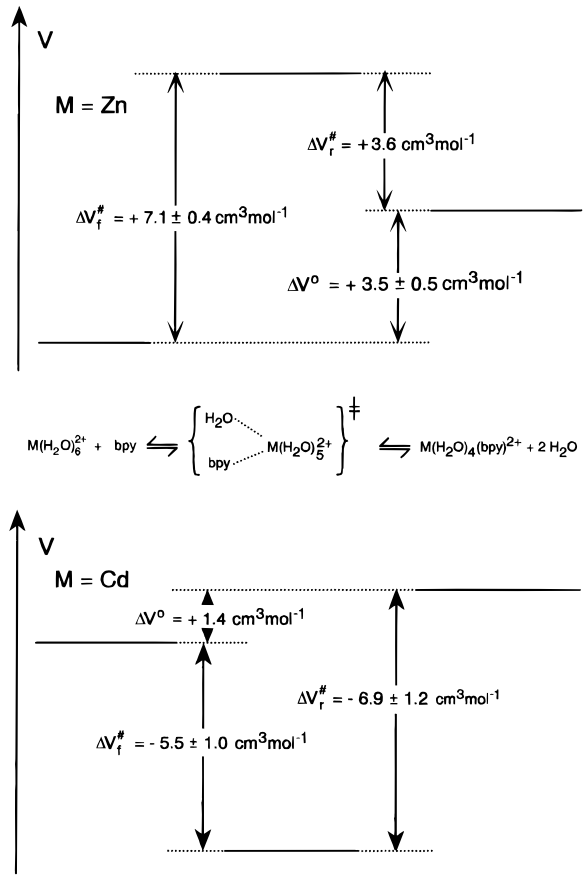

Figure 2. Volume profiles for formation and dissociation of $M(H_2O)_4(bpy)^{2+}$ complexes (M = Zn, Cd). (From refs 166 and 174.)

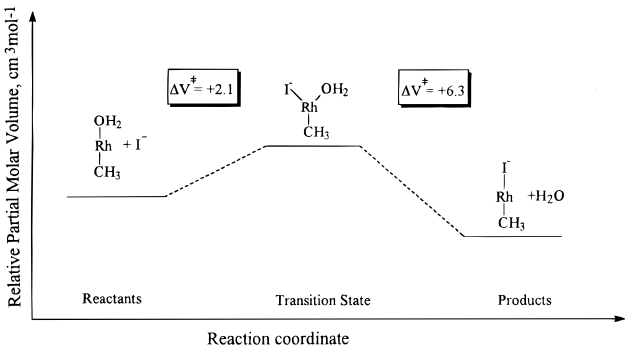

Figure 3. Volume profile for the nucleophilic substitution of $CH_3Rh(H_2O)$ by I^-. (From ref 183.)

substitutions (R = CH_2CF_3). Thus the methyl group is responsible for a bigger trans labilization effect than are either CH_2Cl or CH_2CF_3. Thus the former effect gives rise to an I_d substitution mechanism, whereas the weaker donating groups favor a more associative interchange mechanism. In the case of iodide ion as the nucleophile, the reverse reaction could also be studied permitting the development of a volume profile, (Figure 3) which displays the values from the table which are indicative of an I_d mechanism. The larger value of $\Delta V^{\ddagger}$ for the reverse reaction is probably a consequence of the large partial molar volume of the departing I^-, and the electrostriction effect on the complex due to the charged ligand. The additional potential mechanistic discrimination power of the pressure variable in kinetic investigations has

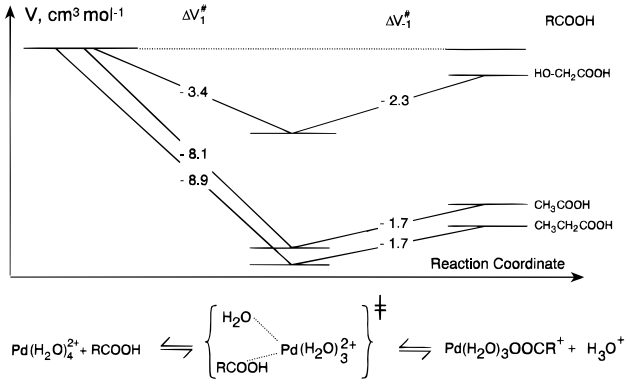

Figure 4. Volume profile for complex formation between $Pd(H_2O)_4^{2+}$ and RCOOH (R = CH_3, CH_3CH_2, CH_2OH). (From ref 191.)

been aptly exploited in *trans*-rhodoxime substitution kinetics.

The formation of several thioether and related complexes from Pd(II) and Pt(II) aqua ions proceeds by an I_a mechanism. The $\Delta V^{\ddagger}$ values for these reactions and the corresponding solvent exchange reactions (vide supra) were said to be of comparable magnitude, and it was reported that there was no obvious correlation between $\Delta V^{\ddagger}$ and the size or steric requirement of the ligands or the steric encumbrance of the first coordination sphere of the complex (entries 498−501).[186] The formation of palladium(II) complexes of sulfur containing ligands in acidic solution is characterized by essentially invariant $\Delta V^{\ddagger}$ values (entries 502−504).[187] This prompted the conclusion that the term "duality behavior" previously introduced is "nonexistent", since variation of electronic property for a common steric character of the ligand changes the reactivity markedly but has no influence on $\Delta V^{\ddagger}$. The reactions are of associative nature. Similar reactions of the tetraaqua Pd(II) ion with other sulfur ligands (entries 498−501) yield $\Delta V^{\ddagger}$ values[186] which span a small range of negative quantities, signifying a similar I_a mechanism, vide infra.

Formation of Pd(II) carboxylate complexes (entries 524−526) from the tetraaqua ion of palladium(II) is characterized by a rate-determining step in which there is significant bond-making in the transition state and the activated complex exhibits trigonal-bipyramidal geometry.[191] Stabilization within the transition state is through the hydrogen bond formed between the entering carboxylic acid and the leaving aqua ligand. The corresponding dissociation reactions (entries 527−529) have also been studied as a function of pressure. The volume profiles for some of these reactions are shown in Figure 4. Anation reactions of alkyl-substituted dien complexes of palladium(II) (entries 518−523), in which coordinated water is substituted by thiourea or methyl substituted thioureas proceed by an associative mechanism which is unaffected by either steric hindrance on the dien ligands or the entering nucleophile.[93]

Binding of ligands such as Ino and IMP to a Pd(II) center in which three coordination sites are nonsubstituting (entries 505−508) occurs by an associative mode of activation.[188] When the nonsubstituting

ligands on Pd(II) ions are en and Et_4en (entries 509−515) each of the observed kinetic processes depends on nucleoside concentration[189] and it is evident that the steric restriction afforded by the ethyl substituents affects the second step in the formation reaction. The binding and dissociation (aquation) of the nucleosides occur associatively.

Entries 498−501 and 577−580 can be considered together as the two reaction series are for the complexation of tetraaqua Pd(II) and Pt(II) ions respectively by unidentate sulfur ligands.[186] In all cases the reactions are judged to proceed by an I_a mechanism, but with the values of $\Delta V^{\ddagger}$ being more negative for the Pt(II) series. Since it was argued that the tetracoordinated aqua cations of the two metals should be of similar molar volumes because the bond distances are similar, the difference in $\Delta V^{\ddagger}$ values is then attributable to the partial molar volumes of the transition state. There is thought to be less extensive orbital overlap in the five-coordinate transition state in the case of Pd(II), which should result in weaker and longer metal−ligand bonds and therefore a less compact structure than in the case of the transition state for the reaction of Pt(II). There is a correlation between $\Delta V^{\ddagger}$ and $\Delta S^{\ddagger}$ for the Pt(II) series but not for the Pd(II) series, again indicating stronger bonding in the transition state for the former series and weaker solvation in the transition state for the Pd(II) series. No obvious correlation could be discerned between the values of $\Delta V^{\ddagger}$ for solvent exchange[95,398,399] and complex formation and with the size and steric requirements of the ligands nor the steric encumbrance in the first coordination sphere of the complex. A further example of Pd(II) reactivity is illustrated[190] by the complex formation and dissociation of the CH_3CN complex (entries 516 and 517). Although formation of both a mono and a bis complex were studied, the latter existing finally in a cis-to-trans ratio of about four following the initial rapid formation of the trans isomer from the mono complex and the slow isomerization to the cis form, the volume data refer to the mono complex only. The values of the activation volume are small and negative in both directions, indicating associative character. Comparative volume profiles could be developed for the corresponding reactions of DMSO[105] and H_2O,[391] demonstrating that since the reverse reactions have statistically equivalent volumes of activation (ca. -1.9 cm^3 mol^{-1}) the volume difference between the reactants for the reverse reaction and the transition state is independent of leaving group when water is the entering ligand.

By employing ^{139}La NMR spectroscopy the formation of a terdentate chelate complex of aqua La^{3+} (entry 556) could be studied.[198] Chelate ring closure was found to be rate determining. Although the reaction volume of $+12.1$ cm^3 mol^{-1} could readily be understood in terms of a strong electrostriction decrease due to charge neutralization upon complex formation, the relatively smaller values of the volumes of activation for the forward and reverse (entry 557) reactions were such that no definite mechanistic assignments were reported.[198]

Variable-pressure UV spectroscopy was employed to study the equilibrium between $Ce(H_2O)_9^{3+}$ and $Ce(H_2O)_8^{3+}$ (entry 558), yielding a value of $+10.9$ cm^3 mol^{-1} for the reaction volume.[199] By considering this value together with the activation volume for water exchange on other trivalent octaaqua lanthanides (Tb and Tm) that had already been determined,[100] it was possible to assign an I_a mechanism to the water exchange on these octaaqua ions. Variable-pressure UV−vis spectroscopy has been used to measure the volume change accompanying the departure of one water molecule from two triaqua europium(III) multidentate complexes (entries 559 and 560).[102] For the edta complex the reaction volume is close to that expected[400] for release of a coordinated water to the bulk solvent and to the value for a comparable process in the preceding table entry. The situation is more complicated in the second complex, as a much smaller positive reaction volume is obtained. It was suggested that this may arise because the binding of the third water molecule in the inner coordination sphere may cause a partial or complete unbinding of a ligand carboxylate arm.

The reaction described by entry 587 is complex kinetically.[207] The initial combination step is accompanied by a negative value of $\Delta V^{\ddagger}$ which is rationalized not in conventional terms but simply by considering a volume decrease due to the hydrogen sulfite ligand being incorporated into the inner coordination sphere of the complex during the activation process. Following this formation process, a step involving linkage isomerization occurs. The latter has a small positive $\Delta V^{\ddagger}$, indicating an intramolecular rearrangement via a loosely bound transition state, in which the Pt−O bond is weakened before a new Pt−S bond is formed.

Two systems were studied in which a Pt−C bond was introduced into the coordination sphere (entries 588−591). In both cases this led to a significant increase in the lability of the complexes, but the volumes of activation clearly demonstrated that no changeover in mechanism occurred, i.e., ligand substitution still follows an associative mechanism.

d. Ligand for Ligand Substitution

In searching for a correlation between leaving group cone angle and volume of activation,[137] for leaving group replacement by CN^- in pentacyanoferrate(II) complexes, departing ligands of widely different cone angles were selected (entries 206−212). The values of $\Delta V^{\ddagger}$ are consistent with a fully dissociative mechanism However, when the activation volumes obtained[137] were considered in combination with values for other leaving groups, no meaningful correlation with a steric property of the leaving group could be established. Entries 210−212 are similar reactions to those of the previous four entries. However, the emphasis in this investigation was a comparison between values of $\Delta V^{\ddagger}$ obtained from conventional high-pressure kinetics and those emerging from calculations based on the surface of activation method[138] whereby rate constants, k for the same reactions are obtained at several salt concentrations in the range up to 6.0 M, and the logarithmic ratios

$\ln(k/k_0)$ (where k_0 is the rate constant when no salt is added) are subsequently plotted against incremental values of the solution surface tension. Parameters derived from such plots lead ultimately to $\Delta V^{\ddagger}$ values, indicated in brackets after the values determined from high-pressure kinetic measurements.[138,142] Agreement between the two methods is reasonably good.

The values of $\Delta V^{\ddagger}$ for substitution of a range of pyridine derivative ligands and other leaving group variants from pentacyanoferrate(II) complex ions by CN^- in aqueous solution are all positive (entries 219−241) and vary little, consistent with a D mechanism.[141] There are reasonable correlations between the logarithm of the rate constants and the pK_a values and also the values of $\Delta V^{\ddagger}$ for uncharged leaving groups from this and other studies. In some cases the addition of a cosolvent (mostly monools) causes changes in the rate constant and $\Delta V^{\ddagger}$ that can be explained easily, while in other cases the interpretation is not unambiguous.

The last group of entries chosen for discussion contains substitution reactions of lanthanide complexes. Particular interest in the kinetics of these reactions and solvent exchange on these ions has been generated by the application of complexes of this general type as NMR imaging agents. The europium complex undergoes the substitution reaction shown (entries 561 and 562) by an interchange mechanism with significantly associative character[200] while the pressure dependence of the kinetics of substitution of the gadolinium complexes (entries 563−566) allows the conclusion that there are large solvational changes associated with the acid-catalyzed dechelation process.[201]

Several examples of ligand substitution reactions for which $\Delta V^{\ddagger}$ values are available have been the subjects of "reanalyses".[401] The objective was to provide improvement in consideration of correlations of leaving group partial molar volumes with measured volumes of activation for reactions such as the base hydrolysis of $Co^{III}(NH_3)_5(Y)$ complexes in which the rate-determining step (within the conjugate base mechanism) is the dissociative departure of Y. Aquation of the same system, substitution of X in $Fe(CN)_5X^{3-}$ complexes (X = amine, substituted pyridine, or substitued pyrazine ligands), substitution of L in $Cr^{III}(TPP)(Cl)(L)$ by 1-methylimidazole in toluene (L = pyridine, quinoline, and PPh_3) and the base hydrolysis and aquation of Cr(III) pentaammine or pentaamine chloro complexes were also considered. No new data were presented, yet the reliability of literature $\Delta V^{\ddagger}$ values was questioned. In this communication, correlations of results were tested by using equations modified from those proposed earlier and by using a cone as a leaving group geometric model. The outcome is an explanation of the observation that there is no correlation between the volume of activation and the partial molar volume of the leaving group for a dissociative substitution process.

A cone model has previously been used in correlating experimental volume of activation data for addition reactions (entries 796−813) with the nucleophile cone angle approach to an osmium carbonyl complex[244] (see also section 2.D).

C. Photoinduced Thermal Substitution Reactions

Flash photolysis techniques have been adopted with great success to initiate a reaction sequence. In these systems, we are interested in the effect of pressure on subsequent thermal reactions. The unstable species generated in solution may have relevance, for instance, in catalytic and biological systems. The pressure dependence of such reactions can once again reveal important mechanistic information. Irradiation of $M(CO)_6$ (M = Cr, Mo, W) in a coordinating solvent (S) produces intermediates of the type $M(CO)_5S$, which can undergo rapid solvent displacement by a nucleophile (L) to produce $M(CO)_5L$ as shown below:

$$M(CO)_6 + S + h\nu \rightarrow M(CO)_5S + CO \qquad \text{fast}$$

$$M(CO)_5S + L \rightarrow M(CO)_5L + S \qquad \text{slow}$$

The data for a series of M, S, and L (entries 602−620 and 664−666) demonstrate the roles played by the size of the metal center (M), the bulkiness of the ligand (L), and the coordination ability of the solvent (S). The data exhibit a trend to more negative (less positive) $\Delta V^{\ddagger}$ values for the larger metal centers.[211,212]

It is also possible to displace the coordinated solvent molecule by ring closure of a potential bidentate ligand such as a P olefin. All members of a series of such reactions for *cis*-$(CO)_4W(S)(PPh_2(CH_2)_nCH{=}CH_2)$ (n = 1 to 4, S = chlorobenzene) (entries 671−674) decrease their reaction rates with increasing pressure. The $\Delta V^{\ddagger}$ data indicate that chelate ring closure for n = 1 and 2 mainly involves an interchange (I_d) mechanism in which the olefin moiety is preassociated with the metal center, followed by rate-determining loss of S. In the case of n = 3 and 4, $\Delta V^{\ddagger}$ reaches the limiting value observed for the dissociation of chlorobenzene and presumably does not involve any significant preassociation.[219]

When the attacking nucleophile is a bidentate ligand, flash photolysis of $M(CO)_6$ results in the reaction sequence:

$$M(CO)_6 + h\nu \rightarrow M(CO)_5 + CO$$

$$M(CO)_5 + S \rightarrow M(CO)_5S \qquad \text{fast}$$

$$M(CO)_5S + N{-}N \rightarrow M(CO)_5N{-}N + S \qquad k_1$$

$$M(CO)_5N{-}N \rightarrow M(CO)_4(N{-}N) + CO \qquad k_2$$

in which ring closure now involves CO displacement in contrast to displacement of S discussed above. The reported data clearly demonstrate that the nature of the metal center and the bulkiness of the N−N ligand control the intimate nature of the CO displacement mechanism. The larger metal centers (Mo and W) tend to exhibit significantly negative $\Delta V^{\ddagger}$ values, suggesting ring closure in an associative way. The smallest Cr center must lose CO prior to ring closure since only in the absence of steric hindrance on the

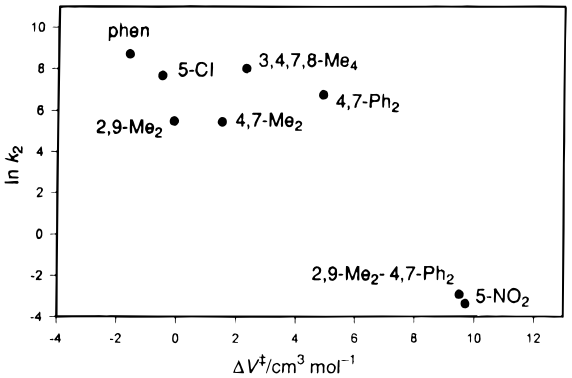

Figure 5. Logarithm of the second-order rate constant (k_2) for the chelation of phen and substituted derivatives when bound to $Mo(CO)_5$ in toluene versus $\Delta V^{\ddagger}$ at 298 K. (From ref 214.)

entering ligand, as in the case of ethylenediamine, can an associative ring closure occur.[210]

More recently, systematic studies of the effect of bulky substituents on bipyridine and phenanthroline (entries 621−638), as well as the influence of the solvent on the ring-closure reactions of $M(CO)_5N-N$ (M = Mo and W) (entries 639−644 and 660−666) were undertaken.[216,218] The results for the series of bipyridine ligands indicate a change in $\Delta V^{\ddagger}$ from small negative to small positive on increasing the steric hindrance on the Mo complex. This can be ascribed to a gradual change in mechanism from associative interchange to dissociative interchange on increasing the steric hindrance on the ligand. A similar trend is observed for the W complexes, although the overall $\Delta V^{\ddagger}$ value remains negative throughout the series of ligands. In this case the values suggest that ring closure in the case of the W complexes remains associative, although a gradual change from limiting associative to associative interchange may occur on increasing the steric hindrance. Throughout the series of complexes the $\Delta V^{\ddagger}$ values are more negative for W than for Mo, which indicates that the W metal center has a greater ability to undergo bond formation with the ring-opened chelate.

A series of studies was also undertaken for substituted phenanthroline complexes of the type $Mo(CO)_5N-N$ (entries 627−638). The ring-closure rate constant k_2 in general decreases with increasing steric hindrance on the ligand, and the apparent correlation in Figure 5 indicates that this trend is accompanied by a pronounced change in $\Delta V^{\ddagger}$ from small negative to significantly positive values. This trend in $\Delta V^{\ddagger}$ in going from faster to slower reactions clearly reveals the position of the transition state in terms of being "early" or "late". For faster reactions, ring closure will occur prior to release of CO (i.e., negative $\Delta V^{\ddagger}$, I_a), whereas the slower reactions will involve more CO bond cleavage (i.e., positive $\Delta V^{\ddagger}$, I_d). The "early" transition state will be closer to the reactant structure in terms of semi-seven-coordination, and the "late" transition state will be closer to the product state, i.e., chelated and total release of CO.[214,215]

The effect of solvent on the rate and associated $\Delta V^{\ddagger}$ value for the ring-closure reactions of $M(CO)_5$phen was studied for M = Mo and W (entries 639−644, 660−666). The orders of magnitude slower ring-closure reaction observed in THF is in agreement with the fact that THF is a more strongly coordinating solvent. This is accompanied by a more negative $\Delta V^{\ddagger}$ value which is ascribed to competition between direct ring closure and indirect ring closure, via the coordination of THF followed by ring closure. Values of $\Delta V^{\ddagger}$ for this reaction in weakly coordinating solvents such as toluene, fluorobenzene, heptane, and chlorobenzene are in many cases rather small, very typical for an interchange (I_a or I_d) mechanism. The significantly more negative value observed for reaction in THF must be related to its direct participation in the ring-closure reaction, presumably via the associative formation of a seven-coordinate intermediate followed by ring closure in a concerted manner.

More recently, similar photoinduced ring-closure reactions were studied in supercritical fluids, e.g., CO_2 and ethane, and the results are discussed in section 2.K.

D. Addition Reactions

The addition of 3,4-dihydro-2*H*-pyran to a chromium-based carbene or indeed to two tungsten-based carbenes proceeds rapidly and the mechanism, independent of metal center, is concerted, synchronous, and a single step.[223] It was further concluded that there is no zwitterionic intermediate or strongly dipolar transition state. The rates at ambient pressure of other similar reactions, in which a range of solvents of widely varying polarity were employed, were mostly solvent independent, permitting the conclusion that the $\Delta V^{\ddagger}$ values of reactions of entries 682, 782, and 783 arise from intrinsic volume changes associated with bond formation. In another study[224] in which chromium- and tungsten-containing compounds (entries 683, 684, 788, and 789) were compared in their reactivity, the $\Delta V^{\ddagger}$ values were all large and negative as were the $\Delta S^{\ddagger}$ values, indicating considerable bond formation in the transition state, and the minor differences in the former parameters were attributed to different geometries, Cr vis a vis W, in the transition state. For the addition reactions (entries 685−691), in CH_3CN, the consequence of varying the electron-withdrawing ability at the para position of the aniline addition agent was examined.[225] The amine basicity controls the rate of bond formation in generating the polar transition state and determines its position (early/late). Overall the reaction is a two-step process leading to a zwitterionic intermediate.

A small number of elimination reactions are included here. Depending on the eliminated group the value of $\Delta V^{\ddagger}$ can either be negative (OR), or positive (NH_2) (entries 692−696).[226] These correspond respectively to an early or a late transition state. Thus the position of the transition state depends on the nature of the reactants.

Of the three types of reaction system containing an iron center in this section, one (entries 697 and 698) is termed an addition[227] but could equally well be termed a substitution. Two equivalents of imidazole can combine in the axial positions of the

complex in DMSO, each being characterized by large positive $\Delta V^{\ddagger}$ values supporting the assignment of a dissociative character in their reactions. The same system has also been studied in acetonitrile, and contrasting features were indicated, one being the complication of self-association of imidazole in CH_3CN. Entries 699−712 cover the addition of 4-substituted pyridines to various dienyl iron compounds in CH_3CN.[228,229] A common mechanism is not applicable; differences depending on the nature of the pyridine substituent and the particular dienyl were noted, and on the basis of the results it was concluded that the amine basicity and steric hindrance in the dienyl ring are crucial parameters in controlling the location of the transition state. Addition of the first CN^- or imidazole to the five-coordinate ferric porphyrin in DMF (entries 713 and 714) is too fast to be measurable by the stopped-flow method.[230] The $\Delta V^{\ddagger}$ values refer to the addition of the second ligand by an associative mechanism.

A large range of coordinated ligands was employed in measurement of the reaction volume of hydroxide or methoxide addition to the Co^{III}(hfac)L series of species (entries 715−740): a wide range of reaction volumes was recorded.[231] They could be interpreted in terms of electrostriction changes, volume differences when L forms crevices in the coordinating sphere and when the ligand is flexible, allowing intrusion of the small solvent (H_2O) molecules.

Entry 745 is a reaction involving a spin-state change upon conversion from a five-coordinate paramagnetic Co(III) species to a six-coordinate diamagnetic Co(III) species, upon formation of the pyridine complex.[234] On a volume basis this represents a novel reaction type. Although metal to ligand bond lengths are expected to change as a consequence of the change of spin state, the contribution to the reaction volume from this source was not as significant as expected.

The reaction volumes for addition of four different solvent molecules to a four-coordinate macrocyclic complex of nickel(II) have been reported[235] (entries 746−749). The values reflect a small volume reduction upon complete transfer of a solvent molecule from the bulk to become coordinated to the nickel center, with somewhat varying degrees of incorporation into the macrocyclic system. The reaction is accompanied by a change in the spin state of nickel from low spin to high spin in the addition reaction direction. By making use of the $\Delta V^{\ddagger}$ value for solvent exchange (CH_3CN, dissociative pathway) from an earlier study,[402] it was possible to construct a volume profile in the case of the addition of CH_3CN. Profiles for G, H, and S are also displayed with the volume profile in Figure 6, and show an interesting difference between the volume and entropy changes. These can be explained by arguing that the ground-state fluxionality between trigonal-bipyramidal and square-planar geometries is lost in the transition state. The mechanism for solvent exchange is dissociative, which is supported by the correspondence between the enthalpy of reaction and enthalpy of activation.

Oxidative addition of CH_3I to rhodium(I) complexes (entries 761−772) proceeds differently in a mechanistic sense depending on the ligands bound to the central metal.[238] For example, the reaction rate of the sacac-containing compound shows no significant solvent dependence, whereas the reactivity of the cupf-containing compound differs significantly in highly polar solvents. The $\Delta V^{\ddagger}$ values are all negative as expected for this type of addition reaction, yet the variation in these values and the different rate/solvent dependencies led to the proposal of the simultaneous formation of two bonds between rhodium and the methyl and iodine moieties, giving rise to a concerted three-centered transition state for the former compound while the cupf compound reacts via formation of a linear transition state and participation of an ion-pair intermediate.

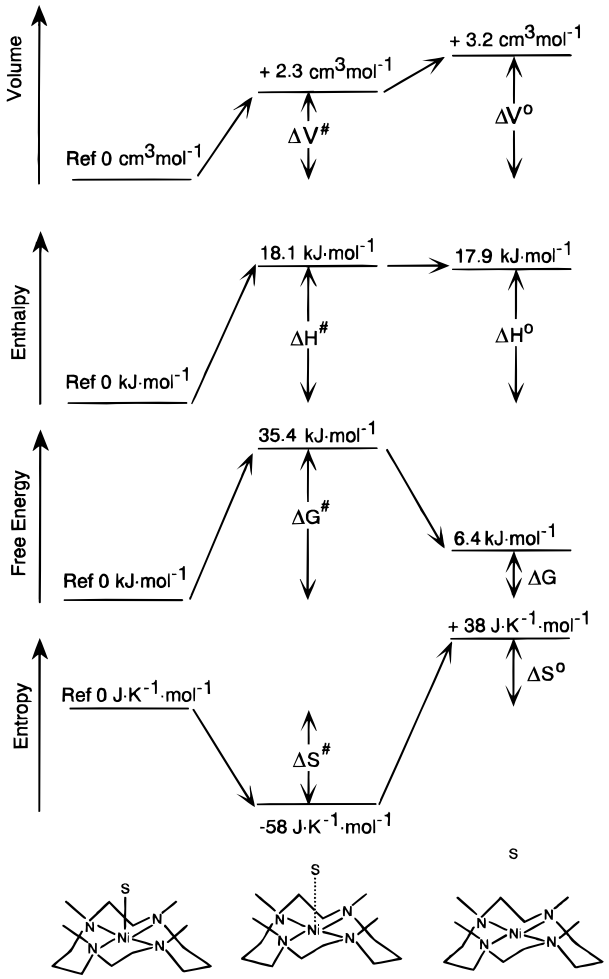

Figure 6. Volume, enthalpy, free energy, and entropy profiles for the reaction of *R,S,R,S*-$[Ni(tmc)(CH_3CN)]^{2+}$ to *R,S,R,S*-$[Ni(tmc)]^{2+}$ + CH_3CN at 25.0 °C. (From ref 235.)

The addition of alkynes to the palladiun compounds (entries 775−779) is characterized by more negative $\Delta V^{\ddagger}$ values for the bulkier diphenylalkyne than for the ethyl analogue.[240] The alkynes can precoordinate to the Pd(II) compound by a bridge opening route, the insertion is nonconcerted to a significant extent and the reaction proceeds with nucleophilic attack of the C1 carbon at the coordinated alkyne.

Addition of pyrrolidine to unsaturated Fischer carbene complexes with M = Cr (entry 681), Mo (entry 750), W (entries 790−795) is a two-step process in which there is a polar transition state for the rate-

determining step and a zwitterionic intermediate.[222] Negative $\Delta V^{\ddagger}$ values indicate substantial bond formation, and since they exhibit only a small solvent dependence the electrostriction component is minor. Finally, in this section, the pressure dependence of the rate constants for addition of several nucleophiles to an osmium decacarbonyl complex (entries 796−813) has been investigated.[244] There is no dependence on the pK_a of the nucleophile, and the volume reduction observed is controlled by steric rather than electronic factors. $\Delta V^{\ddagger}$ shows a remarkably good correlation with the cone angle of each nucleophile. What may be termed a steric threshold is about 160°, above which value $\Delta V^{\ddagger}$ becomes less negative denoting less penetration by the nucleophile, and the osmium phosphorus bond is longer in the transition state.

E. Formation and Dissociation Reactions

Although the majority of entries in this section are reactions in which there is a central transition element, there are a few cases in which the reaction involves either a representative element of small atomic number having very interesting mechanistic features, or a lanthanide element.

Entries 816 and 818 may be considered together.[246] Reaction volumes are of the expected sign. The dissociation constant of HF in water is increased by increasing pressure and the negative reaction volume arises from the contraction of water around the ionic product species compared with that around the undissociated molecules. Likewise the dissociation of NaF has a negative reaction volume resulting from the increase in electrostricted solvent.

Dissociation of the sodium cryptate, (Na^+(C222)) (entry 817) an inclusive form of this type of complex in en as solvent, has been studied by high-pressure NMR spectroscopy, and is characterized by a $\Delta V^{\ddagger}$ value of +8.9 $cm^3\ mol^{-1}$.[247] Projection of the sodium ion into the solvent as well as expansion of the cavity of C222 account for this result. It was noted that the volumes of activation for dissociation of the C221 complex of Na^+ in DMF and DMSO (entries 819 and 820) were smaller[248] and the notion of the potential importance of solvent donicity was addressed by comparing the enthalpies of activation. The solvent of highest donicity, en, has the lowest $\Delta H^{\#}$ reflecting the more favorable interaction of this solvent with Na^+.

The dissociation of a sodium−cryptate complex (entries 819−824) differs somewhat depending on the solvent. Two parallel paths, one solvent assisted and the other acid dependent (dichloroacetic acid), are evident for the dissociation in DMF, whereas the solvent path prevails in the more basic DMSO, and the latter path is barely evident in the less basic CH_3CN.[248] A volume increase due to cage opening, not wholly compensated by electrostriction, is argued to be the explanation for the small positive $\Delta V^{\ddagger}$ values for the solvent-assisted pathway, while the negative values found for the acid-dependent path arise from a consequence of charge localization and electrostriction following hydrogen bond formation between a lone-pair of the cryptand and DCA. An additional noteworthy aspect of this study is that the reactions were monitored by a high-pressure stopped-flow instrument making use of changes in conductance in the solution.

To permit the reaction of hydrogen peroxide with the V(V) species VO_2^+ in strongly acidic medium (entries 826−828) to be studied it was necessary to employ tantalum as the material for construction of the high-pressure stopped-flow instrument.[249] Reaction with the first equivalent of H_2O_2 is complex: three paths are evident, an acid-dependent path, and acid-independent path, and reaction in which the rate is proportional to the inverse of the hydrogen ion concentration, all of which yield positive volumes of activation. This obviously indicates an expanded transition state in each case. The acid-independent path is regarded as an associative attack by an H_2O_2 molecule into a face of the octahedral V(V) ion, followed by rearrangement of that geometry to a distorted pentagonal bipyramid. The second H_2O_2 molecule penetrates the surrounding sphere of the V center, but this volume decrease is compensated for by the volume increase due to elongation of the V−OH_2 bond, resulting in a zero volume of activation.

The conformational equilibrium involving C221 (entries 838−840) will be discussed later in section 2.F.[250] The near zero volumes of activation for copper(II) ion C221 complex formation (entries 831 and 833) in both DMSO and DMF may be explained by compensatory effects of metal ion desolvation and rearrangement of the cryptand for the encirclement of the metal ion.[250]

The hydrogen bridge cleavage reaction by substituted pyridines in chloroform has been studied[251] for a Pd(II) complex and for a second complex, identical except for the replacement of Pd(II) by Pt(II) (entries 834 and 837). Both are associatively driven as may be interpreted from the large negative $\Delta V^{\ddagger}$ values.

F. Isomerization Reactions

In this section activity with respect to the first row of transition metals has centered on but by no means exclusively on isomerization reactions of chromium(III) and cobalt(III) complexes. Exciting new developments have also been recorded for isomerization reactions involving metal cluster compounds of ruthenium, osmium, and iridium.

Although very strictly speaking entries 838−840 should be included in the organic part of this review, the fact that these conformational equilibria are pertinent to metal ion binding studies with the same cryptands and are reported[250] in the same publication persuaded us to include them here. The large positive reaction volumes in each solvent, obtained from ultrasonic absorption spectroscopy, indicate that the conformer with both nitrogen lone pairs of electrons directed to the inside of the molecular cavity has a larger volume than that with one electron pair directed toward the inside and the other directed outside the cavity.

The trans form of $TiCl_4$·2TMPA is slightly favored over the cis form (entry 841) in $CHCl_3$ solution at −30 °C, judging by the small negative reaction volume for cis to trans isomerization.[253] The activation volume

(+6.2 cm^3 mol^{-1}) determined at 67 °C in the same solvent (entry 842) is considered to arise from an intramolecular twist mechanism with an expanded six-coordinate transition state,[64] a mechanism which resembles that advanced[403] for the cis to trans isomerization of $SnCl_4 \cdot 2Me_2S$.

The two chromium(III) complexes (entries 843 and 844) each isomerize in basic solution and release a proton: the negative entropies of activation and volumes of activation arise as a result of solvent electrostriction around separated charge centers in the transition state.[121] Both the reaction volume and activation volume have been determined for a large number of trans to cis isomerizations of cobalt(III) bisethylenediamine−aqua−X complexes (entries 847−855).[255] The former parameter can be correlated with the order of X in the spectrochemical series, as the reaction volume increases when a change in X causes a stronger crystal field. An interchange mechanism was preferred to a D_P mechanism. The latter would involve a tetragonal-pyramidal transition state. It was also considered possible that the $\Delta V^{\ddagger}$ values could contain a component of en chelate ring expansion in the transition state. In the isomerization process water approaches the complex from the opposite side to the side from which the rate-determining water molecule is dissociating, a situation different from water exchange on such complexes in which the incoming water molecule approaches from the side from which water departs. Since the reaction volumes and volumes of activation have both been obtained, the volumes of activation for the cis−trans isomerization are also available[255] (entries 856−864).

The cis−trans isomerization of $ZrCl_4 \cdot 2(MeO)_3PO$ (entry 867) in $CHCl_3$[82,83] exemplifies the difference in mechanism caused by change in the ionic radius of the metal ion, since in this case the mechanism is associative ($\Delta V^{\ddagger} = -1.6$ cm^3 mol^{-1}), whereas the analogous titanium compound undergoes isomerization by a dissociative mechanism ($\Delta V^{\ddagger} = +6.2$ cm^3 mol^{-1}).[64]

The first report on results of high-pressure measurements on metal cluster compound isomerizations illustrated the difficulty in mechanistic diagnosis, as the process is a multistep one.[259] The modestly positive value of $\Delta V^{\ddagger}$ for the trinuclear ruthenium compound (entry 875) was interpreted as an exchange pathway involving migration of one hydride from a doubly bridging coordination mode to a terminal coordination site in the transition state, whereas the near zero $\Delta V^{\ddagger}$ value for a related trinuclear osmium complex (entry 887) was considered to be consistent with exchange of bridging and terminal hydrides and a transition state in which both hydrides are bridging.[259] The solvents for the two systems were different, but this is unlikely to have any mechanistic consequences.

The trinuclear ruthenium carbonyl complexes isomerize in decane (entries 868−870) by different mechanisms depending on the composition of the other ligands.[256] For example the compound in entry 868 has a near zero $\Delta V^{\ddagger}$ and $\Delta S^{\ddagger}$, consistent with an intramolecular process in which there are no appreciable changes in bond lengths upon forming the transition state or there is compensation for any changes. Other possible mechanisms are ruled out because they would either generate distinctly positive (ligand dissociation) or distinctly negative (CO association or bimolecular hydride transfer) volumes of activation. By contrast the compound in entry 869 is characterized by a large positive $\Delta V^{\ddagger}$ value which was accounted for by anchimeric assistance from the methylidene substituent. The isomerization of another trinuclear ruthenium carbonyl compound (entry 870) in decane[257] exhibited a $\Delta V^{\ddagger}$ value about 50% of the magnitude of the reaction volume estimated from solid-state molar volumes. The isomerization involves opening of the Ru_3 framework by cleavage of one Ru−Ru bond, reductive elimination of a C−H bond, breakage of the C−SEt bond, and then formation of a Ru−SEt−Ru bridge, and the connectivity of the carbon atoms to the metal center is changed. The rate-limiting step was judged to be intramolecular with significant metal−metal cleavage and C−S bond cleavage in the transition state. The magnitude of $\Delta V^{\ddagger}$ was considered to be higher than would be accommodated by C−H elimination alone. Furthermore, CO dissociation is not thought to be involved. The isomerization of various geometric variants of the mononuclear ruthenium complexes (entries 871−874) takes place by a dissociative pathway.[258]

The kinetics of rearrangement within several binuclear rhodium compounds (entries 876−883) have been studied as a spontaneous reaction or acid or base assisted.[260] The starting compound contains a metalated and an equatorial phosphine which rearranges to produce the corresponding doubly metalated compounds. Steric hindrance on the initial products is thought to have an influence on reaction product distribution. The cases where the volume of activation has been determined all point toward the importance of compression in the transition state.

In the polynuclear iridium carbonyl complex (entries 888 and 889) isomerization there is no charge change so that electrostriction changes are negligible.[262] The reaction volume for the bridged to unbridged species (entry 888) is close to that calculated on the basis of the molecular parameters rather than the crystal cell data.[262] Intramolecular CO exchange (entry 889) is reasoned to involve the breaking of three M−CO bonds and formation of three additional terminal CO moieties, and the transition state is thought to be the result of the formation in a concerted manner of three semibridging CO units.

G. Electron-Transfer Reactions

Significant progress has been made in the application of high-pressure thermodynamic and kinetic techniques to the study of inorganic and bioinorganic electron-transfer reactions during the period covered by this review. Especially in the case of self-exchange reactions, which represent the simplest symmetrical electron-transfer process, it has been possible to account for the observed pressure effects in terms of the Marcus−Hush theory. In the case of nonsymmetrical electron-transfer reactions, the volume

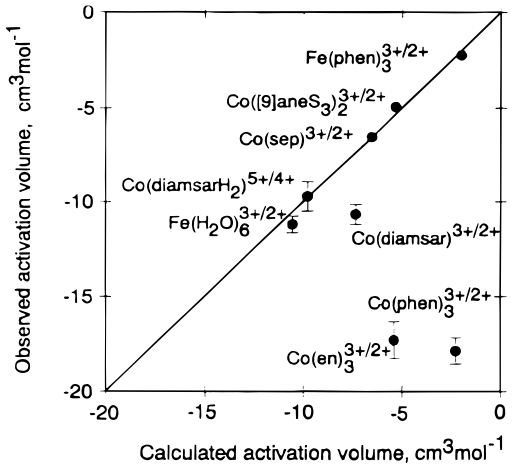

Figure 7. Electron self-exchange reactions: plot of $\Delta V^{\ddagger}$ (calculated) versus $\Delta V^{\ddagger}$ (experimental). sep = sepulchrate = 1,3,6,10,13,16,19-octaazabicyclo[6,6,6]eicosane; [9]aneS3 = 1,4,7-trithiacyclononane; diamsar = diaminosarcophagine = 1,8-diamino-1,3,10,13,16,19-hexaazabicyclo[6,6,6]-eicosane; en = ethylenediamine, phen = 1,10-phenanthroline. (From refs 287 and 299.)

changes are primarily due to solvent reorganization from changes in electrostriction associated with the electron-transfer process. Several reviews, the subject of which is the effect of pressure on electron-transfer reactions, have appeared in the literature.[3,6−8,11,13,14,16,18,404,405] In our discussion of the data we will distinguish between symmetrical and nonsymmetrical electron-transfer processes.

a. Symmetrical Electron-Transfer Reactions

Symmetrical self-exchange reactions are the simplest kind of electron-transfer process, since there is no net chemical reaction and no reaction volume, and therefore in principle the mechanistic interpretation of activation volume data, as in the case of solvent exchange reactions is relatively straightforward. Swaddle and collaborators have made cogent contributions in this area. One of the first interesting observations was that the activation volume for self-exchange on $Fe(H_2O)_6^{3+/2+}$ is ca. 12 cm^3 mol^{-1} more negative than that for the self-exchange in $Fe(H_2O)_5OH^{2+}/Fe(H_2O)_6^{2+}$ (entries 1006 and 1007).[287] This difference could be explained in terms of the operation of an outer-sphere mechanism in the former process and an inner-sphere mechanism in the latter case, since the formation of a hydroxo bridged species will be accompanied by the release of a solvent molecule, i.e., a markedly more positive activation volume. The same group has also studied a series of self-exchange reactions (see entries 1007 and 1043−1049) and found a good correlation between experimental and theoretically calculated values (see Figure 7). In most cases the self-exchange reaction is significantly accelerated by pressure, with the exception of the $Fe(CN)_6^{3-/4-}$ system which proceeds in exactly the opposite direction (i.e., the reaction rate is retarded by pressure). In general, solvent reorganization accounts for the largest contribution toward the observed activation volume. The latter can be accounted for theoretically in terms of contributions resulting from internal reorganization, solvent reorganization, Coulombic or electrostatic work change, and a Debye−Hückel activity coefficient term.[299,406] As can be seen from Figure 7 large deviations were observed for the $Co(en)_3^{3+/2+}$ and $Co(phen)_3^{3+/2+}$ systems where the theoretical volume of activation is between 10 and 15 cm^3 mol^{-1} more positive than the experimental value.[300,302] The deviations are most probably related to the participation of a high-spin to low-spin changeover associated with the electron-transfer process, accounting for an additional volume collapse of ca. 10 cm^3 mol^{-1}.[299]

Another interesting example involves the self-exchange reaction between MnO_4^- and MnO_4^{2-} for which $\Delta V^{\ddagger}$ has a value of −21 cm^3 mol^{-1} (entries 927−929). This reaction is catalyzed by counterions such as Na^+ and K^+ and the catalysis manifests itself in very different $\Delta V^{\ddagger}$ values, viz. +3 and −1 cm^3 mol^{-1}, respectively. Self-exchange reactions in polar organic solvents also exhibit distinctly negative volumes of activation (entries 930−960) but ion pairing with counterions is expected to influence the values. Such ion pairs formed by cationic reactants in nonaqueous solvents are generally less reactive in electron-transfer reactions than the free ions according to Wherland.[272] The experimental $\Delta V^{\ddagger}$ values are expected to be more negative than the calculated ones, since pressure in general breaks up ion pairs by favoring solvation of the separated ions.[404]

Recently Swaddle et al.[45,407] determined volumes of activation for heterogeneous self-exchange reactions of a series of complexes on the surface of an electrode. In general it was found that the numerical values are about 50% of those for the corresponding homogeneous reactions, which resulted in the so-called "fifty percent rule".[45] This trend was shown to be in agreement with theoretical predictions based on an extension of the Marcus theory.[45,407]

b. Nonsymmetrical Electron-Tranfer Reactions

One objective of many mechanistic studies dealing with inorganic electron-transfer reactions has been to distinguish between outer-sphere and inner-sphere mechanisms. High-pressure kinetic methods and analysis of reaction volume profiles have been employed to provide a better understanding of the intimate mechanisms involved in such processes. The differentiation between outer-sphere and inner-sphere mechanisms depends on the nature of the precursor species, Ox//Red in the following scheme, which can either be an ion pair or encounter complex, or a bridged intermediate, respectively:

$$\mathrm{Ox} + \mathrm{Red} \leftrightarrow \mathrm{Ox//Red} \qquad K$$

$$\mathrm{Ox//Red} \rightarrow \mathrm{Ox^-//Red^+} \qquad k_{\mathrm{ET}}$$

$$\mathrm{Ox^-//Red^+} \leftrightarrow \mathrm{Ox^-} + \mathrm{Red^+}$$

This means that the coordination sphere of the reactants remains intact in the former case and is modified by ligand substitution in the latter, which will naturally affect the associated volume changes.

A difficulty encountered in many cases in kinetic studies of outer-sphere electron-transfer processes concerns the separate determination of the precursor

formation constant (K) and the electron-transfer rate constant (k_{ET}) (in the scheme outlined above), from an empirically determined composite parameter. In the majority of cases, precursor formation is a diffusion-controlled step, followed by rate-determining electron transfer. In the presence of an excess of Red, the rate expression is given by

$$k_{obs} = k_{ET}K[\text{Red}]/(1 + K[\text{Red}])$$

In many cases K is small, such that this equation simplifies to $k_{obs} = k_{ET}K[\text{Red}]$, which means that the observed second-order rate constant and the associated activation parameters are composite quantities, viz. $\Delta V^{\ddagger} = \Delta V^{\ddagger}(k_{ET}) + \Delta V(K)$. When K is large enough such that $1 + K[\text{Red}] > 1$, it is possible to separate k_{ET} and K kinetically and also the associated activation parameters, viz. $\Delta V^{\ddagger}(k_{ET})$ and $\Delta V(K)$.[18]

A series of reactions was studied where it was possible to resolve K and k_{ET}, and thereby $\Delta V(K)$ and $\Delta V^{\ddagger}(k_{ET})$. In this case oppositely charged reaction partners were selected as indicated in the following general scheme:

$$Co(NH_3)_5X^{(3-n)+} + Fe(CN)_6^{4-} \leftrightarrow [Co(NH_3)_5X^{(3-n)+}\cdot Fe(CN)_6^{4-}] \quad K$$

$$[Co(NH_3)_5X^{(3-n)+}\cdot Fe(CN)_6^{4-}] \rightarrow Co^{2+} + 5NH_3 + X^{n-} + Fe(CN)_6^{3-} \quad k_{ET}$$

$$X^{n-} = H_2O, Me_2SO, py, Cl^-, N_3^-$$

The data[408] indicated that ion-pair formation is accompanied by close to zero ΔV values. This is rather surprising, since it is generally accepted that ion-pair formation should involve considerable charge neutralization accompanied by strong desolvation due to a decrease in electrostriction. Values of ΔV therefore indicate that the reaction partners most probably exist as solvent-separated ion pairs, i.e., with no significant charge neutralization accompanied by desolvation. It is evident that the electron-transfer steps exhibit a strong pressure-induced deceleration, with most systems having a $\Delta V^{\ddagger}$ value of between +25 and +34 cm^3 mol^{-1}. These values indicate that electron transfer is accompanied by extensive desolvation, most probably related to charge neutralization associated with the electron-transfer process.[279] A simplified model based on partial molar volume data, in which electron transfer occurs from the precursor ion pair $[Co(NH_3)_5X^{(3-n)+}\cdot Fe(CN)_6^{4-}]$ to the successor ion pair $[Co(NH_3)_5X^{(2-n)+}\cdot Fe(CN)_6^{3-}]$, predicts an overall volume increase of ca. 65 cm^3 mol^{-1}. This means that according to the $\Delta V^{\ddagger}$ values reported the transition state for the electron-transfer process lies approximately halfway between the reactant and product states on a volume basis for the precursor and successor ion pairs. The largest volume contribution arises from the oxidation of $Fe(CN)_6^{4-}$ to $Fe(CN)_6^{3-}$, which is accompanied by a large decrease in electrostriction and an increase in partial molar volume of ca. 40 cm^3 mol^{-1} (see entry 1000). Theoretical calculations also confirmed that the transition state for these reactions lies approximately halfway along the reaction coordinate on a volume basis.[279] This first information on the nature of the volume profile for an outer-sphere electron-transfer reaction proved to be in good agreement with results reported subsequently for systems with a low driving force in which it was possible to construct a complete volume profile by studying the effect of pressure on both the forward and reverse reactions, as well as on the overall equilibrium constant (see section 2.L).

Data have also been reported for a series of related complexes containing phosphor−oxo ligands (see entries 1019−1024, 1027−1031). The results can be interpreted in terms of major solvational changes associated with the oxidation of $Fe(CN)_6^{4-}$. Other interesting systems that have been investigated include reduction of aquated Fe(III) by Co(II) complexes (entries 966 and 967), oxidation of Fe(II) complexes by peroxodisulfate (entries 985−990), reduction of Co(III) complexes by Fe(II) complexes in nonaqueous solution (entries 1056−1072), oxidation of Ni(II) complexes by $HO_2^{\bullet}$ (entries 1081−1087), and the reduction of $IrCl_6^{2-}$ by a series of catechols (entries 1132−1144).

Data are also available for the reduction of aquated Fe(III), $Fe(CN)_6^{3-}$, and $Ru(CN)_6^{3-}$ by ascorbic acid and ascorbate ions (entries 969−976, 1120, and 1121). It is an interesting finding that the hexacyano complexes all exhibit a strongly negative volume of activation that mainly results from the increase in electrostriction due to the reduction to $M(CN)_6^{4-}$ (M = Fe, Ru). In the case of the aquated Fe(III) species, the activation volumes are significantly positive; these have been ascribed to an outer-sphere electron-transfer reaction in the case of $Fe(H_2O)_6^{3+}$, but to an inner-sphere reaction in the case of the more labile $Fe(H_2O)_5OH^{2+}$ complex.[279]

Other data include the oxidation of Fe(II) and Co(II) chelated complexes by dioxygen (entries 962−965, 1017, and 1018). Oxidation reactions of chelated Fe(II) complexes are all significantly accelerated by pressure and accompanied by negative volumes of activation. These can be ascribed to the binding of dioxygen that is accompanied by the oxidation of Fe(II) to Fe(III) and the reduction of dioxygen to superoxide and peroxide ions, processes that are all expected to lead to a decrease in partial molar volume. In a recent reinvestigation of the Fe^{II}(edta) oxidation reaction it was possible to resolve the different reaction steps that form part of the oxidation process and to assign the negative volumes of activation in a more detailed way.[409] The formation of a diiron(III) peroxo complex from an alkoxo-bridged diiron(II) complex and dioxygen is also accompanied by a significantly negative volume of activation (entry 961).[273]

In another study[292] it was possible to construct a volume profile for the reversible binding of dioxygen to a Co(II) macrocycle, viz. hexamethylcyclam, to produce $(L)Co-O_2^{2+}$, which is a Co(III)−superoxo species (entries 1017 and 1018). The kinetics of the overall reaction could be studied by flash photolysis, since the dioxygen complex can be photodissociated and the subsequent reequilibration could be followed in the microsecond time range. A combination of the

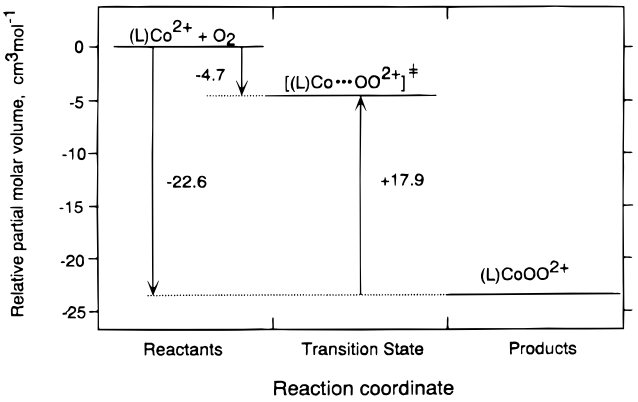

Figure 8. Volume profile for the reaction of O_2 with the Co(II)L complex (L = hexamethylcyclam) at 298 K. (From ref 292.)

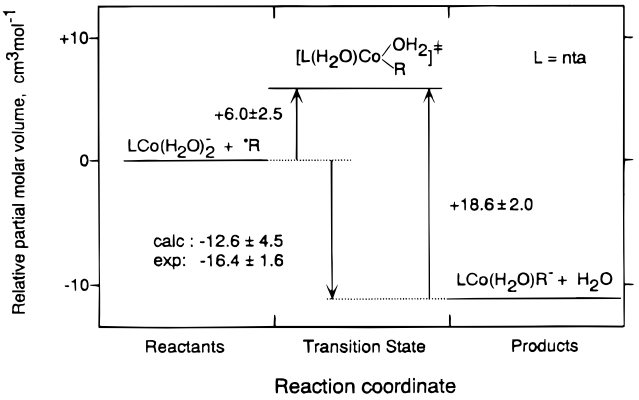

Figure 9. Volume profile for the reaction of methyl radicals with the nitrilotriacetate complex of Co(II) at 298 K. (From refs 290 and 291.)

activation volumes for the binding and release of dioxygen results in a reaction volume that is in very good agreement with the value determined directly from equilibrium measurements as a function of pressure. The volume profile for the reaction is shown in Figure 8. The small volume of activation associated with the forward reaction was interpreted as evidence for a rate-determining interchange of the ligands, water versus dioxygen, which is followed by an intramolecular electron-transfer reaction to form $Co^{III}-O_2^-$. It is the latter process that accounts for the large volume collapse en route to the reaction products. The oxidation of Cu(I) complexes by dioxygen is also characterized by distinctly negative volumes of activation, the reason for which is parallel to that noted for the cobalt complex system above (entries 1089 and 1090).

Oxidation of Cr(II), Co(II), and Ni(II) complexes by alkyl radicals have also been studied as a function of pressure using a high-pressure pulse-radiolysis technique.[39] These reactions are all characterized by negative reaction volumes due to the oxidation of the metal center, and the associated volumes of activation (entries 894−903, 1014−1016, and 1088) can be used to obtain information on the nature of the transition state. The volume profile for the reaction of $Co^{II}(nta)(H_2O)_2^-$ with methyl radicals (CH_3) shown in Figure 9 indicates a significantly higher partial molar volume for the transition state than for either the reactant or product states. This was interpreted

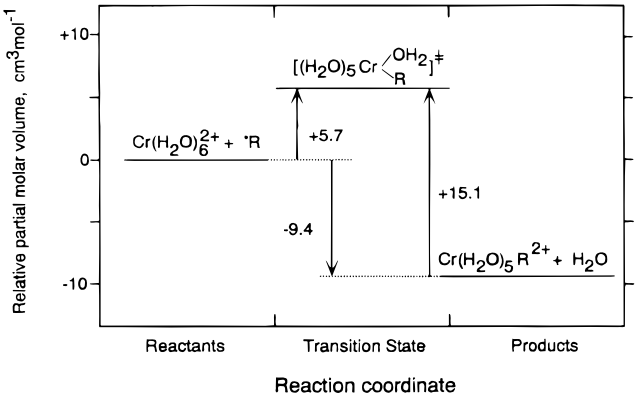

Figure 10. Volume profile for the reaction of an aliphatic radical with aqua Cr(II) species at 298 K. (From ref 265.)

in terms of an I_d substitution controlled mechanism, which is followed by a large volume reduction associated with metal−carbon bond formation accompanied by oxidation of Co(II) to Co(III).

Similar results were obtained for the reaction of $Cr(H_2O)_6^{2+}$ with 10 different aliphatic radicals. Although the overall reaction volume is significantly negative due to the oxidation of Cr(II) to Cr(III), the observed volumes of activation (entries 894−903) are all small and positive. This was interpreted as evidence for the occurrence of an I_d substitution mechanism that is controlled by water exchange on aquated Cr(II). Once again the large volume reduction after formation of the transition state (see volume profile in Figure 10) was ascribed to Cr−R bond formation and the conversion of $Cr^{II}-R$ to $Cr^{III}-R^-$. These and other recent studies on the interaction of metal complexes with free radicals suggest that for nondiffusion controlled processes, the radicals can be treated as normal nucleophiles in ligand substitution processes which are often controlled by solvent exchange on the metal complex, i.e., typical for an inner-sphere electron-transfer process.

For the mechanistic interpretation of activation volume data for electron-transfer reactions, it is important to know the overall reaction volume associated with the redox process. Efforts have, in recent years, focused on the electrochemical determination of reaction volume data from the pressure dependence of the redox potentials. In this area the work has mainly been performed by Swaddle et al. and Tregloan et al. who developed the appropriate high-pressure techniques to conduct such measurements.[44−47] The reported reaction volumes have to be corrected for the effect of pressure with a reference electrode. Tregloan et al.[42] conducted a well-designed set of experiments on a series of $Fe^{III/II}$ couples in which the ligands were varied in order to change the overall charge of the complex (see entries 1000−1005). From a correlation of the cell reaction volume with the difference in the square of the charge on the oxidized and reduced forms of the complexes, it was possible by interpolation to estimate the reaction volume associated with the Ag/Ag^+ reference electrode (see Figure 11) to be -11.9 ± 0.5 cm^3 mol^{-1} at 25 °C and 1.0 M ionic strength. Further measurements on a series of Cr, Co, and Ru complexes (see entries 914, 1038−1044, and 1097−1101) enabled a

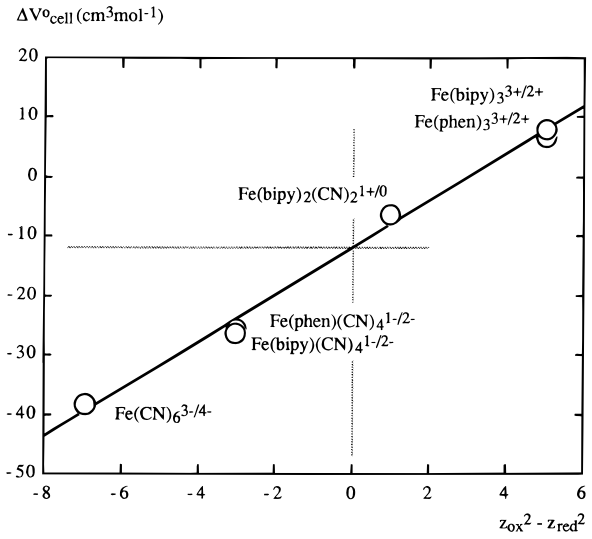

Figure 11. Plot of V^0_{cell} versus $z_{OX}^2 - z_{RED}^2$ for Fe^{II}/Fe^{III} species. (From ref 268.)

systematic differentiation to be made between intrinsic and solvational volume contributions associated with the redox process.[268] The results include examples where intrinsic volume changes are indeed very small, whereas in other cases intrinsic volume changes can be as large as the solvational volume changes.[268]

H. Electrodeposition/Electrochemical Reactions

A number of studies have been performed in which the effect of pressure on electrodeposition and electrochemical reactions was investigated (entries 1145−1167). In many cases these processes are characterized by significantly positive volumes of activation, which were accounted for in terms of the release of solvent molecules during the deposition process.

I. Heterolysis, Homolysis, and Homolytic Fission

In a wide-ranging series of experiments (entries 1168−1201) heterolysis reactions of chromium(III) complexes have been examined.[322−324] The variations include different catalytic anions, different nonparticipating ligands, measurements over a pH range, and different R groups, where the R group connected to chromium is subject to cleavage from it. In the case of a catalytic anion (entries 1173−1181) the catalysis was enhanced with increasing basicity of the anion, and $\Delta V^{\ddagger}$ values are all positive, indicating dissociatively activated heterolysis. Other data[323] indicate the volumes of activation decrease somewhat upon increasing the anion concentration. The dissociative mechanism in this series of reactions involves breakage of a σ chromium−carbon bond accompanied by bond formation to the entering solvent molecule. The coordinated anion exerts a trans labilization effect, and this effect has been quite thoroughly studied when the anion is acetate. Phosphate ion also gives rise to a catalytic effect manifest through its coordination and trans labilizing effect and a dissociatively activated mechanism is induced. In earlier spontaneous heterolysis reactions the value of $\Delta V^{\ddagger}$ was closer to zero, signifying a mutual cancellation of bond formation and bond breakage contributions.[410]

Pressure effects have been used as mechanistic probes for homolytic cleavage of cobalt carbon bonds in cobalamins.[325] Solvents of different viscosities were used. Substantial positive volumes of activation for the Ado-B_{12} and CH_3-B_{12} compounds (entries 1202 and 1205, respectively) were obtained; an exact adjudication of the magnitude of the values for the homolysis reactions was not presented, although it was suggested that the values were relatively large for the cage model for this type of reaction. The neopentyl derivative (entry 1204) has a much lower $\Delta V^{\ddagger}$ value which might arise as a consequence of the higher solvent viscosity at the lower temperature of measurement resulting in a higher cage efficiency. In water the reaction of entry 1203 yields a value of -2.0 cm^3 mol^{-1}. Here there is the complication that there is a dual reaction pathway, since homolysis and heterolysis occur. Thermolysis of the isopropylcobalamin in ethylene glycol/water mixtures proceeds by β-elimination (entries 1206 and 1207), a reaction which is insensitive to pressure at physiological temperature, but whose rate is retarded by pressure at 100 °C (entry 1208).[325]

In a series of papers[326−328] the kinetics of homolysis of alkylcobalamins and model complexes (entries 1209 and 1249) in water when possible, in organic solvents or in water/2-propanol mixtures, have been studied as a function of pressure. The reactions proceed upon homolysis to form a caged pair of radicals, which subsequently are true free radicals, i.e., solvent separated, and then are subject to a radical trap to form the final trapped products. In the reactions of entries 1209−1227 two important features emerge: the R group in the substrate has very little influence, and the temperature variation of $\Delta V^{\ddagger}$ is considerable.[326] This latter observation may be explained by reasoning that at higher temperatures (large $\Delta V^{\ddagger}$ value) there is negligible cage efficiency, whereas at lower temperatures when the value of $\Delta V^{\ddagger}$ is much reduced then the cage efficiency is much higher. This implies that the solvent system viscosity variation with temperature is responsible for this difference. Therefore the pressure and temperature dependence of the rates of reaction of these and of similar systems may be used as a mechanistic probe to identify which radicals have the opportunity to escape the cage. The model reactions[327] (entries 1228−1232) gave results which led to the proposal that there is a similarity between cobalt−carbon and carbon−carbon bond cleavages in 2-propanol mixtures. The measured values of $\Delta V^{\ddagger}$ are composite quantities and this has been addressed[328] (entries 1233−1249). The solvent contribution is termed the transport contribution in these systems. Upon correcting the measured $\Delta V^{\ddagger}$ values to reflect only the homolytic fission intrinsic contribution, the values ranged from -2.0 to $+12.3$ cm^3 mol^{-1}, values which were noted to be measurably smaller than those for similar reactions in aqueous solution.[410,411]

J. Photochemical and Photophysical Processes

The effect of pressure on photochemical processes of inorganic systems has been reviewed elsewhere.[3,6,7,24−28] The applications have mainly focused

on ligand substitution reactions, which can be studied under continuous irradiation, or induced by flash photolysis. Both techniques have been applied in numerous systems and the results obtained will be treated separately.

During continuous irradiation the photochemical conversion, i.e., quantum yield, is measured as a function of pressure. The apparent volume of activation obtained must be corrected for the effect of pressure on all other deactivation processes such as radiative and nonradiative deactivation. Such information can only be obtained from photophysical measurements performed on the system as a function of pressure.[25,28] These complications can lead to a too simplistic interpretation of pressure effects on photochemical reactions as discussed in detail for Cr(III) systems in the literature.[412] These authors[412] concluded in their detailed treatment of earlier published data that the observed pressure effects indeed support an associative mechanism (A or I_a) for ligand labilization regardless of the reactive state responsible, which is in contrast to the earlier conclusions in several theoretical treatments that ligand labilization has a dissociative character in these complexes.

The effect of pressure on the photosubstitution reactions of a series of Ru(II) diimine complexes was studied (entries 1279−1289) in different solvents. The apparent activation volumes are all significantly positive and increase with increasing temperature. The latter trend could be ascribed to a changeover from MLCT to an LF state that is favored by higher temperatures, with the result that the apparent volume of activation mainly represents the photophysical component. The pressure data clearly rule out the possibility of an associative attack by the entering ligand and support an I_d mechanism for the substitution from the LF state. In this system there is thus no evidence for an associative substitution mechanism originating from the MLCT state (see further Discussion).

A series of photosubstitution reactions of the type (entries 1264−1273, 1278, and 1292)

$$M(CO)_6 + L \rightarrow M(CO)_5L + CO$$

$$M = Cr, Mo, W; L = \sigma \text{ donor ligand}$$

was studied as a function of pressure for various L and solvents. For all reactions investigated the photosubstitution quantum yield decreased with increasing pressure and resulted in significantly positive volumes of activation. Under the assumption that nonradiative deactivation is relatively independent of pressure, the apparent positive volumes of activation fit well into the picture of a dissociative mechanism, i.e., release of CO. This dissociation leads to a trigonal-bipyramidal $M(CO)_5$ fragment that can either recombine with CO, be trapped by a solvent molecule or bind to L. The difference in the pressure dependence for the recombination with CO or combination with L can be used to account for the observed activation volumes.

Another series of complexes of the type $W(CO)_4L$, involving either a ligand field (L = pyridine) or a metal to ligand charge-transfer state (L = 4-acetyl- and 4-cyanopyridine) as the lowest excited state, has been studied (entries 1293−1295). In these cases the effects of pressure on both the photosubstitution quantum yield and the excited-state emission lifetime were measured. The model suggests that most of the observed photochemistry in the MLCT state occurs via back population to the LF state. The larger pressure effects observed for the 4-acetyl- and 4-cyanopyridine complexes are consistent with the volume difference expected between the LF and MLCT excited states. The overall positive volumes of activation support a dissociative substitution mechanism as a result of LF excitation.

Numerous data are now available for photosubstitution reactions of the type (entries 1250−1259, 1262, 1263, 1276, 1277, 1296, and 1297)

$$M(CO)_4(phen) + L \rightarrow fac\text{-}M(CO)_3(phen)L + CO$$

$$M = Cr, Mo, W; L = PMe_3, PEt_3$$

There has been some controversy in the literature concerning the nature of the photosubstitution mechanism originating from the lower lying MLCT state. On one hand it was assumed that the observed photosubstitution proceeds dissociatively from the LF excited state, i.e., MLCT excitation is followed by thermal back population of the LF state.[413] On the other hand it was argued that the MLCT states themselves are photoactive and could in principle undergo an associative substitution reaction.[414] To resolve this apparent discrepancy, the effect of pressure on the above reaction as a function of irradiation wavelength, i.e., LF and MLCT excitation, was studied.

The first results for $L = PEt_3$ clearly suggested an associative substitution mechanism for the Mo and W complexes when irradiated directly into the MLCT bands. This is evidenced by negative $\Delta V^{\ddagger}$ values for 546-nm irradiation, in contrast to the positive $\Delta V^{\ddagger}$ values for ligand substitution when LF bands are excited with 366-nm light. In the case of the smaller Cr complex, MLCT excitation still gave a small positive value of $\Delta V^{\ddagger}$ indicative of a dissociative mechanism. The associative character of the MLCT states could be accounted for in terms of partial transfer of electron density from the metal to the phen ligand, by which the metal became more electrophilic and could undergo an associative nucleophilic attack by the entering ligand.

More recently, in a series of studies[329,415,416] there has been a systematic investigation of the influence of the metal center, entering nucleophile, and irradiation wavelength as a function of pressure for various M (M = Cr, Mo, W) and PR_3 (R = Me, Bu^n, Ph). The competition between dissociative LF and associative MLCT ligand substitution could be tuned by selecting the appropriate metal and entering ligand, ligand concentration, and pressure. The typical results displayed in Figure 12 show how an increase in irradiation wavelength from LF to MLCT excitation results in a changeover in the effect of pressure on Φ, viz., a decrease in Φ with increasing pressure for irradiation at 313 and 366 nm, in

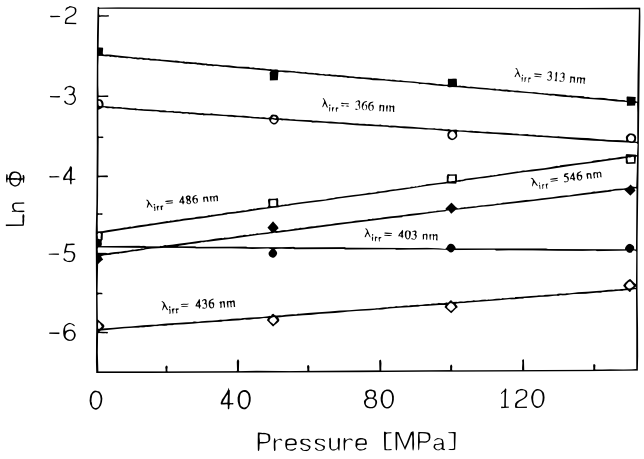

Figure 12. Plot of the natural logarithm of the quantum yield versus pressure at different excitation wavelengths for the reaction $M(CO)_4(phen) + PR_3 \rightarrow (h\nu)$ fac-$M(CO)_3(PR_3)(phen) + CO$ (M = Mo, R = Bu^n). (From ref 416.)

contrast to an increase in Φ with increasing pressure for irradiation at 436−546 nm. The results showed that the size of the metal center and the entering nucleophile determine the irradiation wavelength at which a mechanistic changeover occurs. The bulkier the entering nucleophile, the more difficult it is to observe an associative mechanism resulting from MLCT excitation.

One sytem was studied that involves MLCT photochemistry of a metal−metal-bonded complex (entries 1298 and 1299). Irradiation into the MLCT band of $(CO)_5ReMn(CO)_3$(α-diimine) in CH_2Cl_2 produces $Re(CO)_5Cl$ and $Mn(CO)_3$(α-diimine)Cl, whereas the substitution product $(CO)_5ReMn(CO)_2(PPh_3)$(α-diimine) is formed in the presence of a strong nucleophile (PPh_3). It was suggested that both photochemical reaction paths involve the initial photodissociation of CO from the parent complex. The apparent volumes of activation are very similar and are large positive values, and thus underline the concept of a common reaction step that involved the primary release of CO and support the dissociative nature of the photochemical process.

In the above presentation the importance of a possible influence of pressure on photophysical processes for the interpretation of the apparent volume of activation became obvious. This is of particular interest with respect to the partial molar volume of the excited state from which the photochemical process occurs. For this reason data for the effect of pressure on the excited-state lifetime and the associated activation volumes for radiative and nonradiative deactivation are included in the table (entries 1341−1395). For the quenching of the triplet excited state $^3[Cu(dpp)_2^+]^*$ the pressure effects are very small, which indicates the absence of solvation/desolvation effects or that the MLCT state is significantly distorted from the ground state. Quenching by Cr(III) complexes shows a larger positive volume of activation in the case of the $Cr(hfac)_3$ species, which can be related to the increase in solvent viscosity, since this quenching process approaches the diffusion limit. In contrast, the significantly negative volume of activation for the quenching by $Cr(tfac)_3$ is dominated by an electron-transfer mechanism. Quenching of $Ru(bpy)_3^{2+}$ in the excited state by different quenchers (entries 1373−1382) results in positive activation volumes, of which some are relatively high values. These can be interpreted in terms of an electron-transfer mechanism that involves precursor formation between the excited state and the quencher.

The application of pressure to CH_2Cl_2 solutions of either $Cu(dmp)_2^+$ or $Cu(dpp)_2^+$ led to systematic decreases in the emission lifetimes. The dominant deactivation pathways are nonradiative, and the observed pressure effects can be accounted for in terms of a unimolecular weak coupling mechanism. Other examples for which relatively small pressure effects were observed are $Pt_2(\mu\text{-}\eta^2\text{-}H_2P_2O_5)_4^{4-}$ and $Ir_2(\mu\text{-}\eta^2$-pyrazolate$)_2(COD)_2$ (entries 1389−1395) and a detailed interpretation of the reasons for these observations is given in the literature.

The effect of pressure on the distribution of electronic states has been investigated for the equilibria and dynamics of relaxation between the high spin/low spin configurations of a series of $Fe^{II}L_n$ complexes (entries 1300−1322). Reaction volumes as large as 16 $cm^3\ mol^{-1}$ have been reported for the low spin to high spin transition, depending on the nature of L. It has been argued from X-ray structural data that the intrinsic volume difference should be as large as 25−30 $cm^3\ mol^{-1}$,[338] such that the transition must be accompanied by an increase in electrostriction, i.e., a more tightly solvated high spin state. A combination of these data with the overall reaction volume data enables activation volumes to be calculated for the spin change in both directions. Many of these reactions exhibit absolute activation volumes close to 5 $cm^3\ mol^{-1}$, which means that the spin crossover for these species follows a common mechanism via a transition state located midway between the high and low spin states.

K. Reactions in Supercritical Fluids

Investigation of the potential of supercritical fluids as media for chemical separation and as reaction media for chemical transformations, including those having environmental relevance has become a subject of increasing activity in recent years.[8,417−420] Both catalytic and oxidation processes have been investigated.[421−424] To understand the underlying reaction mechanisms of chemical transformations in supercritical fluids, kinetic studies are essential and have been performed in a limited number of cases. Although activation volumes of chemical reactions in the liquid state have been determined for several decades, relatively little is known about activation volumes in supercritical fluids. There is obviously a difference, in part due to the sensitivity to pressure of the density of a supercritical medium compared with normal condensed liquid media. While activation volumes in liquids are characterized typically by values between −50 and +50 $cm^3\ mol^{-1}$, they can be thousands of $cm^3\ mol^{-1}$ in supercritical fluids, as has been demonstrated for the thermal decomposition of α-chlorobenzyl methyl ether[425] and for other reactions that have been reviewed recently.[418,419] Activation

volumes have been measured for a few simple cases in which for instance ligand substitution reactions are induced by flash photolysis.[216,426] Ring-closure reactions of the type

$$M(CO)_5L{-}L \rightarrow M(CO)_4(L{-}L) + CO$$

M = Mo, W;
L−L = 1,10-phenanthroline, 2,2′-bipyridine

exhibit volumes of activation as large as +7 L mol^{-1} under conditions near the critical point in supercritical ethane and CO_2. The results were interpreted[216] as evidence for a large repulsive contribution to the activation volume associated with the dissociation of CO during the ring-closure reaction. Other examples referred to in the literature[216] include the tautomerization of 2-hydroxypyridine to 2-pyridone and the hydrolysis of methoxynaphthalene in supercritical fluids. These reactions are accompanied by large negative volumes of activation which are associated with an increase in electrostriction.

It follows from these few examples that reaction and activation volume data in supercritical fluid solvents can be orders of magnitude different from those in the liquid state. This is not unexpected if we consider the large difference in partial molar volumes of species in the liquid state relative to the gaseous state. It is reasonable to anticipate considerable progress in this field in the future.

L. Bioinorganic and Biological Reactions

High-pressure kinetic and thermodynamic experiments have been performed on a number of bioinorganic and bioorganic systems that are of biological and biochemical interest and significance. This overall topic has been reviewed in recent years in contributions to a number of monographs.[3,4,6−8,11] The available information focuses on structural effects, hydrolysis processes, substitution reactions, ligation of small molecules by macromolecules, enzyme catalysis, and electron-transfer processes. A selection of these processes will be described and in some cases where a volume profile is available these will be interpreted in some detail.

Conformational changes and folding of proteins can be induced by pressure.[5,6−8,23] It was recently reported[427] that the unfolding of staphylococcal nuclease is accompanied by a volume change of −77 cm^3 mol^{-1}. The associated activation volume for folding (+92 cm^3 mol^{-1}) is much larger than for unfolding (+20 cm^3 mol^{-1}). The pressure-induced unfolding arises from a combination of increased solvation and decreased excluded volume in the unfolded state. In a similar way the helix−coil equilibrium in DNA was found to be very pressure sensitive as a result of solvent interactions in the stabilization and formation of DNA helices. The activation volume for helix formation was found to be −11.8 cm^3 mol^{-1}, as compared to a value of +39.9 cm^3 mol^{-1} for helix unfolding.[428] The authors propose that the activation volume for the forward reaction may arise from the volume change due to charging of the cytosine residues and the formation of base-stacking interactions. The large positive activation volume of strand separation may be a consequence of poor solvent packing of the DNA duplex major groove during dissociation. From the effect of pressure on phospholipid translocation in lipid bilayers,[429] for which a volume of activation of +17 cm^3 mol^{-1} was measured, information on the mechanism by which phospholipids spontaneously flip−flop in membranes could be obtained. The formation of nucleic acid homoduplexes was also found to be accompanied by significant volume changes (between −17 and +7 cm^3 mol^{-1}); the individual values depend on the degree of hydration of the different conformations that can be produced.[430] Other examples include monomer−dimer, tetramer−dimer, octamer−dimer, and octamer−tetramer equilibria all of which are very pressure sensitive (entries 1511−1522).

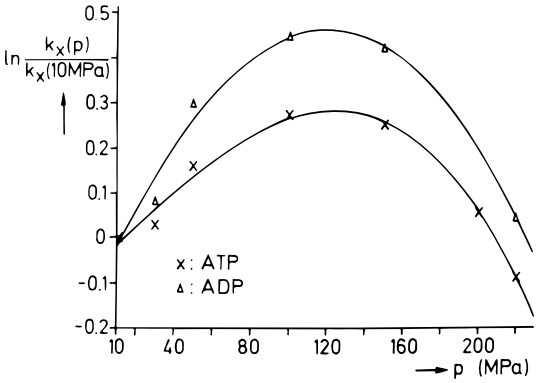

Figure 13. Logarithm of the normalized rate constants for the hydrolysis of ATP and ADP at 353 K versus pressure. (From ref 431.)

Several hydrolysis reactions of biological interest were investigated at elevated pressures. The hydrolyses of ATP and ADP exhibit a peculiar pressure dependence as shown in Figure 13.[431] The increase in rate with increasing pressure in the lower pressure range is ascribed to rate-determining attack by solvent (water). At higher pressure there is a change in rate-limiting step, which is then suggested to be a prior protonation step that is accompanied by partial charge neutralization resulting in a positive volume of activation. Hydrolysis reactions of nucleotide bound phosphate are in general accelerated by pressure, and $\Delta V^{\ddagger}$ values of between −10 and −15 cm^3 mol^{-1} have been reported.[432]

There are a number of important biological processes in which ligand substitution reactions on transition metal centers play an important role. One of these concerns the antitumor activity of platinum complexes, for which it is generally accepted that substitution reactions involving the metal complexes and DNA moieties play a key role in such processes.[433] Such substitution reactions in general follow an associative mechanism and are therefore usually characterized by markedly negative volumes of activation, i.e., the reactions are accelerated by pressure. A detailed account of the pressure dependence of such reactions is given in section 2.B.

A further example concerns the substitution reactions of cobalamins (vitamin B_{12}), reactions which have attracted considerable attention from kineticists (entries 1396−1411). In these systems the usually kinetically inert Co(III) ion is labilized considerably

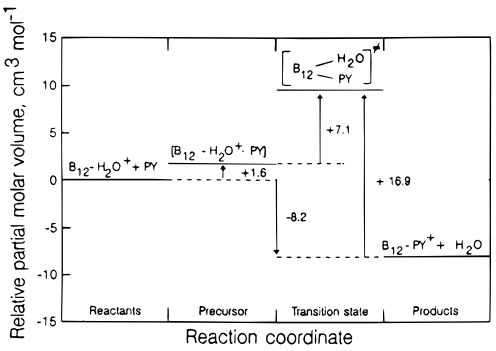

Figure 14. Volume profile for the reaction $B_{12}-H_2O^+ +$ pyridine. (From refs 351 and 352.)

by the corrin ring, and there has been some disagreement in the literature concerning the mechanism of these substitution reactions. The volume of activation results available for complex-formation and reverse aquation reactions of the type

$$B_{12}-H_2O^+ + L^{n-} \rightarrow B_{12}-L^{(1-n)+} + H_2O$$

are all in support of a dissociative (I_d) substitution mechanism. For the reaction of $B_{12}-H_2O^+$ with pyridine,[354] the observed rate constants k_{obs} reached a limiting value at high pyridine concentrations, which was interpreted as evidence for a limiting D mechanism. However, later work[351,352] showed that the curvature of the plot of k_{obs} versus concentration must be due to a precursor formation step preceding the dissociative interchange (I_d) step. The nonlinear concentration dependence enabled a kinetic separation of the precursor formation constant and the rate-determining interchange rate constant to be made, such that a detailed volume diagram for the overall process could be drawn (see Figure 14). The volume profile clearly illustrates the dissociative character of the transition state.

The mechanism of the binding of small molecules such as O_2 and CO to ferrous heme and hemoproteins has been the focus of many investigations in recent years. Model heme complexes were usually employed in an effort to clarify our understanding of the reactions of the corresponding proteins. Two model heme systems and various neutral ligands were used to study the bimolecular addition to the five-coordinate ferrous model heme complexes (entries 1446−1450) using two different photolysis techniques. The reported $\Delta V^{\ddagger}$ data correlate well with the addition rate constants: for the slower reactions, bond formation is rate determining and results in negative $\Delta V^{\ddagger}$ values; for the faster reactions, the processes become diffusion controlled and are slowed by increasing pressure due to the large increase in solvent (toluene) viscosity. In a subsequent study,[364] the reaction of CO with MCPH was studied as a function of pressure in a very viscous medium. The data reported in Figure 15 clearly show a changeover in rate-determining step from bond formation to control by diffusion upon increasing the pressure, i.e., from a $\Delta V^{\ddagger}$ value of -9.6 to a value of $+7.1$ cm^3 mol^{-1}. This is an example of a changeover from activation control to diffusion control where the mechanistic diagnosis

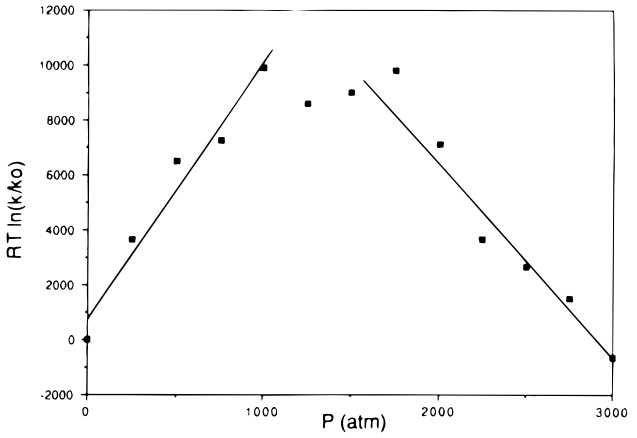

Figure 15. Plot of $RT(\ln(k/k_o))$ versus pressure for the reaction of CO with the intermediate formed by nanosecond laser flash photolysis of MCPH−CO. (From ref 364.)

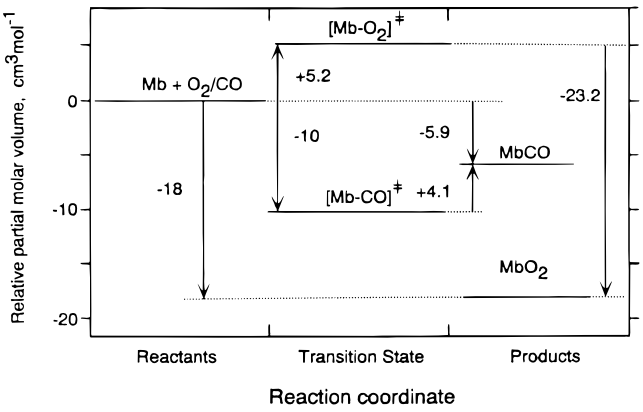

Figure 16. Volume profile for the reactions of CO and O_2 with myoglobin at 298 K. (From ref 360.)

has emerged from kinetic measurements at high pressures.

Similar techniques were applied to study the effect of pressure on the bimolecular association rate constant for the reaction of sperm whale myoglobin with a series of neutral ligands in water (entries 1416−1426). It follows from the data that only the reaction with CO is characterized by a negative $\Delta V^{\ddagger}$ value, which is in line with a bond formation process. The positive $\Delta V^{\ddagger}$ values found for the other ligands were ascribed to the entry of the ligand into the protein pocket, which will be accompanied by pronounced desolvation and presumably conformational changes on the protein chain. The effect of pressure on the escape of the ligand from the protein-separated pair, resulted in distinctly positive $\Delta V^{\ddagger}$ values (entries 1426−1436). These values are consistent with the notion of a "gate" that operates in both directions of the process.

The large difference in $\Delta V^{\ddagger}$ values observed for the binding of O_2 and of CO to deoxymyoglobin stimulated the need to develop a complete volume profile for both systems. The profiles are shown in Figure 16;[360] that for the binding of O_2 is characterized by a substantial increase in volume in proceeding from the reactant state to the transition state, followed by a significant volume reduction when the product state is reached. The observed volume increase was ascribed to rate-determining movement of O_2 through

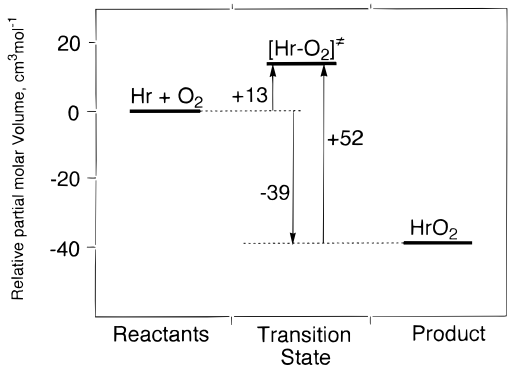

Figure 17. Volume profile for the reaction of hemerythrin with O_2. (From ref 356.)

the protein to the heme pocket, which may involve hydrogen bonding to the distal histidine as well as desolvation. This step is followed by rapid bond formation with the Fe(II) center, during which the change in spin state from high to low, the movement of the Fe(II) center into the porphyrin plane, and the associated conformational changes account for the drastic volume collapse. The overall reaction volume of -18 cm^3 mol^{-1} demonstrates the large volume reduction caused by the binding of O_2. The volume profile for the binding of CO shows a considerable volume decrease on going from the reactant to the transition state, which has been attributed to rate-determining bond formation. The reverse bond cleavage reaction is accompanied by a volume decrease, which may be related to the different bonding mode of CO compared with O_2. This difference in bonding mode must also account for the much smaller absolute reaction volume observed in this case. It should be mentioned that such measurements and their interpretation were criticized by Frauenfelder et al.[434] on the basis of low-temperature high-pressure investigations at <160 K in 75% glycerol solutions. They considered the influence of conformational substates in the interpretation of the pressure data, to account for the different volume changes found for O_2 and CO.

A volume profile was also obtained (Figure 17) for the binding of dioxygen to hemerythrin (entries 1412 and 1413). The $\Delta V^{\ddagger}$ values for the "on" and "off" reactions as well as the overall reaction volume are about twice as large as for the corresponding myoglobin case. In the hemerythrin system two Fe(II) centers are oxidized to Fe(III) during which dioxygen is reduced and bound as hydroperoxide to one Fe(III) center. The $\Delta V^{\ddagger}_{on}$ value can partly be accounted for in terms of desolvation of oxygen during its entrance into the protein. The value is, however, such that it suggests some form of dynamic "breathing" motion of the protein that momentarily causes an opening up of a cleft and permits oxygen to enter the protein. The marked volume decrease that occurs following the formation of the transition state can be ascribed to the oxidation of the iron centers and the reduction of O_2 to O_2^{2-}. The fact that the overall volume reduction is almost double that observed for the oxygenation of myoglobin may indicate similar structural features in oxyhemerythrin and oxymyoglobin. This would suggest that a description of the bonding mode as $Fe^{III}-O_2^-$ or $Fe^{III}-O_2H$ (H from

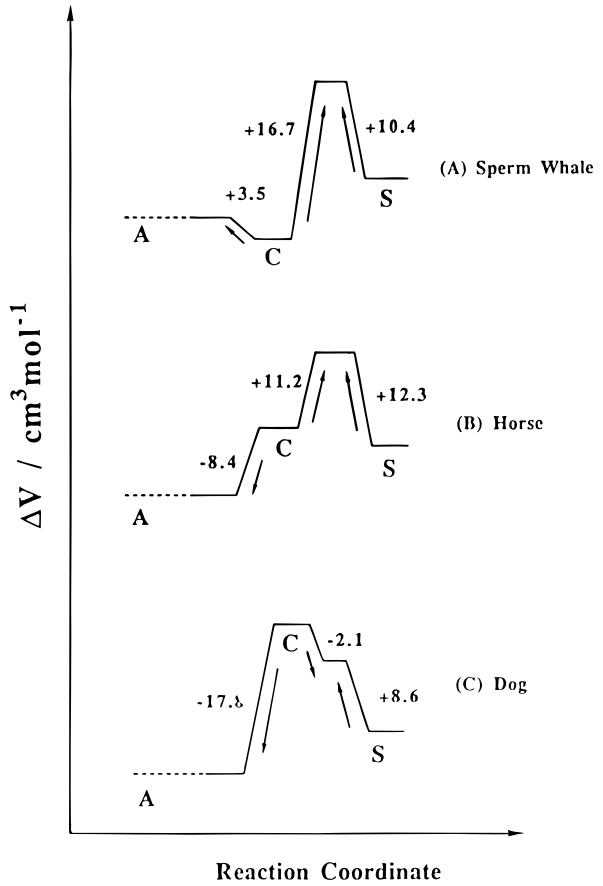

Figure 18. Activation volume diagrams for the binding of O_2 to myoglobins. (From ref 361.)

histidine E7) instead of $Fe^{II}-O_2$, may be more appropriate for oxymyoglobin. Eyring and co-workers[357] studied the uptake of dioxygen by deoxymyohemerythrin and found positive $\Delta V^{\ddagger}$ values for both the uptake and release processes (entries 1414 and 1415). They also concluded that the positive value for the uptake reaction must be due to a different rate-determining step that occurs prior to Fe−O bond formation.

The effect of pressure on the binding kinetics of O_2 and CO to myoglobin was studied in more detail on a milli-, micro-, and nanosecond time scale for sperm whale, horse, and dog myoglobin. The results were analyzed quantitatively in terms of the following three-step mechanism:

$$A(MbL) \leftrightarrow B(Mb\cdot L) \leftrightarrow C(Mb\cdots L) \leftrightarrow S(Mb + L)$$

where A represents the bound species, B the short-lived geminate pair, C the longer lived geminate pair, and S the entirely separated species. The volume profiles for all three myoglobins may be drawn (Figure 18); from these it was concluded that the O_2 diffusion step within the protein matrix is quite different among the three Mb species.[361] It was further suggested that the activation volumes are very sensitive to the amino acid residues adjacent to and flanking the ligand path channel. In the case of CO binding (entries 1425−1441), the overall $\Delta V^{\ddagger}$ was negative, which is consistent with the rate-determining bond formation step.

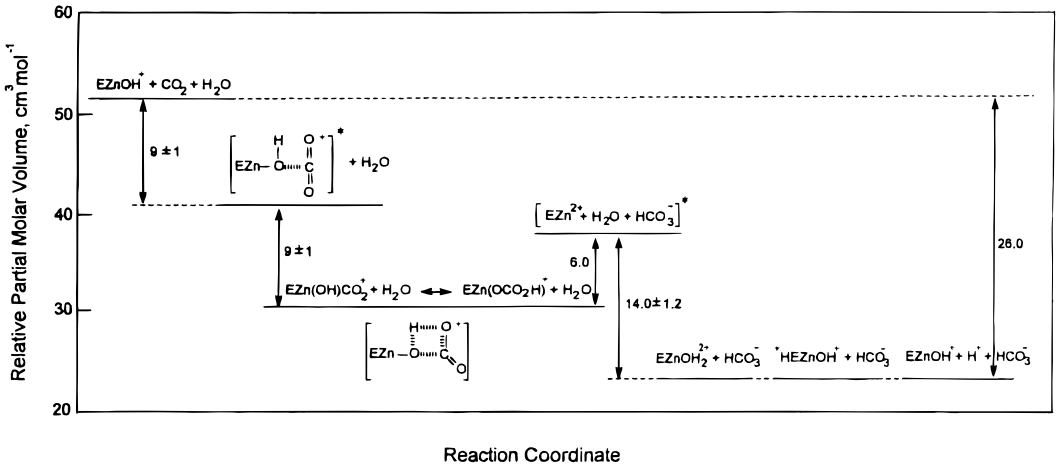

Figure 19. Volume profile for the carbonic anhydrase catalyzed hydration of CO_2 and dehydration of HCO_3^- at 298 K. See ref 369 for details.

The binding of CO to horseradish peroxidase (entries 1458−1469) was studied as a function of pressure, temperature, and solvent. The observed $\Delta V^{\ddagger}$ is the sum of several components: binding of CO, subsequent conformational changes occurring in the protein, and the reorganization of the solvation shell. The authors[365] conclude that these events are interconnected and difficult to analyze independently. The large variation in $\Delta V^{\ddagger}$ under different experimental conditions suggests that solvent reorganization is the predominant factor which drives the response of the system. The binding of CO to various reduced hemoproteins, including several cytochrome P450 variants, chloroperoxidase and lactoperoxidase, was studied under pressure (entries 1470−1485). The activation volumes depend on the nature of the proximal axial heme ligand; the values are relatively small (+1 to +16 $cm^3\ mol^{-1}$) for cysteine (S^-) ligand hemoproteins, and markedly negative (−3 to −36 $cm^3\ mol^{-1}$) for histidine (N) ligand proteins. These results suggest that the CO binding transition state of the S ligand class has a molecular conformation similar to that of the ground state. In the case of the histidine class, the transition state appears to involve protein conformational changes and/or solvational changes. The effect of substrate analogues on the kinetics of recombination of CO to ferrous cytochrome $P450_{CAM}$ has been studied as a function of pressure (entries 1479−1485). A small positive (+4 $cm^3\ mol^{-1}$) $\Delta V^{\ddagger}$ value was found for the binding of CO to the substrate free protein. However, the binding of *d*-camphor and some camphor analogues into the heme pocket resulted in considerably reduced $\Delta V^{\ddagger}$ values to negative quantities (−14 to −32 $cm^3\ mol^{-1}$). This trend suggests that iron−ligand bond formation is the rate-limiting process for the substrate-bound protein.

A number of systems of biological interest have been studied in which the kinetics of molecular association and a subsequent binding step were monitored as a function of pressure. For instance the binding of NADH to liver alcohol dehydrogenase is characterized by significantly positive volumes of activation (entries 1486−1488), i.e., the binding rate is decelerated with increasing pressure. No explanation for this observation was offered. Other examples studied include: binding equilibria in the *lac* repressor system,[435] ribosomal subunit association of *Escherichia coli*,[436] and substrate affinity of an immobilized glucoamylase.[437] Dissociation of the cytochrome b_5−porphyrin cytochrome *c* complex is accompanied by a large volume reduction (entry 1492). This has been ascribed to the removal of solvent from the interface of the two molecules on closest approach, which will result in the rehydration of the bare surface charges upon separation. The effect of pressure has also been monitored during the thermal inactivation of taka-amylase A, and activation and reaction volume data were reported.[438] Ligand binding and kinetic behavior of butyrylcholinesterase from human plasma were also studied under high pressure.[439] Volume changes were determined and the kinetic data showed that binding of substrate to the enzyme led to a pressure-sensitive enzyme conformational state, which did not participate in the catalytic cycle.

The effect of pressure on the CO stretch mode of substrate-free cytochrome P450 was studied; this provided information on the conformational substates of the protein.[440] In another study[441] the effect of norbornane-type substrate binding on the pressure dependence of the spin-state equilibrium of cytochrome P450 was examined. Reaction volumes associated with the high spin to low spin transition varied between −70 and −22 $cm^3\ mol^{-1}$ depending on the substrate employed (camphor, camphorquinone, camphane, norcamphor, and norbornane).

The effect of pressure on some enzyme-catalyzed reactions has been investigated. Activation volumes of subtilisin Carlsberg in organic solvents, particularly with the enzyme hydrated, have a larger magnitude than in aqueous solution.[442] It follows that the primary effect of pressure is to enhance the stripping of water from an enzyme in polar solvents and leads to decreased enzyme activity.[442] Volume profiles have been generated for some catalytic systems.[369,443] In the case of the catalytic activity of carbonic anhydrase, a systematic study of the effect of pressure on all the accessible reaction steps enabled the establishment of a complete volume profile[369] as shown in Figure 19. The volume changes associated with the "CO_2 uptake/decarboxylation"

step and the ligand substitution process (HCO_3^- for H_2O), exhibit different trends with respect to the location of the transition state. In the first part of the catalytic cycle the transition state is located approximately halfway between the reactant and product states, which is in good agreement with the structure of the suggested transition state. The subsequent ligand substitution process is characterized by a transition state that has a significantly higher partial molar volume than either the reactant or product states, which is indicative of a dissociative substitution mechanism. Overall this is a complex system and a complete explanation is best obtained by consulting the original literature.

Several investigators have applied high-pressure techniques in the study of electron-transfer reactions in biological systems. In one of the earliest studies,[442] the reaction rates of the multiheme hydroxylamine oxidoreductase were studied as a function of pressure. By way of comparison, the binding of CO to the dithionite-reduced enzyme was characterized by negative $\Delta V^{\ddagger}$ values (between -14 and -36 cm^3 mol^{-1}), whereas the reduction of the *c* hemes of the enzyme by NH_2OH was characterized by positive or negative $\Delta V^{\ddagger}$ values, depending on the selected temperature and composition of the solvent. In other work[444] the effect of pressure on the electron-transfer kinetics in and around the chloroplast cytochrome *bf* complex was studied. For the reduction of $P700^+$ (reaction center of Photosystem I) by reduced plastocyanin, $\Delta V^{\ddagger}$ was found to be $+9.6$ cm^3 mol^{-1}, compared with a value of -14 cm^3 mol^{-1} for the reduction of oxidized plastocyanin by ascorbate. The kinetics of oxidation of decyl plastoquinol by the *bf* complex gave rise to a $\Delta V^{\ddagger}$ value of $+18$ cm^3 mol^{-1}. The complexity of the systems made an accurate interpretation of the observed pressure effects very difficult, and therefore stimulated further work on less complicated and perhaps more "ideal" systems.

A challenging question concerns the feasibility of the application of high-pressure kinetic and thermodynamic techniques in the study of "long distance" electron-transfer reactions. Do such processes exhibit a characteristic pressure dependence, and to what extent can a volume profile analysis reveal information on the intimate mechanism of the electron-transfer process?

The systems investigated were intermolecular and intramolecular electron-transfer reactions between ruthenium complexes and cytochrome *c* (see entries 1495−1508). A series of intermolecular reactions between chelated cobalt complexes and cytochrome *c* was also studied (see entries 1493 and 1494). A variety of high-pressure experimental techniques, including stopped-flow, flash photolysis, pulse radiolysis, and voltammetry, were employed in these investigations. As the following presentation will show, a remarkably good agreement was found between the volume data obtained with the aid of these different techniques, which clearly demonstrates the complementariness of these methods for the study of electron-transfer processes.

Application of pulse-radiolysis techniques revealed that the following intramolecular and intermolecular electron-transfer reactions all exhibit a significant acceleration with increasing pressure. The reported volumes of activation are -17.7 ± 0.9, -18.3 ± 0.7, and -15.6 ± 0.6 cm^3 mol^{-1}, respectively for the three reactions, and denote a marked volume reduction as reaction proceeds from the reactant to the transition state.[376]

$$(NH_3)_5Ru^{II}-(His33)cyt\ c^{III} \rightarrow (NH_3)_5Ru^{III}-(His33)cyt\ c^{II}$$

$$(NH_3)_5Ru^{II}-(His39)cyt\ c^{III} \rightarrow (NH_3)_5Ru^{III}-(His39)cyt\ c^{II}$$

$$Ru^{II}(NH_3)_6^{2+} + cyt\ c^{III} \rightarrow Ru^{III}(NH_3)_6^{3+} + cyt\ c^{II}$$

At this stage it was uncertain which mechanistic or other features the negative volumes of activation actually represented since overall reaction volumes were not available. However, data in the literature[268] suggested that the oxidation of $Ru(NH_3)_6^{2+}$ to $Ru(NH_3)_6^{3+}$ is accompanied by a volume increase of ca. 30 cm^3 mol^{-1}, which would mean that the activation volumes quoted above could principally be a consequence of volume changes associated with the oxidation of the ruthenium redox partner.

With the purpose of determining the overall reaction volumes and thereby locating the position of the transition state along the reaction coordinate, a series of intermolecular electron-transfer reactions of cyt *c* with pentaammine ruthenium complexes was studied. The sixth ligand on the ruthenium complex was selected in such a way that the overall reaction driving force was sufficiently low so that the reaction kinetics could be studied in both directions.[374,375] The substituents chosen were isonicotinamide (isn), 4-ethylpyridine (etpy), pyridine (py), and 3,5-lutidine (lut) (see entries 1498−1505). The overall reaction can be formulated as

$$Ru^{III}(NH_3)_5L^{3+} + cyt\ c^{II} \leftrightarrow Ru^{II}(NH_3)_5L^{2+} + cyt\ c^{III} \qquad k_f,\ k_b$$

For all the systems investigated the forward reaction was significantly decelerated by pressure, whereas the reverse reaction was equivalently accelerated by presssure. The absolute values of the volumes of activation for the forward and reverse processes are indeed very similar, demonstrating that a similar rearrangement occurs in order to reach the transition state. In addition, the overall reaction volume for these systems could be determined spectrophotometrically by recording the spectrum of an equilibrium mixture of components as a function of pressure, and electrochemically by recording cyclic and differential pulse voltammograms as a function of pressure (entries 1537−1541).[381] A comparison of the reaction volume data demonstrates the good agreement between the values obtained from the difference in the volumes of activation for the forward and reverse reactions, and those obtained thermodynamically. The values show that $|\Delta V^{\ddagger}| \approx 0.5|\Delta V|$, i.e., the transition state lies approximately halfway between

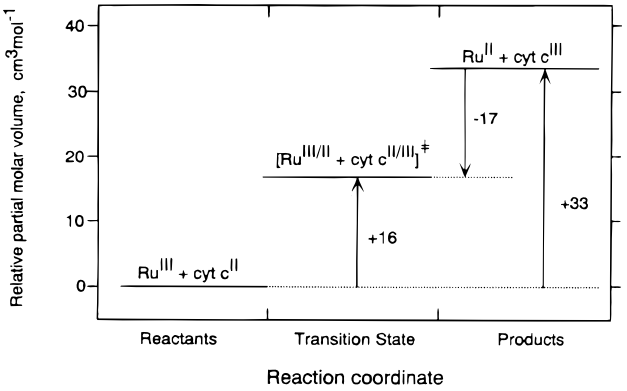

Figure 20. Volume profile for the reaction of an isonicotinamide pentaammine ruthenium complex with cytochrome *c* at 298 K. (From ref 374.)

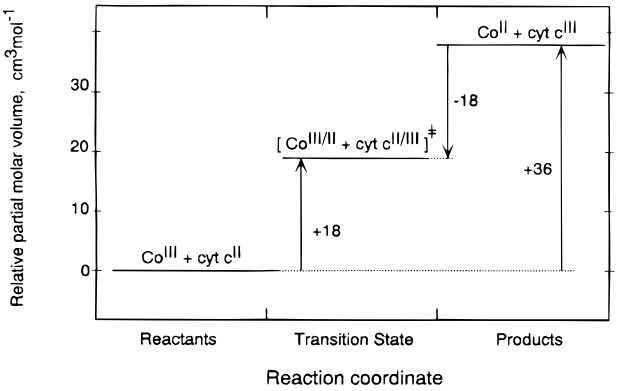

Figure 21. Volume profile for the reversible interaction of $Co^{II/III}$(amines) with cyt $c^{III/II}$ at 25.0 °C at neutral pH. (From refs 372 and 445.)

the reactant and product states on a volume basis, and obviously for electron transfer in either direction. The typical volume profile in Figure 20 illustrates these findings.

Similar results were recently obtained for the redox reactions of a series of cobalt amine complexes with cytochrome *c*.[372,445] In general a good agreement exists between the kinetically and thermodynamically determined parameters, and the typical volume profile in Figure 21 once again demonstrates the location of the transition state with respect to the reactant and product states.

At this point it may be important to ask the question, to what may these volume changes be attributed? It was always argued that the major volume change arises from changes on the redox partner and not on cytochrome *c* itself. This was suggested by the fact that the change in partial molar volume associated with the oxidation of the Ru(II) and Co(II) complexes investigated, as obtained from electrochemical and density measurements, almost fully accounted for the observed overall reaction volume. Thus the reduction of cytochrome *c* can only make a minor contribution toward the overall volume change.

These arguments were apparently not compatible with electrochemical results obtained by Cruanes et al.[382] who reported that the reduction of cytochrome *c* is accompanied by a volume reduction of 24 cm^3 mol^{-1} (entries 1542−1552). This value is so large that it represents virtually all of the total of the reaction volume obtained for the reactions investigated and discussed above. A reinvestigation of the electrochemistry of cytochrome *c* as a function of pressure, using cyclic and differential pulse voltammetric techniques,[381] yielded a reaction volume of -14.0 ± 0.5 cm^3 mol^{-1} for the reaction.

$$\text{cyt } c^{III} + \text{Ag(s)} + \text{Cl}^- \rightarrow \text{cyt } c^{II} + \text{AgCl(s)}$$

A correction for the contribution from the reference electrode could be made on the bases of the data published by Tregloan et al.[47] and of a series of measurements of the potential of the Ag/AgCl (KCl saturated) electrode relative to the Ag/Ag^+ electrode as a function of pressure. The contribution of the reference electrode turned out to be -9.0 ± 0.6 cm^3 mol^{-1}, from which it then followed that the reduction of cytochrome c^{III} is accompanied by a volume decrease of 5.0 ± 0.8 cm^3 mol^{-1}. This contribution is much smaller than reported by Cruanes et al.[382] and is also consistent with the contributions from other arguments referred to above. Thus it can be concluded that the observed activation and reaction volumes mainly arise from volume changes on the ruthenium and cobalt complexes, which in turn will largely be associated with changes in electrostriction in the case of the ammine complexes. The oxidation of the Ru(II) ammine complexes will be accompanied by a large increase in electrostriction and almost no change in the metal−ligand bond length, whereas in the case of the cobalt complexes a significant contribution from intrinsic volume changes associated with the oxidation of Co(II) will partially account for the observed effects.[376]

One system has been investigated in which the effect of pressure on the electron-transfer rate constant yielded information relevant to the actual electron-transfer route. The effect of pressure on distant electronic coupling in $Ru(bpy)_2(im)$-modified His33 and His72 cytochrome *c* derivatives, for which the electron transfer from Fe(II) to Ru(III) is activationless, was investigated (entries 1495−1497).[373] In the case of the His33-modified system the electron-transfer rate constant exhibited no dependence on pressure within experimental error limits. However, the rate constant for the His72-modified protein increased with increasing pressure, corresponding to a $\Delta V^‡$ value of -6 ± 2 cm^3 mol^{-1}. Since this value is exactly opposite that expected for the reduction of Ru(III), the result was interpreted as an increase in electronic coupling at elevated pressure. The application of moderate pressures will cause a slight compression of the protein that in turn shrinks the through-space gaps, key units in the electron-tunneling pathway between the heme and His72. A decrease of 0.46 A in the tunneling path length at a pressure of 150 MPa can account for the observed increase in rate constant. This in turn means that there is an average decrease in the space gap of 0.1 A. The absence of an effect for the His33-modified species is understandable since electronic coupling through covalent and hydrogen bonds will be less pressure sensitive than coupling via van der Waals gaps.[373]

Very recently[446] Morishima and co-workers investigated the effect of pressure on electron-transfer rates in zinc/ruthenium modified myoglobins. The rate constant for electron transfer from photoexcited $^3ZnP^*$ to the $Ru(NH_3)_5^{3+}$ moiety of the protein decreased from 5×10^7 to 55 s^{-1} upon increasing the donor−acceptor distance from 9.5 to 19.3 Å when the ruthenium complex is attached to His70 and His83, respectively. This decrease in rate constant was accompanied by an increase in the associated volume of activation from +4 to +17 cm^3 mol^{-1}. The authors account for this difference in terms of the effect of pressure on the electronic coupling term H_{AB}. However, in the context of the results reported above and the volume changes associated with the reduction of Ru(III) ammine complexes, the gradual increase in $\Delta V^{\ddagger}$ with increasing donor−acceptor distance and with decreasing rate constant could be a clear demonstration of "early" (for the fast) and "late" (for the slow reactions) transition states. Volume changes mainly associated with changes in electrostriction on the ruthenium ammine center will control the solvent reorganization and so account for the "early" (reactant-like) and "late" (product-like) transition states. These results and the conclusions based upon them illustrate the insight that can be obtained regarding the mechanism of long-distance electron-transfer reactions from the application of high-pressure techniques.

M. Theoretical Calculations and Modeling

Computation of partial molar volumes and radii based on overlapping van der Waals spheres has been reported for a wide range of inorganic molecular ions.[447a] The results were compared with experimentally determined partial molar volumes and thermochemical radii. The correlations are remarkably good and may be used to estimate with some confidence the partial molar volume of ions which have not been experimentally determined. The authors venture that the accuracy of the calculated partial molar volumes may be sufficient to calculate molar volumes of transition states.

Various analytical equations have been developed to analyze the dependence of observed rate constants on pressure.[447b] These are especially employed when plots of ln *k* versus pressure deviate from linearity, i.e., when the volume of activation is a function of pressure.

The solvent exchange processes on metal ions and complexes described in section 2.A present ideal reactions to simulate and predict activation volumes theoretically since solvent exchange is a symmetrical reaction and does not involve overall solvational changes. The activation volumes for solvent exchange on the divalent cations of the first row of transition metals determined experimentally exhibit clear evidence for a mechanistic changeover along the series, i.e., from more associative for the earlier, larger cations to a more dissociative one for the later, smaller cations. It has been claimed on the basis of theoretical calculations[384−387] that the interpretation of such activation volume data could be considered faulty, and arguments were presented against a mechanistic changeover along the series. Additional theoretical calculations were needed in order to investigate the validity of the mechanistic proposals that were based on calculations, in an endeavor to resolve the disparate conclusions.

The original studies[384−387,448] involved ab initio self-consistent field (SCF) calculations of the binding energies, ligand-field effects, water exchange reactions, and exchange mechanisms of hexahydrated divalent first row transition metal cations. In subsequent work,[388,449] Rotzinger succeeded in computing the structures of the transition states and intermediates formed during the water exchange reactions of the first row transition metals with ab initio methods at the Hartree−Fock or CAS−SCF (complete active space−SCF) level. It was now possible to generate A, I_a, I_d, and D reaction pathways, and to optimize the structures of the transition and intermediate states. Furthermore, the calculated bond length changes that occurred during the activation process were entirely consistent with the activation volume data, and indicated that an associative interchange mechanism can operate for some metal ions, in contrast to the previous prediction.[387] Density functional theory has also been applied successfully to describe the solvent exchange mechanism for aquated Pd(II), Pt(II), and Zn(II) cations.[389,450] Molecular dynamics simulation studies have been performed on the structure of the first hydration shell of some trivalent lanthanide ions, on the change in coordination number decreasing from 9 to 8 along the series, and on the mechanism of water exchange between hydrated lanthanide ions and bulk water.[451] The latter study demonstrated an excellent agreement with the observed high-pressure kinetic effects, i.e., experimental activation volumes. Finally, molecular dynamics simulations and density functional theory were applied to model water exchange reactions in the second coordination (first solvation) sphere on hexaaquachromium(III).[452]

3. Volume Data for Organic Reactions

A. General Remarks

Our approach has basically been the same as that offered in our previous reviews.[1,2] Thus, since high-pressure kineticists have in many cases measured reaction volumes for the processes of interest as well, these results have been recorded in the Remarks column of Table 2. The results of Holroyd's experiments (in which dynamics led him to deduce reaction volumes) are included in this section. In other cases in which the reaction volume was of primary or even exclusive concern, the data are reported separately (in Table 4). The entry under *T* (°C) in Tables 2−4 reads "ambient" in many instances; this word was employed whenever the original authors used it (or an equivalent such as room temperature), or if no mention was made of the temperature at all.

In our previous review,[1] we called special attention to the fact that many authors had claimed to have made corrections in the volume profiles for compressibility effects. We do so again, as the phrases used in the literature do not always inspire confidence that

Table 2. Activation Volumes of Organic Reactions

No.	reaction	solvent	T/ °C	P/MPa	no of k data	$\Delta V_0^{\neq}$ /cm^{3}mol^{-1}	ref	remarks
1.	CIDEP[a1] decay of 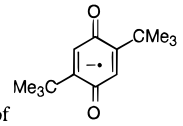	i-PrOH-Et_3N	ambient	39.2	4	+26	453	i-PrOH 91 v%, b1
2.	CIDEP[a1] decay of 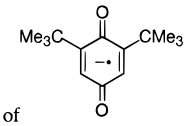	i-PrOH-Et_3N	ambient	39.2	4	+30	453	i-PrOH 91 v%, b1
3.	CIDEP[a1] decay of 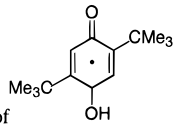	PhH-Et_3N	ambient	39.2	4	+11	453	PhH 91 v%, b1
4.	CIDEP[a1] decay of 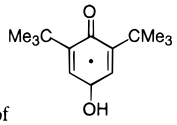	PhH-Et_3N	ambient	39.2	4	+12	453	PhH 91 v%, b1
5.	CIDEP[a1] decay of 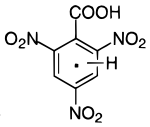	aq i-PrOH	ambient	39.2	4	+11	453, 454	i-PrOH 90 v%, c1
6.	CIDEP[a1] decay of 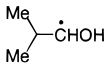	i-BuOH	ambient	39.2	4	+9	453	d1
7.	spin exchange of 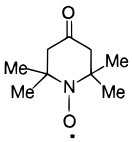	n-pentane	25	64	6	+12.7	455	
8.		n-hexane	25	64	6	12.1	456	
9.		PhH	ambient	50	5	+18.4	457	
10.		PhMe	23	59	7	+13.7	458	
11.		o-$Me_2C_6H_4$	ambient	59	7	+15.3	457	
12.		$PhNO_2$	20	44	4	+13.3	458	
13.		acetone	25	64	6	+8.7	456	
14.		acetone	30	59	7	+7.7	458	
15.		H_2O	15	59	5	-7.6	458	
16.		MeOH	25	59	7	+6.7	458	
17.		EtOH	ambient	59	7	+9.5	457	
18.		i-PrOH	25	59	7	+15.4	458	
19.		i-BuOH	ambient	39	5	+19.6	457	
20.	spin exchange of 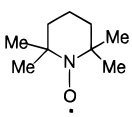	n-pentane	25	64	6	+9.2	455	
21.		n-hexane	25	64	6	+14.3	455	
22.		acetone	25	64	6	+10.7	456	
23.	spin exchange of 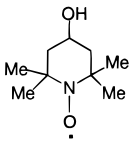	n-pentane	25	64	6	+13.0	455	
24.		n-hexane	25	64	6	+13.3	455	
25.		acetone	25	64	6	+8.1	455	
26.		n-hexane-EtOH	25	64	6	+14.5	455	n-hexane 90 v%.

Table 2. (Continued)

No.	reaction	solvent	T/ °C	P/MPa	no of k data	$\Delta V_0^{\neq}$ /cm^{3}mol^{-1}	ref	remarks
27.	spin exchange of 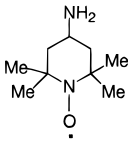	*n*-pentane	25	64	6	+9.9	455	
28.		*n*-hexane	25	64	6	+11.5	455	
29.		acetone	25	64	6	+12.6	455	
30.	spin exchange of 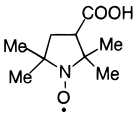	acetone	25	64	6	+12.3	455	
31.	spin exchange of 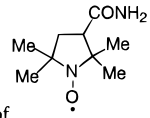	acetone	25	64	6	+10.6	455	
32.	spin exchange of 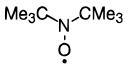	acetone	25	64	6	+7.4	456	
33.	spin exchange of 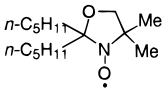	acetone	25	64	6	+10.7	455	
34.	spin exchange of 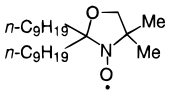	acetone	25	64	6	+11.1	455	
35.		PhMe	25	64	6	+16.6	455	
36.	quenching of $^1O_2$ by solvent	*n*-hexane	25	400	6	-9	459	e1
37.		*cy*-$C_6H_{11}Me$	25	400	6	-6	459	e1
38.		MeCN	25	300	5	-6	459	e1
39.		MeOH	25	300	6	-4	459	e1
40.		PhH	25	110	13	-8.3	460	
41.		PhMe	25	400	9	-10.0	460	
42.		*m*-$Me_2C_6H_4$	25	400	9	-13.0	460	
43.		*o*-$Me_2C_6H_4$	25	400	9	-14.2	460	
44.		*p*-$Me_2C_6H_4$	25	400	9	-19.2	460	
45.		1,3,5-$Me_3C_6H_3$	25	300	7	-20.7	460	
46.		*n*-pentane	25	-	-	-11.9	461	
47.		*cy*-C_6H_{12}	25	80	-	-9.9	461	
48.		CH_2Cl_2	25	-	-	-8.7	461	
49.		$CHCl_3$	25	100	6	-8.0	461	
50.		acetone	25	120	5	-8.2	461	
51.		MeCN	9	-	-	-6.5	461	
52.		MeCN	20	-	-	-6.5	461	
53.		MeCN	24	-	-	-7.9	461	
54.		MeCN	25	120	5	-7.0	461	
55.		MeCN	30	-	-	-7.6	461	
56.		MeCN	34	-	-	-8.7	461	
57.		MeCN	35	-	-	-7.4	461	
58.		MeCN	40	-	-	-7.5	461	
59.		MeCN	45	-	-	-9.0	461	
60.		MeCN	50	-	-	-8.8	461	
61.		MeCN	55	-	-	-8.3	461	
62.		MeCN	65	-	-	-9.4	461	
63.		MeCN	67	-	-	-10.7	461	
64.		PhMe	10	-	-	-8.6	461	
65.		PhMe	25	120	5	-10.3	461	
66.		PhMe	40	-	-	-11.1	461	
67.		PhMe	70	-	-	-14.4	461	
68.		PhCN	25	100	6	-7.2	461	
69.		CCl_4	25	-	-	-10.6	461	
70.		C_6F_6	25	60	-	-9.9	461	
71.		formamide	25	-	-	-4.1	461	
72.		CS_2	25	-	-	-10.5	461	
73.	quenching of $^1O_2$ by DABCO[f1]	PhCN	25	100	4	-10.0	462	
74.		MeCN	25	120	6	-10.8	462	
75.		acetone	25	120	5	-14.6	462	

Table 2. (Continued)

No.	reaction	solvent	T/ °C	P/MPa	no of k data	$\Delta V_0^{\neq}$ /cm^{3}mol^{-1}	ref	remarks
76.	quenching of $^1O_2$ by DABCO[f1]	CH_2Cl_2	25	120	5	-14.9	462	
77.		PhMe	25	120	6	-17.1	462	
78.		$CHCl_3$	25	120	4	-19.0	462	
79.	quenching of $^1O_2$ by piperazine	*n*-hexane	ambient	120	13	-42.0	463	
80.		PhMe	ambient	120	13	-27.4	463	
81.		CH_2Cl_2	ambient	120	13	-28.2	463	
82.		PhCl	ambient	120	13	-24.3	463	
83.		*o*-$Cl_2C_6H_4$	ambient	120	13	-22.6	463	
84.		PhCN	ambient	120	13	-18.8	463	
85.	quenching of $^1O_2$ by *N*,*N*'-dimethylpiperazine	*n*-hexane	ambient	120	13	-35.8	463	
86.		PhMe	ambient	120	13	-23.1	463	
87.		CH_2Cl_2	ambient	120	13	-22.8	463	
88.		PhCl	ambient	120	13	-19.5	463	
89.		*o*-$Cl_2C_6H_4$	ambient	120	13	-16.8	463	
90.		PhCN	ambient	120	13	-15.8	463	
91.	quenching of $^1O_2$ by *N*-methylpiperidine	*n*-hexane	ambient	120	13	-33.3	463	
92.		PhMe	ambient	120	13	-21.5	463	
93.		CH_2Cl_2	ambient	120	13	-21.2	463	
94.		PhCl	ambient	120	13	-18.6	463	
95.		*o*-$Cl_2C_6H_4$	ambient	120	13	-16.6	463	
96.		PhCN	ambient	120	13	-14.7	463	
97.	quenching of $^1O_2$ by quinuclidine	*n*-hexane	ambient	120	13	-35.7	463	
98.		PhMe	ambient	120	13	-22.1	463	
99.		CH_2Cl_2	ambient	120	13	-19.2	463	
100.		PhCl	ambient	120	13	-16.6	463	
101.		*o*-$Cl_2C_6H_4$	ambient	120	13	-16.0	463	
102.		PhCN	ambient	120	13	-12.5	463	
103.	quenching of $^1O_2$ by *N*,*N*,*N*'*N*'-tetramethyl-1,4-phenylenediamine	*n*-hexane	ambient	120	13	-34.2	463	
104.		*cy*-$C_6H_{11}Me$	ambient	120	13	-27.5	463	
105.		PhMe	ambient	120	13	-19.0	463	
106.		CH_2Cl_2	ambient	120	13	-17.6	463	
107.		PhCl	ambient	120	13	-13.9	463	
108.		*o*-$Cl_2C_6H_4$	ambient	120	13	-11.8	463	
109.		MeCN	ambient	120	13	-13.8	463	
110.		PhCN	ambient	120	13	-9.0	463	
111.	quenching of S_1 state of anthracene by O_2	*cy*-$C_6H_{11}Me$	25	400	9	+12	464	
112.	quenching of T_1 state of anthracene by O_2	*cy*-$C_6H_{11}Me$	25	400	9	+6.1	464	
113.	quenching of S_1 state of 9-methylanthracene by O_2	*cy*-$C_6H_{11}Me$	25	700	12	+14	464	
114.	quenching of T_1 state of 9-methylanthracene by O_2	*cy*-$C_6H_{11}Me$	25	400	9	+5.8	464	
115.	quenching of S_1 state of 9,10-dichloroanthracene by O_2	*cy*-$C_6H_{11}Me$	25	700	12	+6	464	
116.	quenching of T_1 state of 9,10-dichloroanthracene by O_2	*cy*-$C_6H_{11}Me$	25	400	9	+5.1	464	
117.	quenching of S_1 state of 9,10-dicyanoanthracene by O_2	*cy*-$C_6H_{11}Me$	25	700	12	-9[g1]	464	h1
118.	quenching of T_1 state of 9-acetylanthracene by O_2	*cy*-$C_6H_{11}Me$	25	400	9	+5[g1]	464	
119.	quenching of S_1 state of perylene by 1-bromonaphthalene (BN)	PhMe	25	150	7	-5.6	465	[BN] = 1.68 mol dm^{-3}
120.		PhMe	25	150	7	-5.7	465	[BN] = 1.44 mol dm^{-3}
121.		PhMe	25	150	7	-6.0	465	[BN] = 1.20 mol dm^{-3}
122.		PhMe	25	150	7	-7.0	465	[BN] = 0.96 mol dm^{-3}
123.		PhMe	25	150	7	-7.4	465	[BN] = 0.72 mol dm^{-3}
124.		PhMe	25	150	7	-7.7	465	[BN] = 0.48 mol dm^{-3}, i1.
125.	quenching of S_1 state of perylene by 1-iodonaphthalene (IN)	PhMe	ambient	150	7	-4.6	465	[IN] = 0.15 mol dm^{-3}
126.	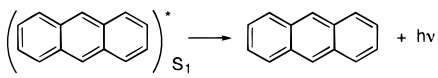	*cy*-$C_6H_{11}Me$	25	300	7	-	466	j1
127.	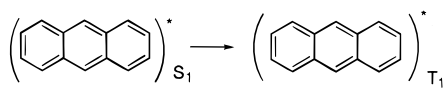	*cy*-$C_6H_{11}Me$	25	300	7	-	466	j1
128.	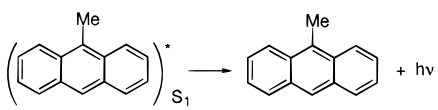	*cy*-$C_6H_{11}Me$	25	300	7	+16[i1]	466	j1

Table 2. (Continued)

No.	reaction	solvent	T/ °C	P/MPa	no of k data	$\Delta V_0^{\neq}$ /cm^{3}mol^{-1}	ref	remarks
129.	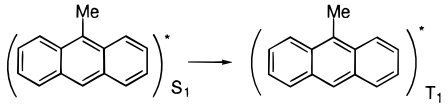	*cy*-$C_6H_{11}Me$	25	300	7	-	466	j1
130.	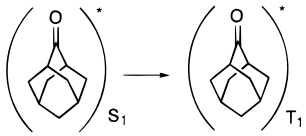	MeCN	25	203	5	-3.2	467	
131.	$e^- + CO_2 \longrightarrow CO_2^-$	2,2,4-trimethylpentane	51	250	9	-64	468	$\Delta V^{\neq}$ = +110 for the reverse process. k1
132.		2,2,4-trimethylpentane	58	-	-	-67	468	$\Delta V^{\neq}$ = +164 for the reverse process. k1
133.		2,2,4-trimethylpentane	67	-	-	-61	468	$\Delta V^{\neq}$ = +150 for the reverse process. k1
134.		2,2,4-trimethylpentane	75	-	-	-49	468	$\Delta V^{\neq}$ = +120 for the reverse process. k1
135.		3-methylpentane	80	-	-	-44	468	$\Delta V^{\neq}$ = +246 for the reverse process. k1
136.		3-methylpentane	90	-	-	-45	468	$\Delta V^{\neq}$ = +220 for the reverse process. k1
137.		3-methylpentane	100	250	12	-31	468	$\Delta V^{\neq}$ = +198 for the reverse process. h1,k1
138.		Me_4Si	23	-	-	-68	468	$\Delta V^{\neq}$ = +106 for the reverse process. k1
139.		Me_4Si	34	-	-	-66	468	$\Delta V^{\neq}$ = +112 for the reverse process. k1
140.		Me_4Si	40	-	-	-52	468	$\Delta V^{\neq}$ = +115 for the reverse process. k1
141.		Me_4Si	48	-	-	-63	468	$\Delta V^{\neq}$ = +121 for the reverse process. k1
142.		Me_4Si	59	-	-	-54	468	$\Delta V^{\neq}$ = +105 for the reverse process. k1
143.		Me_4Si	66	-	-	-63	468	$\Delta V^{\neq}$ = +83 for the reverse process. k1
144.		Me_4Si	81	-	-	-47	468	$\Delta V^{\neq}$ = +85 for the reverse process. k1
145.		2-methylbutane	47	150	7	-59	469	ΔV = -298, h1, k1
146.		2-methylbutane	55	150	12	-66	469	ΔV = -251, h1, k1
147.		2-methylbutane	70	150	13	-51	469	ΔV = -255, h1, k1
148.		2-methylbutane	85	150	10	-51	469	ΔV = -246, k1
149.		2-methylbutane	100	150	12	-46	469	ΔV = -228, k1
150.		2,2-dimethylbutane	24	200	10	-96	469	ΔV = -231, k1
151.		2,2-dimethylbutane	32	-	-	-110	469	ΔV = -271, k1
152.		2,2-dimethylbutane	40	-	-	-81	469	ΔV = -248, k1
153.		2,2-dimethylbutane	44	200	10	-	469	ΔV = -254, k1
154.		2,2-dimethylbutane	60	-	-	-84	469	ΔV = -219, k1
155.		2,2-dimethylbutane	80	200	7	-83	469	ΔV = -193, k1
156.	CH_2=CH-CH=$CH_2^- \longrightarrow CH_2$=CH-CH=$CH_2 + e^-$	2,2-dimethylbutane	8	200	7	+112	470	ΔV = 122, k1, l1
157.		2,2-dimethylbutane	42	300	8	+84	470	ΔV = 100, k1, l1
158.	$o\text{-}Ps^{m1} + PhNO_2 \longrightarrow PhNO_2 + 2\gamma$	*n*-hexane	19	98	11	-329[n1]	471	
159.		PhH	19	49	6	≈0	471	
160.	overall motion of 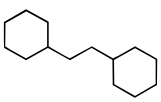	neat	37	-	4	+37.9	472	o1
161.		neat	56	197	5	+30.3	472	o1
162.	overall motion of 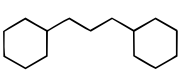	neat	37	-	4	+33.3	472	o1

Table 2. (Continued)

No.	reaction	solvent	T/ °C	P/MPa	no of k data	$\Delta V_0^{\neq}$ /cm^{3}mol^{-1}	ref	remarks
163.	overall motion of 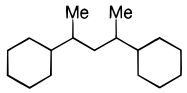	neat	17	-	4	+51.5	472	o1
164.		neat	37	-	5	+43.3	472	o1
165.		neat	56	-	6	+42.4	472	o1
166.	overall motion of 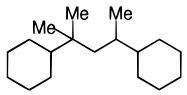	neat	27	-	-	+74.8	472	o1
167.		neat	37	-	9	+58.9	472	o1
168.		neat	46	-	-	+57.1	472	o1
169.		neat	56	-	-	+56.6	472	o1
170.	motion of the methyl groups in 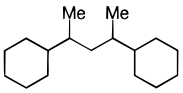	neat	17	-	-	+1.7	472	o1
171.		neat	37	-	-	+7.4	472	o1
172.		neat	56	-	-	+5.4	472	o1
173.	motion of C-1 and the methyl group on C-2 in 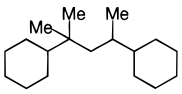	neat	27	-	-	-53.9	472	o1
174.		neat	37	-	-	-10.8	472	o1
175.		neat	46	-	-	-12.2	472	o1
176.		neat	56	-	-	-26.6	472	o1
177.	motion of C-5 in 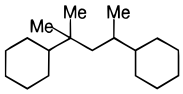	neat	27	-	-	-11.0	472	o1
178		neat	37	-	-	+9.7	472	o1
179.		neat	46	-	-	+16.1	472	o1
180.		neat	56	-	-	+21.6	472	o1
181.	overall motion of (n-Oct)$_4$Sn	neat	17	211	7	+10.0	473	From the relaxation of C-1. o1
182.		neat	37	-	-	+23.9	473	From the relaxation of C-1. o1
183.		neat	56	-	-	+29.0	473	From the relaxation of C-1. o1
184.		neat	17	211	7	+19.8	473	From the relaxation of C-2. o1
185.		neat	37	-	-	+27.6	473	From the relaxation of C-2. o1
186.		neat	56	-	-	+29.5	473	From the relaxation of C-2. o1
187.		neat	17	211	7	+30.0	473	From the relaxation of C-3. o1
188.		neat	37	-	-	+33.5	473	From the relaxation of C-3. o1
189.		neat	56	-	-	+29.5	473	From the relaxation of C-3. o1
190.		neat	17	211	7	+31.0	473	From the relaxation of C-4,5. o1
191.		neat	37	-	-	+32.9	473	From the relaxation of C-4,5. o1
192.		neat	56	-	-	+29.7	473	From the relaxation of C-4,5. o1
193.		neat	17	211	7	+28.0	473	From the relaxation of C-6. o1
194.		neat	37	-	-	+35.3	473	From the relaxation of C-6. o1
195.		neat	56	-	-	+31.5	473	From the relaxation of C-6. o1
196.		neat	17	211	7	+33.8	473	From the relaxation of C-7. o1
197.		neat	37	-	-	+36.7	473	From the relaxation of C-7. o1
198.		neat	56	-	-	+33.7	473	From the relaxation of C-7. o1
199.		neat	17	211	7	+30.5	473	From the relaxation of C-8. o1
200.		neat	37	-	-	+30.8	473	From the relaxation of C-8. o1
201.		neat	56	-	-	+32.1	473	From the relaxation of C-8. o1

Table 2. (Continued)

No.	reaction	solvent	T/ °C	P/MPa	no of k data	$\Delta V_0^{\neq}$ /cm^{3}mol^{-1}	ref	remarks
202.	overall motion of Ph_2CH_2	neat	27	50	5	+19[p1]	474	q1
203.		neat	36	100	5	+16[p1]	474	q1
204.		neat	53	100	5	+15[p1]	474	q1
205.		neat	67	100	5	+15[p1]	474	q1
206.		neat	80	100	5	+14[p1]	474	q1
207.		neat	96	100	5	+13[p1]	474	q1
208.	overall motion of Ph_2O	neat	33	100	5	+22[p1]	474	q1
209.		neat	53	100	5	+21[p1]	474	q1
210.		neat	66	100	5	+17[p1]	474	q1
211.		neat	81	100	5	+16[p1]	474	q1
212.	overall motion of D_2O	neat	10	300	7	-4.8	475	r1
213.		neat	30	300	7	-3.8	475	r1
214.		neat	50	300	7	-2.2	475	r1
215.		MeCN	30	300	7	+4.9	476	r1
216.		$CHCl_3$	30	300	7	+4.0	476	r1
217.		PhH	30	300	7	+0.6	476	r1
218.	overall motion of CD_3CN	neat	30	300	7	+9.0	475	r1
219.	overall motion of $CDCl_3$	$CHCl_3$	30	300	7	+8.2	475	r1 $CDCl_3$ 15 w%.
220.	overall motion of C_6D_6	PhH	30	300	7	+10	475	r1 C_6D_6 3 w%.
221.	reorientation of 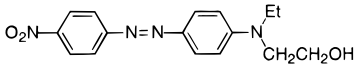	corona poled film of PMMA[s1]	99	272	7	+96	477	
222.		corona poled film of PS[t1]	98	204	6	+211	477	
223.		corona poled film of PC[u1]	124	272	6	+192	477	
224.	reorientation of 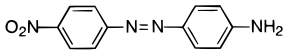	corona poled film of PMMA[s1]	99	272	6	+108	477	
225.		corona poled film of PS[t1]	98	204	7	+228	477	
226.		corona poled film of PC[u1]	124	204	5	+126	477	
227.	reorientation of 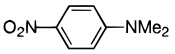	corona poled film of PMMA[s1]	99	272	5	+30	477	
228.		corona poled film of PS[t1]	98	204	5	+162	477	
229.		corona poled film of PC[u1]	124	272	6	+102	477	
230.	First step in the inclusion of 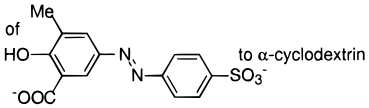	H_2O	15	200	5	-20.9	478	ΔV = -3.6
231.	Second step in the inclusion of 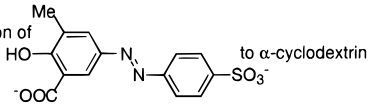	H_2O	15	200	5	-15.8	479	ΔV = +6.1
232.	First step in the inclusion of 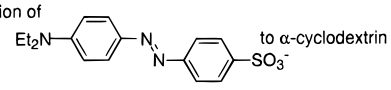	H_2O	15	200	5	-22.1	479	ΔV = -6.2
233.	First step in the inclusion of 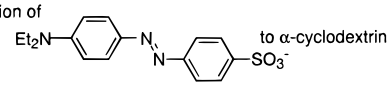	H_2O	15	200	5	-1.8	479	ΔV = +17.0
234.	rotation of the ethylene in $(C_5H_5)Rh(C_2H_4)_2$[v1]	C_6D_6	44.5	-	4	-2	480	
235.		$CDCl_3$	44.5	-	5	-5	480	
236.	rotation of ethylene in $(C_5H_5)Rh(C_2H_4)(C_2F_4)$[w1]	n-pentane-d_{12}	-15	495	12	-3.7[g1]	481	$\Delta V^{\neq} > 0$ at $P > 300$.
237.		n-pentane-d_{12}	0	495	12	-5.5[g1]	481	$\Delta V^{\neq} > 0$ at $P > 300$.

Table 2. (Continued)

No.	reaction	solvent	T/ °C	P/MPa	no of k data	$\Delta V_0^{\neq}$ /cm^{3}mol^{-1}	ref	remarks
238.		cy-$C_6D_{11}CD_3$	-15	493	12	-5.9[g l]	481	$\Delta V^{\neq} > 0$ at $P > 300$.
239.		cy-$C_6D_{11}CD_3$	0	497	12	-3.3[g l]	480	$\Delta V^{\neq} > 0$ at $P > 300$.
240.		CS_2	-15	497	12	-3.6[g l]	481	$\Delta V^{\neq} > 0$ at $P > 300$.
241.		CS_2	0	496	12	-5.9[g l]	481	$\Delta V^{\neq} > 0$ at $P > 300$.
242.	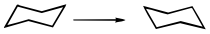	CS_2	-10	470	5	-2.0	482	
243.		n-pentane	9	416	12	+10.6[i l]	483	
244.		cy-$C_6H_{11}Me$	9	400	9	+10.3[i l]	483	
245.	rotation of the phenyl group in 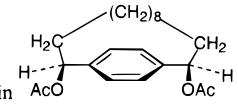	$CDCl_2CDCl_2$	83	300		-5 ~ 10	484	
246.		$CDCl_2CDCl_2$	105	300	8	-6 ~ 7	484	
247.	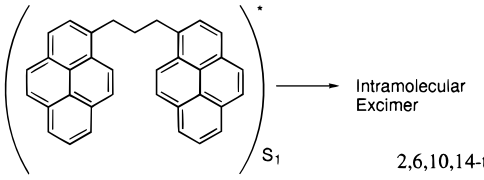	2,6,10,14-tetramethlpentadecane	25	250	11	+24.8	485	
248.			30	500	9	+28.0	486	
249.		acetone	30	600	10	+4.9	487	
250.		n-hexane	30	600	10	+5.9	487	
251.		cy-$C_6H_{11}Me$	30	600	10	+9.6	487	
252.		ethanol	30	600	10	+6.7	487	
253.		i-BuOH	30	600	10	+12.6	487	
254.		SDS[x l] micelles	30	250	6	+5.3	488	
255.		n-$C_{12}H_{25}(OC_2H_4)_5OH$ micelles	30	300	8	+14.2	488	
256.		n-$C_{12}H_{25}(OC_2H_4)_6OH$ micelles	30	300	8	+14.6	488	
257.	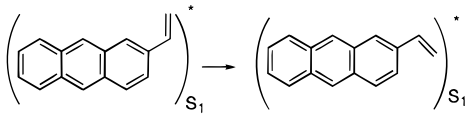	n-pentane	30	500	-	+1.4	489	
258.		n-hexane	30	500	-	+2.7	489	
259.		n-octane	30	500	-	+3.3	489	
260.		n-decane	30	500	-	+3.3	489	
261.	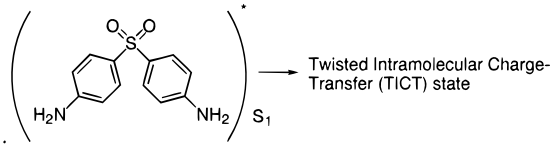	MeOH	30	400	9	-	490	y1
262.		EtOH	30	500	11	-	490	y1
263.		n-PrOH	30	500	6	+2.4	490	y1
264.		n-PrOH	30	500	6	-	491	
265.		n-BuOH	30	500	10	+2.6	490	y1
266.		n-BuOH	30	500	11	-	491	
267.		n-PentOH	30	450	10	+2.9	490	y1
268.		n-PentOH	30	400	5	-	491	
269.	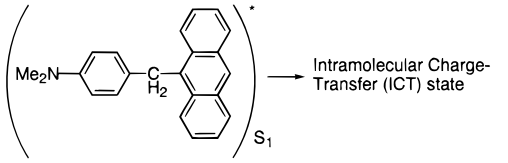	n-PrOH	30	500	-	+7.9	492	
270.		n-PentOH	30	500	-	+1.3	492	

Table 2. (Continued)

No.	reaction	solvent	T/ °C	P/MPa	no of k data	$\Delta V_0^{\neq}$ /cm^{3}mol^{-1}	ref	remarks
271.	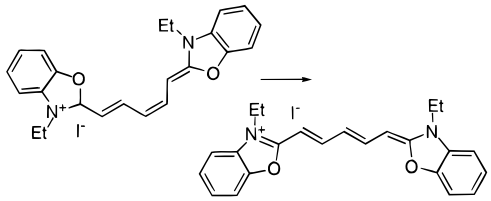	MeOH	30	500	11	+3.5	493	
272.		EtOH	30	500	11	+4.3	493	
273.		*n*-PrOH	30	500	11	+3.8	493	
274.		*n*-BuOH	30	500	11	+3.9	493	
275.	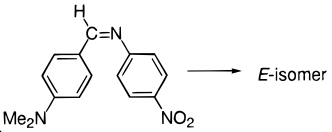	*n*-hexane	25	240	9	-1.2	494	
276.		PhH	25	70	5	-1.2	494	
277.		THF	25	240	9	-1.2	494	
278.		PhCl	25	240	9	-0.8	494	
279.		*o*-$C_6H_4Cl_2$	25	240	9	-1.1	494	
280.		2,4-dicyclohexyl-2-methylpentane	-5	330	12	0.4	495	$\Delta V^{\neq} >> 0$ at high P.
281.		2,4-dicyclohexyl-2-methylpentane	0	360	13	+0.7	495	$\Delta V^{\neq} >> 0$ at high P.
282.		2,4-dicyclohexyl-2-methylpentane	5	360	13	+0.3	495	$\Delta V^{\neq} >> 0$ at high P.
283.		2,4-dicyclohexyl-2-methylpentane	10	390	14	+0.5	495	$\Delta V^{\neq} >> 0$ at high P.
284.		2,4-dicyclohexyl-2-methylpentane	15	420	15	+0.1	495	$\Delta V^{\neq} >> 0$ at high P.
285.		2,4-dicyclohexyl-2-methylpentane	20	420	15	+0.6	495	$\Delta V^{\neq} >> 0$ at high P.
286.		glycerol triacetate	5	420	15	0.0	496	$\Delta V^{\neq} >> 0$ at high P.
287.		glycerol triacetate	10	450	16	+0.3	496	$\Delta V^{\neq} >> 0$ at high P.
288.		glycerol triacetate	15	480	17	+0.3	496	$\Delta V^{\neq} >> 0$ at high P.
289.		glycerol triacetate	20	510	18	+0.1	496	$\Delta V^{\neq} >> 0$ at high P.
290.		glycerol triacetate	25	540	19	0.0	496	$\Delta V^{\neq} >> 0$ at high P.
291.		2-methyl-2,4-pentanediol	-10	420	15	+0.5	496	$\Delta V^{\neq} >> 0$ at high P.
292.		2-methyl-2,4-pentanediol	-5	420	15	+0.6	496	$\Delta V^{\neq} >> 0$ at high P.
293.		2-methyl-2,4-pentanediol	0	480	17	0.0	496	$\Delta V^{\neq} >> 0$ at high P.
294.		2-methyl-2,4-pentanediol	5	480	17	+0.3	496	$\Delta V^{\neq} >> 0$ at high P.
295.		2-methyl-2,4-pentanediol	10	360	13	+0.2	496	$\Delta V^{\neq} >> 0$ at high P.
296.	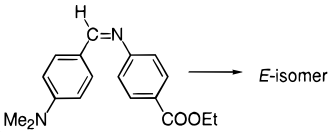	2,4-dicyclohexyl-2-methylpentane	0	300	11	+0.4	495	$\Delta V^{\neq} >> 0$ at high P.
297.		2,4-dicyclohexyl-2-methylpentane	5	360	13	+1.7	495	$\Delta V^{\neq} >> 0$ at high P.
298.		2,4-dicyclohexyl-2-methylpentane	10	390	14	+1.5	495	$\Delta V^{\neq} >> 0$ at high P.
299.		2,4-dicyclohexyl-2-methylpentane	15	390	14	+1.0	495	$\Delta V^{\neq} >> 0$ at high P.
300.		2,4-dicyclohexyl-2-methylpentane	20	420	15	+1.3	495	$\Delta V^{\neq} >> 0$ at high P.
301.		glycerol triacetate	5	450	16	+0.5	496	$\Delta V^{\neq} >> 0$ at high P.
302.		glycerol triacetate	10	480	17	+1.0	496	$\Delta V^{\neq} >> 0$ at high P.
303.		glycerol triacetate	15	450	17	+1.2	496	$\Delta V^{\neq} >> 0$ at high P.
304.		glycerol triacetate	20	570	20	+1.0	496	$\Delta V^{\neq} >> 0$ at high P.
305.		glycerol triacetate	25	570	20	+1.2	496	$\Delta V^{\neq} >> 0$ at high P.
306.		2-methyl-2,4-pentanediol	-5	450	16	+1.7	497	$\Delta V^{\neq} >> 0$ at high P.
307.		2-methyl-2,4-pentanediol	0	510	18	+1.6	497	$\Delta V^{\neq} >> 0$ at high P.
308.		2-methyl-2,4-pentanediol	5	510	18	+1.6	497	$\Delta V^{\neq} >> 0$ at high P.
309.		2-methyl-2,4-pentanediol	10	540	19	+1.8	497	$\Delta V^{\neq} >> 0$ at high P.
310.		2-methyl-2,4-pentanediol	15	540	19	+1.6	497	$\Delta V^{\neq} >> 0$ at high P.
311.	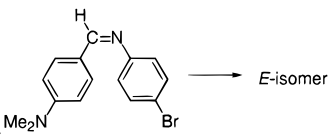	2,4-dicyclohexyl-2-methylpentane	0	450	16	+1.9	495	$\Delta V^{\neq} >> 0$ at high P.
312.		2,4-dicyclohexyl-2-methylpentane	5	450	16	+2.2	495	$\Delta V^{\neq} >> 0$ at high P.
313.		2,4-dicyclohexyl-2-methylpentane	10	510	18	+2.2	495	$\Delta V^{\neq} >> 0$ at high P.
314.		2,4-dicyclohexyl-2-methylpentane	15	510	18	+2.1	495	$\Delta V^{\neq} >> 0$ at high P.

Table 2. (Continued)

No.	reaction	solvent	T/ °C	P/MPa	no of k data	$\Delta V_0^{\neq}$ /cm^{3}mol^{-1}	ref	remarks
315.		2,4-dicyclohexyl-2-methylpentane	20	510	18	+1.3	495	$\Delta V^{\neq} >> 0$ at high P.
316.		glycerol triacetate	5	570	20	+2.1	496	$\Delta V^{\neq} >> 0$ at high P.
317.		glycerol triacetate	10	600	21	+1.9	496	$\Delta V^{\neq} >> 0$ at high P.
318.		glycerol triacetate	15	600	21	+2.4	496	$\Delta V^{\neq} >> 0$ at high P.
319.		glycerol triacetate	20	600	21	+1.8	496	$\Delta V^{\neq} >> 0$ at high P.
320.		glycerol triacetate	25	600	21	+2.6	496	$\Delta V^{\neq} >> 0$ at high P.
321.		2-methyl-2,4-pentanediol	-5	600	21	+2.5	497	$\Delta V^{\neq} >> 0$ at high P.
322.		2-methyl-2,4-pentanediol	0	600	21	+2.3	497	$\Delta V^{\neq} >> 0$ at high P.
323.		2-methyl-2,4-pentanediol	5	600	21	+2.5	497	$\Delta V^{\neq} >> 0$ at high P.
324.		2-methyl-2,4-pentanediol	10	600	21	+2.6	497	$\Delta V^{\neq} >> 0$ at high P.
325.	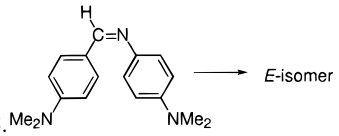	glycerol triacetate	20	600	21	+1.5	496	
326.		glycerol triacetate	25	600	21	+1.0	496	
327.		glycerol triacetate	30	600	21	+2.1	496	
328.		glycerol triacetate	35	600	21	+2.1	496	
329.		glycerol triacetate	40	600	21	+2.4	496	
330.	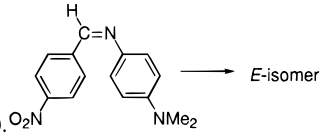	*n*-hexane	25	240	9	+0.3	494	
331.		PhH	25	80	5	+1.5	494	
332.		acetone	25	240	9	+1.2	494	
333.		MeOH	25	240	9	+3.1	494	
334.	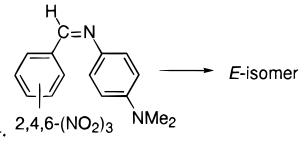	MeOH	25	240	5	-1.7	498	
335.	degenerate isomerization of 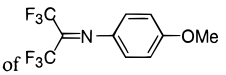	CD_3CN	25	207	8	+3.7	499	
336.	degenerate isomerization of 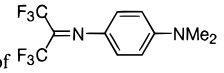	CD_3CN	54	193	7	+0.5	499	
337.	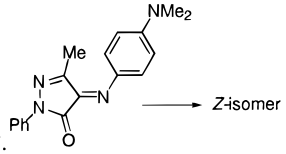	*n*-hexane	25	240	9	+2.3	494	
338.		PhH	25	60	4	+4.2	494	
339.		acetone	25	240	9	+3.7	494	
240.		MeOH	25	240	9	+3.6	494	
341.	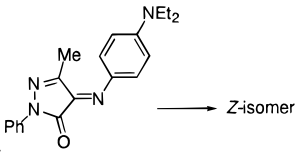	*n*-hexane	25	240	9	+3.0	494	
342.		PhH	25	60	4	+4.2	494	
343.		acetone	25	240	9	+3.7	494	
344.		MeOH	25	240	9	+3.6	494	
345.	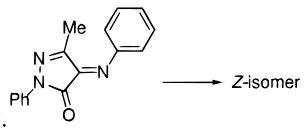	PhH	25	70	5	+1.0	494	
346.		MeOH	25	240	9	+0.1	494	

Table 2. (Continued)

No.	reaction	solvent	T/ °C	P/MPa	no of k data	$\Delta V_0^{\neq}$ /cm^{3}mol^{-1}	ref	remarks
347.	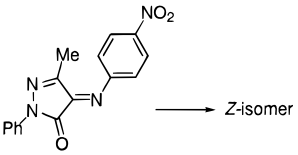	PhH	25	70	5	+5.0	494	
348.		MeOH	25	240	9	-1.0	494	
349.	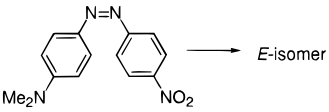	glycerol triacetate	5	600	13	-15.5	496	$\Delta V^{\neq} >> 0$ at high P.
350.		glycerol triacetate	15	600	13	-15.9	496	$\Delta V^{\neq} >> 0$ at high P.
351.		glycerol triacetate	25	800	17	-18.7	496	$\Delta V^{\neq} >> 0$ at high P.
352.		glycerol triacetate	40	800	17	-20.4	496	$\Delta V^{\neq} >> 0$ at high P.
353.		2-methyl-2,4-pentanediol	-5	600	27	-17.4	497	$\Delta V^{\neq} >> 0$ at high P.
354.		2-methyl-2,4-pentanediol	5	600	28	-19.2	497	$\Delta V^{\neq} >> 0$ at high P.
355.		2-methyl-2,4-pentanediol	15	600	28	-18.6	497	$\Delta V^{\neq} >> 0$ at high P.
356.		2-methyl-2,4-pentanediol	25	600	29	-22.8	497	$\Delta V^{\neq} >> 0$ at high P.
357.		2-methyl-2,4-pentanediol	35	600	29	-21.6	497	$\Delta V^{\neq} >> 0$ at high P.
358.	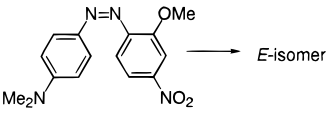	glycerol triacetate	5	600	13	-20.0	496	$\Delta V^{\neq} >> 0$ at high P.
359.		glycerol triacetate	15	600	13	-24.1	496	$\Delta V^{\neq} >> 0$ at high P.
360.		glycerol triacetate	25	600	13	-21.1	496	$\Delta V^{\neq} >> 0$ at high P.
361.		glycerol triacetate	35	600	13	-23.0	496	$\Delta V^{\neq} >> 0$ at high P.
362.		2-methyl-2,4-pentanediol	-5	600	27	-18.7	497	$\Delta V^{\neq} >> 0$ at high P.
363.		2-methyl-2,4-pentanediol	0	600	27	-17.1	497	$\Delta V^{\neq} >> 0$ at high P.
364.		2-methyl-2,4-pentanediol	5	600	28	-20.0	497	$\Delta V^{\neq} >> 0$ at high P.
365.		2-methyl-2,4-pentanediol	15	600	28	-22.3	497	$\Delta V^{\neq} >> 0$ at high P.
366.		2-methyl-2,4-pentanediol	25	600	29	-23.1	497	$\Delta V^{\neq} >> 0$ at high P.
367.		2-methyl-2,4-pentanediol	35	600	29	-22.8	497	$\Delta V^{\neq} >> 0$ at high P.
368.	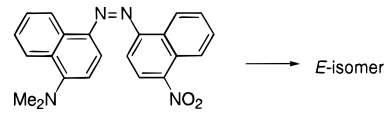	glycerol triacetate	-10	390	18	-16	500	$\Delta V^{\neq} >> 0$ at high P.
369.		glycerol triacetate	-5	390	18	-13	500	$\Delta V^{\neq} >> 0$ at high P.
370.		glycerol triacetate	0	390	20	-21	500	$\Delta V^{\neq} >> 0$ at high P.
371.		glycerol triacetate	5	420	18	-19	500	$\Delta V^{\neq} >> 0$ at high P.
372.	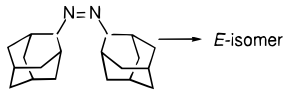	*n*-hexane	21	199	6	+7	501	
373.		EtOH	36	204	6	+5	501	
374.	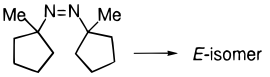	EtOH	9	195	10	+10	501	
375.	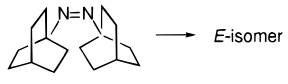	*n*-hexane	36	203	7	+9	501	
376.		EtOH	46	214	7	+7	501	
377.	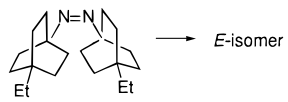	*n*-hexane	36	217	7	+6	501	

Table 2. (Continued)

No.	reaction	solvent	T/ °C	P/MPa	no of k data	$\Delta V_0^{\neq}$ /cm^{3}mol^{-1}	ref	remarks
378.	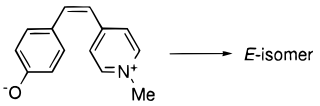	H_2O	15	180	7	+16.5	502	
379.		H_2O	25	210	8	+17.7	502	
380.		H_2O	35	210	8	+18.1	502	
381.		H_2O	45	210	8	+20.0	502	
382.		aq MeOH	25	210	8	+19.1	502	MeOH 20 v%.
383.		aq MeOH	25	210	8	+22.2	502	MeOH 40 v%.
384.	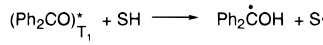	*i*-PrOH	25	400	9	-11.3	503	
385.		*i*-BuOH	25	400	9	-11.0	503	
386.		2-octanol	25	400	14	-7.8	503	h1
387.		5-methyl-3-heptanol	16	400	9	-	503	h1
388.		5-methyl-3-heptanol	25	400	9	-10.1	503	h1
389.		5-methyl-3-heptanol	40	400	9	-	503	h1
390.	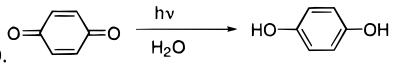	SDS[x1] micelles	35	150	4	-4.7	504	
391.		CTAB[z1] micelles	35	100	4	-22	504	
392.		AOT[a2]/H_2O/hexane reversed micelles	35	150	4	+1.5	504	$[H_2O]/[AOT] = 2$
393.		AOT[a2]/H_2O/hexane reversed micelles	35	150	4	+1.7	504	$[H_2O]/[AOT] = 5$
394.		AOT[a2]/H_2O/hexane reversed micelles	35	150	4	+2.4	504	$[H_2O]/[AOT] = 20$
395.		AOT[a2]/H_2O/hexane reversed micelles	35	100	4	+3.8	504	$[H_2O]/[AOT] = 30$
396.		H_2O	35	150	4	-3.0	504	
397.		*n*-heptane	35	100	4	-3.3	504	
398.	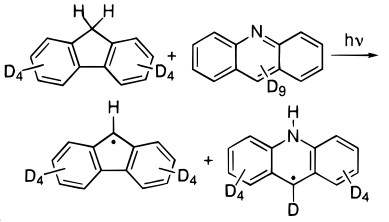	acridine-doped fluorene crystal	27	600	14	+9.3	505	
399.		acridine-doped fluorene crystal	-196	2000	-	+1.6	505	
400.		acridine-doped fluorene crystal	-272	3000	-	+0.03	505	
401.	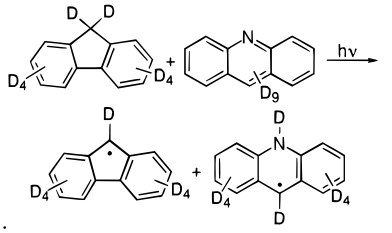	acridine-doped fluorene crystal	27	750	15	+9.7	506	
402.		acridine-doped fluorene crystal	-196	3600	6	≈0	506	
403.	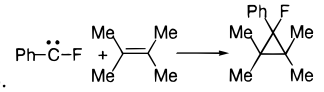	*cy*-$C_6H_{11}Me$	ambient	203	5	-17	507	
404.	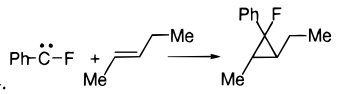	*cy*-$C_6H_{11}Me$	ambient	203	5	-18	507	
405.	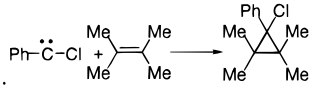	*cy*-$C_6H_{11}Me$	ambient	203	5	-14	507	
406.		MeCN	ambient	203	5	-14	507	
407.	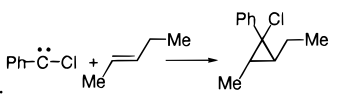	*cy*-$C_6H_{11}Me$	ambient	203	5	-15	507	
408.		MeCN	ambient	203	5	-14	507	

Table 2. (Continued)

No.	reaction	solvent	T/ °C	P/MPa	no of k data	$\Delta V_0^{\neq}$ /cm^{3}mol^{-1}	ref	remarks
409.	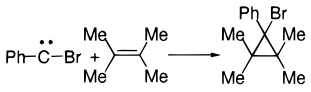	*cy*-$C_6H_{11}Me$	ambient	203	5	-10	507	
410.	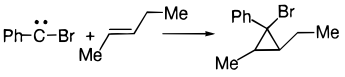	*cy*-$C_6H_{11}Me$	ambient	203	5	-12	507	
411.	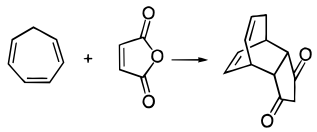	AcOEt	107	130	13	-54	508	
412.	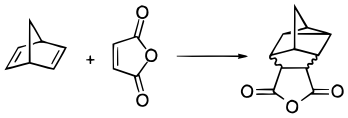	AcOEt	113	100	9	-45	508	ΔV (25 °C) = -29.5
413.	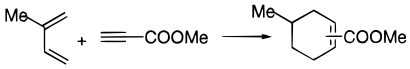	CH_2Cl_2	82	100	11	-43.0	508	ΔV (25 °C) = -39.5
414.	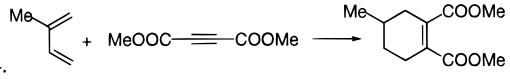	CH_2Cl_2	44	100	11	-45.8	508	ΔV (25 °C) = -39.3
415.	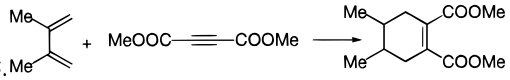	*n*-BuCl	58	80	9	-39.1	508	ΔV (25 °C) = -38.8
416.	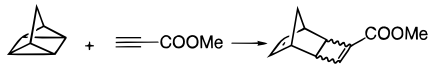	$CHCl_3$	90	100	13	-43.5	508	ΔV (25 °C) = -38.8
417.	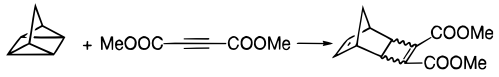	$CHCl_3$	40.5	100	11	-37.3	508	ΔV (25 °C) = -39.4
418.	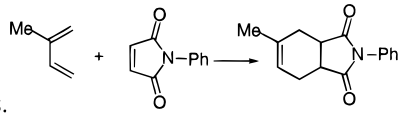	Et_2O	30	90	7	-36.1	509	
419.		Et_2O	30	80	5	-41.7	509	$[AlCl_3]$ = 0.06 mol dm^{-3}
420.		Et_2O	30	80	6	-45.4	509	$[LiClO_4]$ = 2.25 mol dm^{-3}
421.	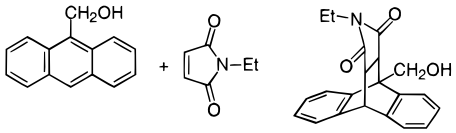	H_2O	45	90	6	-36.0	509	
422.		*n*-BuOH	45	90	7	-31.4	509	
423.		*n*-heptane	45	90	6	-28.6	509	
424.	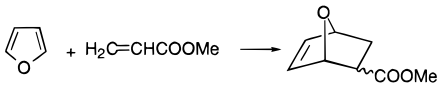	neat	20	1400	16	-18.8	510	ΔV = -30 furan/methyl acrylate = 2
425.	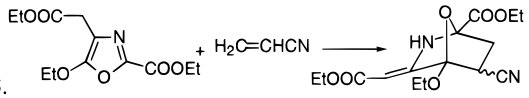	CH_2Cl_2	20	1000	11	-21.3	511	
426.		CH_2Cl_2	30	1000	14	-22.9	511	ΔV = -30.0
		26						
427.		CH_2Cl_2	40	1000	14	-19.2	511	
428.		CH_2Cl_2	50	1000	14	-20.9	511	

Table 2. (Continued)

No.	reaction	solvent	T/ °C	P/MPa	no of k data	$\Delta V_0^{\neq}$ /cm^{3}mol^{-1}	ref	remarks
429.		CH_2Cl_2	60	1000	14	-27.4	511	
430.	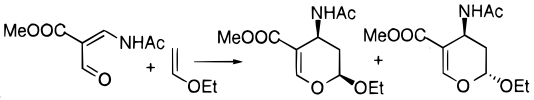	CH_2Cl_2	60	300	10	-25.1	512	$P \geq 40$
431.						-46.1	513	
432.		isodurene	75	300	12	-25.0	512	$P \geq 5$
433.	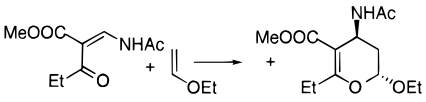	CH_2Cl_2	100	280	9	-45.8	513	$P \geq 50$
434.	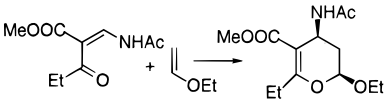	CH_2Cl_2	100	280	9	-40.6	513	$P \geq 50$
435.	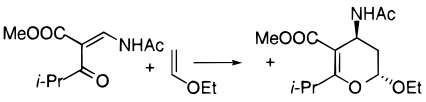	CH_2Cl_2	100	280	9	-46.7	513	$P \geq 50$
436.	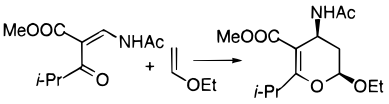	CH_2Cl_2	100	280	9	-41.4	513	$P \geq 50$
437.	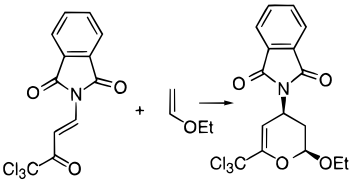	CH_2Cl_2	90	285	17	-40.3	514, 515	$P \geq 40$
438.	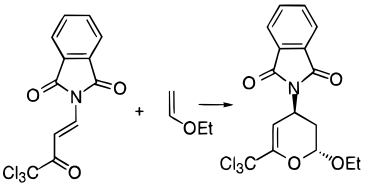	CH_2Cl_2	90	285	17	-31.1	514, 515	$P \geq 40$
439.		*n*-heptane-isodurene	110	300	16	-28.0[b2]	515	$P \geq 25$
440.	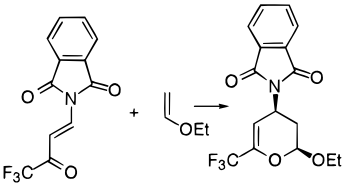	CH_2Cl_2	45	310	18	-37.5	514, 515	$P \geq 20$
441.	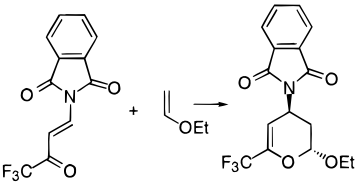	CH_2Cl_2	45	310	18	-31.5	514, 515	$P \geq 20$
442.	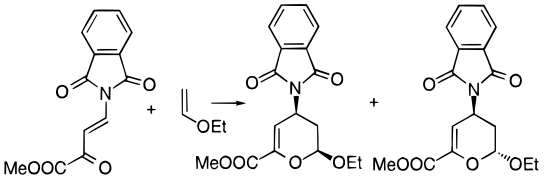	CH_2Cl_2	70	310	17	-32.5	515	$\delta\Delta V^{\neq}$ (= $V^{\neq}_{cis}$ -$V^{\neq}_{trans}$) = -2.4, $P \geq 30$

Table 2. (Continued)

No.	reaction	solvent	T/ °C	P/MPa	no of k data	$\Delta V_0^{\neq}$ /cm^{3}mol^{-1}	ref	remarks
443.	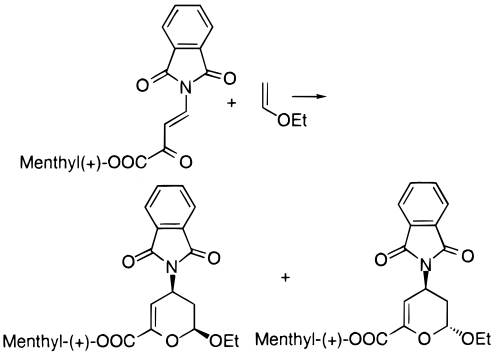	CH_2Cl_2	-	-	-	-20[c2]	515	
444.	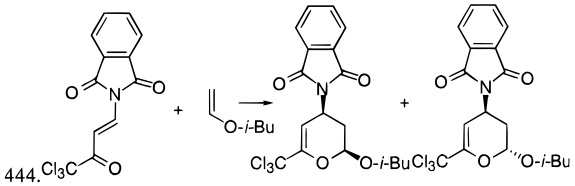	CH_2Cl_2	90	300	13	-35.0	516	$\delta\Delta V^{\neq}$ (= $V^{\neq}_{cis}$ -$V^{\neq}_{trans}$) = -8.9, $P \geq 35$
445.	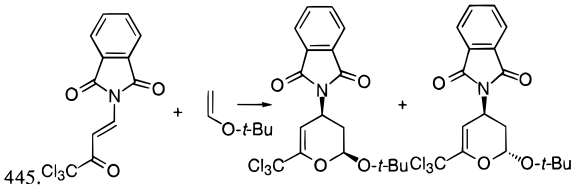	CH_2Cl_2	90	300	12	-29.6	516	$\delta\Delta V^{\neq}$ (= $V^{\neq}_{cis}$ -$V^{\neq}_{trans}$) = -9.0, $P \geq 20$
446.	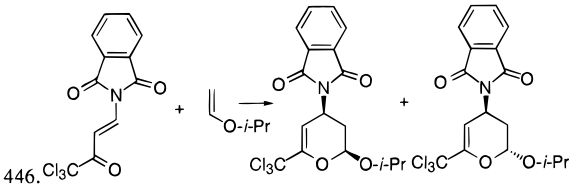	CH_2Cl_2	90	-	-	-32.3	516	$\delta\Delta V^{\neq}$ (=$V^{\neq}_{cis}$ -$V^{\neq}_{trans}$) = -8.7
447.	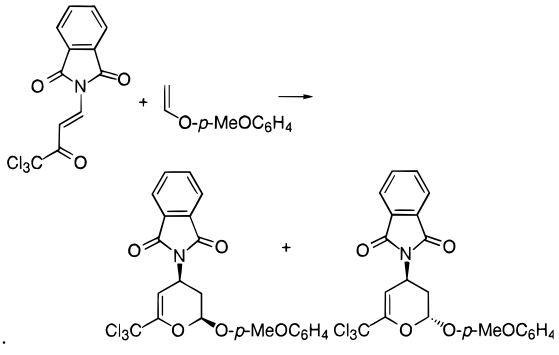	CH_2Cl_2	120	280	13	-24.4	516	$\delta\Delta V^{\neq}$ (= $V^{\neq}_{cis}$ -$V^{\neq}_{trans}$) = -10.9, $P \geq 60$
448.	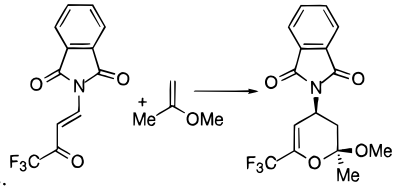	CH_2Cl_2	50	300	11	-37.6	514	$P \geq 50$
449.	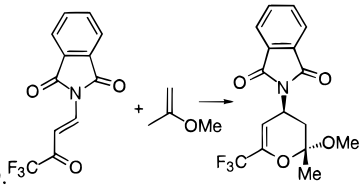	CH_2Cl_2	50	300	11	-41.7	514	$P \geq 50$

Table 2. (Continued)

No.	reaction	solvent	T/ °C	P/MPa	no of k data	$\Delta V_0^{\neq}$ /cm^{3}mol^{-1}	ref	remarks
450.	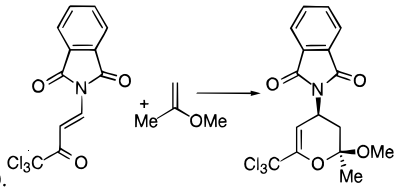	CH_2Cl_2	80	300	10	-43.2	514	$P \geq 50$
451.	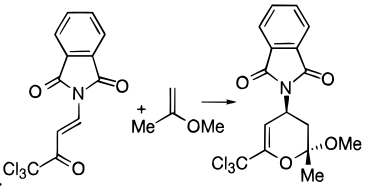	CH_2Cl_2	80	300	10	-42.6	514	$P \geq 50$
452.	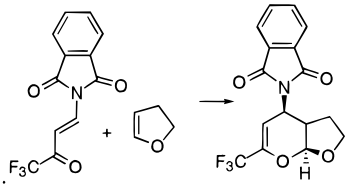	CH_2Cl_2	60	260	8	-41.7	514	$P \geq 50$
453.	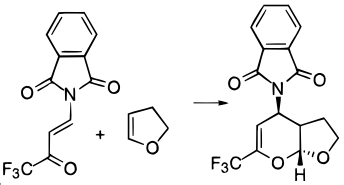	CH_2Cl_2	60	260	8	-37.8	514	$P \geq 50$
454.	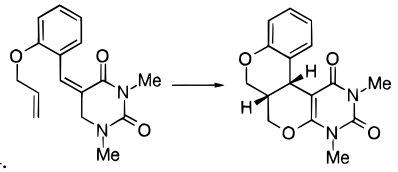	CH_2Cl_2	110	280	8	-33.7	517	ΔV(20 °C) = -30 $P \geq 75$
455.		*n*-BuCl	110	250	6	-30.1	517	$P \geq 50$
456.		THF	110	300	6	-34.8	517	ΔV(20 °C) = -35 $P \geq 75$
457.		MeCN	110	300	6	-17.3	517	ΔV(20 °C) = -15 $P \geq 75$
458.		PhMe	110	300	4	-13.4	517	ΔV(20 °C) = -18 $P \geq 100$
459.	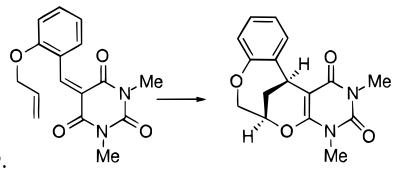	CH_2Cl_2	110	280	8	-32.1	517	$P \geq 75$
460.		*n*-BuCl	110	250	6	-28.0	517	$P \geq 50$
461.		THF	110	300	6	-32.7	517	$P \geq 75$
462.		MeCN	110	300	6	-15.2	517	$P \geq 75$
463.		PhMe	110	300	4	-12.1	517	ΔV(20 °C) = -20 $P \geq 100$
464.	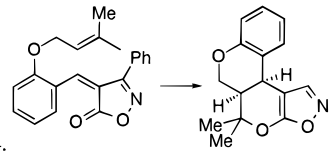	CH_2Cl_2	70	300	8	-19.4	518	$P \geq 40$
465.		CH_2Cl_2	70	300	8	-17.9	518	$P \geq 40$

Table 2. (Continued)

No.	reaction	solvent	T/ °C	P/MPa	no of k data	$\Delta V_0^{\neq}$ /cm^{3}mol^{-1}	ref	remarks
466.	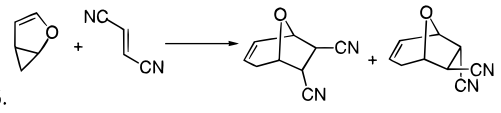	acetone-d_6	70	680	4	-10[g1]	519	$P \geq 25$
467.	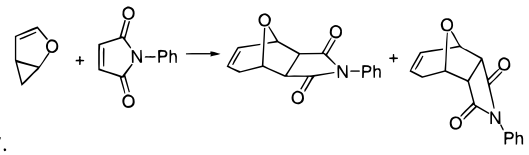	acetone-d_6	70	698	3	-11[g1]	519	
468.	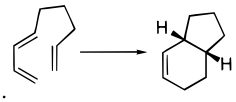	*n*-hexane	153	460	8	-24.8	520	
469.	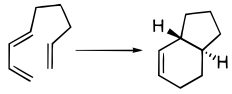	*n*-hexane	153	460	8	-24.8	520	
470.	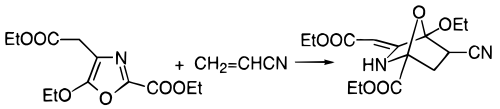	CH_2CHCN	20	1200	14	-20.1	521	ΔV = -24.2
471.		CH_2Cl_2	20	1200	10	-21.3	521	ΔV = -29.0
472.		PhCN	20	1200	11	-16.8	521	
473.		PhH	20	1200	14	-20.5	521	ΔV = -23.8
474.	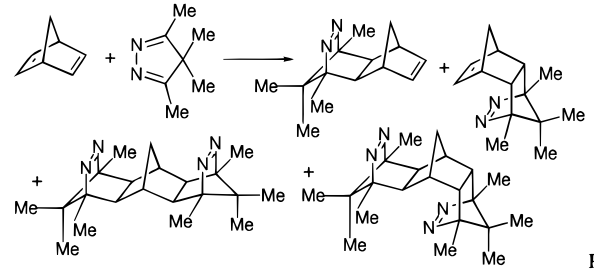	PhMe	130	1000	10	-41	522	ΔV (20 °C) = -28.8
475.	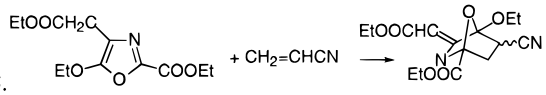	MeCN	20	1200	12	-22	523	-$\Delta V^{\neq}$ increases with P. ΔV (30 °C) = -26
476.		CH_2Cl_2	20	1200	7	-22	523	-$\Delta V^{\neq}$ increases with P. ΔV (30 °C) = -30
477.	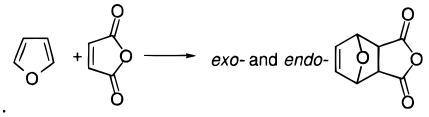	acetone-d_6	20	686	9	-30.5	524	ΔV = -28.0
478.	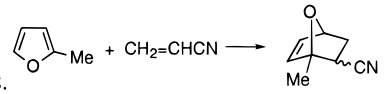	Et_2O	25	-	-	-28.8	525	
479.		Et_2O	25	-	-	-29.3	525	In the presence of $LiClO_4$. d2
480.	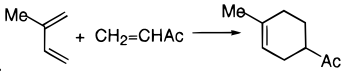	MeCN	34	-	-	-38.0	525	
481.		MeCN	34	-	-	-33.2	525	In the presence of $ZnCl_2$.
482.	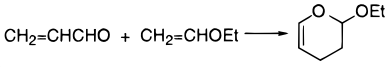	$CHCl_3$	25	-	-	-29.6	525	
483.		$CHCl_3$	25	-	-	-31.7	525	In the presence of $Yb(fod)_3$.

Table 2. (Continued)

No.	reaction	solvent	T/ °C	P/MPa	no of k data	$\Delta V_0^{\neq}$ /cm^{3}mol^{-1}	ref	remarks
484.	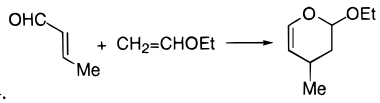	$CHCl_3$	25	-	-	-27.7	525	
485.		$CHCl_3$	25	-	-	-31.9	525	In the presence of $Yb(fod)_3$. e2
486.	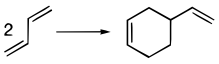	*n*-decane	120	530	14	-38.4	526	ΔV(23 °C) = -33.5 $P \geq 60$
487.	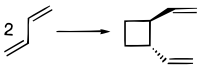	*n*-decane	120	530	14	-20.9	526	ΔV(23 °C) = -24.4 $P \geq 60$
488.	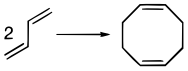	*n*-decane	120	530	14	-34.0	526	ΔV(23 °C) = -43.5 $P \geq 60$
489.	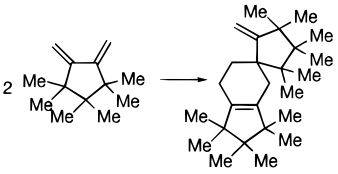	PhMe	79	930	8	-15.8	527	f2, $P \geq 55$, ΔV(21 °C) = -40.8
490.		PhMe	79	930	8	-15.9	527	g2, $P \geq 55$
491.	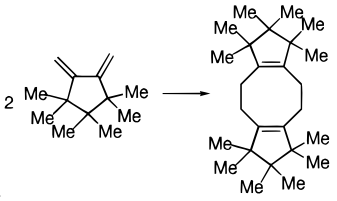	PhMe	79	930	8	-15.5	527	f2, $P \geq 55$
492.		PhMe	79	930	8	-15.5	527	g2, $P \geq 55$
493.	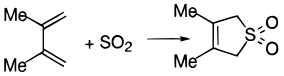	neat	39	100	6	-35.0	528	ΔV = -33
494.	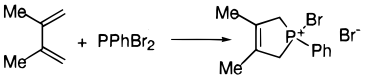	Et_2O	-	380	-	-60	529	ΔV = -38
495.	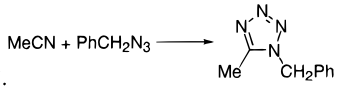	none	130	150	5	-18.3	530	h2, i2
496.		none	139	200	6	-20.5	530	h2
497.		none	149	170	4	-21.3	530	h2
498.		none	158	210	5	-24.4	530	h2
499.	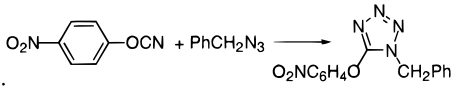	MeCN	80	-	-	-14.5	531	j2, k2
500.		MeCN	80	-	-	-18.2	531	j2, l2
501.		MeCN	80	-	-	-23.4	531	j2, m2
502.		CH_2Cl_2	80	1400	5	-18.4	531	n2
503.	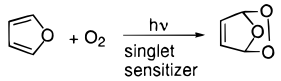	*cy*-$C_6H_{11}Me$	25	400	9	-	532	
504.	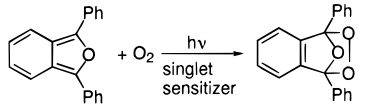	*cy*-$C_6H_{11}Me$	25	400	6	-19	532	h1

Table 2. (Continued)

No.	reaction	solvent	T/ °C	P/MPa	no of k data	$\Delta V_0^{\neq}$ /cm^{3}mol^{-1}	ref	remarks
505.		*n*-hexane	25	400	6	-14	532	
506.		2,2,4,4,6,8,8-Me$_6$-nonane	25	200	8	-6	532	h1
507.		MeCN	25	300	5	-15	532	
508.		MeOH	25	300	5	-20	532	
509.	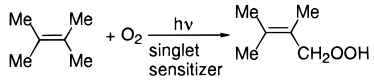	*n*-hexane	25	120	5	-35.1	533	
510.		PhMe	25	120	5	-26.4	533	
511.		CH_2Cl_2	25	120	5	-25.8	533	
512.		PhCl	25	120	5	-24.0	533	
513.		*o*-$C_6H_4Cl_2$	25	120	5	-21.9	533	
514.		PhCN	25	120	5	-20.7	533	
515.	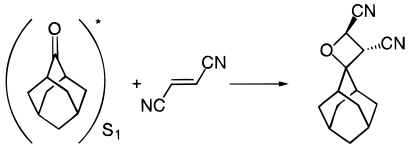	MeCN	25	203	5	+1.0	467	
516.	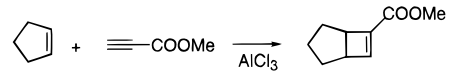	PhH	25	242	7	-20.5	534	ΔV(25 °C) = -28
517.	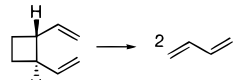	*n*-heptane	160	300	8	+5.0	535	ΔV(20 °C) = +26.4 $P \geq 20$
518.	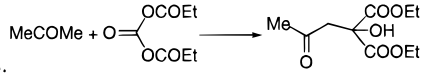	acetone	97	142	5	-45.1	536	ΔV(20 °C) = -33.9
519.	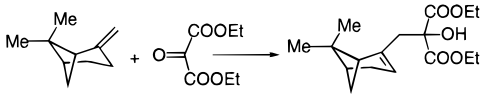	CH_2Cl_2	52	90.5	6	-34.5	536, 537	ΔV(25 °C) = -29.4
520.	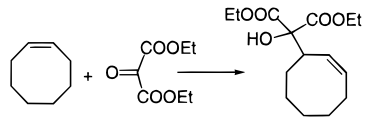	CH_2Cl_2	100	106	6	-33	537	$P \geq 530$
521.	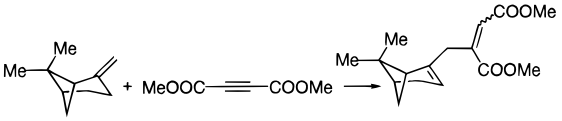	CH_2Cl_2	96	93	7	-55.8	536, 537	ΔV(25 °C) = -35.4
522.	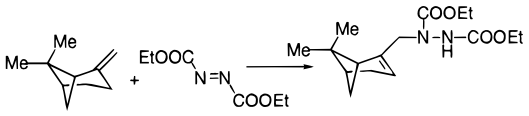	CH_2Cl_2	23	-	-	-22(25 °C)	537	ΔV(25 °C) = -35.4
523.	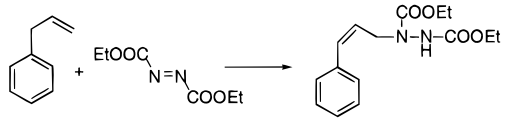	PhMe	50	100	12	-27.0(25°C)	537	ΔV(25 °C) = -35.8
524.	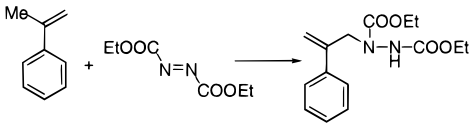	PhMe	23	-	-	-22(25 °C)	537	ΔV(25 °C) = -32.0
525.	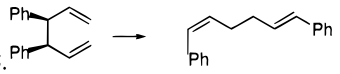	*n*-hexane	128	585	9	-13.3	520	

Table 2. (Continued)

No.	reaction	solvent	T/ °C	P/MPa	no of k data	$\Delta V_0^{\neq}$ /cm^{3}mol^{-1}	ref	remarks
526.	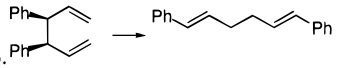	*n*-hexane	128	585	9	-8.8	520	
527.	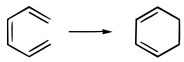	PhMe	101	600	9	-9.8	520	
528.	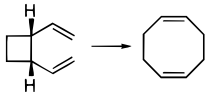	*n*-heptane	70	300	8	-14.1	535	ΔV(20 °C) = -12.8 $P \geq 20$
529.	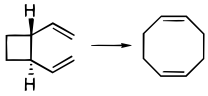	*n*-heptane	160	300	8	+4.1	535	ΔV(20 °C) = -17.4 $P \geq 20$
530.	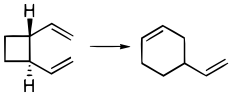	*n*-heptane	160	300	8	+4.2	535	ΔV(20 °C) = -9.6 $P \geq 20$
531.	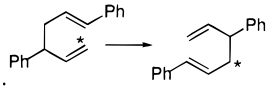	C_6D_6	162	600	9	-9.1	535	
532.	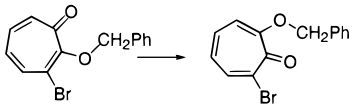	*i*-PrPh	130	160	5	-11.1	538	
533.		*n*-HexOH	130	160	5	-10.1	538	
534.	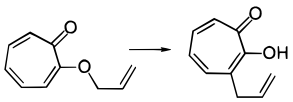	PhBr	120	160	5	-10.6	538	
535.	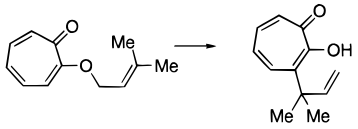	PhBr	120	160	5	-18.2	538	
536.	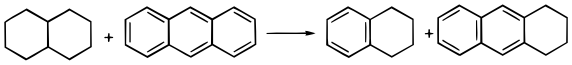	none	400	55.2	2	-55	539	o2
537.	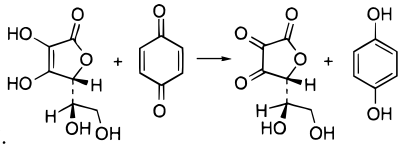	H_2O	25	90	6	-20	540	unbuffered.
538.		H_2O	25	100	5	-15	540	pH 2.00.
539.		H_2O	25	100	4	-16	540	pH 2.65.
540.		H_2O	25	90	6	-13	540	pH 3.00.
541.		H_2O	25	70	4	-4	540	pH 4.87.
542.	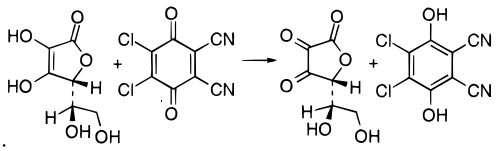	H_2O	25	90	6	-16	540	Unbuffered.
543.	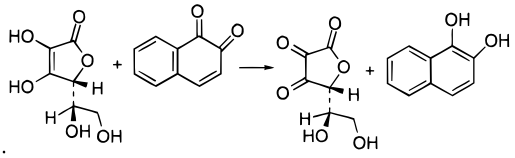	H_2O	25	90	6	-14	540	Unbuffered.

Table 2. (Continued)

No.	reaction	solvent	T/ °C	P/MPa	no of k data	$\Delta V_0^{\neq}$ /cm^{3}mol^{-1}	ref	remarks
544.	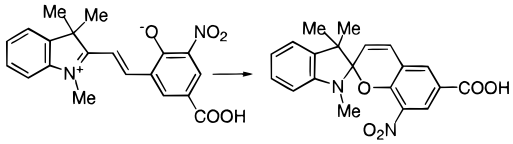	$CHCl_3$	30	120	4	+16.2	541	ΔV = +15.6, p2
545.		CH_2ClCH_2Cl	30	120	4	+16.7	541	ΔV = +18.6, p2
546.		acetone	30	120	4	+22.3	541	ΔV = +22.3, p2
547.		DMSO	30	60	3	+11.5	541	ΔV = +7.9, p2
548.	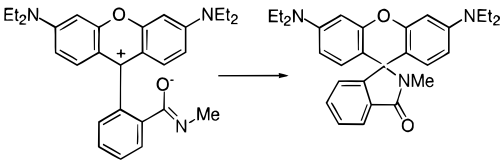	$CHCl_3$	40	120	4	+10.9	542	
549.		PhCl	40	120	4	+7.0	542	
550.		CH_2ClCH_2Cl	40	120	4	+8.4	542	
551.		MeCN	40	120	4	+3.1	542	
552.	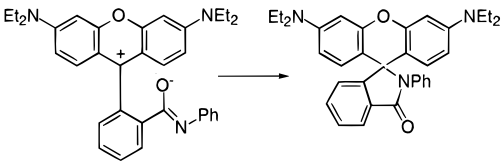	$CHCl_3$	40	100	4	+5.5	542	
553.		PhCl	40	100	4	+5.1	542	
554.		CH_2ClCH_2Cl	40	100	4	+5.6	542	
555.		MeCN	40	100	4	+4.7	542	
556.	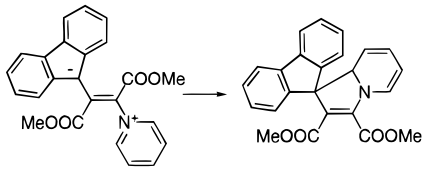	*cy*-$C_6H_{11}Me$	30	118	4	+3.3	543	
557.		PhMe	30	118	4	+4.8	543	
558.		PhCl	30	118	4	+6.1	543	
559.		Acetone	30	118	4	+6.9	543	
560.		MeCN	30	118	4	+7.7	543	
561.	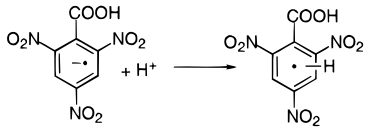	aq *i*-PrOH	ambient	39.2	5	+25/26	454, 544	*i*-PrOH 90 v%
562.	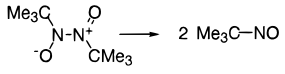	CCl_4	25	123	6	+7.7	545	ΔV = +36
563.	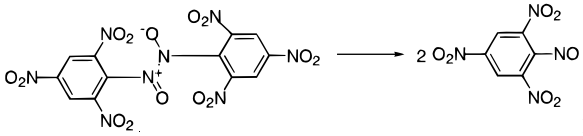	MeCN	25	196	5	+5.1	546	ΔV = +21.4
564.	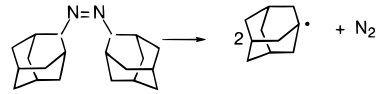	*n*-hexane	21	199	6	+17	501	
565.		EtOH	36	204	6	+22	501	
566.	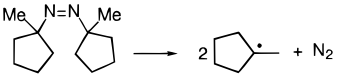	EtOH	9	195	10	+16	501	
567.	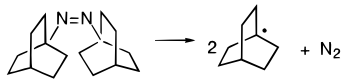	*n*-hexane	36	203	7	+13	501	
568.		EtOH	46	214	7	+9	501	

Table 2. (Continued)

No.	reaction	solvent	T/ °C	P/MPa	no of k data	$\Delta V_0^{\neq}$ /cm^{3}mol^{-1}	ref	remarks
569.	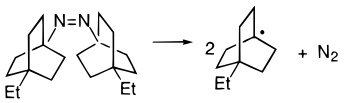	*n*-hexane	36	217	7	+16	501	
570.	decomposition of $Me_3COOCMe_3$	2-methoxytetrahydropyran (MTHP)	130	1400	9	+10.5	547	
571.		2-ethoxytetrahydropyran	130	1400	9	+11.5	547	
572.		PhH-MTHP	130	1400	9	+3.9	547	PhH 70 mol%.
573.		*n*-heptane	120	180	6	+7	548	
574.	decomposition of $(PhCOO)_2$	*n*-heptane	145	200	4	+1.2	549	$P \geq 50$
575.	decomposition of $(n\text{-}C_7H_{15}COO)_2$	*n*-heptane	80	250	5	+3.0	549	$P \geq 50$
576.	decomposition of $[Me_3CCH_2CH(Me)CH_2COO]_2$	*n*-heptane	80	250	6	+2.9	549	
577.	decomposition of RDX 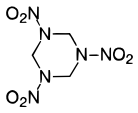	THF	170	103	11	-12	550	
578.	decomposition of HMX 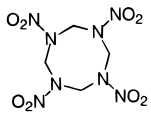	MeCN	205	103	8	+25	550	
579.		NaCl	280-300	6500	2-3	+4.1	551	$\Delta V^{\neq} < 0$ at $P > 6000$ $P \geq 3600$
580.	decomposition of 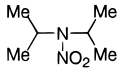	PhH	203	-	-	+47	550	
581.	decomposition of 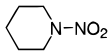	PhH	240	-	-	+34	550	
582.	decomposition of 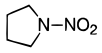	PhH	235	-	-	+48	550	
583.	decomposition of 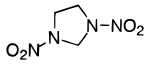	THF	163	-	-	+18	550	
584.	decomposition of 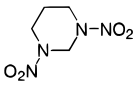	THF	205	-	-	+15	550	
585.	decomposition of 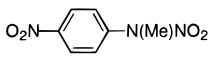	PhMe-piperidine	100	-	-	+39	550	PhMe 95 v%.
586.	decomposition of 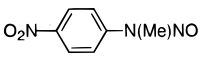	PhMe-piperidine	140	-	-	+12	550	PhMe 95 v%.
587.	decomposition of 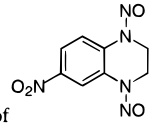	PhMe-piperidine	85	-	-	-3.5	550	PhMe 95 v%.
588.	decomposition of 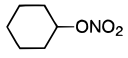	tetralin	170	1000	11	+12	550	$\Delta V^{\neq} < 0$ at $P > 600$.
589.	decomposition of 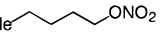	tetralin	160	-	-	+17	552	
590.	decomposition of *N*-nitrodimethylamine	2,2,4-trimethylpentane	227	103	6	+30	553	$P \geq 12.4$
591.	decomposition of nitromethane	NaCl	140	5000	4	0 >	554	$P \geq 2000$

Table 2. (Continued)

No.	reaction	solvent	T/ °C	P/MPa	no of k data	$\Delta V_0^{\neq}$ /cm^{3}mol^{-1}	ref	remarks
592.	decomposition of  in the presence of piperidine	THF	80	1300	4	-13	555	$P \geq 600$
593.		THF	130	800	5	-18	555	$P \geq 200$
594.	decomposition of  in the presence of piperidine	THF	200	600	4	+3.5	555	
595.	decomposition of  in the presence of piperidine	THF	235	1000	6	-13	555	$P \geq 80$
596.	decay of 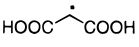	single crystal	70	200	4	+35	556	q2
597.	decay of 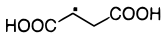	single crystal	105	200	4	+32	556	q2
598.	decay of 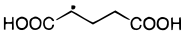	single crystal	66	200	4	+45	556	q2
599.	decay of 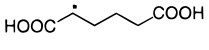	single crystal	100	200	4	+39	556	q2
600.	decay of 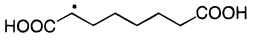	single crystal	112	200	4	+43	556	q2
601.	decay of 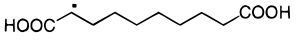	single crystal	87	200	4	+50	556	q2
602.	co-polymerization of α-methylstyrene with oxygen	neat	50	3	8	-1800	557	
603.	ethanolysis of MeBr	EtOH	40	98	3	-21	558	
604.		EtOH	60	98	5	-26	559	
605.	hydrolysis of EtBr	H_2O	25	98	4	-11/12	559	
606.	hydrolysis of *n*-PrBr	H_2O	25	98	4	-11/12	559	
607.	ethanolysis of *n*-PrBr	EtOH	40	98	4	-26	559	
608.	hydrolysis of *n*-BuBr	H_2O	25	98	4	-9	559	
609.	ehanolysis of *n*-BuBr	EtOH	25	98	4	-24	559	
610.	ethanolysis of *tert*-BuCl	EtOH	40	98	5	-29	558	
611.	ethanolysis of *tert*-BuBr	EtOH	40	98	5	-24	558	
612.	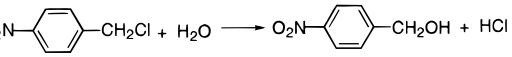	aq MeCN	25	80	5	-30.3	560	MeCN 95 v%
613.	solvolysis of 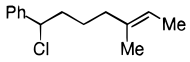	aq EtOH	45	100	5	-13.3	561	EtOH 80 %
614.	solvolysis of 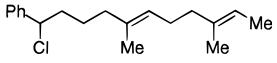	aq EtOH	45	100	6	-24.0	561	EtOH 80 %
615.	solvolysis of 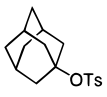	EtOH	20	80	4	-13.0	562	
616.		EtOH	25	80	4	-13.4	562	
617.		EtOH	30	80	4	-13.6	562	
618.		aq EtOH	25	80	4	-12.7	562	EtOH 95 v%
619.		aq EtOH	15	80	4	-11.3	562	EtOH 90 v%
620.		aq EtOH	20	80	4	-11.7	562	EtOH 90 v%
621.		aq EtOH	25	80	4	-12.1	562	EtOH 90 v%
622.		aq EtOH	15	80	4	-11.7	562	EtOH 85 v%
623.		MeOH	15	80	4	-13.0	562	
624.		MeOH	20	80	4	-13.7	562	
625.		MeOH	25	80	4	-13.9	562	
626.	solvolysis of PhCOCl	aq EtOH	10	200	5	-15.5	563	EtOH 95 w%
627.		aq EtOH	10	200	5	-15.1	563	EtOH 90 w%
628.		aq EtOH	20	200	5	-15.7	563	EtOH 95 w%
629.		aq EtOH	20	200	5	-15.5	563	EtOH 90 w%
630.		aq acetone	15	200	5	-21.3	563	acetone 95 w%

Table 2. (Continued)

No.	reaction	solvent	T/ °C	P/MPa	no of k data	$\Delta V_0^{\neq}$ /cm^{3}mol^{-1}	ref	remarks
631.		aq acetone	15	200	5	-17.3	563	acetone 90 w%
632.		aq acetone	25	200	5	-18.5	563	acetone 95 w%
633.		aq acetone	25	200	5	-17.0	563	acetone 90 w%
634.		aq 1,4-dioxane	15	200	5	-19.8	563	dioxane 95 w%
635.		aq 1,4-dioxane	15	200	5	-25.7	563	dioxane 90 w%
636.		aq 1,4-dioxane	25	200	5	-20.9	563	dioxane 95 w%
637.		aq 1,4-dioxane	25	200	5	-27.1	563	dioxane 90 w%
638.	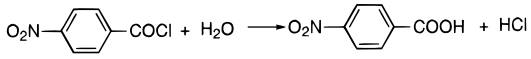	aq MeCN	40	80	4	-26.3	560	MeCN 95 v%
639.	solvolysis of 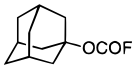	aqMeOH	40	100	4	-30.0	564	MeOH 80 %
640.		aqMeOH	50	100	4	-35.4	564	MeOH 80 %
641.		aqMeOH	40	100	4	-32.6	564	MeOH 90 %
642.		aqMeOH	50	100	4	-39.4	564	MeOH 90 %
643.		aqEtOH	40	100	4	-27.7	564	EtOH 60 %
644.		aqEtOH	50	100	4	-34.3	564	EtOH 60 %
645.		aqEtOH	40	100	4	-29.3	564	EtOH 70 %
646.		aqEtOH	50	100	4	-36.3	564	EtOH 70 %
647.		aqEtOH	40	100	4	-31.7	564	EtOH 80 %
648.		aqEtOH	50	100	4	-37.0	564	EtOH 80 %
649.		aqEtOH	50	100	4	-35.8	564	EtOH 90 %
650.		aq CF_3CH_2OH	35	50	3	-13.7	564	TFE 90 w%
651.		aq CF_3CH_2OH	35	50	3	-12.7	564	TFE 80 w%
652.		aq CF_3CH_2OH	35	50	3	-12.0	564	TFE 70 w%
653.	solvolysis of MeOCOCl	EtOH	20	80	4	-21.7	562	
654.		EtOH	25	80	4	-24.6	562	
655.		aq EtOH	20	80	4	-22.9	562	EtOH 90 v%
656.		aq EtOH	25	80	4	-25.6	562	EtOH 90 v%
657.		aq EtOH	20	80	4	-23.8	562	EtOH 80 v%
658.		aq EtOH	25	80	4	-25.9	562	EtOH 80 v%
659.		MeOH	20	80	4	-23.3	562	
660.		MeOH	25	80	4	-25.2	562	
661.		aq MeOH	20	80	4	-23.4	562	MeOH 90 v%
662.		aq MeOH	25	80	4	-25.5	562	MeOH 90 v%
663.		aq MeOH	20	80	4	-23.7	562	MeOH 80 v%
664.		aq MeOH	25	80	4	-25.8	562	MeOH 80 v%
665.	solvolysis of PhOCOCl	EtOH	5	50	3	-29.2	562	
666.		EtOH	10	50	3	-34.2	562	
667.		aq EtOH	5	50	3	-32.8	562	EtOH 90 v%
668.		aq EtOH	10	50	3	-35.3	562	EtOH 90 v%
669.		aq EtOH	5	50	3	-34.4	562	EtOH 80 v%
670.		aq EtOH	10	50	3	-36.8	562	EtOH 80 v%
671.		MeOH	5	50	3	-33.8	562	
672.		MeOH	10	50	3	-36.2	562	
673.	solvolysis of 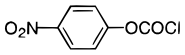	aq MeCN	10	80	4	-22.9	560	MeCN 95 v%
674.	solvolysis of 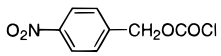	MeOH	25	80	5	-40.3	560	
675.		EtOH	25	80	4	-55.7	560	
676.	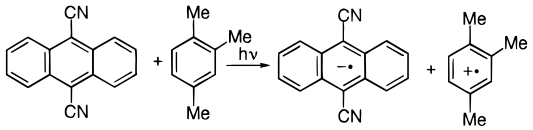	MeCN	25	256	6	+6.8[r2]	565	$\delta\Delta V^{\neq}$ = -9.3[s2]
677.	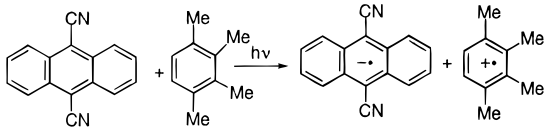	MeCN	25	256	6	+6.5[r2]	565	$\delta\Delta V^{\neq}$ = -8.2[s2]
678.	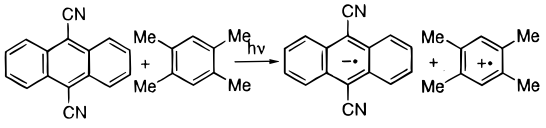	MeCN	25	256	6	+6.7[r2]	565	$\delta\Delta V^{\neq}$ = -8.1[s2]

Table 2. (Continued)

No.	reaction	solvent	T/ °C	P/MPa	no of k data	$\Delta V_0^{\neq}$ /cm^{3}mol^{-1}	ref	remarks
679.	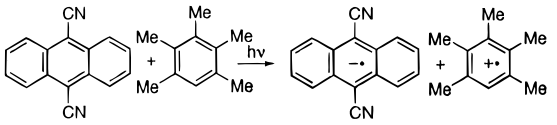	MeCN	25	256	6	+9.6[r2]	565	$\delta\Delta V^{\neq}$ = -10.6[s2]
680.	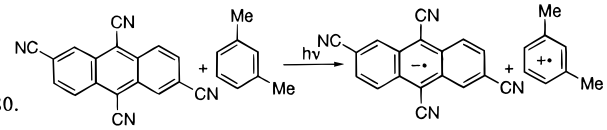	MeCN	25	256	6	+7.7[r2]	565	$\delta\Delta V^{\neq}$ = -8.4[s2]
681.	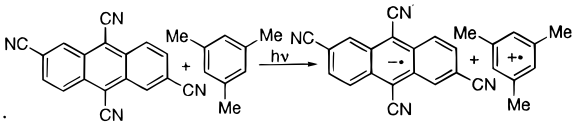	MeCN	25	256	6	+7.8[r2]	565	$\delta\Delta V^{\neq}$ = -8.2[s2]
682.	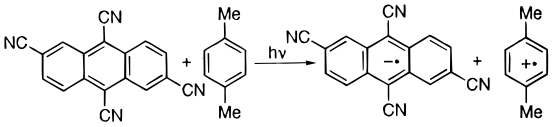	MeCN	25	256	6	+7.6[r2]	565	$\delta\Delta V^{\neq}$ = -8.1[s2]
683.	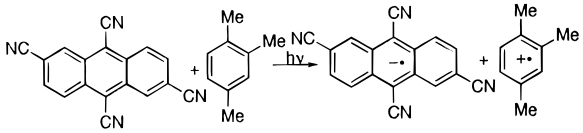	MeCN	25	256	6	+6.9[r2]	565	$\delta\Delta V^{\neq}$ = -7.1[s2]
684.	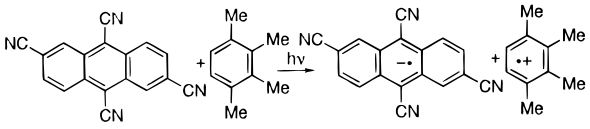	MeCN	25	256	6	+7.3[r2]	565	$\delta\Delta V^{\neq}$ = -7.4[s2]
685.	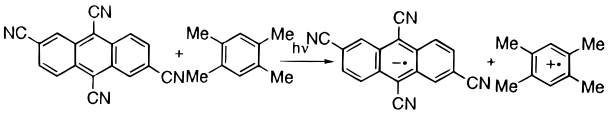	MeCN	25	256	6	+7.4[r2]	565	$\delta\Delta V^{\neq}$ = -7.7[s2]
686.	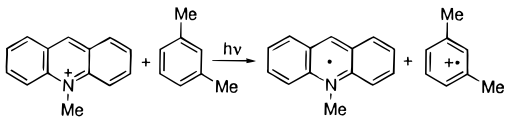	MeCN	25	256	6	+9.0[r2]	565	$\delta\Delta V^{\neq}$ = -11.0[s2]
687.	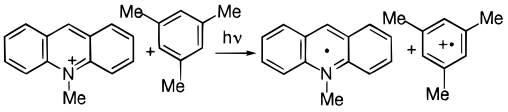	MeCN	25	256	6	+10.3[r2]	565	$\delta\Delta V^{\neq}$ = -11.6[s2]
688.	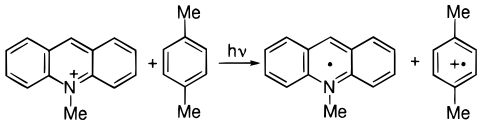	MeCN	25	256	6	+11.0[r2]	565	$\delta\Delta V^{\neq}$ = -12.2[s2]
689.	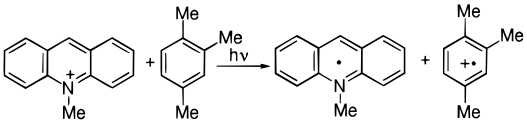	MeCN	25	256	6	+9.5[r2]	565	$\delta\Delta V^{\neq}$ = -10.0[s2]
690.	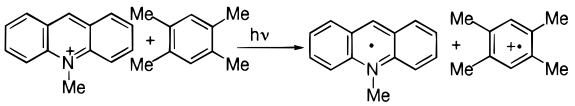	MeCN	25	256	6	+9.2[r2]	565	$\delta\Delta V^{\neq}$ = -9.6[s2]
691.	p-$BrC_6H_4SO_3CH_2CH_2Ph + C_5H_5N \rightarrow C_5H_5N^+CH_2CH_2Ph + BrC_6H_4SO_3^-$	MeCN	40	100	3	-12.3	566	
692.		MeCN	45	200	5	-16.9	567	
693.		MeCN	50	150	4	-10.3	566	
694.		MeCN	50	200	5	-15.9	567	

Table 2. (Continued)

No.	reaction	solvent	T/ °C	P/MPa	no of k data	$\Delta V_0^{\neq}$ /cm^{3}mol^{-1}	ref	remarks
695.		MeCN	50	200	5	-18.6[g l]	568	
696.		MeCN	55	200	5	-15.6	567	
697.		MeCN	60	150	4	-9.6	566	
	m-$NO_2C_6H_4SO_3CH_2CH_2Ph + C_5H_5N \longrightarrow$ $C_5H_5N^+CH_2CH_2Ph + m\text{-}NO_2C_6H_4SO_3^-$							
698.		MeCN	50	200	5	-4.3[g l]	566	
699.	*p*-$ClC_6H_4SO_3CH_2CH_2Ph + C_5H_5N \longrightarrow C_5H_5N^+CH_2CH_2Ph + ClC_6H_4SO_3^-$	MeCN	50	200	5	-9.2[g l]	566	
700.	$PhSO_3CH_2CH_2Ph + C_5H_5N \longrightarrow C_5H_5N^+CH_2CH_2Ph + PhSO_3^-$	MeCN	50	200	5	-15.4[g l]	566	
701.	*p*-$MeC_6H_4SO_3CH_2CH_2Ph + C_5H_5N \longrightarrow C_5H_5N^+CH_2CH_2Ph + MeC_6H_4SO_3^-$	MeCN	50	200	5	-18.6[g l]	566	
	p-$BrC_6H_4SO_3CH_2CH_2Ph$ + 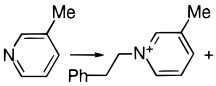 + $BrC_6H_4SO_3^-$							
702.		MeCN	45	200	5	-15.3	567	
703.		MeCN	50	200	5	-14.4	567	
704.		MeCN	50	200	5	-13.5[g l]	568	
705.		MeCN	55	200	5	-13.5	567	
	p-$BrC_6H_4SO_3CH_2CH_2Ph$ + 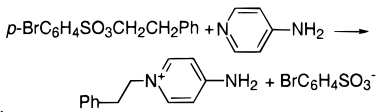							
706.		MeCN	45	200	5	-12.6	567	
707.		MeCN	50	200	5	-12.3	567	
708.		MeCN	50	200	5	-15.0[g l]	568	
709.		MeCN	55	200	5	-11.4	567	
	p-$BrC_6H_4SO_3CH_2CH_2Ph$ + 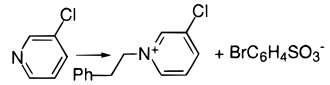							
710.		MeCN	50	200	4	-12.8[g l]	568	$P \geq 50$.
	p-$BrC_6H_4SO_3CH_2CH_2Ph$ + 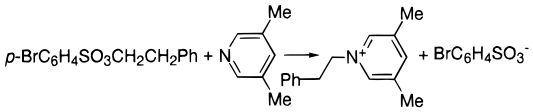							
711.		MeCN	35	200	5	-15.5	568	
712.		MeCN	40	200	5	-15.2	568	
713.		MeCN	45	200	5	-15.7	567	
714.		MeCN	45	200	5	-14.6	568	
715.		MeCN	50	200	5	-15.4	567	
716.		MeCN	50	200	5	-14.3	568	
717.		MeCN	55	200	5	-13.8	567	
718.	*p*-$BrC_6H_4SO_3CH_2COPh + C_5H_5N \longrightarrow C_5H_5N^+CH_2COPh + BrC_6H_4SO_3^-$	MeCN	35	150	4	-14.6	569	
719.		MeCN	45	150	4	-13.7	569	
720.		MeCN	55	150	4	-13.3	569	
	p-$BrC_6H_4SO_3CH_2COPh$ + 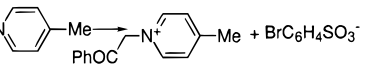 + $BrC_6H_4SO_3^-$							
721.		MeCN	45	150	4	-16.5[g l]	569	
	p-$BrC_6H_4SO_3CH_2COPh$ + 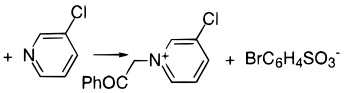							
722.		MeCN	45	150	4	-14.1[g l]	569	
	p-$BrC_6H_4SO_3CH_2COPh$ + 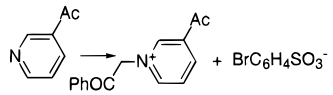							
723.		MeCN	45	150	4	-14.3[g l]	569	
	p-$BrC_6H_4SO_3CH_2COPh$ + 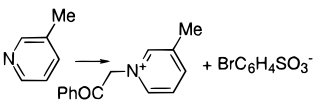							
724.		MeCN	45	150	4	-18.4[g l]	569	
725.	$PhCH_2Cl + C_5H_5N \longrightarrow C_5H_5N^+CH_2Ph + Cl^-$	DMF	40	200	6	-5.1	570	
726.		DMF	50	200	6	-8.1	570	
727.	*p*-$NO_2C_6H_4CH_2Cl + C_5H_5N \longrightarrow C_5H_5N^+CH_2C_6H_4NO_2 + Cl^-$	DMF	40	200	6	-4.5	570	
728.		DMF	50	200	6	-7.1	570	

Table 2. (Continued)

No.	reaction	solvent	T/ °C	P/MPa	no of k data	$\Delta V_0^{\neq}$ /cm^{3}mol^{-1}	ref	remarks
729.	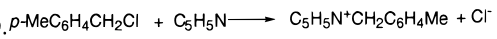	DMF	40	200	6	-5.5	570	
730.		DMF	50	200	6	-10.9	570	
731.	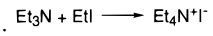	MeOH	40	200	7	-33.1	571	
732.		EtOH	40	200	7	-29.7	571	
733.		*n*-PrOH	40	200	7	-27.3	571	
734.		*n*-BuOH	40	200	7	-26.5	571	
735.		*n*-PentOH	40	200	7	-26.2	571	
736.		*i*-PrOH	40	200	7	-31.2	571	
737.		*sec*-BuOH	40	200	7	-28.2	571	
738.	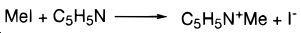	MeCN	45	110	7	-28.5	572	
739.	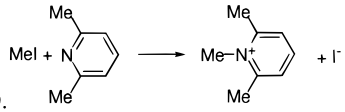	MeCN	45	110	6	-30.8	572	
740.	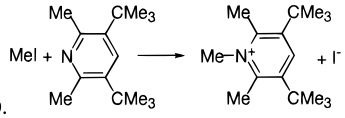	MeCN	45	120	6	-32.5	572	
741.	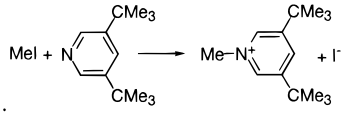	MeCN	45	100	6	-21.4	572	
742.	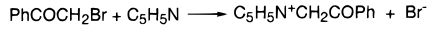	MeOH	40	100	8	-19.9	573	ΔV (40 °C) = -31.9
743.	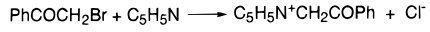	MeOH	40	100	3	-30	573	$P \geq 40$
744.	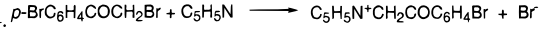	MeOH	40	100	5	-19.8	573	ΔV (40 °C) = -26.0
745.	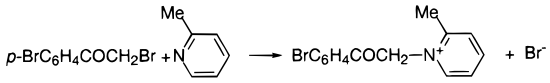	MeOH	40	100	3	-48	573	ΔV (40 °C) = -32 $P \geq 40$
746.	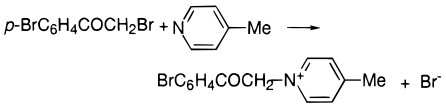	MeOH	40	100	5	-16.9	573	ΔV (40 °C) = -31.3
747.	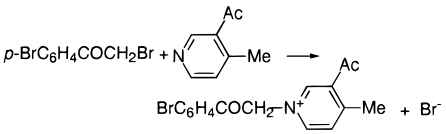	MeOH	40	100	5	-22.1	573	ΔV (40 °C) = -32
748.	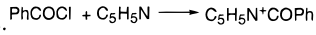	MeCN	10	100	4	-41.1	574	
749.		MeCN	20	100	4	-45.6	574	
750.	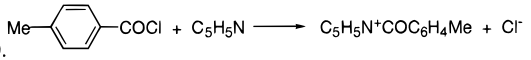	MeCN	10	100	4	-38.4	574	
751.		MeCN	20	100	4	-39.7	574	
752.	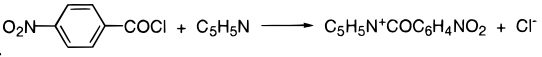	MeCN	10	100	4	-53.5	574	
753.		MeCN	20	100	4	-38.3	574	
754.	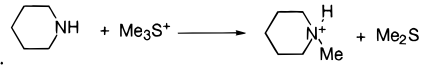	-	-	-	-	-3	575	
755.	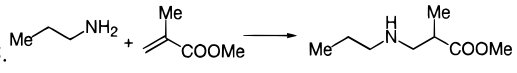	MeCN	36	-	-	-48	576	
756.	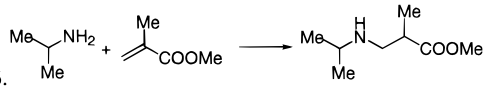	MeCN	36	-	-	-50	576	

Table 2. (Continued)

No.	reaction	solvent	T/ °C	P/MPa	no of k data	$\Delta V_0^{\neq}$ /cm^{3}mol^{-1}	ref	remarks
757.	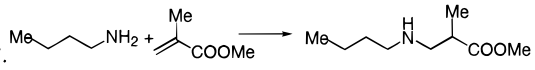	MeCN	36	-	-	-49	576	
758.	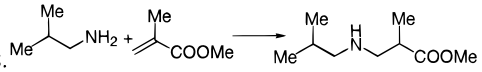	MeCN	36	-	-	-53	576	
759.	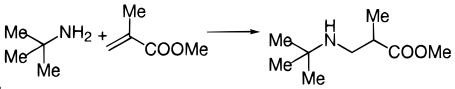	MeCN	36	-	-	-53	576	
760.	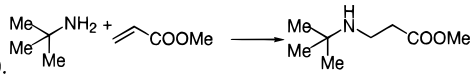	MeCN	36	-	-	-42	576	
761.	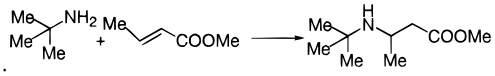	MeCN	36	-	-	-45	576	
762.	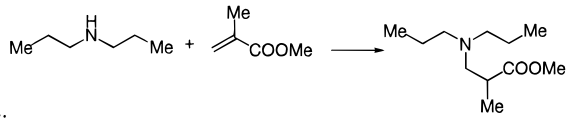	MeCN	36	-	-	-51	576	
763.	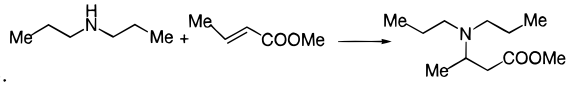	MeCN	36	-	-	-46	576	
764.	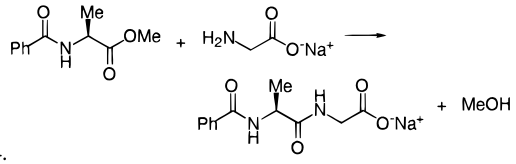	MeOH	52	660	8	-19.3	577	
765.	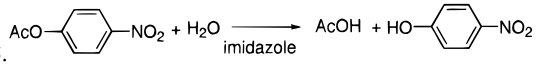	H_2O	15	100	4	-17[g1]	578	
766.		H_2O	25	100	4	-11.8	578	
767.		H_2O	35	60	4	-16[g1]	578	
768.		AOT[a2]/H_2O/hexane reversed micelles	15	100	4	-10[g1]	578	$[H_2O]/[AOT] = 12.1$
769.		AOT[a2]/H_2O/hexane reversed micelles	15	100	4	-12[g1]	578	$[H_2O]/[AOT] = 23.4$
770.		AOT[a2]/H_2O/hexane reversed micelles	25	100	7	-3.2	578	$[H_2O]/[AOT] = 11.2$
771.		AOT[a2]/H_2O/hexane reversed micelles	25	100	4	-6.4	578	$[H_2O]/[AOT] = 12.9$
772.		AOT[a2]/H_2O/hexane reversed micelles	25	100	4	-10.4	578	$[H_2O]/[AOT] = 23.7$
773.		AOT[a2]/H_2O/hexane reversed micelles	25	100	4	-14.4	578	$[H_2O]/[AOT] = 35.2$
774.		AOT[a2]/H_2O/hexane reversed micelles	25	100	4	-15.2	578	$[H_2O]/[AOT] = 38.7$
775.		AOT[a2]/H_2O/hexane reversed micelles	25	100	4	-16.0	578	$[H_2O]/[AOT] = 39.9$
776.		AOT[a2]/H_2O/hexane reversed micelles	35	100	6	-16[g1]	578	$[H_2O]/[AOT] = 12.2$
777.		AOT[a2]/H_2O/hexane reversed micelles	35	100	4	-11[g1]	578	$[H_2O]/[AOT] = 24.6$
778.		AOT[a2]/H_2O/hexane reversed micelles	35	80	4	-19[g1]	578	$[H_2O]/[AOT] = 34.4$
779.	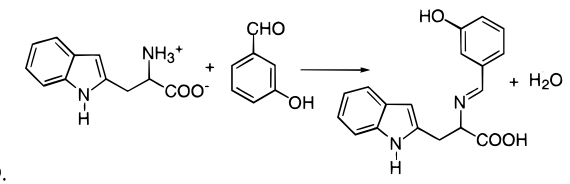	H_2O	70	80	5	-10	579	
780.	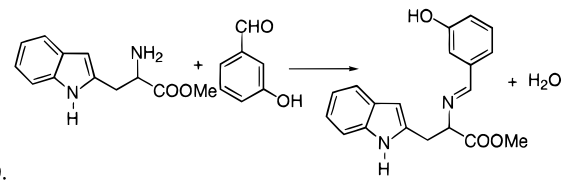	H_2O	20	60	4	-16	579	

Table 2. (Continued)

No.	reaction	solvent	T/ °C	P/MPa	no of k data	$\Delta V_0^{\neq}$ /cm^{3}mol^{-1}	ref	remarks
781.	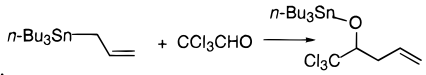	n-$Bu_3SnCH_2CHCH_2$	37.5	80	5	-33.4	239	
782.	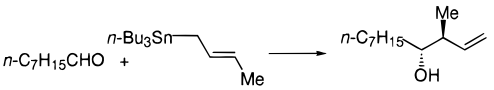	$CHCl_3$	30	800	4	-29.1	580	$P \geq 300$
783.	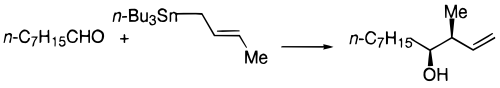	$CHCl_3$	30	800	4	-34.1	580	$P \geq 300$
784.	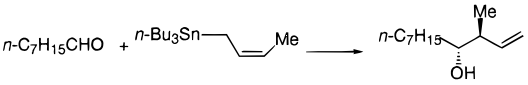	$CHCl_3$	30	800	4	-34.4	580	$P \geq 300$
785.	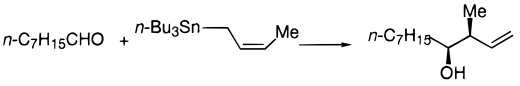	$CHCl_3$	30	800	4	-30.1	580	$P \geq 300$
786.	$Me_4Sn + I_2 \longrightarrow Me_3SnI + MeI$	CCl_4	10	120	5	-48.2	581	
787.		MeOH	10	160	6	-38.8	582	
788.		CCl_4	25	120	5	-54.8	581	
789.		MeOH	25	160	6	-45.1	582	
790.		CCl_4	35	120	5	-59.9	581	
791.		MeOH	35	160	6	-52.7	582	
792.	$Me_4Sn + I_2 \longrightarrow Me_3SnI + MeI$	hexane	10	160	6	-51.0	583	
793.		hexane	25	160	6	-59.6	583	
794.		hexane	35	160	6	-65.0	583	
795.		acetone	10	160	6	-39.4	583	
796.		acetone	25	160	6	-45.3	583	
797.		acetone	35	160	6	-51.0	583	
798.	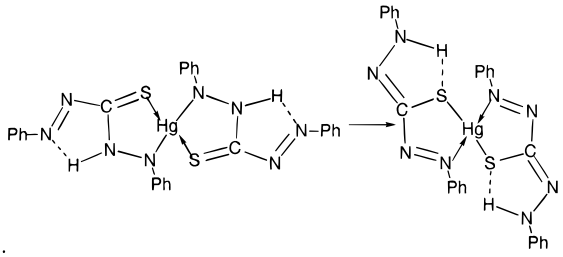	PhMe	20	120	5	+7.0	584	
799.		CCl_4	20	90	5	+7.0	584	
800.		PhCl	20	120	5	+6.6	584	
801.		CH_2ClCH_2Cl	20	120	5	+5.7	584	
802.		$PhNO_2$	20	90	4	+5.2	584	
803.	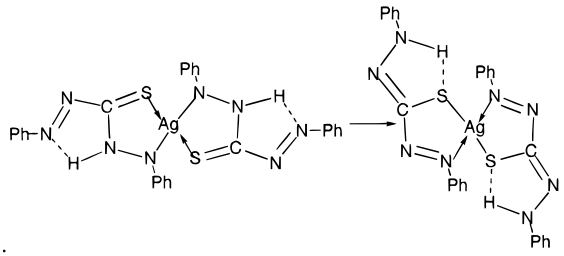	CH_2Cl_2	20	90	4	+5.9	584	
804.		CH_2Cl CH_2Cl	20	120	5	+7.9	584	
805.		$PhNO_2$	20	80	4	+6.4	584	
806.	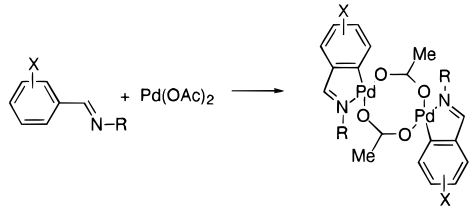 X = H, R = n-Pr	PhMe	45	101	5	-12	585	

Table 2. (Continued)

No.	reaction	solvent	T/ °C	P/MPa	no of k data	$\Delta V_0^{\neq}$ /cm^{3}mol^{-1}	ref	remarks
807.		AcOH	25	101	4	-17	586	
808.	X = H, R = Ph	PhMe	70	101	5	-23	585	
809.		AcOH	25	86	7	-18	586	
810.	X = 4-MeO, R = Ph	PhMe	50	101	5	-24	585	
811.		AcOH	20	101	4	-15	586	
812.	X= 2-NO_2, R = Ph	PhMe	70	101	5	-23	585	
813.		AcOH	20	101	5	-12	586	
814.	X= 3-NO_2, R = Ph	PhMe	70	101	5	-21	585	
815.		AcOH	20	101	4	-16	586	
816.	X= 4-NO_2, R = Ph	PhMe	70	71	4	-25	585	
817.		AcOH	20	91	4	-17	586	
818.	X = H, R = CH_2Ph	PhMe	50	101	6	-15	585	
819.		AcOH	35	101	5	-15	586	
820.		AcOH	45	101	3	-16	586	
821.	X = 4-Cl, R = CH_2Ph	PhMe	60	122	6	-12	585	
822.		AcOH	20	101	4	-17	586	
823.	X = 3-NO_2, R = CH_2Ph	PhMe	50	101	5	-15	585	
824.	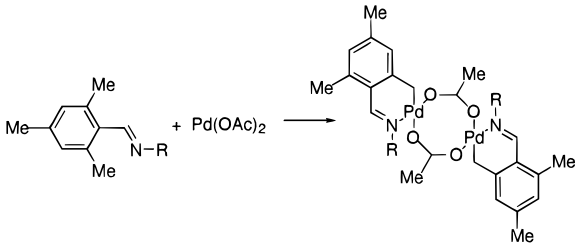	AcOH	45	101	4	-16	586	
825.	R = Ph	PhMe	60	101	5	-24	585	
826.		AcOH	25	91	6	-17	586	
827.	R= 2-MeC_6H_4	PhMe	70	101	5	-20	585	
828.		AcOH	20	101	4	-11	586	
	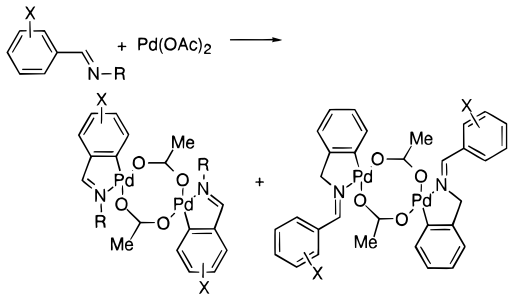 X = 2-NO_2, R = CH_2Ph							
829.		PhMe	50	101	5	-11	585	
830.		AcOH	45	101	3	-17	586	
831.	X = H 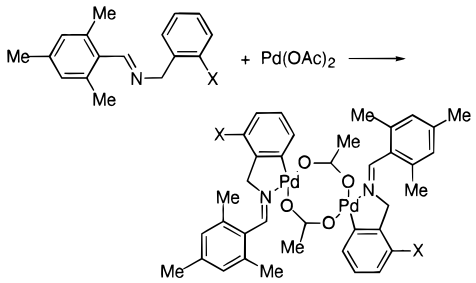	PhMe	50	101	5	-12	585	
832.		AcOH	20	101	4	-11	586	
833.		AcOH	30	101	4	-15	586	
834.	X = Me	PhMe	50	101	5	-17	585	
835.		AcOH	30	101	4	-13	586	

Table 2. (Continued)

No.	reaction	solvent	T/ °C	P/MPa	no of k data	$\Delta V_0^{\neq}$ /cm^{3}mol^{-1}	ref	remarks
836.	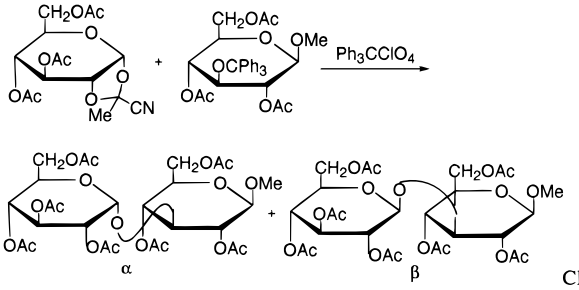	CH_2Cl_2	20	1400	9	-8	587	t2
837.	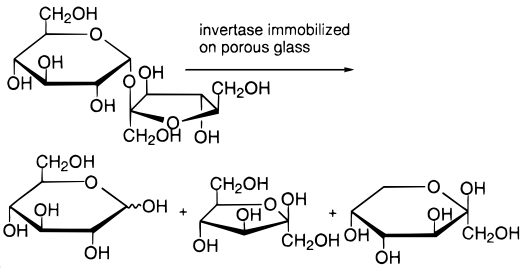	H_2O	30	127	5	-29	588	$\Delta V^{\neq} > 0$ at $P > 50$.
838.	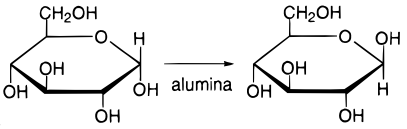	H_2O	40	90	4	+22	589	
839.	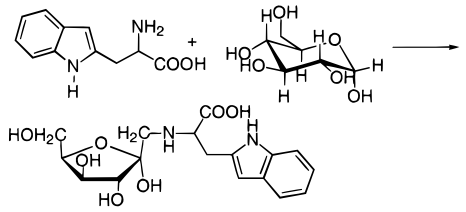	MeOH	70	60	4	-17	579	
840.	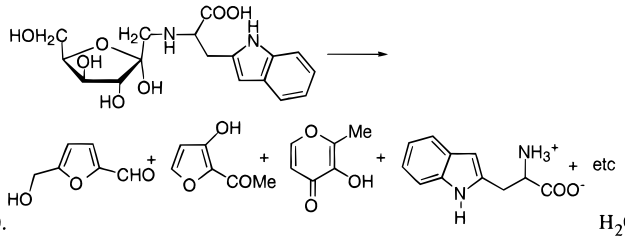	H_2O	95	60	4	+17	579	
841. hydrolysis of maltose catalyzed by immobilized glucoamylase		H_2O	25	127	4	+1	590	ΔV = -4 for Michaelis constant
842. hydrolysis of maltotriose catalyzed by immobilized glucoamylase		H_2O	25	98	4	+1	590	ΔV = -4 for Michaelis constant
843. H^+-catalyzed hydrogen exchange of $CH_3CONHCH_3$ with H_2O		H_2O	66	400	17	+1.7	591	[amide] = 16 mol%.
844. OH^--catalyzed hydrogen exchange of $CH_3CONHCH_3$ with H_2O		H_2O	66	400	17	+11.0	591	[amide] = 16 mol%.
845. uncatalyzed hydrogen exchange of $CH_3CONHCH_3$ with H_2O		H_2O	66	400	17	-9.0	591	[amide] = 16 mol%.
846.	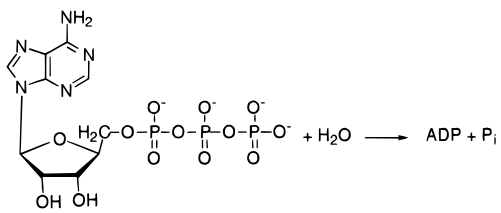	H_2O	80	220	7	-15	431	$\Delta V^{\neq} > 0$ at P>120
847. ADP + H_2O ⟶ AMP + Pi		H_2O	80	220	6	-15	431	$\Delta V^{\neq} > 0$ at P>120

Table 2. (Continued)

No.	reaction	solvent	T/ °C	P/MPa	no of k data	$\Delta V_0^{\neq}$ /cm^{3}mol^{-1}	ref	remarks
848.	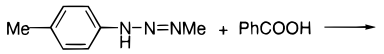 $MeC_6H_4NH_2$ + $PhCOOMe$ + N_2	$CHCl_3$	29.8	100	8	-15	592	
849.		MeCN	29.8	120	6	-4	592	
850.	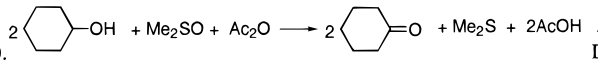	DMSO	58	100	5	-25.2	593	
851.	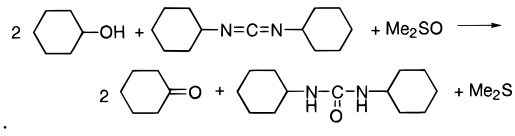	DMSO-$CHCl_3$	31	102	6	-34	593	DMSO 25 v%.
852.	$MeCH(NHCl)COO^- + H_2O \longrightarrow MeCHO + NH_3 + HCl + CO_2$	H_2O	26	250	28	+50	594	$\Delta V^{\neq} \approx 0$ at $P > 100$.
853.	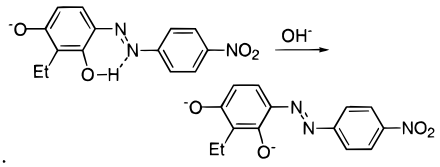	aqDMSO	25	200	6	-22	595	DMSO 80 v%.

[a1] Chemically induced dynamic electron polarization. [b1] Observed by laser flash photolysis of the quinone solution. [c1] Observed by laser flash photolysis of the benzoic acid solution in the presence of hydrogen chloride. The CIDEP signal followed a double exponential decay. The faster decay was assigned to the protonation of the anion radical, and the slower decay was assigned to the spin−lattice relaxation of the neutral radical. [d1] Observed by laser flash photolysis of the benzophenone solution. [e1] Measured indirectly by monitoring the concentration of diphenylisobenzofuran. [f1] 1,4-Diazabicyclo[2.2.2]octane. [g1] Calculated by one of the authors (T.A.). [h1] The log $k - P$ plot shows a maximum. [i1] Extrapolated value for [1-Br$C_{10}H_7$] = 0: $\Delta V_0^{\ddagger} = -8.6$. [j1] The rate constants were calculated from the fluorescene lifetime in *J. Phys. Chem.* (**1993**, *97*, 177) and the fluorescence quantum yield reported previously (Tanaka, F. *Rev. Phys. Chem. Jpn.* **1974**, *44*, 65). [k1] For the pressure ranges and the results for other temperatures, see the original paper. [l1] For the results in hexane, see: Holroyd, R. A.; Schwarz, H. A.; Stradowska, E.; Ninomiya, S.; Itoh, K.; Nishikawa, M. *J. Phys. Chem.* **1994**, *98*, 7142. [m1] *Ortho*-positronium. [n1] Pressure-averaged ($P \leq 10$ MPa) activation volume. [o1] From ^{13}C spin−lattice relaxation rates. [p1] Estimated from the figure. [q1] From depolarized light scattering. [r1] From ^2H spin−lattice relaxation rates. [s1] Poly(methyl methacrylate). [t1] Polystyrene. [u1] Poly(bisphenol A carbonate). [v1] Cyclopentadienyldiethylenerhodium(I). [w1] Cyclopentadienylethylenetetrafluoroethylenerhodium(I). [x1] Sodium dodecyl sulfate. [y1] For the related works, see also: Hara, K. *Physica B* **1986**, *139* & *140*, 705; Hara, K.; Kometani, N.; Kajimoto, O. *J. Phys. Chem.* **1996**, *100*, 1488. [z1] Hexadecyltrimethylammonium bromide. [a2] Aerosol-OT (Tokyo Kasei): sodium di(2-ethylhexyl) sulfosuccinate, $NaO_3SCH(COOC_8H_{17})CH_2COOC_8H_{17}$. [b2] For the overall reaction. $\delta\Delta V^{\ddagger} = V^{\ddagger}_{cis} - V^{\ddagger}_{trans} = -5.3$. [c2] Pressure-averaged ($P \leq 300$ MPa) activation volume. [d2] The endo/exo ratio (= 35/65) did not change with pressure. [e2] Cis/trans = 70/30 (0.1 MPa), 75/25 (300 MPa). [f2] In the presence of bis(3-*tert*-butyl-4-hydroxy-5-methylphenyl) sulfide as a radical chain inhibitor. [g2] In the presence of diphenylamine as a radical chain inhibitor. [h2] Acetonitrile 89 mol %. [i2] ΔV values: −35.6 (30 °C), −39.9 (50 °C), −44.8 (60 °C). [j2] ΔV values: −28.8 (30 °C), −33.0 (50 °C), −35.6 (65 °C). [k2] Aryl cyanate 3.94 mol %, benzyl azide 15.8 mol %. [l2] Aryl cyanate 7.24 mol %, benzyl azide 7.24 mol %. [m2] Aryl cyanate 9.40 mol %, benzyl azide 3.92 mol %. [n2] Aryl cyanate 2.78 mol %, benzyl azide 2.78 mol %. [o2] Anthracene (40 mg) in 0.2 mL of decalin. For the reaction of decalin with coal, $\Delta V^{\ddagger} = -70$. [p2] Pressure effects on the reverse reaction were also measured. [q2] The radicals were created by γ-irradiation. [r2] From the pressure dependence of the quantum yield for the free radical ion formation in the irradiation of the donor and the acceptor solution. [s2] $\delta\Delta V^{\ddagger} = \Delta V^{\ddagger}$ (back electron transfer) − $\Delta V^{\ddagger}$ (ion pair separation). [t2] $\delta\Delta V^{\ddagger} = V^{\ddagger}(\alpha) - V^{\ddagger}(\beta) = +5$.

these corrections were made properly, and readers who wish to consult the original papers should be alert to that complication. Table 2 contains a few results obtained in solid media such as films and host crystals; this was done despite the title of this article, in instances where related reactions were studied in solutions under pressure. The reader will surely be aware of the fact that a solid subject to a uniaxial stress cannot be considered to be under hydrostatic pressure, and volume changes calculated on that basis, while of interest, must be regarded with some reservation. As before, the text does not offer comment on every single entry in the table; rather, we sought to call attention only to especially useful and interesting chemistry.

The rate at which new and additional data on high-pressure effects in organic reactions are accumulating continues unabated, at about 100 per year; however, the nature of the processes investigated is clearly changing. Where our previous reviews dealt almost exclusively with well-known and traditional reactions such as displacements, additions, eliminations, and pericyclic chemistry, the interests of the community has in the past decade shifted to new areas, including fast processes in which the use of transition state theory may become questionable, electron transport in organic media, reactions in supercritical fluids, and so on. In some of these areas, the interpretation of the data is by no means straightforward, or widely agreed to, and it may therefore be anticipated that high-pressure organic chemistry will continue as a lively territory for research.

B. Comments on Table 2

Sueishi[453,454] has used the CIDEP phenomenon to open up to high-pressure scrutiny chemical reactions

with half-lives in the sub-microsecond domain (entries 1−6). For example, the photoreduction of 2,4,6-trinitrobenzoic acid in aqueous 2-propanol containing chloride ion involves the radical anion the decay of which can be followed by means of emission in the electron spin frequency regime. The nine-line spectrum (due to H-3, H-5, and the *p*-nitro group) decays in two stages which were identified by means of their pressure dependence. The first step is a rapid protonation to give a neutral free radical the ESR spectrum of which is virtually identical with that of the precursor; support for this interpretation is provided by the activation volume of +26 cm^3 mol^{-1}. The second phase was not identified precisely, but the $\Delta V^{\ddagger}$ value of +11 cm^3 mol^{-1} suggests that diffusion is an important part of the process, as the solvent viscosity has a pressure dependence which corresponds approximately to that volume change.

The same group has looked into the bimolecular spin exchange of stable free radicals such as tempone (2,2,6,6-tetramethyl-4-piperidone *N*-oxide; entries 7−34). The technique used was to study the effect of pressure on the change in line broadening that occurs when the concentration is varied.[455−458] The process is inhibited by the application of pressure, and it was initially postulated[458] that diffusion control was the reason. Especially convincing was the fact that $\Delta V^{\ddagger}$ is negative in water, for indeed, the viscosity of water decreases when the pressure is raised within the range used. However, $\Delta V^{\ddagger}$ is generally somewhat smaller than what would be anticipated on the basis of the Smoluchowski equation.[457] The deviations are largest in protic solvents, prompting the assumption that encounter complexes first form in such media. These complexes were estimated to involve a negative contribution to $\Delta V^{\ddagger}$, of about 3.5 cm^3 mol^{-1}. Still later experiments with a wider variety of solvents as well as of radicals showed that the process is much more complex than previously believed, as some of the largest deviations from simple diffusion control occur in aprotic media such as acetone and hexane. Exchange probability and a steric factor were considered; further insights are likely to emerge from future investigations. The large difference between the activation volumes in pentane and hexane (entries 20 and 21) is especially remarkable.

Somewhat similar mechanisms have been considered for the quenching of singlet oxygen (entries 36−110). The process is accelerated by the application of pressure;[459] the negative activation volumes are explained[460] by the formation of encounter complexes with the solvent. The contractions are larger in those solvents which have low ionization potentials; presumably the complexes have considerably dipolar character. When the quenching is mediated by nitrogen-containing solutes, this polar nature of the intermediate is well-demonstrated by the strong solvent dependence: $\Delta V^{\ddagger}$ is the more strongly negative the less polar the solvent.[462,463] In *n*-hexane, for example, $\Delta V^{\ddagger}$ reaches values as low as −40 cm^3 mol^{-1}.

The rates of quenching of both singlet and triplet states of anthracenes by oxygen in methylcyclohexane (entries 111−118) are in most instances reduced at high pressure.[464] Increased solvent viscosity is responsible; but since the activation volumes are only about half of what would be expected on that basis, encounter complexes are also thought to play a role. The negative value for the 9,10-dicyano derivative is not understood at present. The pressure-promoted quenching of the ^1S state of perylene by 1-bromo- and 1-iodonaphthalenes in toluene is readily attributed to[465] and in accord with exciplex formation (stacking).

A very nice contribution to our knowledge of high-pressure phenomena has been made by Holroyd and co-workers (entries 131−157). It has long been known that charged species in solution bring about electrostriction, a phenomenon well-explained by the Drude−Nernst equation. The relation predicts that the contraction should become exceptionally large in hydrocarbon media, because of their nonpolar nature. This prediction has never been verified for the simple reason that the necessary solutions could not be prepared. However, the predicted exceedingly large pressure effects have now been observed by the Holroyd group in pulse radiolysis experiments aimed at the process of electron attachment to various molecules in hydrocarbon liquids.[468−470]

Their studies fall into two categories: the study of transport phenomena of electrons and that of their reactivity. Both provide information on partial molar volumes. In the experiments, liquid samples are exposed to a pulse of X-rays from a van de Graaff accelerator, which generates excess electrons and ions; hence, the current observed immediately after the pulses measures the electron concentration in the liquid. This makes it possible to determine excess electron mobilities if the liquid is free from electron-capturing impurities, and the rates of electron attachment to solutes deliberately added.

Studies of this sort shed light on the nature of electron traps in nonpolar liquids In some, such as tetramethylsilane,[596] the electron mobility is very high, indicating that the electron remains untrapped, or quasi-free. However, in many other liquids such as *n*-alkanes,[597] some alkenes,[598] and xylenes,[599] the mobility is low and strongly affected by the pressure. In the *n*-alkanes and in 1-pentene,[600] the mobility gradually decreases as the pressure is raised to 300 MPa; but in *o*- and *m*-xylene as well as in cyclohexene, the mobility increases with pressure.

To explain these effects, a two-state model was assumed for the low-mobility liquids in which quasi-free and trapped electrons are in equilibrium. The observed mobility then depends on the position of that equilibrium, and the pressure dependence thus gives the sign and magnitude of the volume change associated with the trapping of electrons. For *n*-hexane, *n*-pentane, and 1-pentene, ΔV_0 at 25 °C equals −22, −28, and −27 cm^3 mol^{-1}, respectively, while in cyclohexene and *o*- and *m*-xylene, ΔV_0 equals 4, 21, and 22 cm^3 mol^{-1}, respectively. Holroyd assumes the partial molar volume of the quasi-free electron to be zero, and that the observed volume changes reflect the partial molar volume of the trapped electron. Two terms contribute to this partial volume: electrostriction by the trapped electron, and the size of the cavity holding it; both are large and of opposite sign, which explains the appar-

ently capricious differences between these liquids. The cavity radii are thought to range from 3.2 to 3.6 Å (and thus, their volumes from 83 to 108 $cm^3\ mol^{-1}$), and thence the electrostriction terms can be estimated as approximately $-100 \pm 25\ cm^3\ mol^{-1}$.

Electron capture by solutes also occurs with large volume changes. In general, both attachment and detachment rates can be measured. Solutes that have been studied include carbon dioxide,[468,469] pyrimidine,[601] butadienes,[470,602] benzene,[603] and toluene.[604,605] Attachment to these solutes is unfavorable in the gas phase (their electron affinities are negative), but in solution the polarization of molecules surrounding the ions stabilizes them, rendering the free energies for capture negative.

The equilibrium constants for these reactions increase with pressure, and reaction volumes range from -90 to $-200\ cm^3\ mol^{-1}$ for these solutes in liquids such as tetramethylsilane and hexane.[468−470,601−604] These large values must be ascribed to electrostriction; a contribution from the formation of a "glass shell" has also been suggested.[605] As expected, these electron attachment reactions also show large decreases in entropy (-25 to -40 eu). It is found that the relation

$$\Delta S/\Delta V = \alpha/\beta$$

applies to these reactions, where α is the coefficient of thermal expansion and β is the compressibility. Thus, the change in organization of the liquid by an ion in a nonpolar solvent is directly related to the density change.

A related case[471] is the capture of positronium by nitrobenzene (entries 158 and 159). In hexane, this species is thought to occupy a large "bubble" which collapses or is greatly reduced in size during the capture process; in benzene, which more nearly resembles nitrobenzene, there is no discernible pressure effect. Further investigations with other substrates and media are clearly desirable.

High-pressure NMR continues to provide new insights into physical and chemical phenomena. Experiments by Gillies et al.[472] furnish a very nice example: these authors measured the effect of pressure on ^{13}C relaxation times and were able to relate their findings to rotational and translational motions through their volume requirements (entries 160−201). The precision of the results was low, nearly 20 $cm^3\ mol^{-1}$ in one instance, and averaging perhaps 5 $cm^3\ mol^{-1}$ for most others; nevertheless, comparing the data derived for several dicyclohexylalkanes and their temperature dependence reveals some enticing insights. The molecular shapes clearly influence these motions; thus, the more crowded species require the largest spaces to exercise them. The needed expansions generally diminish as the temperature is raised and the neat liquids become more tenuous. Surprisingly, the volume changes required for methyl group rotations are negative: these groups rotate more easily at high pressures than under ambient conditions. The drastic temperature variations in these cases can at present also not really be understood. In tetra-*n*-octyltin, the volume requirements for carbon relaxation increase with distance from the central tin atom—a finding which makes intuitive sense.[473]

Similar results (entries 202−211) were obtained in part by a German group[474] by means of Raleigh scattering experiments; as might be expected, they find smaller (though still positive) activation volumes for the smaller molecules of diphenylmethane and diphenyl ether. These volume changes again diminish as the temperature is raised. An interesting and intuitively reasonable finding is that the more polar ether requires a larger space for overall motion than the isoelectronic hydrocarbon does. The still smaller molecules of acetonitrile, chloroform and benzene demand smaller volume expansions still, as Nakahara[475] found by studying the deuteron relaxation times under pressure. D_2O in solution in these solvents requires even less space, and that for neat D_2O is negative. As the authors noted, however, quantitative interpretation is difficult, in part because of the complications introduced by hydrogen bonding.[476]

The importance of the medium viscosity in molecular motion is underscored by data obtained by Brower and Hayden in polymeric films.[477] As might be expected, the positive activation volumes for the reorientation of rodlike molecules are extremely large, the more so the larger the solute. The nature of the polymer also has a substantial influence, with polystyrene exhibiting the largest pressure effect for all solutes.

Merbach's group[478,479] has been able to uncover the complete volume profile of the two-step inclusion of two azo dyes in α-cyclodextrin in water (entries 230−233). Both steps are accelerated, and both transition states are at volume minima. An intriguing sequence of events was proposed to account for the data, based on contributions from desolvation and resolvation of the sulfonate group, the original presence of two water molecules in the cavity, and hydrogen bonds between the host and parts of the dye. Jonas has studied several degenerate conformational processes (entries 234−242) which at low pressure have small, negative activation volumes.[480−482] As expected for internal rotations, the increase in crowding in the approach to the transition states leads to a reduced volume, although the Authors chose to interpret their data rather differently, in terms of Kramers theory. The same is true for the NMR coalescence of the two methyl groups in *N*,*N*-dimethyltrichloroacetamide;[483] the activation volume for this process is positive as was observed by Lüdemann for a host of amides.[1] A negative activation volume was found by Yamada and Sera[484] for the phenyl group rotation inside the cavity of a [12]paracyclophane, and they interpreted this classically as the result of more efficient space utilization in the transition state (entries 245−246).

Hara has in a series of impressive papers[485−493] drawn attention to the proposition that Kramers theory is more useful than transition-state theory to analyze pressure effects on fast reactions with activation energies of 5 kcal mol^{-1} or less, and even above that value, it can make a substantial contribution (entries 247−274). A fundamental reason for this is that Kramers theory is based on a treatment of

chemical reactions as viscous flow processes, in which medium viscosity is an important parameter. The fast process of excimer formation in 1,3-dipyrenylpropane is a good example, with the pressure coefficient of the rate constant clearly related to the solvent viscosity, and not at all to the solvent polarity. Thus, in the long-chain solvent 2,6,10,14-tetramethylpentadecane,[485] the viscosity part of the activation volume is as large as 28 $cm^3\ mol^{-1}$ while the intrinsic part is only $-2.5\ cm^3\ mol^{-1}$. Hara was able to use this probe as a device to gauge medium viscosity inside micelles.[488] However, his assumption[493] that transition-state theory cannot be applied to the ground-state isomerization of the oxadicarbocyanine shown in entries 271−274 seems unreasonable, if one considers the relatively large activation energy (14 kcal mol^{-1}) and the relatively nonviscous solvents used. The small positive activation volumes observed are reasonably explained as resulting from relief of the steric congestion existing in the initial state. The matter is discussed further at the end of this paper.

Asano has made an extensive study of the $Z \rightarrow E$ isomerization of 1,2-diphenyl substituted imines, azo compounds, and olefins (entries 275−371); the results have played a decisive role in the elucidation of the mechanisms involved.[494,498,499,502] Initially, a heterolytic cleavage of the carbon−nitrogen π bond followed by a rotation of the remaining single bond had been proposed for some *N*-alkylidineanilines on the basis of substituent effects.[606] However, it is now generally agreed that the reaction is brought about by the inversion of the nitrogen atom.[607] When the alkylidine group is an electron-withdrawing one such as hexafluoroisopropylidine, the reaction is accelerated by both electron-donating and -withdrawing substituents on the aniline moiety. The accelerations by the former groups were expected for the inversion mechanism because the electron attracting substituent should promote the conjugation of the lone pair on the nitrogen atom with the phenyl ring; however, the acceleration by the latter type of substituent was surprising, and invoked to suggest the intervention of the rotation mechanism. If the reaction proceeds via a highly polar rotational transition state, large negative activation volumes should be observed as in the push−pull substituted azobenzenes.[608] The activation volumes listed in entries 334−336 clearly rule out the rotation mechanism. The small solvent effects[494,499] also support this conclusion. The situation is the same in (phenylimino)pyrazolones.[494] On the basis of these experimental results, an inversion transition state was proposed in which the aniline moiety is in conjugation with the C−N π bond;[494,499] it was supported by ab initio calculations.[498]

Large positive activation volumes in the isomerization of a stilbazolium betaine in aqueous solution[502] demonstrates that this reaction proceeds by rotation through the quinoid structure. The activation volume increases with temperature and with the addition of methanol, as expected for a desolvation process.

The small positive activation volumes for the isomerization of azoalkanes leave some room for uncertainty. They do not appear to rule out a radical mechanism, but Neuman[501] has concluded that the reaction proceeds via nitrogen inversion. His conclusion is based on a comparison of these values with that of 1,2-bis(1-norbornyl)diazine[609] (+6.1 $cm^3\ mol^{-1}$ at 85 °C). The reaction volume was 11.5 $cm^3\ mol^{-1}$ at 25 °C, and the volume increase in the activation step could be attributed to the increase in the freedom of motion of the bicyclic groups. However, the temperatures (9−46 °C) were rather lower in Neuman's reactions and the stabilities of the alkyl radicals are much higher than that of the 1-norbornyl radical. In view of these differences, it is difficult to exclude the possibility of the isomerization through the diazenyl radical.

The photoreduction of benzophenone in alcohols has been studied by Okamoto,[503] who found negative activation volumes for the hydrogen abstraction by the triplet as might be expected for atom transfers. In 2-octanol, a maximum was seen in the ln k vs P plots, indicating that diffusion is beginning to be rate limiting; this did not happen with solutions in the lower alcohol homologues which are presumably less viscous. Also, in 5-methyl-3-heptanol, such a maximum was seen at 15 °C but not at 40 °C; this, too, hints at the onset of the influence of viscosity. Tamura[504] similarly studied the photoreduction of benzoquinone and observed generally small pressure effects, but in the presence of cetyltrimethylammonium bromide micelles, a considerable (apparent) acceleration was noticed. The authors also found that benzoquinone steeply raises the critical micelle concentration, and attributed the pressure effect to that. Chan's data on the photoreduction of fluorene by acridine[505,506] seem at variance with the other observations on such reactions, but as noted earlier, it is questionable whether rate data gathered in solid crystalline media can be confidently interpreted in terms of hydrostatic pressure effects (entries 398−402).

In collaboration with Moss, the Turro group has used laser flash photolysis technology to obtain the absolute rates of capture of various carbenes by olefins.[507] The carbenes were formed from the corresponding diazirines. The results in entries 403−410, with the activation volumes ranging from −10 to $-18\ cm^3\ mol^{-1}$, are consistent with early transition states involving the formation of two bonds, although intermediate complex formation is not ruled out.

The synthetic importance of the Diels−Alder reaction and its remarkable acceleration by pressure have led to much continued attention to this chemistry in several laboratories (entries 411−492). Thus, Jenner has reported[508] several new cases in which α,β-unsaturated esters and their analogues serve as the dienophiles; they show activation volumes even more negative than the reaction volumes. Secondary orbital interactions continue as one attractive interpretation of this phenomenon. Isaacs et al.[509] have found that the use of Lewis acids to catalyze the cycloaddition of isoprene to *N*-phenylmaleimide leads to more negative activation volumes; bonding between the acids and the dienophile is a reasonable explanation for this observation. The same explanation may also apply to the solvent effect reported by

these authors.

Zhulin reports two Diels−Alder reactions with activation volumes rather less negative than expected; he advances the unconventional view that this is "due to a change in the dynamic properties of the solvent, and not to the change of volume in the formation of the activated complex".[510,511] However, methylene chloride is not especially known for unusual solvent behavior at any pressure, and perhaps other cycloadditions should be studied in this medium before definite conclusions are reached.

The groups of Buback and Tietze have published their results with many Diels−Alder pairs.[512−518] The data are generally in the range now expected for the [4+2] cycloaddition of α,β-unsaturated ketones to vinyl ethers, but two points are worth noting. First, where both cis and trans stereoisomers are produced, the former uniformly have the more compact transition states. This is consistent with our knowledge of the smaller volume requirements of crowded molecules. The other fact that stands out is that in internal Diels−Alder reactions, with both diene and dienophile part of the same molecule, the activation volumes are reduced to substantially less negative values. This is reasonable if one considers that such substrates need not go through the process of creating an encounter complex.

The homofuran shown in entries 466 and 467 have remarkably small negative activation volumes which clearly indicate a different mechanism, and Klärner has proposed[519] that the reaction involves a prior opening of the bicyclic structure to give the moderately dipolar form shown:

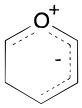

A very important paper by Klärner[526] in 1994 decisively broke new ground in the long-debated question whether concerted pericyclic reactions are more strongly accelerated by pressure than stepwise analogues. He was able to mimick the activation and reaction volumes for both types of process by means of a Monte Carlo computer simulation based on a hard-sphere model, and the excellent agreement between observed and calculated volume changes strongly reinforces the notion that they are indicative of the basic mechanisms (entries 486−488). This development is especially important because of the doubts about the existence of truly concerted reactions that have been expressed on many occasions by Firestone. His misgivings have led him to question the high-pressure argument, and to summarize his analysis[610] with the statement: "...the activation and reaction volumes are not useful criteria of the Diels−Alder mechanism." The diradical reactions depicted in entries 489−492 and their modest negative activation volumes are also clear demonstrations of the power of the argument.

The cheletropic reactions of 2,3-dimethylbuta-1,3-diene (entries 493−494) are clearly concerted.[528,529] The formation of the dibromophenylphosphine ion-pair adduct has the very large activation volume of −60 cm^3 mol^{-1}; in that instance, the charge formation leads to additional contraction.[529] Just the opposite feature may be the reason that the dipolar cycloadditions of benzyl azide (entries 495−502) are only moderately accelerated by pressure[530,531] although these reactions are concerted by all other criteria; it seems likely that the disappearance of formal charges during reaction is responsible. From that point of view, the reaction volumes would be informative in these cases.

The photocycloaddition of singlet oxygen to furan and to 1,3-diphenylisobenzofuran (entries 503−508) is accelerated by pressure,[532] which is unsurprising in view of the two newly forming bonds. The solvent effect was interpreted as indicative of a contribution by the solvent viscosity. In the photo reaction of singlet oxygen with tetramethylethylene (entries 509−514), both the large pressure-induced acceleration of the rate and the solvent effect clearly hint at a highly polar intermediate; a Foote perepoxide with $\mu = 3.4$ D was proposed:[533]

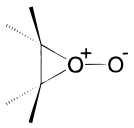

Turro's group has been able to measure[467] the [2+2] photocycloaddition by singlet adamantanone to fumaronitrile. The reaction is only barely affected by pressure, and complicated by the pressure-enhanced intersystem crossing; however, this had the benefit of allowing the measurement of an activation volume for the sensitized olefin isomerization. With some of the steps dependent on the viscosity, and others correlating only with the dielectric constant of the medium, the interpretation is too complex for analysis here, and the original paper should be consulted (entry 515).

The cycloaddition of methyl propynoate to cyclopentene with aluminum chloride catalysis (entry 516)[534] reveals a volume decrease in the transition state, which seems rather moderate for the proposed zwitterionic intermediate. A diradical species could be considered. From the point of view of that possibility, it would be interesting to study the stereochemistry of some open-chain olefins.

The several ene reactions studied at high pressure (entries 518−524) are clearly of a concerted nature[536,537] except in the case of the azo compounds; in that case, the much reduced contraction in the transition state suggests that a diradical mechanism is operating. Sigmatropic shifts (entries 525−535) are subject to moderate pressure acceleration resulting from the assumption of a cyclic conformation; the bond-making and -breaking parts should largely cancel.[520] A very nice confirmation comes from a study of the 1,2-divinylcyclobutanes.[535] The cis isomer gives 1,5-cyclooctadiene at 70 °C with an activation volume of −14 cm^3 mol^{-1}; by contrast, the trans isomer requires 160 °C before it finally reacts to give a mixture of the cyclooctadiene, 4-vinylcyclohexene and butadiene, the activation volume being about +5 cm^3 mol^{-1} for all three processes. Sugiyama and

Takeshita[538] found that 1,9- and 1,5-sigmatropic shifts are accelerated by pressure in comparable ways; they also demonstrated that increased hindrance (as in entry 535) increases the contraction. The hydrogen group transfer process[539] shown in entry 536 clearly requires the close approach of the Decalin and anthracene molecules: $\Delta V^{\ddagger} = -55$ cm^3 mol^{-1}, in an interesting contrast with the results shown in entries 537−543.[540]

Nishimura et al.[541−543] have studied the conversion of several zwitterions and the spiroforms depicted in entries 544−560. Both the activation and reaction volumes are positive, as might be expected when neutralization of charge is part of the process. Interestingly, the effect of neutralization is larger than the contraction due to the new bond, but the difference becomes smaller in more polar solvents, as is expected on the basis of the Drude−Nernst formalism: the more polar (and hence self-constricted) solvents are least subject to electrostriction by ionic charges. The decomposition of nitroso dimers (entries 562 and 563) is retarded by pressure, as should be expected from bond cleavage reactions; the disappearance of the formal charges may also have played a role.[545,546]

Neuman[501] has contributed further insights into the decomposition of azo compounds (entries 564−569): it is now clear that while one bond breaks initially, diffusion to separate radicals is a critical part of the reaction. This causes the positive activation volumes to be larger than in the case of most single bond scission processes; they contrast with peroxide decomposition[549] (entries 570−576; no return, early transition states).

Naud and Brower[550] have conducted a courageous investigation of the decomposition of various explosives under pressure (entries 577−595). The activation volumes are positive in most cases, and the authors postulate N−N bond cleavage as the rate-controlling step; however, RDX and 6-nitro-1,2-dinitroso-1,2,3,4-tetrahydroquinoxaline have negative activation volumes. Both of these compounds can aromatize by means of E1 elimination (of HNO_2 and HNO, respectively), and it may be presumed that they do so. The same mechanism applies to cyclohexyl nitrate. Elimination also drives the thermal decomposition of 2-nitropropane and 2-methyl-2-nitropropane.[555] The decay of α radicals derived from crystalline dicarboxylic acids is inhibited[556] very strongly by pressure, but again, the pressure in such circumstances is at best approximately hydrostatic (entries 596−601).

Solvolysis experiments by Itsuki[558,559] and others show mostly normal values understandable in terms of Drude−Nernst theory, as explained in our earlier reviews (entries 603−675). Thus, in ethanol, substantially more negative activation volumes are found than in water, as expected from the less polar nature of the alcohol; the *tert*-butyl chloride is more strongly accelerated than the bromide because of the smaller size of the chloride anion. The chloride depicted in entry 614 has an activation volume much more negative than that in entry 613; this was attributed[561] to extended participation (bond formation) and the preformation of the necessary bicyclic (more crowded) conformation. Kyong's experiments[562] in generating the 1-adamantyl cation show clearly that at higher temperatures, $\Delta V^{\ddagger}$ becomes more negative due to the more expanded state of the solvent. The effect of solvent composition is more difficult to account for, as aqueous organic solvents may adopt different structures depending on the water content. The radical ion pair separation processes shown in entries 676−690 were studied by Turro.[565] Pressure was found to inhibit them. This is of course opposite to what is normally expected and found for this type of process. The authors favored the increase in solvent viscosity as the explanation. If the charges are more localized in the ion pair than in the separate ions, that could also account for the pressure effect.

The Menschutkin reaction, long known for its pressure sensitivity, continues to draw the attention of the high-pressure kineticists (entries 691−754). Yoh's group has reported the reactions of variously substituted pyridines in acetonitrile, over a range of temperatures. These authors found that ρ steadily decreases as the pressure is raised, and attributed this fact to the increase in density of the solvent, and hence, to decreased electrostriction (the opposite is true for the phenacyl sulfonates).[566−569] A comparison with the known pressure effects on the corresponding benzyl sulfonates led the authors to conclude that the former have "more S_N2 character" in the transition state.

Entries 739−741 show that the same increase in $-\Delta V^{\ddagger}$ which results from steric hindrance also obtains from the buttressing of that effect.[572] Entries 742−747 describe the pressure effects for the reaction of various pyridines with phenacyl halides;[573] the most noticeable effects are those of the use of chloride as the leaving group versus that of bromide, and the effect of a hindering *o*-methyl group. Brower's finding of a very modest pressure acceleration when the substrate already carries a positive charge which becomes delocalized in the transition state is also of interest.[575]

Jenner[576] has made a thorough study of the Michael reaction at high pressures (entries 755−763). This reaction resembles the Menschutkin chemistry in that the formation of a new bond and a pair of charges are both expected to contribute to contraction, and the results fully bear this out: values of $-\Delta V^{\ddagger}$ as large as 50 cm^3 mol^{-1} or more are commonly encountered. The conversion of esters into amides[577] and the imidazole-catalyzed hydrolysis of phenyl acetate esters[578] are standard cases of the contraction always seen in the formation of a tetrahedral intermediate (entries 764−778). The former reaction has acquired synthetic usefulness as it is often sluggish under ambient conditions; the latter was found to have a pressure response strongly dependent on the presence and concentration of sodium bis(2-ethylhexyl)sulfosuccinate micelles. Aggregation of these micelles was postulated to account for this observation.

The reaction of aldehydes with allyltri-*n*-butylstannanes (entries 781−785) has large negative activation volumes consistent with concerted cyclic tran-

sition states as proposed by Isaacs[239] and Yamamoto.[580] The metathesis reaction of iodine and tetramethylstannane (entries 786−797) is strongly enhanced by pressure, and both the solvent and temperature effects suggest that charge development characterizes the transition state.[581−583] The isomerization shown in entries 798−805 is consistent with the cleavage of two hydrogen bonds, although an accounting of that sort is hazardous in view of the extensive double-bond relocation that must accompany the reaction.[584]

The reaction of palladium acetate with imines to give the complex structures shown in entries 806−835 all have negative activation volumes as might be expected from the multiple-bond formations taking place. The reactions of imines derived from anilines are accelerated substantially more by pressure than those of *N*-propyl- and *N*-benzylimines, which is surely related to the more severe crowding in the transition states.[585] Entries 836−842 show reactions of carbohydrate and their derivatives; most were catalyzed by solids, and although the results show intriguing variations, they can presently not be confidently interpreted.

The acid-catalyzed, base-catalyzed, and uncatalyzed proton exchange processes of the NH proton in *N*-methylacetamide (entries 843−845) furnish an interesting example of the effects of charge and charge delocalization on the volume profile.[591] Simple proton exchange between oxygen and nitrogen (acid catalysis) is essentially unaffected by pressure; base catalysis is retarded because the charge, concentrated in hydroxide, becomes delocalized in the amide anion, and in the "uncatalyzed" reaction (catalyzed by water), charge and bond formation accelerate the process. These results are important in that departures from these values observed in peptides and proteins may furnish information about the physical state of these macromolecules in aqueous solution.

The adenosine phosphate hydrolyses[431] (entries 846−847, already commented on in the section on biological reactions) are further examples of evidence that metaphosphate is not an intermediate in these reactions.[1] The activation volume of the triazine decomposition in chloroform[592] as depicted in entry 848 is surely the result of a proton transfer to N-1 to give an ion pair, followed by—or perhaps concerted with—methyl transfer to oxygen. The importance of the charges becomes clear from the much-reduced value of $\Delta V^{\ddagger}$ in acetonitrile (entry 849); the further decomposition of the resulting intermediate to give nitrogen follows in rapid subsequent steps.

The reactions of entries 850 and 851 resemble the Kornblum oxidation of primary halides to aldehydes by dimethyl sulfoxide.[593] In that process, sulfur alkylation occurs in the first step, and that is likely to be the case here, as may be deduced from the substantial negative activation volume and its dependence on the solvent. The very large positive value seen in the fragmentation taking place in entry 852 is surely a reflection of the multiple-bond cleavages,[594] although the precise sequence of events in this reaction cannot be deduced from this experiment alone. The ionization of the resorcinol monoanion to the dianion (entry 853) is expected to be strongly promoted by pressure in view of the concomitant concentration of charge, and this is indeed observed.[595]

C. Comments on Table 3

The difference in activation volume between multiple products in the same reaction is simply the difference in partial molar volume of the two transition states. This difference will often simply reflect or resemble the difference in partial molar volume of the products themselves. Thus, the smaller volume will often be that which leads to the more crowded products. For example, in the third entry, the partial molar volume of the less crowded trans adduct is probably larger by several $cm^3\ mol^{-1}$ than the cis epimer, and this volume difference is foreshadowed by $V_2^{\ddagger} - V_1^{\ddagger}$ which has a value of $+5.5\ cm^3\ mol^{-1}$ (it will be understood that differences in initial state must be taken into account when the reactions are not competing but simultaneous, as in entries 13 and 14).

Occasionally, significant information can be derived from such results. In the case of the 1,4-dicyanonaphthalene-sensitized photo-Diels−Alder reaction of 1,3-cyclohexadiene (entry 7), the identity of the smaller of the endo and exo transition states depends on the solvent: a clear indication that the mechanisms in the two solvents are different. The authors[612] postulate the occurrence of different types of ion pairs in the two solvents. In the case of the two products from 1,3,8-nonatriene (entry 10), the Diels−Alder transition state is smaller than the activated complex of the 1,5-sigmatropic shift; this is surely related at least in part to the larger parachor of the two extra double bonds in the triene product.

D. Comments on Table 4

It has become a fairly routine practice among high-pressure kineticists to measure not only volumes of activation but the reaction volumes as well, so that the complete volume profile of the reaction can be drawn; in fact, the individual partial molar volumes of the components are known in many cases. In Table 4, the pressure range and number of measurements are not always recorded as several methods are in use to determine the reaction volume, and not all of them employ pressure. A number of reaction volumes measured as a secondary goal were reported in Table 2; they require no further comment here. This section is devoted to instances in which the reaction volume was the primary objective, or where new methods were used to determine it.

Conway has used the buoyancy−balance method to determine the partial volumes of several organic bases and their conjugate acids in water;[620] the resulting ionization volumes are shown in entries 1−16. The electrostriction effect and its increase upon a second protonation are evident. Somsen[621] has reported the partial volumes of nine polybasic acids in water; some of the results differ substantially from data shown in earlier literature.

Table 3. Activation Volume Differences of Organic Reactions

No.	reaction	solvent	T/ °C	P/MPa	no of ratio data	$\delta\Delta V_0^{\neq}$ /cm^{3}mol^{-1}	ref	remarks
1.	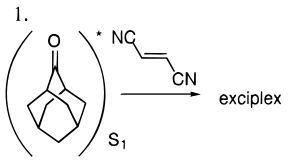					0		
	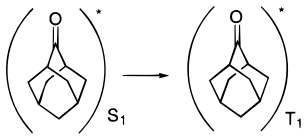	MeCN	25	203	5	-3.7	467	
2.	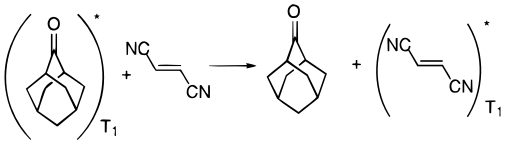					0		
	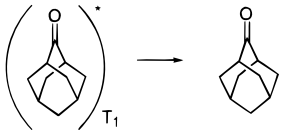	MeCN	25	203	5	+7.4	467	
3.	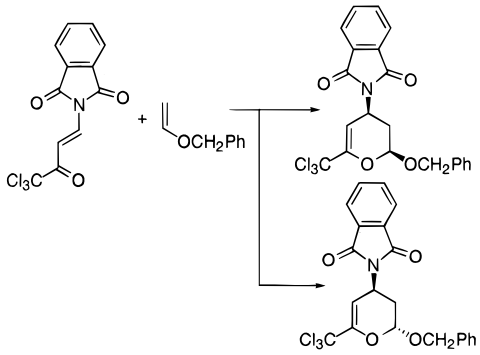	CH_2Cl_2	55	550	12	+5.5	516	
4.	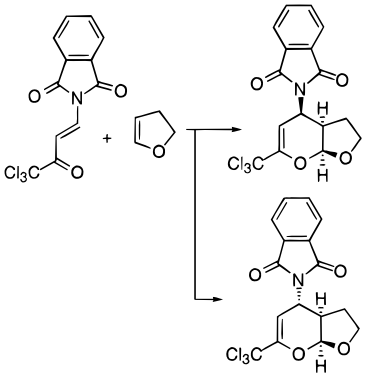	CH_2Cl_2	90	250	7	+7.3	514	$P \geq 25$
5.	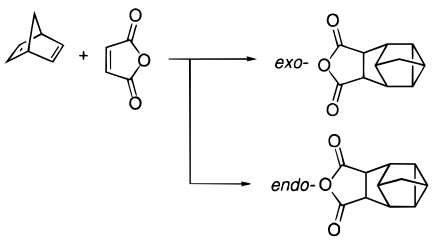	AcOEt	100	1000	4	-3.1[a]	518	$\delta\Delta V^{\neq}$(25 °C) = -3.4

Table 3. (Continued)

No.	reaction	solvent	T/ °C	P/MPa	no of ratio data	$\delta\Delta V_0^{\neq}$ /cm^{3}mol^{-1}	ref	remarks
6.	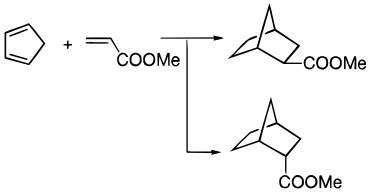					0		
		CO_2	35	30	5	-3.7	611	At 10 MPa.
		CO_2	45	30	3	-5.9	611	At 10 MPa.
7.	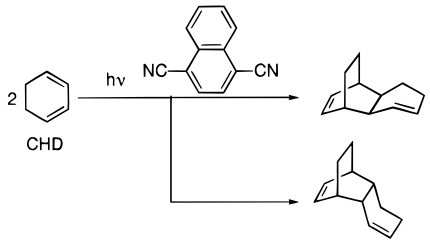					0		
		MeCN	25	203	5	+2.0	612	[CHD] = 0.1 mol dm^{-3}
		MeCN	25	203	5	+2.4	612	[CHD] = 0.16 mol dm^{-3}
		MeCN	25	203	5	+1.6	612	[CHD] = 0.4 mol dm^{-3}
		MeCN	25	203	5	+1.2	612	[CHD] = 1.06 mol dm^{-3}
		PhH	25	203	5	-11.1	612	[CHD] = 0.08 mol dm^{-3}
		PhH	25	203	5	-8.7	612	[CHD] = 0.16 mol dm^{-3}
		PhH	25	203	5	-10.7	612	[CHD] = 0.4 mol dm^{-3}
		PhH	25	203	5	-11.6	612	[CHD] = 1.0 mol dm^{-3}
8.	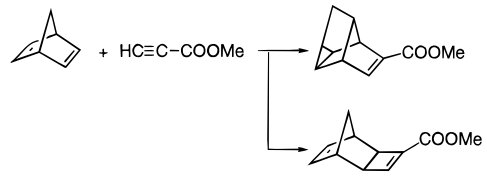					0		
		PhH	ambient	300	2	+12.5	525	b
		CH_2Cl_2	ambient	300	2	+12.5	525	c
9.	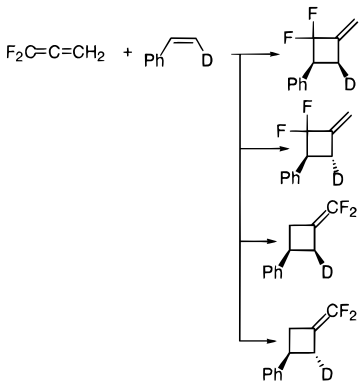					0		
		none	ambient	1300	6	+2.4[a]	613	$P \geq 180$
		none	ambient	1300	6	-2.0[a]	613	$P \geq 180$
		none	ambient	1300	6	+0.2[a]	613	$P \geq 180$
10.	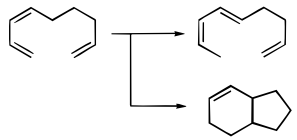					0		
		n-hexane	150	770	2	-8.1[a]	520, 614	
11.	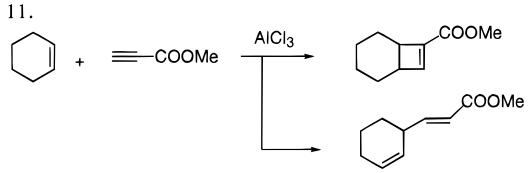					0		
		PhMe	25	900	3	≈0	534	

Table 3. Activation Volume Differences of Organic Reactions

No.	reaction	solvent	T/ °C	P/MPa	no of ratio data	$\delta\Delta V_0^{\neq}$ /cm^{3}mol^{-1}	ref	remarks
12.	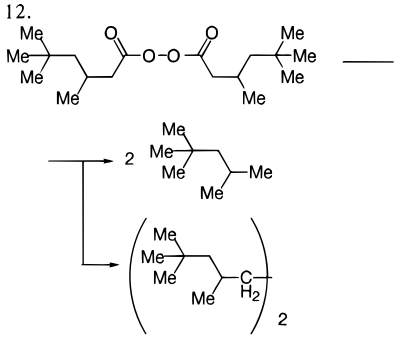					0		
		n-heptane	80	200	5	−2.7[a]	549	
		n-pentadecane	80	200	6	−2.6[a]	549	
13.	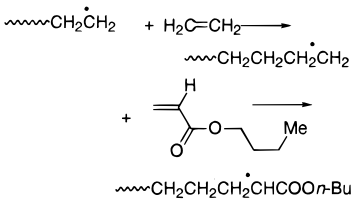					0		
		none	200	250	3	+5.1	615	$P \geq 150$
14.	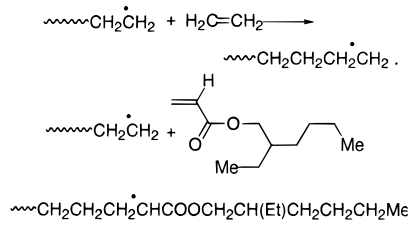					0		
		none	200	250	3	+8.2	616	$P \geq 150$
15.	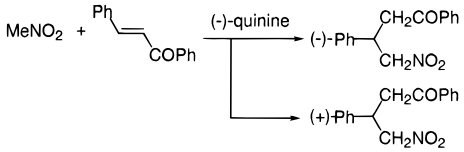					0		
		PhMe	ambient	1500	4	-0.6	617	$P \geq 400$, d
16.	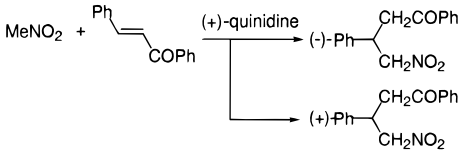					0		
		PhMe	ambient	900	4	+0.3	617	$P \geq 400$
17.	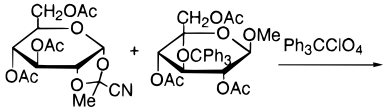					0		
	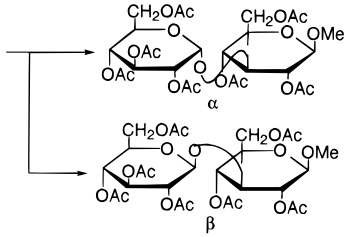	CH_2Cl_2	20	1300	8	-4.2	618	
		CH_2ClCH_2Cl	20	300	3	-10	618	
		CH_2Cl_2 -CH_2ClCH_2Cl	20	600	3	-4.7	618	CH_2Cl_2 30%

Table 3. (Continued)

No.	reaction	solvent	*T*/ °C	*P*/MPa	no of ratio data	$\delta\Delta V_0^{\neq}$ /cm^{3}mol^{-1}	ref	remarks
18.	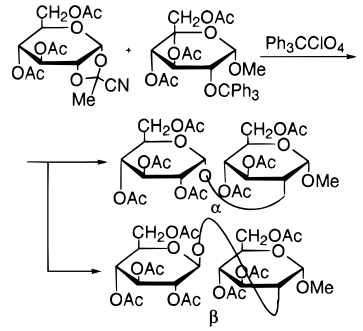					0		
		CH_2Cl_2	20	1400	8	-8.5	619	

[a] Calculated by one of the authors (T.A.). [b] In the presence of $AlCl_3$. For other reactions, see the original. [c] In the presence of $ZrCl_4$. For other reactions, see the original. [d] Both the enantiomer excess and the chemical yield increase with increasing pressure.

The application of photothermal and photoacoustic methods[48,51] has made possible the study of volume profiles difficult to obtain with other techniques. For instance, the $E \rightarrow Z$ photoisomerizations of 3,3′-diethyloxadicarbocyanine iodide (entry 26) and the monocarbo analogue (entry 27) have reaction volumes of −29 and ∼0 cm^3 mol^{-1}, respectively; if it is assumed that these changes are due to solvation changes, the structures of the products shown can be deduced from the dipole moments calculated for them[53] (see also entries 271−274 of Table 2).

Entries 28−33 resulted from measurements of reaction volumes by means of photoacoustic calorimetry. Two of these values (entries 28 and 32) seem improbably high; the authors ascribed them to the fact that the starting materials have substantially larger dipole moments than the products, and hence would interact more strongly with the solvents.[622] Subsequent measurements for diphenylcyclopropenone have averaged at about +24 cm^3 mol^{-1}; the reasons for the discrepancy have been discussed by Schmidt.[624] An Italian group[626] has measured the reaction volume of the photorearrangement of *o*-nitrobenzaldehyde to nitrosobenzoate in water as a function of pH; the sign change was attributed to the neutralization of the proton released in the process. Zimmt[627] found the reaction volume for the generation of excited singlet tetraphenylethylene to be large and negative, and attributed that result to the strongly dipolar character of this state, with a dipole moment of about 6 D. The relaxation of the zwitterion resulting from the photoexcitation shown in entry 38 in alkanes is characterized by an expansion of 14 cm^3 mol^{-1}.[628] Similar effects were seen by Braslavsky and co-workers[56,58] (entries 37 and 39−41).

The conformational equilibrium for 1,1,2-trichloroethane has been studied by Yamada and Sera,[629] who found the more crowded gauche conformer to be favored by high pressure. Tamura[630] has been able to deduce the ionization volumes of a number of highly deactivated anilines, in a study of the Hammett acidity function at high pressure. The trend in the data shows that the effect of the deactivating groups is to diminish charge delocalization. The 1,7-prototropic shift depicted in entries 50−62 was attributed by Nishimura et al.[631] to the greater ability of the naphthoquinone form to engage the solvent in H bonding, a finding which is in accord also with the more negative values found in the water content of the solvent was raised. The intramolecular hydrogen bonds shown[632] to form as in entries 63−69 are about the same as those characterizing external H bonds such as those observed by Schulman[633] (entry 70) for neat methanol at eight temperatures from 5 to 119 °C: 3 cm^3 mol^{-1} of H bonds. The equilibrium between the lactone and zwitterionic froms of rhodamine B in primary alcohol solvents shifts toward the latter under high pressure,[634] the more so the less polar the alcohol; these effects are commonly expected and observed. The negative reaction volumes are rather small, presumably because of the delocalized nature of the charges (which is responsible for the ring opening in the first place). The difference in ΔV between the apparently similar reactions shown in entries 75 and 76 is due to the fact that the latter is intramolecular—the association of two molecules accounts for the major part of the contraction as noted by the authors.[635]

The dimerization of nitrosobenzenes causes much larger contractions, since the dimers have local charges associated with the oxygen and nitrogen atoms.[636] The small volume diminutions usually noted for charge-transfer complexation were shown by Kim[637] to be somewhat temperature-dependent: the complexes may possibly be somewhat looser at the higher temperatures. The association process of pyridinium iodides amounts to a net neutralization, so that the reaction volumes are positive in that case.[638] The negative reaction volumes for the process shown in entries 102−111 seem very large for simple H bond—and/or charge-transfer complex formation; they appear to be more characteristic of ion-pair formation, as the authors[639] suggested for the reactions of the quinone with proton sponge (entries 112−115). In fact, amine interactions with hydrogalvinoxyl have reaction volumes so large that free

Table 4. Reaction Volumes of Organic Reactions

No.	reaction	solvent	T/ °C	P/MPa	no of K data	ΔV /cm^{3}mol^{-1}	ref	remarks
1.	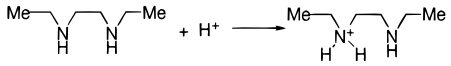	H_2O	25	-	-	-7.1	620	
2.	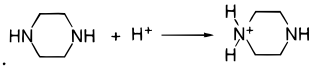	H_2O	25	-	-	-5.6	620	
3.	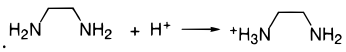	H_2O	25	-	-	-6.6	620	
4.	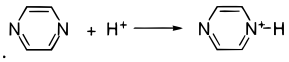	H_2O	25	-	-	-6.3	620	
5.	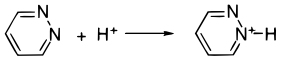	H_2O	25	-	-	-4.4	620	
6.	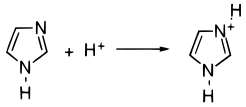	H_2O	25	-	-	-1.7	620	
7.	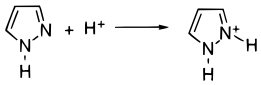	H_2O	25	-	-	-2.3	620	
8.	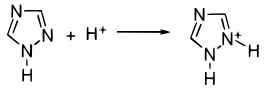	H_2O	25	-	-	-3.9	620	
9.	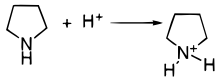	H_2O	25	-	-	-4.3	620	
10.	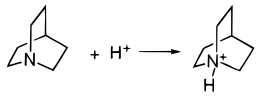	H_2O	25	-	-	-3.5	620	
11.	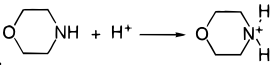	H_2O	25	-	-	-7.3	620	
12.	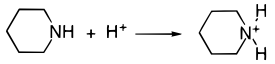	H_2O	25	-	-	-2.2	620	
13.	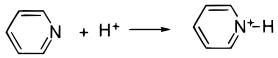	H_2O	25	-	-	-4.5	620	
14.	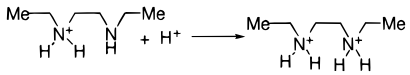	H_2O	25	-	-	-15.9	620	
15.	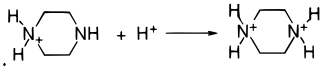	H_2O	25	-	-	-13.4	620	
16.	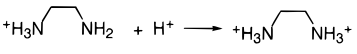	H_2O	25		-	-11.8	620	
17.	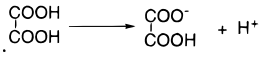	H_2O	25	-	-	-7.5	621	
18.	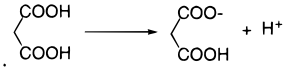	H_2O	25	-	-	-6.6	621	

Table 4. (Continued)

No.	reaction	solvent	T/ °C	P/MPa	no of K data	ΔV /cm^{3}mol^{-1}	ref	remarks
19.	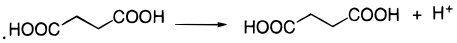	H_2O	25	-	-	-8.0	621	
20.	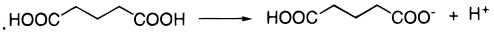	H_2O	25	-	-	-23.0	621	
21.	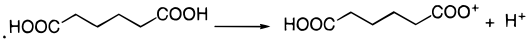	H_2O	25	-	-	-7.3	621	
22.	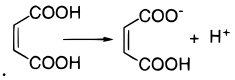	H_2O	25	-	-	-5.5	621	
23.	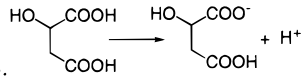	H_2O	25	-	-	-6.0	621	
24.	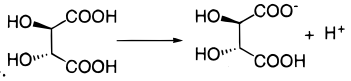	H_2O	25	-	-	-12.0	621	
25.	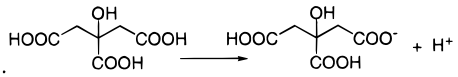	H_2O	25	-	-	-14.8	621	
26.	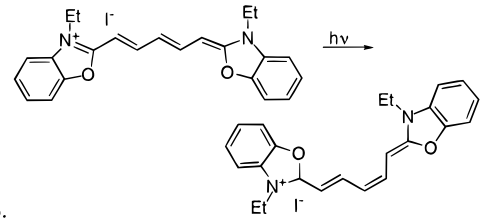	H_2O	6-25	-	-	-29	53	
27.	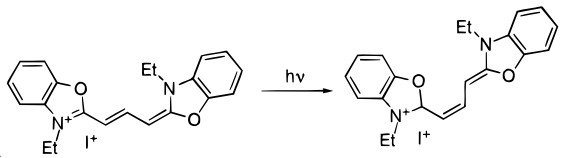	H_2O	6-25	-	-	≈0	53	
28.	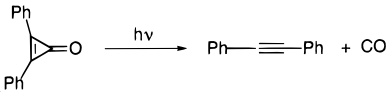	MeCN	ambient	-	-	+60.1	622	
29.		alkanes	ambient	-	-	+23	623	
30.		alkanes	ambient	-	-	+22.3	624	
31.		*n*-heptane	ambient	-	-	+23.6	625	
32.	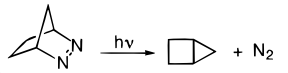	MeCN	ambient	-	-	+48.5	622	
33.	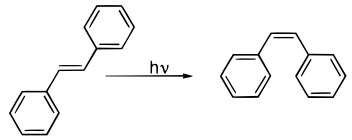	MeCN	ambient-	-	+5.6		622	
34.	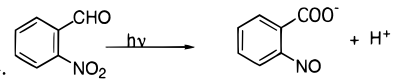	H_2O	3.9	-	-	-52	626	pH < 9.5.
35.	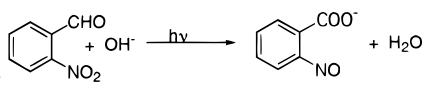	H_2O	3.9	-	-	+24.5	626	pH < 9.5.
36.	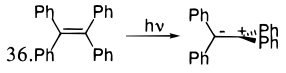	alkanes	23	-	-	-29	627	

Table 4. (Continued)

No.	reaction	solvent	T/ °C	P/MPa	no of K data	ΔV /cm^{3}mol^{-1}	ref	remarks
37.	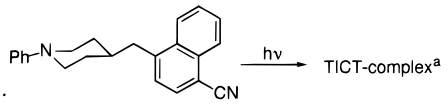	alkanes	20	-	-	-40	56	
38.	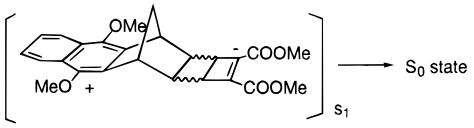	alkanes	20	-	-	+14	628	
39.	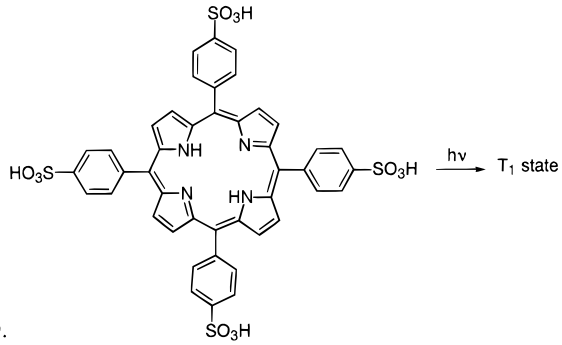	D_2O	22	-	-	-10	58	pH 7.8.
40.	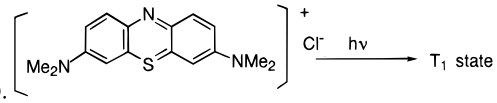	D_2O	22	-	-	-1.5	58	pH 7.8.
41.	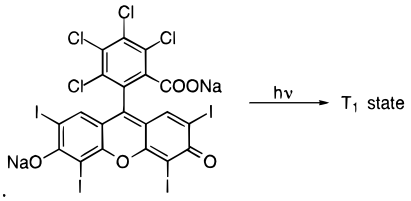	D_2O	22	-	-	+1	58	pH 7.8.
42.	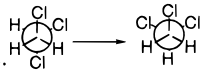	neat	45	320	12	-3.9	629	With 10 mol% cyclopentane.
43.	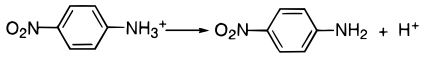	aq H_2SO_4	25	150	6	+5.5	630	
44.	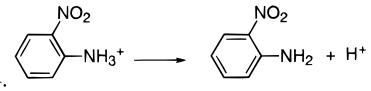	aq H_2SO_4	25	150	6	+7.8	630	
45.	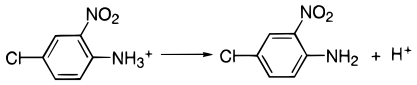	aq H_2SO_4	25	150	6	+11.3	630	
46.	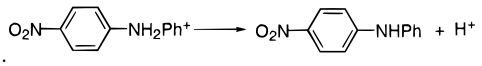	aq H_2SO_4	25	150	6	+15.8	630	
47.	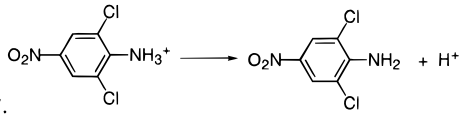	aq H_2SO_4	25	150	6	+14.2	630	
48.	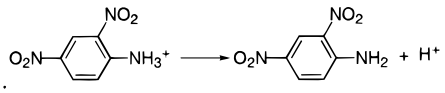	aq H_2SO_4	25	150	6	+13.7	630	

Table 4. (Continued)

No.	reaction	solvent	*T*/ °C	*P*/MPa	no of *K* data	ΔV /cm^{3}mol^{-1}	ref	remarks
49.	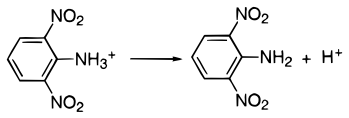	aq H_2SO_4	25	150	6	+21.0	630	
50.	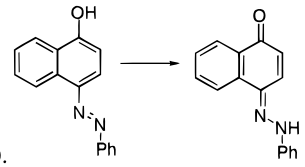	EtOH	25	98	4	-2.3	631	
51.		aq EtOH	25	118	4	-3.0	631	EtOH 80 v%.
52.		aq EtOH	25	118	4	-3.4	631	EtOH 70 v%.
53.		aq EtOH	25	118	4	-4.8	631	EtOH 60 v%
54.		aq EtOH	25	118	4	-5.2	631	EtOH 50 v%
55.		aq EtOH	25	118	4	-6.4	631	EtOH 40 v%.
56.		aq acetone	25	98	4	-2.3	631	acetone 95 v%
57.		aq acetone	25	98	4	-3.4	631	acetone 90 v%
58.		aq acetone	25	98	4	-4.0	631	acetone 80 v%
59.		aq acetone	25	98	4	-4.8	631	acetone 70 v%
60.		aq acetone	25	98	4	-5.0	631	acetone 60 v%
61.		aq acetone	25	98	4	-5.8	631	acetone 50 v%
62.		aq acetone	25	98	4	-6.8	631	acetone 40 v%
63.	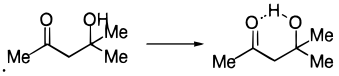	CCl_4	25	107	-	-4.0	632	
64.		CS_2	25	128	-	-3.9	632	
65.	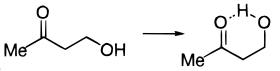	CCl_4	25	107	-	-1.7	632	
66.		CS_2	25	128	-	-3.0	632	
67.	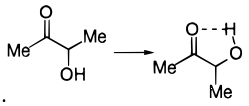	CCl_4	25	107	-	-2.2	632	
68.	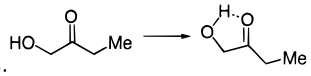	CCl_4	25	107	-	-3.1	632	
69.	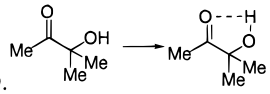	CCl_4	25	107	-	-3.7	632	
70.	4 MeOH ⟶ tetramer	neat	5-119	103	6	-11	633	
71.	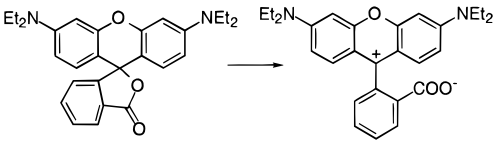	MeOH	25	88	4	-4.2	634	
72.		EtOH	25	88	4	-4.7	634	
73.		*n*-PrOH	25	88	4	-6.1	634	
74.		*n*-PentOH	25	88	4	-12.2	634	
75.	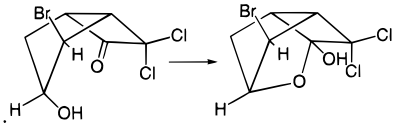	DMSO/$CDCl_3$	29	200	3	-3.2	635	DMSO 20 wt%
76.	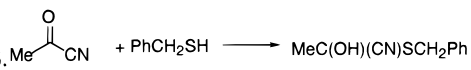	CDCl3	30	114	6	-13.0	635	
77.	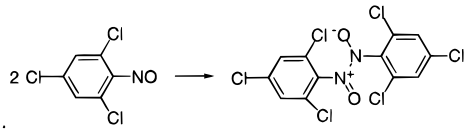	CCl_4	25	123	6	-20.7	636	

Table 4. (Continued)

No.	reaction	solvent	T/ °C	P/MPa	no of K data	ΔV /cm^{3}mol^{-1}	ref	remarks
78.	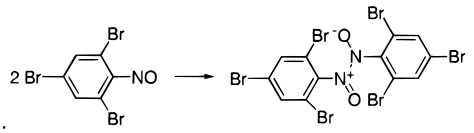	CCl_4	25	123	6	-18.9	636	
79.	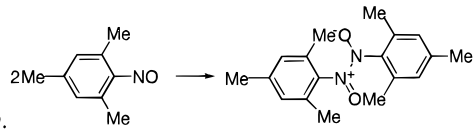	CCl_4	25	123	6	-22.7	636	
80.	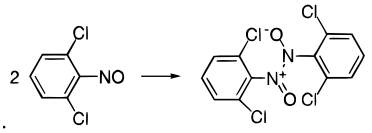	CCl_4	25	123	6	-16.9	636	
81.	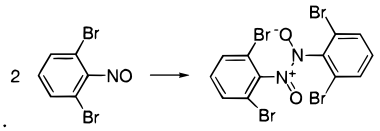	CCl_4	25	123	6	-17.2	636	
82.	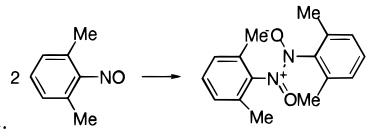	CCl_4	25	123	6	-20.0	636	
83.	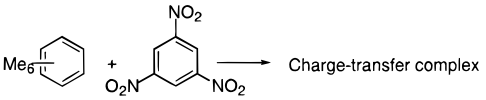	CCl_4	25	140	5	-6.5	637	
84.		CCl_4	40	140	5	-5.7	637	
85.		CCl_4	50	140	5	-4.4	637	
86.	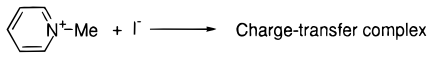	aq EtOH	25	200	5	-0.9[b]	638	EtOH 95 v%. ln k - P plot concave up.
87.		aq EtOH	30	200	5	-0.8[b]	638	EtOH 95 v%. ln k - P plot concave up.
88.		aq EtOH	35	200	5	-1.1[b]	638	EtOH 95 v%. ln k - P plot concave up.
89.		aq EtOH	40	200	5	-1.4[b]	638	EtOH 95 v%. ln k - P plot concave up.
90.	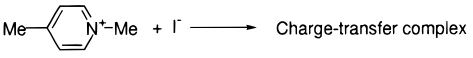	aq EtOH	25	200	5	-2.8[b]	638	EtOH 95 v%. ln k - P plot concave up.
91.		aq EtOH	30	200	5	-3.1[b]	638	EtOH 95 v%. ln k - P plot concave up.
92.		aq EtOH	35	200	5	-2.3[b]	638	EtOH 95 v%. ln k - P plot concave up.
93.		aq EtOH	40	200	5	-2.5[b]	638	EtOH 95 v%. ln k - P plot concave up.
94.	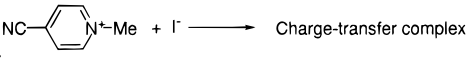	aq EtOH	25	200	5	-4.8[b]	638	EtOH 95 v%.
95.		aq EtOH	30	200	5	-5.8[b]	638	EtOH 95 v%.
96.		aq EtOH	35	200	5	-4.5[b]	638	EtOH 95 v%.
97.		aq EtOH	40	200	5	-6.7[b]	638	EtOH 95 v%.

Table 4. (Continued)

No.	reaction	solvent	T/ °C	P/MPa	no of K data	ΔV /cm^{3}mol^{-1}	ref	remarks
98.	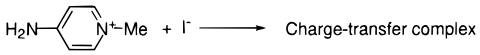	aq EtOH	25	200	5	-6.0[b]	638	EtOH 95 v%.
99.		aq EtOH	30	200	5	-5.5[b]	638	EtOH 95 v%.
100.		aq EtOH	35	200	5	-6.4[b]	638	EtOH 95 v%.
101.		aq EtOH	40	200	5	-5.5[b]	638	EtOH 95 v%.
102.	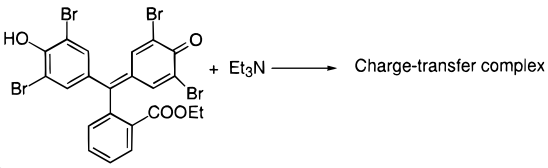	$CHCl_3$	25	-	-	-23.2	639	
103.		PhMe	25	-	-	-24.9	639	
104.		1,4-dioxane	25	-	-	-22.3	639	
105.	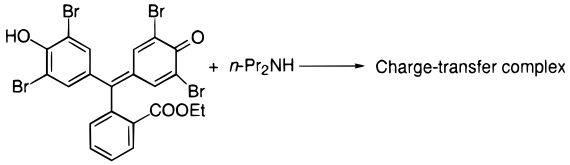	PhCl	25	-	-	-31.1	639	
106.		CH_2ClCH_2Cl	25	-	-	-35.3	639	
107.		1,4-dioxane	25	-	-	-23.1	639	
108.	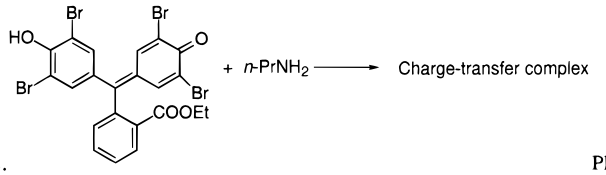	PhH	25	-	-	-31.5	639	
109.		PhCl	25	-	-	-31.5	639	
110.		CH_2ClCH_2Cl	25	-	-	-34.8	639	
111.		1,4-dioxane	25	-	-	-31.9	639	
112.	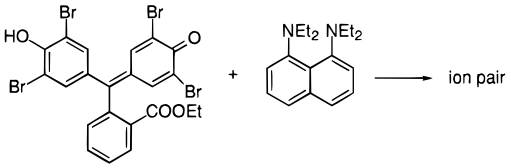	PhH	25	-	-	-35.4	639	
113.		PhMe	25	-	-	-35.8	639	
114.		$CHCl_3$	25	-	-	-38.5	639	
115.		*n*-BuCl	25	-	-	-30.7	639	
116.	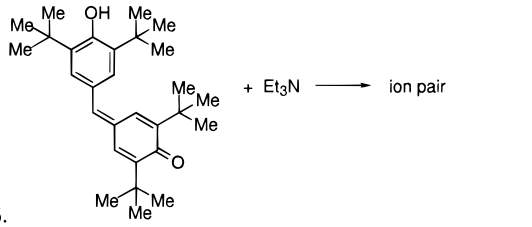	MeCN	25	82	4	-40.7	640	
117.	+ $Et_2NCH_2CH_2OH$ → ion pair	MeCN	25	73	5	-40.8	640	
118.	+ $Me_2NCH_2CH_2OH$ → ion pair	MeCN	25	73	5	-34.2	640	
119.	+ *n*-Pr_2NH → ion pair	MeCN	25	73	5	-38.2	640	
120.	+ *t*-$BuNH_2$ → ion pair	MeCN	25	73	5	-35.4	640	
121.	+ *n*-$PrNH_2$ → ion pair	MeCN	25	73	5	-44.4	640	
122.	+ *n*-$BuNH_2$ → ion pair	MeCN	25	73	5	-42.9	640	
123.	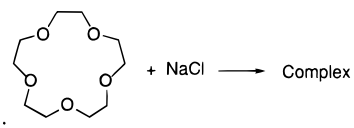	MeOH	25?	-	-	+14	641	
124.	+ NaI → Complex	MeOH	25?	-	-	+15	641	
125.	+ KI → Complex	MeOH	25?	-	-	+11	641	
126.	+ CsI → Complex	MeOH	25?	-	-	+1	641	

Table 4. (Continued)

No.	reaction	solvent	T/ °C	P/MPa	no of K data	ΔV /cm^{3}mol^{-1}	ref	remarks
127.	+ NaI ⟶ Complex	MeCN	25?	-	-	+21	641	
128.	+ KI ⟶ Complex	MeCN	25?	-	-	+13	641	
129.	+ CsI ⟶ Complex	MeCN	25?	-	-	-13	641	
130.	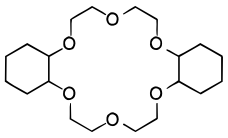 + NaI ⟶ Complex	MeOH	25?	-	-	+19	641	
131.	+ KI ⟶ Complex	MeOH	25?	-	-	+12	641	
132.	+ CsI ⟶ Complex	MeOH	25?	-	-	+8	641	
133.	+ NaI ⟶ Complex	MeCN	25?	-	-	+19	641	
134.	+ KI ⟶ Complex	MeCN	25?	-	-	+12	641	
135.	+ CsI ⟶ Complex	MeCN	25?	-	-	+16	641	
136.	+ NaI ⟶ Complex	DMSO	25?	-	-	-9	641	
137.	+ KI ⟶ Complex	DMSO	25?	-	-	-13	641	
138.	+ CsI ⟶ Complex	DMSO	25?	-	-	+10	641	
139.	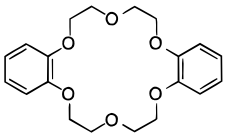 + NaI ⟶ Complex	MeCN	25?	-	-	+25	641	
140.	+ KI ⟶ Complex	MeCN	25?	-	-	+22	641	
141.	+ CsI ⟶ Complex	MeCN	25?	-	-	+17	641	
142.	+ NaI ⟶ Complex	DMSO	25?	-	-	+4	641	
143.	+ KI ⟶ Complex	DMSO	25?	-	-	+2	641	
144.	+ CsI ⟶ Complex	DMSO	25?	-	-	-3	641	
145.	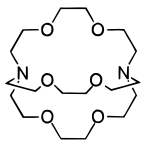 + NaCl ⟶ Complex	MeOH	25?	-	-	+15	641	
146.	+ KCl ⟶ Complex	MeOH	25?	-	-	+13	641	
147.	+ CsCl ⟶ Complex	MeOH	25?	-	-	+10	641	
148.	+ NaI ⟶ Complex	MeOH	25?	-	-	+16	641	
149.	+ KI ⟶ Complex	MeOH	25?	-	-	+13	641	
150.	+ CsI ⟶ Complex	MeOH	25?	-	-	+10	641	
151.	+ NaI ⟶ Complex	MeCN	25?	-	-	+25	641	
152.	+ KI ⟶ Complex	MeCN	25?	-	-	+16	641	
153.	+ CsI ⟶ Complex	MeCN	25?	-	-	+11	641	
154.	+ NaI ⟶ Complex	DMSO	25?	-	-	+2	641	
155.	+ KI ⟶ Complex	DMSO	25?	-	-	+1	641	
156.	+ CsI ⟶ Complex	DMSO	25?	-	-	+3	641	
157.	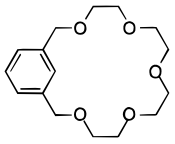 + t-BuNH$_3^+$ ⟶ Hydrogen-bonded complex	MeOH	33.5	150	4	-4.2	642	
158.	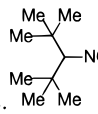 + β-cyclodextrin ⟶ Inclusion complex	H_2O	ambient	59	7	+5	643	
159.	2 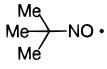 ⟶ 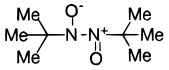	CO_2	35	110	-	-33	644	At P > 80
160.		CO_2	35	110	-	+1000	644	At P < 70
161.	3 MeOD ⟶ trimer	CO_2	40	45	8	-62.3	645	X_{MeOD} 0.062
162.		CO_2	40	-	-	-54.8	645	X_{MeOD} 0.031

Table 4. (Continued)

No.	reaction	solvent	T/ °C	P/MPa	no of K data	ΔV /cm^{3}mol^{-1}	ref	remarks
163.		ethane	40	45	9	-47.8	645	X_{MeOD} 0.062
164.		ethane	40	-	-	-32.9	645	X_{MeOD} 0.031
165.	4 MeOD ⟶ tetramer	CO_2	40	45	8	-79.2	645	X_{MeOD} 0.062
166.		CO_2	40	-	-	-65.9	645	X_{MeOD} 0.031
167.		ethane	40	45	9	-62.2	645	X_{MeOD} 0.062
168.		ethane	40	-	-	-42.3	645	X_{MeOD} 0.031
169.		heptane	40	45	6	-6.9	645	X_{MeOD} 0.062
170.		heptane	40	-	-	-13.7	645	X_{MeOD} 0.031
171.	5 MeOD ⟶ pentamer	CO_2	40	45	8	-96.2	645	X_{MeOD} 0.062
172.		CO_2	40	-	-	-76.9	645	X_{MeOD} 0.031
173.		ethane	40	45	9	-76.8	645	X_{MeOD} 0.062
174.		ethane	40	-	-	-51.5	645	X_{MeOD} 0.031
175.	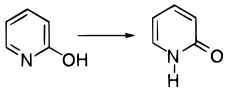	CHF_2CH_3	130	21	17	-1400[c]	646	$\Delta V \approx 0$ at 20
176.		propane	120	21	13	-900[c]	646	$\Delta V \approx 0$ at 20 MPa.

a. Twisted intramolecular charge-transfer complex.
b. Calculated by one of the present authors (T. A.).
c. At the maximum compressibility of the fluid.

ions seem likely to be formed; ion association would be highly hindered.[640]

Letcher and Kay[641] have reported an extensive set of volume data on the complexation of alkali halide salts with crown ethers and cryptands in various solvents. In most instances, simple trends can be discerned and understood. Thus, most of the reaction volumes are positive, which is the result of the desolvation of the cations which is necessary before binding can take place. For this reason, the expansion is generally least for the heavier alkali metals. In dimethyl sulfoxide, complexation does not offer much advantage over solvation, and it probably does not occur. It also appears that the cesium cation is too large to form a complex with 15-crown-5, but the negative value in acetonitrile suggests that it may bind two crown molecules; on the other hand, it is not obvious why the values for sodium and potassium iodides with dicyclohexyl-18-crown-6 in dimethyl sulfoxide should be negative while that for cesium iodide is positive. Yamada and Sera[642] made a high-pressure NMR study of the interaction of *tert*-butylammonium perchlorate with 1,3-xylyl-18-crown-5 in methanol; they interpret the negative value of the reaction volume as indicative of a cation strongly hydrogen-bonded to three oxygen atoms at one face of the crown. High-pressure ESR was used by Sueishi et al.[643] to evaluate the inclusion of di-*tert*-butyl nitroxide in β-cyclodextrin; they find that water can be packed in the cavity more efficiently than the solute.

There are a few cases in which the reaction volume was measured in supercritical media. Nakahara[644] found that in carbon dioxide, a normal value of -33 cm^3 mol^{-1} applies to the dimerization of 2-methyl-2-nitrosopropane at high pressure, but this changes to about $+1000$ cm^3 mol^{-1} near the critical density. Smith[645] studied the association of methanol and found negative values for the volume change per H bond far larger than normal if the medium is supercritical carbon dioxide or ethane. Similarly, large contractions were reported for the isomerization of 2-hydroxypyridine in supercritical propane and 1,1-difluoroethane, in an excellent paper by Johnston.[646] This phenomenon is further discussed below.

This section may close with a few related observations in micellar phenomena, not all of which resulted in volume measurements but which are certainly of interest. The association of ions of like charge increases electrostriction and that of ions of opposite charge diminishes it; hence it is not obvious what the volume consequence of micellization will be. Positive values of 5−10 cm^3 mol^{-1} are in fact found for alkanesulfonate, alkanoate, and ammonium salts.[647] In a number of instances,[648−650] the critical micelle concentration reached a maximum at a pressure of 100 to 130 MPa. Papers by Sugihara[651] and Yamanaka[652] should also be consulted. Additional observations of interest to high-pressure afficionada's have been reported on conformational equilibria in proteins,[653] on electrochemistry,[654] and on polymerization at constant volume.[655]

E. Other Pressure Effects

In this section we discuss several projects that have produced information on molar volumes, volume changes, and volume differences but which for one reason or another were not readily incorporated in Tables 2−4.

The commercialization of extraction by means of supercritical carbon dioxide has sparked a great deal of interest in chemistry in such media. Knowledge of the volume behavior of stable solutes under such conditions will obviously be important in understanding the variation of rates in such media. Eckert[655]

has developed a new and precise protocol to measure partial molar volumes of solutes in the critical region; data were provided for naphthalene, carbon tetrabromide, and camphor in carbon dioxide and ethylene. His results show extreme variability in the partial volume of solutes; values of many liters per mole are observed near the critical point of the solvent. Thus, one may expect that under these conditions, activation and reaction volumes will be large and difficult to interpret: the lion's share of these volume differences will be due to solution compressibilities, and not to changes in bonding. Measurements of the complete volume profiles will be helpful in understanding the results. While several authors have reported activation volumes in supercritical solvents, it should be noted that they cannot be directly compared with the $\Delta V^{\ddagger}$ values discussed earlier because they cannot be extrapolated to zero pressure.

Several Diels−Alder reactions have been studied in supercritical media. Paulitis[656] studied the cycloaddition of maleic anhydride and isoprene in carbon dioxide, and found that the activation volume resembles that in the liquid phase at pressures of ca. 10 MPa, but drops steeply to far more negative values near the critical pressure of 72.8 atm. Ikushima et al.[657] reported work on the same reaction, with methyl acrylate as the dienophile; these workers also found a deep minimum in $\Delta V^{\ddagger}$, of 750 cm^3 mol^{-1} at 7.5 MPa. As important, the product distribution was also strongly affected; the ratio of 4- to 5-carbomethoxy-1-methylcyclohexene, which is about 200 at atmospheric pressure, is reduced to 0.6 at the critical pressure and then returns to about 7 at 20 MPa. Similar findings were reported by Tester;[658] in contrast, Isaacs[659] found no unusual behavior for the reaction of quinine with cyclopentadiene.

In other reactions, Johnston[660] reported the unimolecular decomposition of α-chlorobenzyl methyl ether in 1,1-difluoroethane; this is an example of a more polar reaction. In this case also, a deep minimum is seen at the critical pressure. Extreme variations are also seen in the data on cyclohexane oxidation gathered by Mukhopadhyay;[661] very large positive activation volumes were encountered by Klein[662] in the pyrolysis of benzyl phenyl ether and dibenzyl ether, as well as extreme negative values for the hydrolysis of dibenzyl ether, phenethyl phenyl ether, and guaiacol. The effect of using supercritical fluoroform as a medium on the enantioselectivity of protease enzymes has been reported by Russell.[663] The acid-catalyzed elimination of water from 1-propanol at 375 °C also shows large variations in $\Delta V^{\ddagger}$ near water's critical point,[664] falling from 1200 cm^3 mol^{-1} to 70 at much higher pressures. A very recent study of electron attachment to NO in supercritical ethane indicates that activation volumes for this reaction approach −30 dm^3 mol^{-1} near critical conditions.[665]

What the available data seem to say is that the extreme behavior occurs near the critical point, and returns to more normal at temperatures well above the critical. Thus, Brower has reported the thermal decomposition of simple nitro compounds at temperatures and pressures well beyond the critical values, and conventional interpretations suffice. The reaction of nitromethane[666] was found to have an activation volume of −85 cm^3 mol^{-1} throughout the pressure range of 25−125 MPa, in accord with a simple polar mechanism. Nitrobenzene[667] reacts in benzene by hydrogen abstraction, as was deduced from the main product (fully deuterated biphenyl if hexadeuteriobenzene was used) and from the activation volume of −46 cm^3 mol^{-1}. Several other aromatic nitro compounds react analogously; when the nitro group is *ortho* to a methyl group, intramolecular abstraction also occurs.

Supercritical conditions have also been employed in the realm of fast reactions. Johnston has reported[668] modest changes in the product ratios in the photodimerization of isophorone (three dimers form) at high pressures of carbon dioxide and fluoroform. Randolph[669] has studied the spin exchange of the di-*tert*-butyl nitroxide radical in ethane; at 35 °C and 4 MPa, the activation volume reaches a maximum of 7500 cm^3 mol^{-1}. Eckert[670] has measured the activation volume of formation of the exciplex of naphthalene with triethylamine in carbon dioxide; he finds that $-\Delta V^{\ddagger}$ has a maximum of 14 000 cm^3 mol^{-1} at 8 MPa. A much reduced maximum (2500 cm^3 mol^{-1}) is observed at 50 °C. A similar extremum was observed by Brennecke and Chateauneuf[671] in the photoreduction of triplet benzophenone by 2-propanol in carbon dioxide near its critical point; the same behavior is seen with ethane and fluoroform media.[672] When pulse radiolysis is used to generate benzhydryl cation, its capture by tetramethylethylene or triethylamine in fluoroform and ethane is again subject to large rate effects near the critical points.[673]

True has reported the activation volumes for several inversion processes by means of a method resembling a protocol developed by one of the present authors:[674] measurement of the rate constant of a nonpolar unimolecular process both in the gas phase and in solution can be used to calculate $\Delta V^{\ddagger}$ without the need for high-pressure experiments. It is assumed that the reactant molecules in the solution are subject to a pressure equal to the internal pressure P_i of the solvent; this quantity can be calculated from the compressibility and the coefficient of thermal expansion. True[675] measured the rate of inversion of 1,3,5-trimethylhexahydro-1,3,5-triazine in the gas phase from ^1H NMR line-shape changes as a function of the pressure of added sulfur hexafluoride, and calculated an activation volume of +1 cm^3 mol^{-1} by comparing it with the rate in deuteriochloroform; this solvent was assumed to have an internal pressure of 500 MPa. The positive value was attributed to the need for nitrogen inversion to accompany the conformation change of the ring. Similar experiments with cyclohexane,[676] tetrahydropyran,[677] cyclohexyl fluoride,[678] *N*,*N*-dimethylpiperazine,[679] and *N*-methylmorpholine[680] were also reported (−4, −5, −8, +4, and −9 cm^3 mol^{-1}, respectively). If these results can be confirmed by direct high-pressure measurements, this would greatly strengthen confidence in the methodology. A somewhat related experiment has been reported by Kiselev and Konovalov.[681] These

authors measured the rate of the Diels−Alder cycloaddition in a number of solvents including lithium perchlorate solutions in diethyl ether, calculated a $\Delta V^{\ddagger}$ value on the basis of the alleged internal pressures of these media, and compared it with the value derived from high-pressure measurements in acetonitrile. The results were −22 and −18 $cm^3\ mol^{-1}$, respectively. Although the agreement seems impressive, some reservation is in order in this case. Both values are suspiciously low; it is furthermore doubtful that the method can be applied to reactions involving electrolytes at any stage or in any role. Dailey's contention[682] that the role of the lithium salt is not to augment the internal pressure of the medium[683] but to serve as a Lewis acid catalyst (not mentioned by the authors) has not been refuted.

F. Viscosity Dependence of Reaction Rates

The results of most of the reactions portrayed in Tables 2−4 can be discussed adequately in terms of TST, which assumes that equilibrium prevails between the initial state and the activated complex. However, especially the advent of means to study low-barrier reactions and reactions in slowly relaxing media has emphasized the need for alternative theories in which this assumption is avoided. This section is devoted to that need.

a. Description of Medium Effects in Terms of Stochastic Dynamics

Recent developments in the theory of chemical reactions are strongly focused on elementary processes proceeding in condensed phases; they include studies of solvation effects on chemical kinetics as an essential ingredient. The emphasis is on possible deviations of observed kinetics from predictions based on traditional TST. It is now conventional to discuss dynamic solvent effects in terms of friction created by the solute environment. The simplest dynamical equations containing friction forces are (GRF = Gaussian random force)

one-dimensional generalized Langevin equation

$$m\ddot{x} + \int_0^t \xi(t-\tau)\dot{x}(t)\,d\tau + \frac{\partial U}{\partial x} = \mathrm{GRF} \qquad (1)$$

Langevin or Kramers equation

$$m\ddot{x} + \gamma\dot{x} + \frac{\partial U(x)}{\partial x} = \mathrm{GRF} \qquad (2)$$

the simplest two-dimensional stochastic dynamical equation without memory effects

$$m\ddot{x} + \frac{\partial U(x,y)}{\partial x} = 0$$

$$\gamma\dot{y} + \frac{\partial U(x,y)}{\partial y} = \mathrm{GRF} \qquad (3)$$

Agmon−Hopfield equation

$$\frac{\partial F}{\partial t} = \text{diffusion term} - \text{sink term}$$

$$\text{diffusion term} = D\frac{\partial^2 F}{\partial y^2} + \frac{D}{k_B T}\frac{\partial}{\partial y}\left(F\frac{\partial U(y)}{\partial y}\right) \qquad (4)$$

$$\text{sink term} = \nu(y)F$$

Dynamical variables (coordinates) x and y are associated with a reactive chemical system (reaction coordinate x) and collective medium motion (medium mode y); the dots represent time derivatives ($\dot{x} = dx/dt$, etc.). The acceleration term with $\ddot{y}$ is disregarded in second eq 3. Potentials governing dynamic behavior are $U(x)$, $U(y)$ (one-dimensional), and $U(x,y)$ (two-dimensional). In the context of condensed phase kinetics, they are referred to as free energy profiles or surfaces. Stochastic elements are brought in eqs 1−3 by GRFs together with dissipative terms proportional to velocities $\dot{x}$ or $\dot{y}$. Equations 1 and 2 differ by their dissipative terms; in eq 1 this term contains an integral of $\dot{x}(t)$. At any given instant t, the dynamics of the system x is governed by its evolution over the preceding time interval $(0,t)$. Equation 1 is, therefore, often referred to as a stochastic equation with memory, and the corresponding integral kernel $\xi(t-\tau)$ as the memory kernel. Equation 2 is a special case of eq 1 with kernel $\xi(t-\tau) = \gamma\delta(t-\tau)$ where $\delta(t-\tau)$ means Dirac delta function. It does not involve memory effects. The number γ is called the friction constant.

For chemically reactive systems the free energy surfaces represent a pair of spatially resolved regions (reactants and products) separated by an energy barrier. They are usually treated as double-well functions. Equation 2 with a double-well potential is called Kramers equation. Equation 3 is more general than eq 4 and can be reduced to it when time scales associated with chemical (τ_x) and medium (τ_y) variables obey the inequality:

$$\tau_y/\tau_x \gg 1 \qquad (5)$$

i.e., it applies when the chemical variable is "fast" and the medium variable is "slow". In this extreme case, slow medium motion determines the total kinetics; eq 4 is formulated for the probability distribution function $F(y,t)$ and describes its time evolution. The diffusion term describes spatial diffusion with the diffusion constant D. The sink term is a sink representing the escape of "particles" y due to a chemical reaction; $\nu(y)$ is an y-dependent rate constant usually taken in Arrhenius form

$$\nu(y) = \nu_0 \exp\left(-\frac{V(y)}{k_B T}\right) \qquad (6)$$

with a y-dependent activation energy $V(y)$. This reaction is associated with an activated process proceeding along fast chemical coordinate x. The diffusion coefficient D in eq 4 and the friction constant γ in eq 3 are connected by the Einstein relation:

$$D = \frac{k_B T}{\gamma} \tag{7}$$

The usually approximate but important methodologies developed to extract kinetic information from eqs 1−4 are generally presented either in the form of explicit expressions or as calculational algorithms for rate constants. A brief overview and additional information on eqs 1−4 are given in the Appendix.

b. Relation to Measurements of Pressure

A peculiarity of stochastic dynamics is the presence of dissipative terms (the second terms of eqs 1 and 2 and second eq 3) and random forces. The energy of a dynamical system is not conserved due to these terms which implies an energy exchange with the environment. In eq 4, a counterpart of these non-Newtonian forces is diffusion motion governed by the diffusion term. The corresponding dissipative coefficients such as ξ, γ, and D are closely related to the shear viscosity η of the medium; for instance, when x represents the motion of spherical particles of radius a, the friction coefficient of eq 2 is given by the Stokes formula

$$\gamma = 6\pi a\eta \tag{8}$$

Further examples are discussed in section 3.F.f.i.

Studies of the dependence of reaction rate on viscosity provide important information on dynamical medium effects in chemical reactions.

A straightforward way to do a viscosity-dependent kinetic experiment is to perform it in a series of solvents of varying viscosity; many experiments of this sort have been reported. The approach has two significant disadvantages: the viscosity range variation is usually limited to 1 order of magnitude, and static solvent effects may change such important kinetic parameter as the activation energy. Reaction free energy surfaces are normally solvent-dependent which gives rise to static effects and hinders the separation of dynamic effects from experimental data.

The alternative approach to tune viscosity changes by means of pressure variations with the same solvent has proved to be extremely successful. By this means, viscosity variations of several orders of magnitude have become available. Of course, the problem of pressure dependence of free energy surface is inherent in this approach; its treatment is discussed below.

c. E/Z and Z/E Isomerizations in Solution

We shall exemplify the experimental studies of the viscosity dependence of reaction rates with *Z*/*E* rearrangements of olefins, imines, and azo compounds:

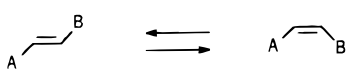

(9)

where A and B are usually aromatic rings such as in stilbene; such isomerizations can, in principle, proceed both in ground (S0) and singlet-excited (S1) states. They may involve elementary steps specified by the scheme of energy levels shown in Figure 22.

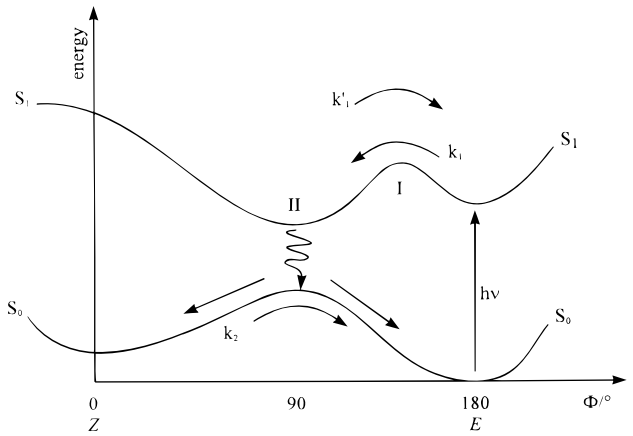

Figure 22. Two-level kinetic scheme representing the photocycle of *E*/*Z* (S_1) and *Z*/*E* (S_0) isomerizations, eq 9. Rotation angle Φ is a measure of a reaction coordinate.

The twist angle $\hat{O}$ associated with the internal rotation is the essential variable describing the evolution along the reaction coordinate for C═C and N═N bridges. Ground-state reactions with C═N bridges are a special case for which an inversion mechanism at the nitrogen center[496−498] causes the electronic structure of the TS to be quite different.

The photoinduced reaction, schematically shown in Figure 22, proceeds as follows. A stable *E* molecule on the S_0 free energy surface is photoexcited to the S_1 surface from which, surmounting a small potential barrier in configuration I, it drops to the intermediate state II, the twisted configuration at the minimum of S_1. It makes a transition to the top of the S_0 surface; about half of its population relaxes along the S_0 surface to the *Z* form and half relaxes to the original *E* form. In the overall process, surmounting the potential barrier on the S_1 surface, is rate limiting; the corresponding rate constant is k_1. Then, measuring the rise of population in the *Z* form, this rate constant can be determined. The *Z* form is metastable on S_0 surface; hence it is gradually transformed back to the *E* form after surmounting the potential barrier with rate constant k_2. By varying experimental conditions, the excited- and ground-state reaction kinetics can be measured.

Another important reaction is the twisted intramolecular charge transfer (TICT) which also proceeds in both excited and ground states. Only the photoreaction has been systematically examined in many solvents. A typical example is the process[684]

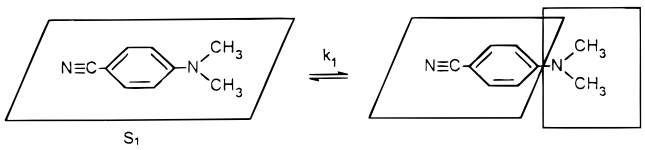

(10)

The planar reactant molecule in its S_1 state undergoes an isomerization into a twisted configuration corresponding to point II in Figure 22. This change is accompanied by a strong change in intramolecular polarization. The evolution which follows is that

Table 5. Experimental Data for *E* → *Z* Reaction 9 in the Excited S_1 State

reaction, no.	solvent[a]	*T*, K	pressure range (*P*, MPa)	viscosity range (η, mPa s)	rate constant range (k, 10^9 s^{-1})	E_a, kJ mol^{-1}	β	ref(s)
1. (*E*)-stilbene (ES) 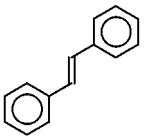	*n*-C_kH_{2k+2} (*l*)							
	$k = 2-4$	295−303	1−600	(38−152) × 10^{-3}	31−5	7.5		690−692
	C_2H_6 (*sc*)	306−433	3−430	(10−130) × 10^{-3}	86−13		∼0.5	692
	C_3H_8 (*sc*)	384	22−400	(70−430) × 10^{-3}	54−29			692
	CO_2 (*sc*)	297, 335	7−500	(35−420) × 10^{-3}	65−11	7−8		692
	SF_6 (*sc*)	298−330	6−140	(75−180) × 10^{-3}	61−13			692
	Xe (*sc*)	298	10−160	(100−150) × 10^{-3}	48−30			692
	CHF_3 (*sc*)	330	110−310		68−56			692
	n-$C_kH_{2k+1}OH$							
	$k = 1, 2$	298	0.1−595	0.57−42.7	23−2.3		depends on viscosity	693, 694
	$k = 3, 4$	298−445		15−60			0.3−0.5	693, 694
2. (1*E*, 3*Z*)-1,4-diphenyl-1,3-butadiene (DPB) 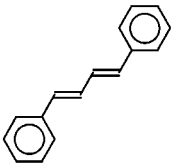	C_2H_6 (*g*, *sc*)	306−4212	3−290	(13−85) × 10^{-3}	50−3.5			695
	C_3H_8 (*g*, *sc*)	393	13−450	(52−420) × 10^{-3}	20−7			695
	n-C_4H_{10} (*g*, *sc*)	407	0.34	10 × 10^{-3}	40			695
	CO_2 (*g*, *sc*)	332−384	5−380	(19−38) × 10^{-3}	50−19			695
	SF_6 (*g*, *sc*)	364−388	3.3		30			695
	n-C_kH_{2k+2} (*l*), $k = 2-4$	298	0.24−620	(39−1300) × 10^{-3}	60−5	10−11	1	695, 696
	n-C_kH_{2k+2}, $k = 5-12$	298	0.1−547	0.23−11.4	1.54−0.18			696
	n-$C_kH_{2k+1}OH$, $k = 1-5$	298	0.1−675	0.57−159	26.5−0.5		0.99−1.03	693
3. (*Z*)-stilbene 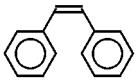	*n*-C_kH_{2k+2}, $k = 5, 6, 8, 9$	295, 390	0.1−385	0.23−7.9	(3−0.3) × 10^3	negligible	1	697, 698
	MeOH	295	0.1−320	0.57−1.38	(0.8−2) × 10^3			697
	MeCN	295	0.1−315	0.37−0.93	(1.2−2.8) × 10^3			697
	PMMA (polymethyl methacrylate)	295	0.1					697
4. 2-vinylanthracene (2VA) 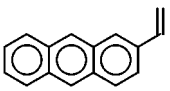	C_2H_6, CO_2 (*sc*)	323	6−12	0.02−0.045				489
	n-C_kH_{2k+2}, $k = 5, 6, 8, 10$	303	0.1−500	0.2−7.2	0.2−0.11		0.4	489b
5. 2-isopropenylanthracene 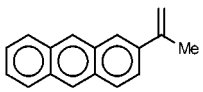	*n*-C_kH_{2k+2}, $k = 5-12$	303	0.1−490	0.2−8.8	2−0.3			699
						15.5	0.23	700

[a] Notation: gas phase (*g*), liquid phase (*l*), supercritical fluid (*sc*).

described for reaction 9. The viscosity dependence of k_1 has been measured by several research groups,[490,491,684−689] some of them using high-pressure experiments.[490,491,688,689]

d. Organization of the Tables

Summaries of experimental data concerned with reactions 9 and 10 are listed in Tables 5−7. Pressure-dependent experiments and those with the solvent variation are treated separately. We emphasize ranges within which pressure, viscosity, and rate constants were varied. Reliable theoretical conclusions are possible only when these ranges are wide enough. Rate constants k in Table 5 correspond either to k_1 or to k'_1 in Figure 22. For ground-state reactions (Table 6) k corresponds to k_2. The viscosity and rate constant ranges in several cases were estimated from the figures given in the original works. Observed activation energies E_a embody a rough measure of the height of reaction barrier for the corresponding elementary process.

In Table 7, we list values of viscosity coefficients β (see eq 12 below) experimentally estimated for both *E*/*Z* photoreaction and TICT (10). They have mainly been obtained by experiments performed at ambient pressure with various solvents. A great variety of solvents was studied. The TICT experiments with varying pressure are also included (see footnote c). Usually accurate separation of static effects (see section 3.F.e) was not made for entries in Table 7.

e. Static Effects in Isomerization Reactions

Static medium effects are interpreted as changes of the reaction free energy surface by the solute environment. Essential among them are changes of heights of free energy barriers, i.e., of classical activation energies. When a solute charge distribution changes in the course of a reaction they become obvious. This effect is known for excited-state isomerizations. Even in hydrocarbon reactants, such as (*E*)-stilbene, the S_1 twisted configuration II (the minimum on S_1 curve, Figure 22) is strongly polarized in a narrow range of twisting angle $\hat{O}$ near 90°; this effect has been called "sudden polarization".[711−715] Although its early estimates seem to be exaggerated, quantum-chemical studies of model systems[714−724] and experiment[725] support significant charge separation in excited configuration II. No such estimates are available for TS configurations of photoreactions

Table 6. Experimental Data for $Z \rightarrow E$ Reaction 9 in the Ground S_0 State

compound[a] (X and substituents in the second ring are indicated)	solvent[b]	T, °C	pressure range (P, MPa)	viscosity range (log η, Pa s)	rate constant range[c] (k, s^{-1}) at lowest temperature	E_a, kJ mol^{-1} (at 0.1 MPa)	β	ref(s)
1. X = N, 4-NO_2	EtOH	5	0.1−800	−2.9−(−1.3)	8.5−144	49.7		495b
DNAB	AcOMe	5−40	0.1−600	no data	0.1−1.5	48.6		unpublished
	GTA	5−40	0.1−800	1−7	0.32 (1.35) 0.10	49.5	0.59−0.74	496
	MPD	−5 to 35	0.1−600	1−7	1.7 (4.35) 1.1	50.3	0.28−0.42	497
2. X = N, 2-MeO, 4-NO_2	GTA	5−35	0.1−600	1−6	0.09 (0.50) 0.04	50.8	0.51−0.56	496
DMNAB	MPD	−5 to 35	0.1−600	1−7	0.69 (1.86) 0.45	50.2	0.28−0.31	
3. X = CH, 4-NO_2	GTA	5−25	0.1−540	1−4	219−45.9	53.5	0.66	496
DBNA	MPD	−10 to 10	0.1−480	1−6	64.8−17.0	53.5	0.53	497
	DCMP	−5 to 20	0.1−420	1−8	2.6−0.6	54.6	0.52	495
4. X = CH, 4-Br	GTA	5−25	0.1−600	1−6	0.37−0.097	71.3	0.73	496
DBBA	MPD	−5 to 10	0.1−600	1−7	0.055−0.018	72.9	0.67	497
	DCMP	0−20	0.1−510	1−9	0.43−0.03	67.2	0.66	495
5. X = CH, 4-COOEt	GTA	5−25	0.1−570	1−5	10.5−2.12	62.6	0.68	496
DBEA	MPD	−5 to 15	0.1−540	1−5	3.45−1.4	62.3	0.61	497
	DCMP	0−20	0.1−420	2−7	7.44−3.32	58.6	0.56	495
6. X = CH, 4-NMe_2 DBDA	GTA	20−35	0.1−600	1−5	0.069−0.024	75.4	0.22−0.35	496
7. 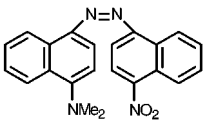	GTA	−10 to 10	0.1−400	−1 to 6	941 (1270) 4.7	27.2	0.60−0.54	497

[a] Compounds of the general structure: 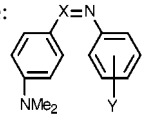 [b] Glycerol triacetate, GTA; 2-methyl-2,4-pentanediol, MPD; 2,4-dicyclohexyl-2-methylpentane, DCMP. [c] The figure in brackets (if it is present) corresponds to the maximum of the kinetic curve (see Figure 24).

(point I in Figure 22) but some polarization at this TS point for (*E*)-stilbene and 1,4-diphenylbutadiene (DPB) is confirmed implicitly by a significiant lowering of activation barriers in polar alcohols as compared to hydrocarbon solvents (see Table 5).[693,694,726−728] Solvent effects on the potential barrier have been also assumed for (*E*)-stilbene in hydrocarbon solvents,[690−692,729−732] where polar effect is not expected. The barrier height varied linearly with the solvent density. The origin of this effect may be due to changes of cavitation[733−735] and dispersion energies.

For ground-state isomerizations with much larger barriers, polarization effects are usually less significant unless polar substituents are present and a reaction proceeds in a polar solvent; lowering of the energy barrier is especially important when the electronic push−pull mechanism is promoted by a pair of substituents, one of which is an electron donor and the other is an electron acceptor. This mechanism is efficient for compounds with N═N double bond bridges; compounds such as 4-(dimethylamino)-4′-nitroazobenzene (DNAB) and 4-(dimethylamino)-2′-methoxy-4′-nitroazobenzene (DMNAB) (see Table 6) provide a typical example.[495b,496,736,737] However, the polar effect seems to be absent in the case of C═N bridges where the reactive motion changes from an internal rotation to inversion at the nitrogen center.

Variations in rate due to static solvent effects can be comparable in magnitude with or even larger than purely dynamical effects. A basic difficulty in the interpretation of viscosity dependencies in a series of solvents is a necessity of an accurate appraisal of these changes.

Static effects can also be present in the case of a compressed single solvent. Thus, in ground-state reactions, large negative activation volumes are typical for push−pull substituted azobenzenes.[495b,496] Provided that polar effects are neglibible, however, static effects of pressure are expected to be small. In this case a simple mechanical model of activation volumes attributes effects of pressure to changes in the size of the cavity corresponding to the excluded volume of a solute. In an isomerization reaction, a solute mainly changes the shape of its cavity, rather than the size. This is in contrast to the drastic cavity changes in bond-forming reactions such as the Diels−Alder reaction.[738,739] The small observed activation volumes (<1−2 cm^3 mol^{-1}) observed for many isomerizations confirm this point of view.

Finally, a comment must be made about a connection of observed Arrhenius activation energies E_a and heights of the corresponding free energy barriers. A direct identification is invalid because of many reasons. Among them, in viscosity-dependent experiments, there is a viscosity contribution to E_a. This correction (of order of several kilojoules per mole) can change the estimated barrier height. The effect is important especially for low barrier photoisomerizations.[691,694,726,732,740] It is often eliminated by the use of isoviscosity activation energies; the barrier height appears to be constant in the isoviscosity Arrhenius plots throughout the homologous series. Unfortunately, this separation is not always reliable.[692,731,732]

Table 7. Viscosity Coefficients β for Several Isomerization and TICT Reactions in the Excited S_1 State

compound	β	ref(s)
ES[a]	0.7	701
ES[a]	0.32	702
DPB[a]	0.59 (hydrocarbons)	703
DPB[a]	0.92 (alcohols)	704
DPB[a]	0.51 (nitriles)	705
DODCI[b]	0.26 (ground state)	706
DODCI[b]	0.43 (excited state)	706
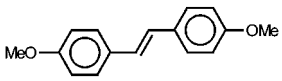	0.44 (nitriles)	705
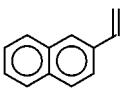	0.2	699, 700, 707
	0	700, 707
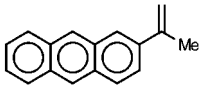	0.23	699, 700
	0.4	699 (*P*)
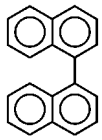	1	708, 709
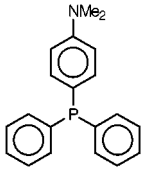	0.7 (EtOH)	688, 689
	0.44 (*n*-PrOH)	710 (*P*)
	0.3−0.35 (n-$C_kH_{2k+1}OH$, k = 4, 5, 8)	710 (*P*)
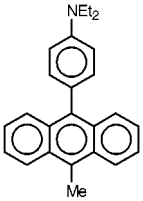	0.7 (*n*-PrOH)	492 (*P*)
	0.1−0.2 (*n*-PentOH)	492 (*P*)
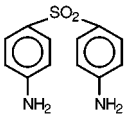	0.2 (*n*-PrOH and higher alcohols)	490, 491 (*P*)

[a] Abbreviations are borrowed from Table 5. [b] 3,3′-Diethyloxadicarbocyanine iodide. [c] "(*P*)" indicates pressure-tuned experiments in a single solvent.

f. Dynamic Medium Effects in Isomerization Reactions

i. Interpretation of Friction Coefficients in Terms of Viscosity. Discussions of dynamical solvent effects in reaction rates are, as a rule, based on the Langevin or Kramers equation, eq 2. For isomerization reaction, when the reactive motion can hardly be viewed as a translation of a spherical particle, several workers have suggested the use of rotational diffusion periods of the solute particle as a measure of the solute−solvent friction of the Kramers model. This quantity is available from spectroscopic measurements; and its theoretical estimate from modifications of the Stokes formula (8) have been discussed.[701,741−744]

In the two-dimensional eq 3, the interpretation of γ must be different. This is the friction corresponding to a purely medium coordinate y. In the context of reaction dynamics, y is a collective medium mode;[745] that is to say, a strongly correlated motion of a large ensemble of solvent particles. Generally, two types of collective modes are involved in an isomerization process. One consists of an adjustment of solvent dipolar particles to the solute charge distribution varying in the course of a reaction (the polarization coordinate); the second represents their displacements accompanying a change of the cavity shape (the shape coordinate). The first type of motion is mainly governed by electric forces while the second is associated with changes of a cavitation free energy.[733−735] Correspondingly, we encounter two types of friction: dielectric and hydrodynamic ones. Elementary motions of medium particles, which form a collective mode after their superposition, are frequently treated as molecular rotations in both these cases. The corresponding relaxation constant for this model is the Debye period τ_D.[746] It works for nonpolar solvents. For a purpose of description of the polarization-type collective mode in charge-transfer processes (with dielectric friction), the longitudinal period τ_L is more appropriate;[746,747] it is defined as $\tau_L = \tau_D(\epsilon_\infty/\epsilon_0)$, where ϵ_0 and ϵ_∞ are static and optic dielectric permittivities. The simplest expression for γ is[748,749]

$$\gamma = \frac{4\pi\epsilon_0\epsilon_\infty}{\epsilon_0 - \epsilon_\infty}\tau_L \qquad (11)$$

More sophisticated treatments have been discussed.[750−754] Periods τ_D and τ_L show a clear correlation with viscosity changes induced by pressure.[755−757]

Dynamic variables x and y in eqs 1−4, as applied to elementary chemical processes, are microscopic quantities and one needs to consider whether macroscopic relations such as eqs 8 or 11 are appropriate to describe their relaxation. In a theoretical treatment at a truly microscopic level, relaxation constants should be extracted by calculating time correlation functions for respective variables[754,758−762] which has recently become available through molecular dynamics and other computational techniques developed in the theory of liquids. Fortunately, microscopic relaxation parameters correlate reasonably well with macroscopic viscosities, as measurements of rotational relaxation constants (microscopic characteristics) for (*E*)-stilbene in hydrocarbon solvents demonstrate within a wide pressure range.[743] It is thus seen that, independently of the microscopic mechanism of friction effects, their clear correlation with macroscopic shear viscosity is observed. This reveals a rationale behind using the macroscopic viscosity as a measure of strength of the dissipative terms in stochastic eqs 1−3. The same is true for the diffusion coefficient D in eq 4 because it is related to γ in eq 3 by the Einstein relation (7).

When the generalized Langevin eq 1 is used, an explicit expression for the kernel $\xi(\tau)$ is needed. Its parametrization has been discussed in the literature.[701,702,705,763−769]

ii. Viscosity Dependence of Photoisomerization Reaction Rates. As noted above, significant preliminary work is necessary in order to correct observed viscosity dependencies of reaction rates for

static effects. For *Z*/*E* photoisomerizations this has been done very well by Troe and Schroeder et al.[690−697,740,770] The so-revealed dynamical effects are conventionally discussed in terms of one-dimensional stochastic dynamics and the corresponding Kramers−Grote−Hynes (KGH) kinetic treatment.[692,726,731,732,771] High and low viscosity ranges should be considered separately in terms of this approach, as discussed in the Appendix.

In the high viscosity limit, rate constants change according to the inverse power law:

$$k \sim \eta^{-\beta} \qquad (0 < \beta < 1) \tag{12}$$

Kramers theory predicts that $\beta = 1$ in this strong friction kinetic regime. Such sort of dependence has been observed for DPB[693,695] (Table 5).

Probably, β is also close to unity in (*Z*)-stilbene,[697,729,772] tetraphenylethylene, and (*E*)-1-[1-indanyliden]indan ("stiff stilbene").[692] A fractional β value is more usual, however (see Tables 5 and 7). Many authors have interpreted this result in terms of the Grote−Hynes (GH) [767,768] generalization of the Kramers approach, when the generalized Langevin equation, eq 1, with memory effects is considered instead of its Kramers limiting case.[489,489b,699,701,702,726,727,764−766] However, alternative explanations have been also suggested.[690−692,730−732,770]

The GH theory actually provides an approximate expression for the rate constant generated by eq 1 (see the Appendix). No explicit derivation of expression 12 from the GH theory has been achieved. The GH treatment generally predicts a decay of the rate constant weaker than $1/\gamma$ in accord with many experimental trends and also with empirical formula (12). This formula is flexible enough to reproduce the desired result within a limited viscosity range. Many authors did not try to explicitly extract β values from their data. This caution is understandable due to ambiguity in separating static effects (section 3.F.e) from the experimental viscosity dependence. Some of the data included in Table 7 are open to criticism from this point.

The GH rate expression for large and intermediate friction ranges combined with the special Kramers approach for treatment of the low friction range constitute the KGH theory. The Kramers theory predicts an increase of the rate with increase of viscosity in the low viscosity range; this corresponds to the so-called "energy diffusion mechanism". Much effort has been expended in searches of this kinetic regime. It was detected[695,730,740,773] at much lower viscosities (and in lower pressure range) than those expected on the basis of the KGH theory. This effect has only been observed in supercritical state of hydrocarbon solvents, i.e., at very low solvent densities. This density shift can be explained as a dimensionality effect. According to the energy diffusion mechanism, slow thermal activation of reactant molecules becomes rate limiting. In the one-dimensional KGH treatment, the activation is due to the random force (GRF) which is directly connected to the friction coefficient γ via fluctuation−dissipation theorem.[758] This is the origin of a linear viscosity dependence of rate constant in the low friction range. In KGH theory, γ is associated with the one-dimensional *x* motion. On the other hand, in polyatomic chemical systems other intramolecular modes can promote *x* activation due to an intermode energy exchange. As a result, the kinetic regime in which activation stage becomes rate limiting is shifted to smaller γ values. The total dependence of the rate over the whole viscosity range studied was described in terms of a combined treatment,[690,692,731] where the energy diffusion limit is described in terms of a standard Lindenmann approach of the theory of gas-phase unimolecular reactions.[774] The medium and large viscosity behavior is interpreted in terms of the Kramers model. The combined rate expression is

$$k = \frac{k_0[M]k_\infty}{k_0[M] + k_\infty}\left[\sqrt{\left(\frac{\gamma}{2m\omega^\ddagger}\right)^2 + 1} - \frac{\gamma}{2m\omega^\ddagger}\right] \tag{13}$$

where k_0 is the collision rate constant and $[M]$ is the concentration of solvent particles; $k_0[M]$ represents the activation rate (the low-pressure limiting rate coefficient). The high-pressure gas-phase limit is denoted as k_∞ and calculated by means of the technique of RRKM theory.[774]

The second factor in eq 13 represents a prefactor of the Kramers rate expression (see the Appendix, eqs A1 and A2) normalized to 1 when $\gamma \to 0$. Here $\omega^\ddagger$ represents the frequency of the free energy profile at the top of the barrier. In this way the inverse viscosity law (12) with $\beta = 1$ is obtained in the high friction limit.

iii. Viscosity Dependence of Ground-State Isomerization Reaction Rates. A distinctive feature of *Z*/*E* isomerization in the ground state is the high activation barrier ($E_a \geq 50$ kJ/mol). Reaction rates are lower than those observed in photoisomerizations by many orders of magnitude. This makes their dynamical interpretation more definite because the relative significance of static effects decreases.

The most important observations have been made by studying pressure effects in high viscosity solvents,[495,495b,496,497] see Table 6. Their heuristic interpretation suggests a two-step reaction mechanism[496,763,775] according to which an isomerization process involves a rearrangement of a solvation shell as a necessary ingredient. This process is considered as a separate kinetic step with rate constant k_f. The rate constant for the solute transformation in an idealized nonviscous medium (viscosity effects neglected) is denoted as k_{iso}. Then the total observed rate expression is

$$\frac{1}{k} = \frac{1}{k_{iso}} + \frac{1}{k_f} \tag{14}$$

It is supposed that at low pressure $k_f \gg k_{iso}$ and extrapolation gives

$$k_{iso} = \lim_{P \to 0} k \tag{15}$$

It is also assumed that the pressure dependence of k_{iso} obeys the conventional approach accepted in high-pressure kinetics. Because this treatment, introducing activation volume as a measure of pressure

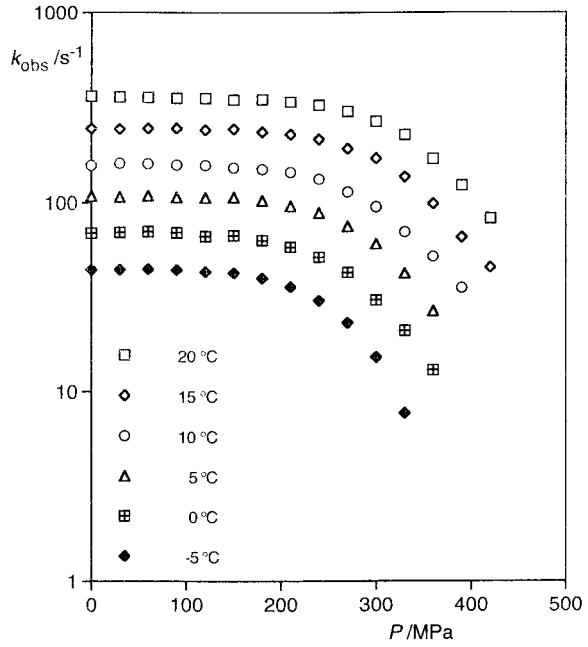

Figure 23. Pressure dependence of the rate constant $k = k_{obs}$ for the ground state *Z*/*E* isomerization of DBNA in DCMP.

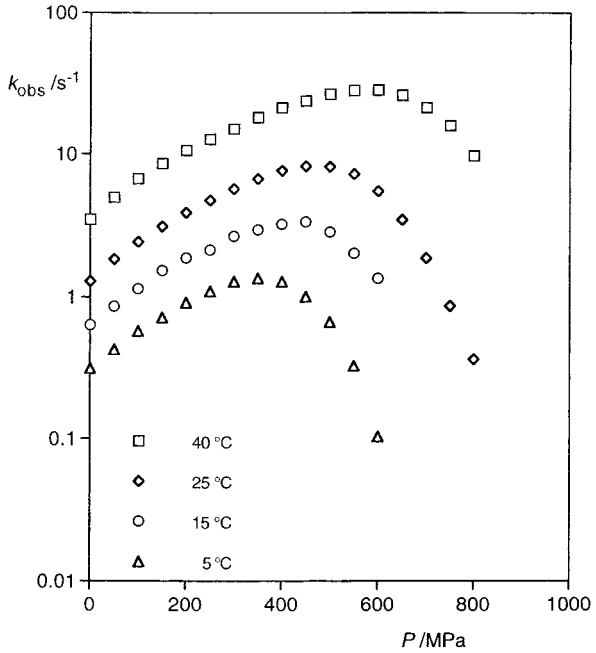

Figure 24. Pressure dependence of the rate constant $k = k_{obs}$ for the ground state *Z*/*E* isomerization of DNAB in GTA.

dependence, is essentially based on the standard TST, one assumes that

$$k_{iso}(P) = k_{TST}(P) = k_{TST}(\eta) \qquad (16)$$

where the η dependence is introduced via the experimentally measured monotonic function $\eta(P)$. It is important to note that k_{TST} accounts for static pressure effects and therefore formulas 14−16 provide an efficient procedure for the extraction of purely dynamical viscosity effects from observed rate constants.

For instance, in Figure 23 for DBNA in DCMP, k_{iso} is pressure-independent (nearly zero activation volume) but for DNAB in GTA in Figure 24 a significiant negative activation volume is observed due to electrostriction in its polar TS.[496,763] It is reasonable to assume that the medium reorganization rate constant k_f can be described in terms of KGH theory so that eq 12 holds. The corresponding values of β are listed in Table 6.

Kinetic curves such as those shown in Figures 23 and 24 have been observed for other reactions.[776,777] They are well-described in terms of a two-dimensional stochastic eq 3 in which x is a chemical coordinate (the isomerization coordinate for the present case) and y is a collective medium mode. A simplified version of eq 3, the Agmon−Hopfield (AH) eq 4, was applied to analyze the pressure dependence of Diels−Alder reactions and nonequilibrium solvation effects, leading to curves shown in Figures 23 and 24 were predicted.[778,779] Generally, a phenomenological two-step eq 14 can be mapped on the theoretical rate expression of the AH model giving:[780]

$$\frac{1}{\langle k \rangle} = \frac{1}{k_{TST}} + \frac{1}{k_f} \qquad k_{TST} = \lim_{\eta \to 0} \langle k \rangle \qquad (17)$$

where $\langle k \rangle$ is an averaged rate constant (an inverse survival period) reducing to the usual monomolecular rate constant when the kinetics are true exponential. Averaging is necessary when kinetics are polyexponential, a typical situation for the AH model in the high friction region (see the Appendix). By using these definitions, the equation defining k_f can be derived from the AH model.[781,782] An empirical interpretation of k_f as a rate of solvent reorganization seems to be successful.[495−497,763] Expressions for k_f beyond its KGH estimate are available.[780,782] They provide an interpretation of the inverse-power law (12).[783] When $\gamma \to \infty$, k_f behaves asymptotically as $1/\gamma$[784,785] but in the intermediate range a weaker dependence is expected in accord with eq 12.

iv. Interrelation of the Two Theoretical Approaches and Their Validity. Our interpretation of kinetics of photoisomerization and thermal isomerization reactions followed the original literature and used two theoretical models: the KGH theory for photoreactions and a two-step mechanism closely related to the AH theory for thermal reactions. As shown in the Appendix, these two kinetics are incompatible to a significant extent. The non-TST kinetic regimes they describe are essentially different. The KGH model is one-dimensional and its non-TST region corresponds to a low-friction limit for a single reaction coordinate x. The AH model is two-dimensional and its non-TST region corresponds to a high-friction limit for the medium coordinate y. The two theories partially overlap in the regions of high friction of the KGH and of low friction of the AH approaches; these regions include the TST kinetic regime as well.

Several authors have mentioned that an explicit multidimensional dynamical study is desirable for a true understanding of the recent kinetic experimental material in the field of condensed phase reac-

tions.[692,726,731,732] Invoking the AH model brings a semiquantitative background to this idea.

Some experimental data support its AH interpretation of the non-TST kinetics for ground-state isomerizations.[497,763,775] Furthermore, a polyexponential kinetic behavior, missing in the KGH approach, is an ingredient of the AH kinetics. Nonexponential kinetic evolution curves are frequently observed in ultrafast spectroscopic experiments testing solvation dynamics in electron-transfer systems[751,752,786−794] including *Z*/*E* isomerization and TICT reactions in polar solvents.[688,689,698,709] Interpretation of this effect in terms of the AH equation[795,796] is now conventional.[792−794] Nonetheless, it should be remembered that both KGH and AH approaches involve serious approximations. A consistent unifying description of two-dimensional reaction dynamics is possible only in terms of a more sophisticated stochastic theory[785,797] including both these models as opposite limiting cases.

G. Appendix: Rate Expressions of Stochastic Theories

a. Kramers–Grote–Hynes (KGH) Theory

The Kramers equation, eq 2, describes a rate of escape of particles from one-dimensional potential well as shown in Figure 25. The potential profile is characterized by the barrier height $U^{\ddagger}$, and two force constants: λ_0 at the bottom of the well and $(-\lambda^{\ddagger}) > 0$ at the barrier top. The corresponding frequencies are defined as $\omega_0^2 = \lambda_0/m$ and $(\omega^{\ddagger})^2 = -\lambda^{\ddagger}/m$. The rate expressions are approximately estimated for different ranges of the friction constant.[767] In the intermediate and large γ range the result is

$$k = \frac{\Omega}{2\pi}\left(\frac{\lambda_0}{\lambda^{\ddagger}}\right)^{1/2} \exp\left(-\frac{U^{\ddagger}}{k_B T}\right) \qquad \text{(A1)}$$

$$\Omega = \sqrt{(\gamma/2m)^2 + (\omega^{\ddagger})^2} - \frac{\gamma}{2m} \qquad \text{(A2)}$$

where the motion in the vicinity of the barrier top (see Figure 25) is considered as a rate-limiting process; Ω is the decay frequency. The asymptotic case of large γ reduces to the $1/\gamma$ (and $1/\eta$) dependency of the rate:

$$k = \frac{\omega_0 \omega^{\ddagger}}{2\pi}\left(\frac{m}{\gamma}\right) \exp\left(-\frac{U^{\ddagger}}{k_B T}\right) \qquad \text{(A3)}$$

If eqs A1 and A2 are formally extended to the region of low friction then the result

$$k = \frac{\omega_0}{2\pi} \exp\left(-\frac{U^{\ddagger}}{k_B T}\right) = k_{TST} \qquad \text{(A4)}$$

is obtained, which is equivalent to the application of the TST without allowance for the influence of the medium.

In fact, eqs A1 and A2 are invalid in the low friction limit where the rate-limiting process changes its physical nature. Here a thermal activation of molecules in the reactant well limits the escape rate. The corresponding rate constant is proportional to γ. This is the so-called energy diffusion kinetic regime. The two asymptotic kinetic regimes are connected by a smooth curve with a maximum, where $k_{max} < k_{TST}$, as shown in Figure 26.

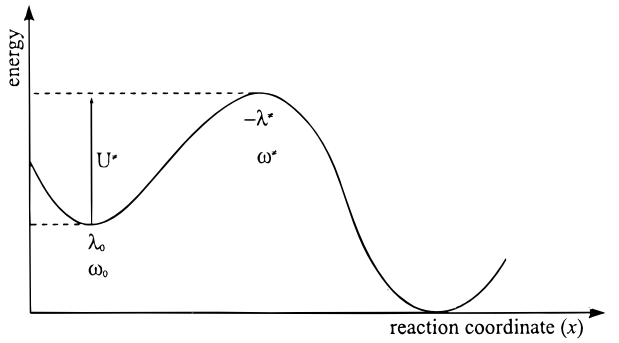

Figure 25. The free energy profile used in the one-dimensional KGH theory; $U^{\ddagger}$ is the height of the barrier, λ_0 and $-\lambda^{\ddagger}$ are force constants at the reactant minimum and at the top of the barrier, ω_0 and $\omega^{\ddagger}$ are the corresponding frequencies.

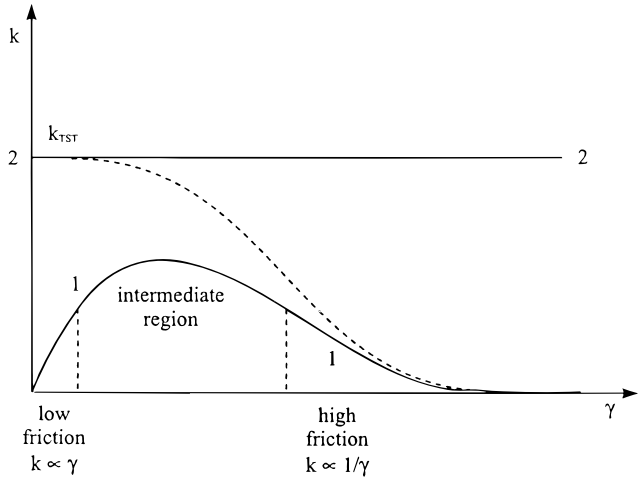

Figure 26. Dependence of the rate constant k on the friction coefficient γ in the Kramers theory (curve 1) and in the one-dimensional TST (straight line 2 and formula (A4)). The region of the high and low friction are described by simple asymptotic formulas, dashed curve represents calculations by eqs A1 and A2.

For the generalized Langevin equation, eq 1, the same Arrhenius expression (A1) operates in the regime when surmounting the barrier is a limiting kinetic step. Only the decay frequency Ω is changed: this is a root of a transcendent equation originally derived by Grote and Hynes.[768] In the low-friction limit the energy diffusion kinetic regime works and friction dependence of the rate is qualitatively the same as in the Kramers case[767,769,798,799] (for eq 1 the integral $\int_0^{\infty}\xi(\tau)\,d(\tau)$ is a measure of the friction strength). The rate expression (A1) valid in the intermediate and strong friction range is an essence of the one-dimensional KGH theory. It can also be extended to multidimensional systems by an appropriate change of the equation determining the decay frequency Ω and by substituting the factor $(\lambda_0/\lambda^{\ddagger})^{1/2}$ by a more complicated combination of all force constants characterizing the reactant well and the barrier top.[767,800−804]

It should be noted that the two kinetic regimes present in the KGH approximation do not at all exhaust the diversity of kinetic behavior inherent to the generalized Langevin eq 1.

b. Kinetic Regimes Corresponding to the AH Equation

A two-dimensional stochastic dynamics as presented by eq 3 exposes several kinetic regimes. A somewhat simplified picture is obtained in terms of its reduced version, namely the AH eq 4. This reduction is legitimate in the limit (5) when the relaxation of medium coordinate y is slower than the escape rate along reaction coordinate x.[784] Kinetic behavior generated by the AH equation was discussed in original papers of Agmon and Hopfield,[805,806] later by Sumi, Marcus, and Nadler[795,796] and, most recently, by Berezhkovsky and Zitserman.[784,807]

The total picture can be reconstructed in terms of several key quantities:

$$k_e = \lim_{\gamma \to 0} k \approx k_{TST}$$

$$U_y^{\ddagger} = \frac{\lambda (y^{\ddagger} - y_0)^2}{2} \qquad \text{(A5)}$$

$$\omega = \frac{1}{\tau_y} = \frac{\lambda D}{k_B T}$$

The quantity k_e is a rate constant corresponding to the two-dimensional KGH treatment of eq 3 simplified to a quasi-one-dimensional form according to the basic approximation (5), reducing eq 3 to the AH equation. It has an Arrhenius temperature dependence but it is slightly distinguished from a standard one-dimensional TST expression (A4) and can be considered as a two-dimensional k_{TST}. In second eq A5, $U_y^{\ddagger}$ is a contribution to the potential barrier due to the medium coordinate. It is extracted from a two-dimensional free energy surface $U(x,y)$ of eq 3. The cross section of this free energy surface along coordinate y (the potential $U(y)$ of eq 4) can be considered as a parabola with force constant λ; the quantity $(y^{\ddagger} - y_0)$ is a shift of the TS position relative to the reactant minimum along the medium mode. Finally, the medium frequency ω is the inverse relaxation period for the y motion establishing its time scale; it is closely related to the diffusion coefficient D.

Now we can construct a pair of dimensionless parameters mainly determining the AH kinetics, namely, k_e/ω and $\epsilon = U_y^{\ddagger}/k_B T$. The first one defines a ratio of time scales for a relaxation of y and a reaction along x, thus specifying the same ratio as given in eq 5. The second is a measure of a medium reorganization energy at the TS.

A numerical investigation of the rate as a function of these parameters[808] resulted in the scheme shown in Figure 27. In the region I, the quasi-two-dimensional KGH kinetics with rate constant $k \approx k_e$ are a good approximation. As discussed above, k_e can be considered as a two-dimensional TST rate constant and, therefore, region I can be identified with the TST region of the two-step mechanism discussed in section 3.F.f.iii. Note that always $k/k_e < 1$; region III represents exponential kinetics with the rate constant $k \ll k_e$. The regime is promoted by a slow diffusion-like mode y. The rate here shows a non-Arrhenius temperature dependence.[784,805] This region can be associated with the "non-TST" region of the two-step mechanism discussed in the section 3.F.f.iii.[496,763,775] Finally, region II shows a polyexponential kinetic evolution which cannot be described in terms of a rate constant. That regime has been disregarded in the two-step model.

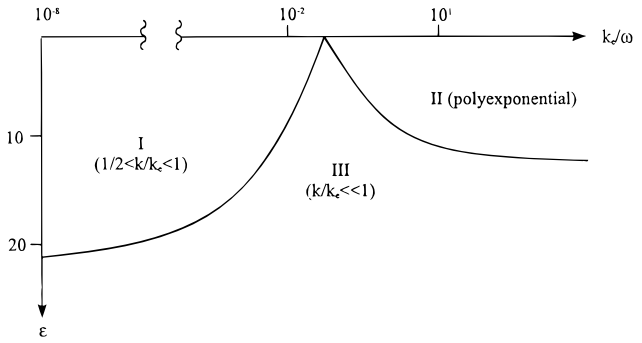

Figure 27. Scheme of kinetic regimes for the AH eq 4.[808] See eq A5 for notation; $\epsilon = U_y^{\ddagger}/k_B T$.

4. Acknowledgments

A.D. is pleased to acknowledge financial support from the Alexander von Humboldt Foundation that enabled him to participate in this project. R.v.E. gratefully acknowledges financial support from the Deutsche Forschungsgemeinschaft, the Volkswagen Foundation, the Fonds der Chemischen Industrie, and the Max-Buchner Forschungsstiftung. R.v.E. and C.D.H. sincerely appreciate the excellent collaborations with current and earlier members of their research group. T.A. is grateful to the Ministry of Education, Science, Sports and Culture of Japan for financial support of his work (Grant No. 0845204). M.V.B. is grateful to the Russian Fund of Basic Research for financial support of his work (Project No. 96-03-32544). W.leN. thanks the National Science Foundation for support of his work in this area.

5. References

(1) van Eldik, R.; Asano, T.; le Noble, W. J. *Chem. Rev.* **1989**, *89*, 549.
(2) Asano, T.; le Noble, W. J. *Chem. Rev.* **1978**, *78*, 407.
(3) van Eldik, R., Ed. *Inorganic High-Pressure Chemistry: Kinetics and Mechanisms*; Elsevier: Amsterdam, 1986.
(4) le Noble, W. J., Ed. *Organic High-Pressure Chemistry*; Elsevier: Amsterdam, 1988.
(5) Jurczak, J., Baranowski, B., Eds. *High-Pressure Chemical Synthesis*; Elsevier: Amsterdam, 1989.
(6) van Eldik, R., Jonas, J., Eds. *High-Pressure Chemistry and Biochemistry*; NATO ASI Series C197; Reidel: Dordrecht, 1987.
(7) Winter, R., Jonas, J., Eds. *High-Pressure Chemistry, Biochemistry and Materials Science*; NATO ASI Series C401; Kluwer: Dordrecht, 1993.
(8) van Eldik, R., Hubbard, C. D., Eds. *Chemistry under Extreme or Non-Classical Conditions*; Wiley: New York, 1997.
(9) Diehl, P., Fluck, E., Günther, H., Kosfeld, R., Seelig, J., Eds. *High-Pressure NMR*; Springer: Heidelberg, 1991.
(10) Sherman, W. F.; Stadtmuller, A. A., Eds. *Experimental Techniques in High-Pressure Research*; Wiley: Chichester, 1987.

(11) Holzapfel, W. B., Isaacs, N., Eds. *High-Pressure Techniques in Chemistry and Physics*; Oxford: Oxford, 1997.
(12) Taniguchi, Y., Senoo, M., Hara, K., Eds. *High-Pressure Liquids and Solutions*; Elsevier: Amsterdam, 1994.
(13) van Eldik, R. et al. In *Mechanisms of Inorganic and Organometallic Reactions*; Twigg, M., Ed.; Plenum: New York, 1988, Vol. 5, p 377; 1989, Vol. 6, p 437; 1991, Vol. 7, p 371; 1994, Vol. 8, p 399.
(14) van Eldik, R.; Merbach, A. E. *Comments Inorg. Chem.* **1992**, *12*, 341.
(15) van Eldik, R. *Pure Appl. Chem.* **1992**, *64*, 1439.
(16) van Eldik, R. In *Perspectives in Coordination Chemistry*; Williams, A. F., Floriani, C., Merbach, A. E., Eds.; VHCH: Basel, 1992; p 52.
(17) van Eldik, R. *Organomet. Org. Synth.* **1993**, *4*, 27.
(18) van Eldik, R. *High Pressure Res.* **1991**, *6*, 251.
(19) Hubbard, C. D.; van Eldik, R. *Instrum. Sci. Technol.* **1995**, *22*, 1.
(20) Frey, U.; Powell, D. H.; Merbach A. E. In *Dynamics of Solutions and Fluid Mixtures by NMR*; Delpuech, J.-J., Ed.; Wiley: Chichester, 1995; p 263.
(21) Lincoln, S. F.; Merbach, A. E. *Adv. Inorg. Chem.* **1995**, *42*, 1.
(22) Frey, U.; Helm, L.; Merbach, A. E.; Roulet, R. In *Advanced Applications of NMR to Organometallic Chemistry*; Gielen, M., Willem, R., Wrackmeyer, B., Eds.; Wiley: Chichester, 1996; p 193.
(23) Lüdemann. H.-D. *Pol. J. Chem.* **1996**, *70*, 387. See also specific sections in refs 3 and 6−8: e.g. the Chapter by Heremans in ref 8.
(24) Klärner, F.-G.; Diedrich, M. K. In *The Chemistry of Dienes and Polyenes, Vol. 1*; Rapaport, Z., Ed.; Wiley: New York, 1997; Chapter 12.
(25) Jenner, G. *Tetrahedron* **1997**, *53*, 2669.
(26) Buback, M. *Pure Appl. Chem.* **1996**, *68*, 1501.
(27) Buback, M. *Angew. Chem., Int. Ed. Engl.* **1991**, *30*, 641.
(28) Isaacs, N. *Tetrahedron* **1991**, *47*, 8463.
(29) Silva, J. L.; Weber, G. *Annu. Rev. Phys. Chem.* **1993**, *44*, 89.
(30) Wieland S.; van Eldik, R. *Coord. Chem. Rev.* **1990**, *97*, 185.
(31) Ford, P. C.; Crane, D. R. *Coord. Chem. Rev.* **1992**, *111*, 153.
(32) Stochel, G. Coord. *Chem. Rev.* **1992**, *114*, 269.
(33) van Eldik, R. *Pure Appl. Chem.* **1993**, *65*, 2603.
(34) Stochel, G.; van Eldik, R. *Coord. Chem. Rev.* **1997**, *159*, 153.
(35) Viana, C. A. N. *Pure Appl. Chem.* **1996**, *68*, 1541.
(36) Yonker, C. R.; Wallen, S. L.; Linehan, J. C. *J. Supercrit. Fluids* **1995**, *8*, 250.
(37) Hoffmann, M. M.; Conradi, M. S. *Rev. Sci. Instrum.* **1997**, *68*, 159.
(38) Cusanelli, A.; Nicula-Dadci, L.; Frey, U.; Merbach A. E. *Inorg. Chem.* **1997**, *36*, 2211.
(39) Wishart, J. F.; van Eldik, R. *Rev. Sci. Instrum.* **1992**, *63*, 3224.
(40) Spitzer, M.; Gärtig, F.; van Eldik, R. *Rev. Sci. Instrum.* **1988**, *59*, 2092.
(41) van Eldik, R.; Gaede, W.; Wieland, S.; Kraft, J.; Spitzer, M.; Palmer, D. A. *Rev. Sci. Instrum.* **1993**, *64*, 1355.
(42) Bugnon, P.; Laurenczy, G.; Ducommun, Y.; Sauvageat, P.-Y.; Merbach, A. E.; Ith, R.; Tschanz, R.; Doludda, M.; Bergbauer, R.; Grell, E. *Anal. Chem.* **1996**, *68*, 3045.
(43) Ji, Q.; Eyring, E. M.; van Eldik, R.; Bal Reddy, K.; Goates, S. R.; Lee, M. L. *Rev. Sci. Instrum.* **1995**, *66*, 222.
(44) Doine, H.; Whitcombe, T. W.; Swaddle, T. W. *Can. J. Chem.* **1992**, *70*, 81.
(45) Fu, Y.; Swaddle, T. W. *Chem. Commun.* **1996**, 1171.
(46) Sachinidis, J. I.; Shalders, R. D.; Tregloan, P. A. *J. Electroanal. Chem. Interfacial Electrochem.* **1992**, *327*, 219.
(47) Sachinidis, J. I.; Shalders, R. D.; Tregloan, P. A. *Inorg. Chem.* **1994**, *33*, 6180.
(48) Braslavsky, S. E.; Heibel, G. E. *Chem. Rev.* **1992**, *92*, 1381.
(49) Peters, K. S. *Angew. Chem.* **1994**, *106*, 301.
(50) Westrick, J. A.; Goodman, J. L.; Peters, K. S. *Biochemistry* **1987**, *26*, 8313.
(51) Schulenberg, P. J.; Rohr, M.; Gärtner, W.; Braslavsky, S. E. *Biophys. J.* **1994**, *66*, 838.
(52) Schulenberg, P. J.; Gärtner, W.; Braslavsky, S. E. *J. Phys. Chem.* **1995**, *99*, 9617.
(53) Churio, M. S.; Angermund, K. P.; Braslavsky, S. E. *J. Phys. Chem.* **1994**, *98*, 1776.
(54) Jiwan, J.-L. H.; Wegewijs, B.; Indelli, M. T.; Scandola, F.; Braslavsky, S. E. *Recl. Trav. Chim. Pays-Bas* **1995**, *114*, 542.
(55) Jiwan, J.-L. H.; Chibisov, A. K.; Braslavsky, S. E. *J. Phys. Chem.* **1995**, *99*, 10246.
(56) Wegewijs, B.; Verhoeven, J. W.; Braslavsky, S. E. *J. Phys. Chem.* **1996**, *100*, 8890.
(57) Gensch, T.; Churio, M. S.; Braslavsky, S. E.; Schaffner, K. *Photochem. Photobiol.* **1996**, *63*, 719.
(58) Gensch, T.; Braslavsky, S. E. *J. Phys. Chem. B* **1997**, *101*, 101.
(59) Pittet, P.-A.; Elbaze, G.; Helm, L.; Merbach, A. E. *Inorg. Chem.* **1990**, *29*, 1936.
(60) Ammann, C.; Helm, L.; Merbach, A. E. *Z. Phys. Chem. Neue Folge* **1987**, *155*, 145.
(61) Helm, L.; Hugi, A. D.; Merbach, A. E. *Inorg. Chem.* **1987**, *26*, 1763.
(62) Dellavia, I.; Helm, L.; Merbach, A. E. *Inorg. Chem.* **1992**, *31*, 4151.
(63) Dellavia, I.; Helm, L.; Merbach, A. E. *Inorg. Chem.* **1992**, *31*, 2230.
(64) Turin, E.; Nielson, R. M.; Merbach, A. E. *Inorg. Chim. Acta* **1987**, *134*, 79.
(65) Dellavia, I.; Sauvageat, P.-Y.; Helm, L.; Ducommun, Y.; Merbach, A. E. *Inorg. Chem.* **1992**, *31*, 792.
(66) Gonzalez, G.; Moullet, B.; Martinez, M.; Merbach, A. E. *Inorg. Chem.* **1994**, *33*, 2330.
(67) Funahashi, S.; Ishii, M.; Tanaka, M. *Chem. Lett. (Chem. Soc. Jpn.)* **1987**, 871.
(68) Cossy, C.; Helm, L.; Merbach, A. E. *Helv. Chim. Acta* **1987**, *70*, 1516.
(69) Fielding, L.; Moore, P. *J. Chem. Soc., Chem. Commun.* **1988**, 49.
(70) Ishii, M.; Funahashi, S.; Tanaka, M. *Inorg. Chem.* **1988**, *27*, 3192.
(71) Aizawa, S.; Matsuda, K.; Tajima, T.; Maeda, M.; Sugata, T.; Funahashi, S. *Inorg. Chem.* **1995**, *34*, 2042.
(72) Mizuno, M.; Funahashi, S.; Nakasuka, N.; Tanaka, M. *Inorg. Chem.* **1991**, *30*, 1550.
(73) Mizuno, M.; Funahashi, S.; Nakasuka, N.; Tanaka, M. *Bull. Chem. Soc. Jpn.* **1991**, *64*, 1988.
(74) Aizawa, S.-I.; Iida, S.; Matsuda, K.; Funahashi, S. *Inorg. Chem.* **1996**, *35*, 1338.
(75) Bradley, S. M.; Doine, H.; Krouse, H. R.; Sisley, M. J.; Swaddle, T. W. *Aust. J. Chem.* **1988**, *41*, 1323.
(76) Fielding, L.; Moore, P. *J. Chem. Soc., Dalton Trans.* **1989**, 873.
(77) Ishii, M.; Funahashi, S.; Ishihara, K.; Tanaka, M. *Bull. Chem. Soc. Jpn.* **1989**, *62*, 1852.
(78) Soyama, S.; Ishii, M.; Funahashi, S.; Tanaka, M. *Inorg. Chem.* **1992**, *31*, 536.
(79) Powell, D. H.; Furrer, P.; Pittet, P.-A.; Merbach, A. E. *J. Phys. Chem.* **1995**, *99*, 16622.
(80) Powell, D. H.; Merbach, A. E.; Fabian, I.; Schindler, S.; van Eldik, R. *Inorg. Chem.* **1994**, *33*, 4468.
(81) Helm, L.; Hugi-Cleary, D.; Merbach, A. E. *J. Am. Chem. Soc.* **1987**, *109*, 4444.
(82) Turin-Rossier, M.; Hugi-Cleary, D.; Frey, U.; Merbach, A. E. *Inorg. Chem.* **1990**, *29*, 1374.
(83) Frey, U.; Helm, L.; Merbach, A. E. *Helv. Chim. Acta* **1990**, *73*, 199.
(84) Nagasawa, A.; Tanaka, H. K.; Miyoshi, M.; Saito, K. *Inorg. Chem.* **1987**, *26*, 4035.
(85) Doine, H.; Ishihara, K.; Krouse, H. R.; Swaddle, T. W. *Inorg. Chem.* **1987**, *26*, 3240.
(86) Bernhard, P.; Helm, L.; Ludi, A.; Merbach, A. E.; Rapaport, I. *Inorg. Chem.* **1988**, *27*, 873.
(87) Bürgi, H. B.; Hummel, W.; Ludi, A.; Merbach, A. E.; Pittet, P. A.; Stebler-Röthlisberger, M. *Inorg. Chem.* **1988**, *27*, 1358.
(88) Luginbühl, W.; Zbinden, P.; Pittet, P.-A.; Armbruster, T.; Bürgi, H.-B.; Merbach, A. E.; Ludi, A. *Inorg. Chem.* **1991**, *30*, 2350.
(89) Laurenczy, G.; Rapaport, I.; Zbinden, D.; Merbach, A. E. *Magn. Reson. Chem.* **1991**, *29*, S45.
(90) Dadci, L.; Elias, H.; Frey, U.; Hörnig, A.; Koelle, U.; Merbach, A. E.; Paulus, H.; Schneider, J. S. *Inorg. Chem.* **1995**, *34*, 306.
(91) Pittet, P.-A.; Dadci, L.; Zbinden, P.; Abou-Hamdan, A.; Merbach, A. E. *Inorg. Chim. Acta* **1993**, *206*, 135.
(92) Helm, L.; Merbach, A. E.; Kotowski, M.; van Eldik, R. *High Pressure Res.* **1989**, *2*, 49.
(93) Berger, J.; Kotowski, M.; van Eldik, R.; Frey, U.; Helm, L.; Merbach, A. E. *Inorg. Chem.* **1989**, *28*, 3759.
(94) Frey, U.; Elmroth, S.; Moullet, B.; Elding, L. I.; Merbach, A. E. *Inorg. Chem.* **1991**, *30*, 5033.
(95) Hallinan, N.; Besancon, V.; Forster, M.; Elbaze, G.; Ducommun, Y.; Merbach, A. E. *Inorg. Chem.* **1991**, *30*, 1112.
(96) Powell, D. H.; Dhubhghaill, O. M. N.; Pubanz, D.; Helm, L.; Lebedev, Y. S.; Schlaepfer, W.; Merbach, A. E. *J. Am. Chem. Soc.* **1996**, *118*, 9333.
(97) Micskei, K.; Helm, L.; Brücher, E.; Merbach, A. E. *Inorg. Chem.* **1993**, *32*, 3844.
(98) Toth, E.; Pubanz, D.; Vauthey, S.; Helm, L.; Merbach, A. E. *Chem. Eur. J.* **1996**, *2*, 1607.
(99) Toth, E.; Vauthey, S.; Pubanz, D.; Merbach, A. E. *Inorg. Chem.* **1996**, *35*, 3375.
(100) Cossy, C.; Helm, L.; Merbach, A. E. *Inorg. Chim. Acta* **1987**, *139*, 147.
(101) Cossy, C.; Helm, L.; Merbach, A. E. *Inorg. Chem.* **1989**, *28*, 2699.
(102) Graeppi, N.; Powell, D. H.; Laurenczy, G.; Zekany, L.; Merbach, A. E. *Inorg. Chim. Acta* **1995**, *235*, 311.
(103) Frey, U.; Li, Z.-W.; Matras, A. *Inorg. Chem.* **1996**, *35*, 981.
(104) Cusanelli, A.; Frey, U.; Richens, D. T.; Merbach, A. E. *J. Am. Chem. Soc.* **1996**, *118*, 5265.
(105) Ducommun, Y.; Helm, L.; Merbach, A. E.; Hellquist, B.; Elding, L. I. *Inorg. Chem.* **1989**, *28*, 377.
(106) Frey, U.; Helm, L.; Merbach, A. E.; Romeo, R. *J. Am. Chem. Soc.* **1989**, *111*, 8161.

(107) Burki, N.; Abou-Hamdan, A.; Lincoln, S. F.; Merbach, A. E.; Vincent, S. J. F. *Inorg. Chim. Acta* **1993**, *207*, 27.
(108) Inamo, M.; Ishihara, K.; Funahashi, S.; Ducommun, Y.; Merbach, A. E.; Tanaka, M. *Inorg. Chem.* **1991**, *30*, 1580.
(109) Ishihara, K.; Mouri, Y.; Funahashi, S.; Tanaka, M. *Inorg. Chem.* **1991**, *30*, 2356.
(110) Kura, G.; Arigata, H. *Polyhedron* **1993**, *12*, 567.
(111) Sauvageat, P.-Y.; Ducommun, Y.; Merbach, A. E. *Helv. Chim. Acta* **1989**, *72*, 1801.
(112) Kuroiwa, Y.; Harada, M.; Tomiyasu, H.; Fukutoni, H. *Inorg. Chim. Acta* **1988**, *147*, 7.
(113) Chung, J.-J.; Choi, J.-H.; Kim, E.-K. *Daehan Hwahak Hwoejee* **1989**, *33*, 582.
(114) Beswick, C. L.; Shalders, R. D.; Swaddle, T. W. *Inorg. Chem.* **1996**, *35*, 991.
(115) Kita, S.; Shibata, M.; Uchida, K. *Bull. Chem. Soc. Jpn.* **1992**, *65*, 3253.
(116) Zhang, S.; Bajaj, H. C.; Zang, V.; Dobson, G. R.; van Eldik, R. *Organometallics* **1992**, *11*, 3901.
(117) Lawrance, G. A.; Martinez, M.; Skelton, B. W.; van Eldik, R.; White, A. H. *Aust. J. Chem.* **1992**, *45*, 351.
(118) House, D. A.; Bal Reddy, K.; van Eldik, R. *Inorg. Chim. Acta* **1991**, *186*, 5.
(119) Wieland, S.; van Eldik, R. *Organometallics* **1991**, *10*, 3110.
(120) (a) Curtis, N. J.; Lawrence, G. A.; van Eldik, R. *Inorg. Chem.* **1989**, *28*, 329. (b) Gonzalez, G.; Martinez, M.; Rodriquez, E. *J. Chem. Soc., Dalton Trans.* **1995**, 891.
(121) Guardado, P.; Lawrence, G. A.; van Eldik, R. *Inorg. Chem.* **1989**, *28*, 976.
(122) Inamo, M.; Sumi, T.; Nakagawa, S.; Funahashi, S.; Tanaka, M. *Inorg. Chem.* **1989**, *28*, 2688.
(123) Chung, J. J.; Kim, H. T.; Bek, S. O. *J. Korean Chem. Soc.* **1989**, *33*, 164.
(124) Awad, H. H.; Dobson, C. B.; Dobson, G. R.; Leipoldt, J. G.; Schneider, K.; van Eldik, R.; Wood, H. E. *Inorg. Chem.* **1989**, *28*, 1654.
(125) Suvachittanont, S.; van Eldik, R. *Inorg. Chem.* **1989**, *28*, 3660.
(126) Zhang, S.; Dobson, G. R.; Zhang, V.; Bajaj, H. C.; van Eldik, R. *Inorg. Chem.* **1990**, *29*, 3477.
(127) Schneider, K. J.; van Eldik, R. *Organometallics* **1990**, *9*, 1235.
(128) Chung, J. J.; Choi, J. H.; Kim, D. J. *Taehan Hwahakhoe Chi* **1987**, *31*, 375.
(129) bin Ali, R.; Burgess, J.; Guardado, P. *Transition Met. Chem.* **1989**, *13*, 126.
(130) Schmidt, G.; Paulus, H.; van Eldik, R.; Elias, H. *Inorg. Chem.* **1988**, *27*, 3211.
(131) Elias, H.; Schmidt, G.; Küppers, H.-J.; Saher, M.; Wieghardt, K.; Nuber, B.; Weiss, J. *Inorg. Chem.* **1989**, *28*, 3021.
(132) Ducommun, Y.; Nichols, P. J.; Merbach, A. E. *Inorg. Chem.* **1989**, *28*, 2643.
(133) Takagi, M.; Ishihara, K. *Inorg. Chim. Acta* **1995**, *232*, 157.
(134) Fabian, I.; van Eldik, R. *Inorg. Chem.* **1993**, *32*, 3339.
(135) Alshehri, S.; Burgess, J.; Hubbard, C. D. *Transition Met. Chem.* **1993**, *18*, 228.
(136) Funahashi, S.; Sengoku, K.; Amari, T.; Tanaka, M. *J. Solution Chem.* **1988**, *17*, 109.
(137) Alshehri, S.; Burgess, J. *Inorg. Chim. Acta* **1991**, *181*, 153.
(138) Al-Alousy, A.; Alsheri, S.; Burgess, J.; del Mar Graciani, M.; Moya, M.-L.; Munoz, E.; Rodriguez, A.; Sanchez, F. *Transition Met. Chem.* **1993**, *18*, 179.
(139) Stochel, G.; van Eldik, R.; Hejmo, E.; Stasicka, Z. *Inorg. Chem.* **1988**, *27*, 2767.
(140) Stochel, G.; van Eldik, R. *Inorg. Chim. Acta* **1989**, *155*, 95.
(141) Alshehri, S.; Burgess, J.; van Eldik, R.; Hubbard, C. D. *Inorg. Chim. Acta* **1995**, *240*, 305.
(142) Barrios, A.; Graciani, M. d. M.; Jimenez, R.; Munoz, E.; Sanchez, F.; Moya, M. L.; Alshehri, S.; Burgess, J. *Transition Met. Chem.* **1992**, *17*, 231.
(143) Al-Alousy, A.; Alshehri, S.; Burgess, J.; Graciani, M. d. M.; Moya, M. L.; Munoz, E.; Rodriguez, A.; Sanchez, F. *Transition Met. Chem.* **1993**, *18*, 179.
(144) Reddy, K. B.; van Eldik, R. *Inorg. Chem.* **1991**, *30*, 596.
(145) Stochel, G.; Chatlas, J.; Martinez, P.; van Eldik, R. *Inorg. Chem.* **1992**, *31*, 5480.
(146) Stochel, G.; van Eldik, R. *Inorg. Chim. Acta* **1991**, *190*, 55.
(147) Blandamer, M. J.; Burgess, J.; Cowles, H. J.; Horn, I. M.; Engberts, J. B. F. N.; Galema, S. A.; Hubbard, C. D. *J. Chem. Soc., Faraday Trans. 1* **1989**, *85*, 3733.
(148) Birus, M.; van Eldik, R. *Inorg. Chem.* **1991**, *30*, 4559.
(149) Burgess, J.; Galema, S. A.; Hubbard, C. D. *Polyhedron* **1991**, *10*, 703.
(150) Blandamer, M. J.; Burgess, J.; Fawcett, J.; Guardado, P.; Hubbard, C. D.; Nuttall, S.; Prouse, L. J. S.; Radulovic, S.; Russell, D. R. *Inorg. Chem.* **1992**, *31*, 1383.
(151) Blandamer, M. J.; Burgess, J.; Duce, P. P.; Elvidge, D. L.; Guardado, P.; Hubbard, C. D.; Ibechem, J. *J. Chem. Soc., Faraday Trans.* **1992**, *88*, 215.
(152) Grace, M. R.; Swaddle, T. W. *Inorg. Chem.* **1992**, *31*, 4674.
(153) Burgess, J.; Hubbard, C. D. *Inorg. Chem.* **1988**, *27*, 2548.
(154) Laurenczy, G.; Bugnon, P.; Merbach, A. E. *Inorg. Chim. Acta* **1992**, *198*, 159.
(155) Jolley, W. H.; Stranks, D. R.; Swaddle, T. W. *Inorg. Chem.* **1992**, *31*, 507.
(156) Kitamura, Y.; Matsuzaki, S.; Butou, T. *Polyhedron* **1991**, *10*, 1449.
(157) Diab, H.; Hendry, P.; Ludi, A.; Reddy, K. B.; van Eldik, R. *Inorg. Chim. Acta* **1990**, *175*, 83.
(158) Leipoldt, J. G.; Purcell, W.; Meyer, H. *Polyhedron* **1991**, *10*, 1379.
(159) Marques, H. M.; Breet, E. L. J.; Prinsloo, F. F. *J. Chem. Soc., Dalton Trans.* **1991**, 2941.
(160) Kitamura, Y.; Takamoto, T.; Kuroda, K. *Inorg. Chim. Acta* **1989**, *159*, 181.
(161) Kitamura, Y.; Taneda, S.; Kuroda, K. *Inorg. Chim. Acta* **1989**, *156*, 31.
(162) Fowless, A. D.; Lawrance, G. A.; Stranks, D. R.; Sullivan, T. R.; Vanderhoek, N. *Aust. J. Chem.* **1988**, *41*, 1263.
(163) Kitamura, Y.; Lawrance, G. A.; van Eldik, R. *Inorg. Chem.* **1989**, *28*, 333.
(164) Park, Y. C.; Cho, Y. J. *Bull. Korean Chem. Soc.* **1988**, *9*, 1.
(165) Chung, J. J.; Bek, S. O. *J. Korean Chem. Soc.* **1988**, *32*, 318.
(166) Itoh, T.; Kitamura, Y.; Yoshitani, K. *Inorg. Chem.* **1988**, *27*, 996.
(167) (a) Lamprecht, G. J.; Leipoldt, J. G.; Swaddle, T. W. *Inorg. Chim. Acta* **1987**, *129*, 21. (b) Leipoldt, J. G.; Steynberg, E. C.; van Eldik, R. *Inorg. Chem.* **1987**, *26*, 3068.
(168) House, D. A.; van Eldik, R. *Aust. J. Chem.* **1993**, *46*, 1775.
(169) Ishihara, K.; Kitamura, Y. *Polyhedron* **1996**, *15*, 2969.
(170) Kitamura, Y.; Muneta, H.; Watanabe, K. *Bull. Chem. Soc. Jpn.* **1996**, *69*, 101.
(171) Amari, T.; Funahashi, S.; Tanaka, M. *Inorg. Chem.* **1988**, *27*, 3368.
(172) (a) Tanaka, T.; Hida, T.; Funahashi, S.; Tanaka, M. *J. Am. Chem. Soc.* **1991**, *113*, 1259. (b) Laurenczy, G.; Ducommun, Y.; Merbach, A. E. *Inorg. Chem.* **1989**, *28*, 3024.
(173) Kawaizumi, F. *J. Solution Chem.* **1995**, *24*, 651.
(174) Ducommun, Y.; Laurenczy, G.; Merbach, A. E. *Inorg. Chem.* **1988**, *27*, 1148.
(175) Abu-Gharib, E. A.; bin Ali, R.; Blandamer, M. J.; Burgess, J. *Transition Met. Chem.* **1987**, *12*, 371.
(176) Ritchens, D. T.; Ducommun, Y.; Merbach, A. E. *J. Am. Chem. Soc.* **1987**, *109*, 603.
(177) Bajaj, H. C.; van Eldik, R. *Inorg. Chem.* **1990**, *29*, 2855.
(178) Neto, B. S. L.; Franco, D. W.; van Eldik, R. *J. Chem. Soc., Dalton Trans.* **1995**, 463.
(179) Bajaj, H. J.; van Eldik, R. *Inorg. Chem.* **1988**, *27*, 4052.
(180) Bajaj, H. J.; van Eldik, R. *Inorg. Chem.* **1989**, *28*, 1980.
(181) Ford, P. C.; Taube, D. J.; van Eldik, R. *Organometallics* **1987**, *6*, 125.
(182) Cloete, E.; Breet, E.; van Eldik, R. *J. Chem. Soc., Dalton Trans.* **1995**, 3591.
(183) Dücker-Benfer, C.; Dreos, R.; van Eldik, R. *Angew. Chem., Int. Ed. Engl.* **1995**, *34*, 2245.
(184) Vest, P.; Anhaus, J.; Bajaj, H. C.; van Eldik, R. *Organometallics* **1991**, *10*, 818.
(185) Aizawa, S.; Iida, T.; Funahashi, S. *Inorg. Chem.* **1996**, *35*, 5163.
(186) Elmroth, S.; Bugarcic, Z.; Elding, L. I. *Inorg. Chem.* **1992**, *31*, 3551.
(187) Shi, T.; Elding, L. *Inorg. Chem.* **1996**, *35*, 5941.
(188) Prinsloo, F. F.; Pienaar, J. J.; van Eldik, R. *J. Chem. Soc., Dalton Trans.* **1995**, 3581.
(189) Hohmann, H.; Hellquist, B.; van Eldik, R. *Inorg. Chem.* **1992**, *31*, 345.
(190) Hellquist, B.; Elding, L. I.; Ducommun, Y. *Inorg. Chem.* **1988**, *27*, 3620.
(191) Shi, T.; Elding, L. I. *Inorg. Chem.* **1996**, *35*, 735.
(192) Suvachittanant, S.; Hohmann, H.; van Eldik, R.; Reedijk, J. *Inorg. Chem.* **1993**, *32*, 4544.
(193) Kotowski, M.; Begum, S.; Leipold, J. G.; van Eldik, R. *Inorg. Chem.* **1988**, *27*, 4472.
(194) Ducommun, Y.; Elding, L. I.; Hellquist, B.; Merbach, A. E. *Inorg. Chem.* **1987**, *26*, 1759.
(195) Breet, E. L. J.; van Eldik, R. *Inorg. Chem.* **1987**, *26*, 2517.
(196) Mahal, G.; van Eldik, R. *Inorg. Chem.* **1987**, *26*, 2838.
(197) Pienaar, J. J.; Kotowski, M.; van Eldik, R. *Inorg. Chem.* **1989**, *28*, 373.
(198) Ducommun, Y.; Helm, L. I.; Laurenczy, G.; Merbach, A. E. *Inorg. Chim. Acta* **1989**, *158*, 3.
(199) Laurenczy, G.; Merbach, A. E. *Helv. Chim. Acta* **1988**, *71*, 1971.
(200) Shi, Y.; Ji, Q.; Eyring, E. M.; van Eldik, R. *J. Chem. Soc., Dalton Trans.* **1996**, 2127.
(201) Reddy, K. B.; Cao, S.; Orr, E. C.; Fabian, I.; van Eldik, R.; Eyring, E. M. *J. Chem. Soc., Dalton Trans.* **1994**, 2497.
(202) Burgess, J.; Smith, A. E. *Transition Met. Chem.* **1987**, *12*, 140.
(203) Laurenczy, G.; Lukas, F.; Roulet, R. *Organometallics* **1996**, *15*, 848.
(204) Kondo, Y.; Ishikawa, M.; Ishihara, K. *Inorg. Chim. Acta* **1996**, *241*, 81.
(205) Jestin, J.-L.; Chottard, J.-C.; Frey, U.; Laurenczy, G.; Merbach, A. E. *Inorg. Chem.* **1994**, *33*, 4277.

(206) Schmülling, M.; Lippert, B.; van Eldik, R. *Inorg. Chem.* **1994**, *33*, 3276.
(207) Berglund, J.; Voigt, R.; Franaeus, S.; Elding, L. I. *Inorg. Chem.* **1994**, *33*, 3346.
(208) (a) Schmülling, M.; Grove, D. M.; van Koten, G.; van Eldik, R.; Veldman, N.; Spek, A. L. *Organometallics* **1996**, *15*, 1384. (b) Schmülling, M.; Ryabov, A. D.; van Eldik, R. *J. Chem. Soc., Dalton Trans.* **1994**, 1257.
(209) House, D. A.; van Eldik, R. *Inorg. Chim. Acta* **1995**, *230*, 29.
(210) Reddy, K. B.; van Eldik, R. *Organometallics* **1990**, *9*, 1418.
(211) Zhang, S.; Zang, V.; Dobson, G. R.; van Eldik, R. *Inorg. Chem.* **1991**, *30*, 355.
(212) Zhang, S.; Zang, V.; Bajaj, H. C.; Dobson, G. R. *J. Organomet. Chem.* **1990**, *397*, 279.
(213) Reddy, K. B.; Hoffmann, R.; Konya, G.; van Eldik, R.; Eyring, E. M. *Organometallics* **1992**, *11*, 2319.
(214) Cao, S.; Shi, Y.; Hollmann, J.; van Eldik, R.; Eyring, E. M. *J. Chem. Soc., Dalton Trans.* **1996**, 1629.
(215) Reddy, K. B.; Brady, B. R.; Eyring, E. M.; van Eldik, R. *J. Organomet. Chem.* **1992**, *440*, 113.
(216) Ji, Q.; Eyring, E. M.; van Eldik, R.; Johnston, K. P.; Goates, S. R.; Lee, M. L. *J. Phys. Chem.* **1995**, *99*, 13461.
(217) Reddy, K. B.; van Eldik, R. *Inorg. Chim. Acta* **1990**, *169*, 13.
(218) Cao, S.; Reddy, K. B.; Eyring, E. M.; van Eldik, R. *Organometallics* **1994**, *13*, 91.
(219) Zang, V.; Zhang, S.; Dobson, C. B.; Dobson, G. R.; van Eldik, R. *Organometallics* **1992**, *11*, 1154.
(220) Rowe, L. M.; Atkinson, G. *J. Solution Chem.* **1990**, *19*, 149.
(221) Rowe, L. M.; Tran, L. B.; Atkinson, G. *J. Solution Chem.* **1989**, *18*, 675.
(222) Pipoh, R.; van Eldik, R.; Henkel, G. *Organometallics* **1993**, *12*, 2236.
(223) Pipoh, R.; van Eldik, R.; Wang, S. L. B.; Wulff, W. D. *Organometallics* **1992**, *11*, 490.
(224) Schneider, K. J.; Neubrand, A.; van Eldik, R.; Fischer, H. *Organometallics* **1992**, *11*, 267.
(225) Pipoh, R.; van Eldik, R. *Organometallics* **1993**, *12*, 2668.
(226) Cohen, H.; van Eldik, R.; Gaede, W.; Gerhard, A.; Goldstein, S.; Czapski, G.; Meyerstein, D. *Inorg. Chim. Acta* **1994**, *227*, 57.
(227) Funahashi, S.; Ishii, M.; Tanaka, M.; Uchiyama, N. *Inorg. Chim. Acta* **1987**, *128*, 169.
(228) Odiaka, T. I.; van Eldik, R. *J. Organomet. Chem.* **1992**, *438*, 131.
(229) Odiaka, T. I.; van Eldik, R. *J. Chem. Soc., Dalton Trans.* **1992**, 2215.
(230) Otake, H.; Miyata, A.; Tomiyasu, H. *Inorg. Chim. Acta* **1990**, *168*, 153.
(231) Yoshitani, K.; Kitamura, Y.; Shibata, A. *Polyhedron* **1994**, *13*, 2483.
(232) Kojima, K. *Bull. Chem. Soc. Jpn.* **1987**, *60*, 603.
(233) Kojima, K. *Bull. Chem. Soc. Jpn.* **1988**, *61*, 385.
(234) Matsuda, J.; Kojima, K. *Inorg. Chem.* **1990**, *29*, 138.
(235) Crick, I. S.; Tregloan, P. A. *Inorg. Chim. Acta* **1988**, *142*, 291.
(236) Trümbach, D.; Kritzenberger, J.; Yersin, H. *Inorg. Chim. Acta* **1994**, *216*, 245.
(237) van Zyl, G. J.; Lamprecht, G. J.; Leipoldt, J. G.; Swaddle, T. W. *Inorg. Chim. Acta* **1988**, *143*, 223.
(238) Venter, J. A.; Leipoldt, J. G.; van Eldik, R. *Inorg. Chem.* **1991**, *30*, 2207.
(239) Dücker-Benfer, C.; van Eldik, R.; Canty, A. J. *Organometallics* **1994**, *13*, 3.
(240) Ryabov, A. D.; van Eldik, R.; Le Borgne, G.; Pfeffer, M. *Organometallics* **1993**, *12*, 1386.
(241) Isaacs, N. S.; Maksimovic, L.; Rintoul, G. B.; Young, D. J. *J. Chem. Soc., Chem. Commun.* **1992**, 1749.
(242) Cheung, C. K.; le Noble, W. J.; Merbach, A. E.; Schulman, E. M.; Yamada, H. *J. Am. Chem. Soc.* **1987**, *109*, 7206.
(243) Pipoh, R.; Martinez, P.; van Eldik, R. *Ber. Bunsen-Ges. Phys. Chem.* **1993**, *97*, 1435.
(244) Neubrand, A.; Poe, A. J.; van Eldik, R. *Organometallics* **1995**, *14*, 3249.
(245) Skauge, A. R. L.; Shalders, R. D.; Swaddle, T. W. *Can. J. Chem.* **1996**, *74*, 1998.
(246) Usha, A. V.; Atkinson, G. *J. Solution Chem.* **1992**, *21*, 477.
(247) Aizawa, S.; Funahashi, S. *Bull. Chem. Soc. Jpn.* **1994**, *67*, 1048.
(248) Ishihara, K.; Miura, H.; Funahashi, S.; Tanaka, M. *Inorg. Chem.* **1988**, *27*, 1706.
(249) Funahashi, S.; Ishihara, K.; Inamo, M.; Tanaka, M. *Inorg. Chim. Acta* **1989**, *157*, 65.
(250) Tanaka, T.; Hida, T.; Funahashi, S.; Tanaka, M. *J. Am. Chem. Soc.* **1991**, *113*, 1259.
(251) Ryabov, A. D.; Kuzmina, L. G.; Polyakov, V. A.; Kazankov, G. M.; Ryabova, E. S.; Pfeffer, M.; van Eldik, R. *J. Chem. Soc., Dalton Trans.* **1995**, 999.
(252) Petovsky, O.; van Eldik, R.; Hushen, P.; Espenson, J. H. *J. Chem. Soc., Dalton Trans.* **1995**, 133.
(253) Merbach, A. E.; Nielson, R. M.; Turin, E. *Inorg. Chim. Acta* **1987**, *134*, 67.
(254) Ioset, J.; Helm, L.; Merbach, A.; Roulet, R.; Grepioni, F.; Braga, D. *Helv. Chim. Acta* **1989**, *71*, 1458.
(255) Kitamura, Y.; Takamoto, T.; Yoshitani, K. *Inorg. Chem.* **1988**, *27*, 1382.
(256) Safarowic, F. J.; Keister, J. B. *Organometallics* **1996**, *15*, 3310.
(257) Paw, W. I.; Bower, D. K.; Bierdeman, D. J.; Keister, J. B.; Schulman, E. M. *J. Coord. Chem.* **1996**, *39*, 199.
(258) Krassowski, D. W.; Nelson, J. H.; Brower, K. R.; Hauenstein, D.; Jacobsen, R. A. *Inorg. Chem.* **1988**, *27*, 4294.
(259) Keister, J. B.; Frey, U.; Zbinden, D.; Merbach, A. E. *Organometallics* **1991**, *10*, 1497.
(260) Estevan, F.; Gonzalez, G.; Lahuerta, P.; Martinez, M.; Peris, E.; van Eldik, R. *J. Chem. Soc., Dalton Trans.* **1996**, 1045.
(261) Kiplinger, J. L.; Richmond, T. G.; Arif, A. M.; Dücker-Benfer, C.; van Eldik, R. *Organometallics* **1996**, *15*, 1545.
(262) Orlandi, A.; Frey, U.; Suardi, G.; Merbach, A. E.; Roulet, R. *Inorg. Chem.* **1992**, *31*, 1304.
(263) Laurenczy, G.; Bondietti, G.; Merbach, A. E.; Moullet, B.; Roulet, R. *Helv. Chim. Acta* **1994**, *77*, 547.
(264) Virtanen, P. O.; Kuikkanen, T.; Rauma, T. *Finn. Chem. Lett.* **1987**, *14*, 162.
(265) van Eldik, R.; Gaede, W.; Cohen, H.; Meyerstein, D. *Inorg. Chem.* **1992**, *31*, 3695.
(266) Gaede, W.; van Eldik, R. *Inorg. Chem.* **1994**, *33*, 2204.
(267) Gaede, W.; Gerhard, A.; van Eldik, R.; Cohen, H.; Meyerstein, D. *J. Chem. Soc., Dalton Trans.* **1993**, 2065.
(268) Sachinidis, J. I.; Shalders, R. D.; Tregloan, P. A. *Inorg. Chem.* **1996**, *35*, 2497.
(269) Anderson, K. A.; Wherland, S. *Inorg. Chem.* **1991**, *30*, 624.
(270) Prinsloo, F. F.; Pienaar, J. J.; van Eldik, R. *J. Chem. Soc., Dalton Trans.* **1996**, 4393.
(271) Spiccia, L.; Swaddle, T. W. *Inorg. Chem.* **1987**, *26*, 2265.
(272) Stebler, M.; Nielson, R. M.; Siems, W. F.; Hunt, J. P.; Dodgen, H. W.; Wherland, S. *Inorg. Chem.* **1988**, *27*, 2893.
(273) Feig, A. L.; Becker, M.; Schindler, S.; van Eldik, R.; Lippard, S. J. *Inorg. Chem.* **1996**, *35*, 2589.
(274) Zang, V.; van Eldik, R. *Inorg. Chem.* **1990**, *29*, 1705.
(275) Grace, M. R.; Takagi, H.; Swaddle, T. W. *Inorg. Chem.* **1994**, *33*, 1915.
(276) Lewis, N. A.; McNeer, R. R.; Taveras, D. V. *Inorg. Chim. Acta* **1994**, *225*, 89.
(277) Kagayama, N.; Sekiguchi, M.; Inada, Y.; Takagi, H. D.; Funahashi, S. *Inorg. Chem.* **1994**, *33*, 1881.
(278) Bänsch, B.; Martinez, P.; Zuluaga, J.; Uribe, D.; van Eldik, R. *Z. Phys. Chem.* **1991**, *170*, 59.
(279) Bänsch, B.; Martinez, P.; Uribe, D.; Zuluaga, J.; van Eldik, R. *Inorg. Chem.* **1991**, *30*, 4555.
(280) Heiber-Langer, I.; Hooper, A. B.; Balny, C. *Biophys. Chem.* **1992**, *43*, 265.
(281) Hubbard, C. D.; Bajaj, H. C.; van Eldik, R.; Burgess, J.; Blundell, N. J. *Inorg. Chim. Acta* **1991**, *183*, 1.
(282) Doine, H.; Swaddle, T. W. *Can. J. Chem.* **1988**, *66*, 2763.
(283) Khoshtariya, D. E.; Billing, R.; Ackermann, M.; van Eldik, R. *J. Chem. Soc., Faraday Trans.* **1995**, *91*, 1625.
(284) Kirchner, K.; Dang, S.-Q.; Stebler, M.; Dodgen, H. W.; Wherland, S.; Hunt, J. P. *Inorg. Chem.* **1989**, *28*, 3604.
(285) Blundell, N. J.; Burgess, J.; Hubbard, C. D. *Inorg. Chim. Acta* **1989**, *155*, 165.
(286) Doine, H.; Whitcombe, T. W.; Swaddle, T. W. *Can. J. Chem.* **1992**, *70*, 81.
(287) Jolley, W. H.; Stranks, D. R.; Swaddle, T. W. *Inorg. Chem.* **1990**, *29*, 1948.
(288) Takagi, H.; Swaddle, T. W. *Inorg. Chem.* **1992**, *31*, 4669.
(289) Martinez, M.; Pitarque, M.-A.; van Eldik, R. *J. Chem. Soc., Dalton Trans.* **1994**, 3159.
(290) van Eldik, R.; Cohen, H.; Meyerstein, D. *Angew. Chem., Int. Ed. Engl.* **1991**, *103*, 1177.
(291) van Eldik, R.; Cohen, H.; Meyerstein, D. *Angew. Chem.* **1991**, *103*, 1177.
(292) Zhang, M.; van Eldik, R.; Espenson, J. H.; Bakac, A. *Inorg. Chem.* **1994**, *33*, 130.
(293) Martinez, M.; Pitarque, M.-A.; van Eldik, R. *J. Chem. Soc., Dalton Trans.* **1996**, 2665.
(294) Guardado, P.; van Eldik, R. *Inorg. Chem.* **1990**, *29*, 3473.
(295) Martinez, M.; Pitarque, M.-A. *J. Chem. Soc., Dalton Trans.* **1995**, 4107.
(296) Krack, I.; van Eldik, R. *Inorg. Chem.* **1989**, *28*, 851.
(297) Park, Y. C.; Kim, S. S. *J. Korean Chem. Soc.* **1989**, *33*, 273.
(298) Krack, I.; van Eldik, R. *Inorg. Chem.* **1990**, *29*, 1700.
(299) Shalders, R. D.; Swaddle, T. W. *Inorg. Chem.* **1995**, *34*, 4815.
(300) Jolley, W. H.; Stranks, D. R.; Swaddle, T. W. *Inorg. Chem.* **1990**, *29*, 385.
(301) Doine, H.; Swaddle, T. W. *Inorg. Chem.* **1991**, *30*, 1858.
(302) Grace, M. R.; Swaddle, T. W. *Inorg. Chem.* **1993**, *32*, 5597.
(303) Bänsch, B.; Martinez, P.; van Eldik, R. *J. Phys. Chem.* **1992**, *96*, 234.
(304) Murguia, M. A.; Wherland, S. *Inorg. Chem.* **1991**, *30*, 139.
(305) Ebihara, M.; Sasaki, Y.; Saito, K.; Tero-Kubota, S. *Bull. Chem. Soc. Jpn.* **1987**, *60*, 391.
(306) bin Ali, R.; Blandamer, M. J.; Burgess, J.; Guardado, P.; Sanchez, F. *Inorg. Chim. Acta* **1987**, *131*, 59.

(307) Endo, K.; Nagasawa, A.; Ninomiya, T.; Saito, K.; Sasaki, Y. *Inorg. Chem.* **1987**, *26*, 2164.
(308) Meshulam, A.; Cohen, H.; van Eldik, R.; Meyerstein, D. *Inorg. Chem.* **1992**, *31*, 2151.
(309) van Eldik, R.; Cohen, H.; Meshulam, A.; Meyerstein, D. *Inorg. Chem.* **1990**, *29*, 4156.
(310) Goldstein, S.; Czapski, G.; van Eldik, R.; Cohen, H.; Meyerstein, D. *J. Phys. Chem.* **1991**, *95*, 1282.
(311) Becker, M.; Schindler, S.; van Eldik, R. *Inorg. Chem.* **1994**, *33*, 5370.
(312) Cohen, H.; van Eldik, R.; Masarwa, M.; Meyerstein, D. *Inorg. Chim. Acta* **1990**, *177*, 31.
(313) Doine, H.; Yano, Y.; Swaddle, T. W. *Inorg. Chem.* **1989**, *28*, 2319.
(314) Goldstein, S.; Czapski, G.; Cohen, H.; Meyerstein, D.; van Eldik, R. *Inorg. Chem.* **1994**, *33*, 3255.
(315) Lewis, N. A.; Obeng, Y. S.; Taveras, D. V.; van Eldik, R. *J. Am. Chem. Soc.* **1989**, *111*, 924.
(316) Kirchner, K.; Dodgen, H. W.; Wherland, S.; Hunt, J. P. *Inorg. Chem.* **1989**, *28*.
(317) Doine, H.; Swaddle, T. W. *Inorg. Chem.* **1988**, *27*, 665.
(318) Anderson, K. A.; Kirchner, K.; Dodgen, H. W.; Hunt, J. P.; Wherland, S. *Inorg. Chem.* **1992**, *31*, 2605.
(319) Hubbard, C. D.; Gerhard, A.; van Eldik, R. *Inorg. Chem.* **1991**, *30*, 5023.
(320) Franklin, T. C.; Mathew, S. A. *J. Electrochem. Soc.* **1989**, *136*, 3627.
(321) Franklin, T. C.; Mathew, S. A. *J. Electrochem. Soc.* **1987**, *134*, 760.
(322) Gaede, W.; van Eldik, R. *Inorg. Chim. Acta* **1994**, *215*, 173.
(323) Gaede, W.; van Eldik, R.; Cohen, H.; Meyerstein, D. *Inorg. Chem.* **1993**, *32*, 1997.
(324) Cohen, H.; Gaede, W.; Gerhard, A.; Meyerstein, D.; van Eldik, R. *Inorg. Chem.* **1992**, *31*, 3805.
(325) Gamelkoorn, H. J.; de Bolster, M. W. G.; Balt, S. *Recl. Trav. Chim. Pays-Bas* **1992**, *111*, 178.
(326) Gerards, L. E. H.; de Bolster, M. W. G.; Balt, S. *Inorg. Chim. Acta* **1992**, *192*, 287.
(327) de Bolster, M. W. G.; Kranenburg, R. A. C. *Inorg. Chim. Acta* **1991**, *183*, 119.
(328) Wolowiec, S.; Balt, S.; de Bolster, M. W. G. *Inorg. Chim. Acta* **1991**, *181*, 131.
(329) Wen-Fu, F.; van Eldik, R. *Inorg. Chim. Acta* **1996**, *251*, 341.
(330) Friesen, D. A.; Lee, S. H.; Lilie, J.; Waltz, W. L.; Vincze, L. *Inorg. Chem.* **1991**, *30*, 1975.
(331) Wieland, S.; Reddy, K. B.; van Eldik, R. *Organometallics* **1990**, *9*, 1802.
(332) Wieland, S.; van Eldik, R. *J. Phys. Chem.* **1990**, *94*, 5865.
(333) Ryba, D. W.; van Eldik, R.; Ford, P. C. *Organometallics* **1993**, *12*, 104.
(334) Fetterolf, M. L.; Offen, H. W. *Inorg. Chem.* **1987**, *26*, 1070.
(335) Wieland, S.; van Eldik, R.; Crane, D. R.; Ford, P. C. *Inorg. Chem.* **1989**, *28*, 3663.
(336) Wieland, S.; van Eldik, R. *J. Chem. Soc., Chem. Commun.* **1989**, 367.
(337) Rossenaar, B. D.; van der Graaf, T.; van Eldik, R.; Langford, C. H.; Stufkens, D. J.; Vleck, A. *Inorg. Chem.* **1994**, *33*, 2865.
(338) McGarvey, J. J.; Lawthers, I.; Heremans, K.; Toftlund, H. *Inorg. Chem.* **1990**, *29*, 252.
(339) Crane, D. R.; Ford, P. C. *J. Am. Chem. Soc.* **1990**, *112*, 6871.
(340) Wieland, S.; van Eldik, R. *J. Chem. Soc., Chem. Commun.* **1989**, 367.
(341) Maupin, C. L.; Meskers, S. C. J.; Dekkers, H. P. J. M.; Riehl, J. P. *J. Chem. Soc., Chem. Commun.* **1996**, 2457.
(342) Friesen, D. A.; Lee, S. H.; Nashiem, R. E.; Mezyk, S. P.; Waltz, W. L. *Inorg. Chem.* **1995**, *34*, 4026.
(343) Friesen, D. A.; Lee, S. H.; Lilie, J.; Waltz, W. L.; Vincze, L. *Inorg. Chem.* **1991**, *30*, 1975.
(344) Vincze, L.; Friesen, D. A. *Inorg. Chem.* **1992**, *31*, 4950.
(345) Crane, D. R.; Ford, P. C. *Inorg. Chem.* **1993**, *32*, 2391.
(346) Crane, D. R.; DiBenedetto, J.; Palmer, C. E. A.; McMillin, D. R.; Ford, P. C. *Inorg. Chem.* **1988**, *27*, 3698.
(347) Crane, D. R.; Ford, P. C. *J. Am. Chem. Soc.* **1991**, *113*, 8510.
(348) Hiraga, T.; Kitamura, N.; Kim, H.-B.; Tazuke, S.; Mori, N. *J. Phys. Chem.* **1989**, *93*, 2940.
(349) Fetterolf, M. L.; Offen, H. W. *J. Phys. Chem.* **1988**, *92*, 3437.
(350) Fetterolf, M. L.; Ford, P. C.; Friedman, A. E.; Yang, Y. Y.; Offen, H. *J. Phys. Chem.* **1988**, *92*, 3760.
(351) Prinsloo, F. F.; Meier, M.; van Eldik, R. *Inorg. Chem.* **1994**, *33*, 900.
(352) Meier, M.; van Eldik, R. *Inorg. Chem.* **1993**, *32*, 2635.
(353) Stochel, G.; van Eldik, R.; Kunkley, H.; Vogler, A. *Inorg. Chem.* **1989**, *28*, 4314.
(354) Stochel, G.; van Eldik, R. *Inorg. Chem.* **1990**, *29*, 2075.
(355) Prinsloo, F. F.; Breet, E. L. J.; van Eldik, R. *J. Chem. Soc., Dalton Trans.* **1995**, 685.
(356) Projahn, H.-D.; Schindler, S.; van Eldik, R.; Fortier, D. G.; Andrew, C. R.; Sykes, A. G. *Inorg. Chem.* **1995**, *34*, 5935.
(357) Lloyd, C. R.; Eyring, E. M.; Ellis, W. R. *J. Am. Chem. Soc.* **1995**, *117*, 11993.
(358) Projahn, H.-D.; Dreher, C.; van Eldik, R. *J. Am. Chem. Soc.* **1990**, *112*, 17.
(359) Taube, D. J.; Projahn, H.-D.; van Eldik, R.; Magde, D.; Traylor, T. G. *J. Am. Chem. Soc.* **1990**, *112*, 6880.
(360) Projahn, H.-D.; van Eldik, R. *Inorg. Chem.* **1991**, *30*, 3288.
(361) Adachi, S.; Morishima, I. *J. Biol. Chem.* **1989**, *264*, 18896.
(362) Unno, M.; Ishimori, K.; Morishima, I. *Biochemistry* **1991**, *30*, 10679.
(363) Unno, M.; Ishimori, K.; Morishima, I. *Biochemistry* **1990**, *29*, 10199.
(364) Traylor, T. G.; Luo, J.; Simon, J. A.; Ford, P. C. *J. Am. Chem. Soc.* **1992**, *114*, 4340.
(365) Balny, C.; Travers, F. *Biophys. Chem.* **1989**, *33*, 237.
(366) Lange, R.; Heiber-Langer, I.; Bonfils, C.; Fabre, I.; Negishi, M.; Balny, C. *Biophys. J.* **1994**, *66*, 89.
(367) Unno, M.; Ishimori, K.; Ishimura, Y.; Morishima, I. *Biochemistry* **1994**, *33*, 9762.
(368) Balny, C.; Saldana, J.-L.; Dahan, N. *Anal. Biochem.* **1987**, *163*, 309.
(369) Zhang, X.; Hubbard, C. D.; van Eldik, R. *J. Phys. Chem.* **1996**, *100*, 9161.
(370) Kornblatt, J. A.; bon Hoa, G. H.; Heremans, K. *Biochemistry* **1988**, *27*, 5122.
(371) Kornblatt, J. A.; bon Hoa, G. H.; Eltis, L.; Mauk, A. G. *J. Am. Chem. Soc.* **1988**, *110*, 5909.
(372) Meier, M.; van Eldik, R. *Inorg. Chim. Acta* **1994**, *225*, 95.
(373) Meier, M.; van Eldik, R.; Chang, I.-J.; Mines, G. A.; Wuttke, D. S.; Winkler, J. R.; Gray, H. B. *J. Am. Chem. Soc.* **1994**, *116*, 1577.
(374) Meier, M.; Sun, J.; Wishart, J. F.; van Eldik, R. *Inorg. Chem.* **1996**, *35*, 1564.
(375) Bänsch, B.; Meier, M.; Martinez, P.; van Eldik, R.; Su, L.; Sun, J.; Isied, S. S.; Wishart, J. F. *Inorg. Chem.* **1994**, *33*, 4744.
(376) Wishart, J. F.; van Eldik, R.; Sun, J.; Su, C.; Isied, S. S. *Inorg. Chem.* **1992**, *31*, 3986.
(377) Scarlata, S. F.; Ropp, T.; Royer, C. A. *Biochemistry* **1989**, *28*, 6637.
(378) Ruan, K.; Weber, G. *Biochemistry* **1988**, *27*, 3295.
(379) Hoganson, C. W.; Windsor, M. W.; Farkas, D. I.; Parson, W. W. *Biochim. Biophys. Acta* **1990**, *892*, 275.
(380) di Primo, C.; Hui Bon Hoa, G.; Douzou, P.; Sligar, S. *Eur. J. Biochem.* **1990**, *193*, 383.
(381) Sun, J.; Wishart, J. F.; van Eldik, R.; Shalders, R. D.; Swaddle, T. W. *J. Am. Chem. Soc.* **1995**, *117*, 2600.
(382) Cruanes, M. T.; Rodgers, K. K.; Sligar, S. G. *J. Am. Chem. Soc.* **1992**, *114*, 9660.
(383) Langford, C. H.; Gray, H. B. *Ligand Substitution Processes*; W. A. Benjamin: New York, 1965.
(384) Akesson, R.; Petterson, L. G. M.; Sandström, M.; Siegbahn, P. E. M.; Wahlgren, U. *J. Phys. Chem.* **1992**, *96*, 10773.
(385) Akesson, R.; Petterson, L. G. M.; Sandström, M.; Siegbahn, P. E. M.; Wahlgren, U. *J. Phys. Chem.* **1993**, *97*, 3765.
(386) Akesson, R.; Petterson, L. G. M.; Sandström, M.; Wahlgren, U. *J. Am. Chem. Soc.* **1994**, *116*, 8691.
(387) Akesson, R.; Petterson, L. G. M.; Sandström, M.; Wahlgren, U. *J. Am. Chem. Soc.* **1994**, *116*, 8705.
(388) Rotzinger, F. P. *J. Am. Chem. Soc.* **1996**, *118*, 6760.
(389) Hartmann, M.; Clark, T.; van Eldik, R. *J. Am. Chem. Soc.* **1997**, *119*, 5867.
(390) Hugi, A. D.; Helm, L.; Merbach, A. E. *Helv. Chim. Acta* **1985**, *68*, 508.
(391) Ducommun, Y.; Newman, K. E.; Merbach, A. E. *Inorg. Chem.* **1980**, *19*, 3696.
(392) Ducommun, Y.; Newman, K. E.; Merbach, A. E. *J. Am. Chem.* Soc. **1979**, *101*, 5588.
(393) Sisley, M. J.; Yano, Y.; Swaddle, T. W. *Inorg. Chem.* **1982**, *21*, 1141.
(394) Burgess, J.; Hubbard, C. D. *Comments Inorg. Chem.* **1995**, *17*, 283.
(395) Blandamer, M. J.; Burgess, J. *Pure Appl. Chem.* **1979**, *51*, 2087.
(396) Blandamer, M. J.; Burgess, J. *Coord. Chem. Rev.* **1980**, *31*, 93.
(397) Blandamer, M. J.; Burgess, J. *Pure Appl. Chem.* **1983**, *55*, 55.
(398) Helm, L.; Elding, L. I.; Merbach, A. E. *Helv. Chim. Acta* **1984**, *67*, 1453.
(399) Helm, L.; Elding, L. I.; Merbach, A. E. *Inorg. Chem.* **1985**, *24*, 1719.
(400) Swaddle, T. W. *Inorg. Chem.* **1983**, *22*, 2663.
(401) Jordan, R. B. *Inorg. Chem.* **1996**, *35*, 3725.
(402) Helm, L.; Meier, P.; Merbach, A. E.; Tregloan, P. A. *Inorg. Chim. Acta* **1983**, *73*, 1.
(403) Knight, C. T. G.; Merbach, A. E. *Inorg. Chem.* **1985**, *24*, 576.
(404) Wherland, S. *Coord. Chem. Rev.* **1993**, *123*, 169.
(405) Swaddle, T. W. *Can. J. Chem.* **1996**, *74*, 631.
(406) Swaddle, T. W. *Inorg. Chem.* **1990**, *29*, 5017.
(407) Fu, Y.; Swaddle, T. W. *J. Am. Chem. Soc.* **1997**, *119*, 7137.
(408) Krack, I.; van Eldik, R. *Inorg. Chem.* **1986**, *25*, 1743.
(409) Seibig, S.; van Eldik, R. *Inorg. Chem.* **1997**, *36*, 4115.
(410) Sisley, M. J.; Rinderman, W.; van Eldik, R.; Swaddle, T. W. *J. Am. Chem. Soc.* **1984**, *106*, 7432.

(411) Ishihara, K.; Swaddle, T. W. *Can. J. Chem.* **1986**, *54*, 2168.
(412) Endicott, J. F.; Ryu, C. K. *Comments Inorg. Chem.* **1987**, *6*, 91.
(413) Manuta, D. M.; Lees, A. J. *Inorg. Chem.* **1986**, *25*, 1354.
(414) van Dijk, H. K.; Servaas, P. C.; Stufkens, D. J.; Oskam, A. *Inorg. Chim. Acta* **1985**, *104*, 179.
(415) Fu, W.-F.; van Eldik, R. *Organometallics* **1997**, *16*, 572.
(416) Fu, W.-F.; van Eldik, R. *Inorg. Chem.* **1998**, *37*, 1044.
(417) Bright, F. V., McNally, M. E. P., Eds. *Supercritical Fluid Technology*; ACS Symp. Ser. 488; American Chemical Society: Washington, DC, 1992.
(418) Kiran, E., Levelt Sengers, J. M. H., Eds. *Supercritical Fluids Fundamentals for Application*; NATO ASI Series E 273; Kluwer: Dordrecht, 1994.
(419) Kiran E., Brennecke, J. F., Eds. *Supercritical Fluid Engineering Science*; ACS Symp. Ser. 514; American Chemical Society: Washington, DC, 1993.
(420) Saito, S. *J. Supercrit. Fluids* **1995**, *8*, 177.
(421) Jessop, P. G.; Ikariya, T.; Noyori, R. *Science* **1995**, *269*, 1065.
(422) Jessop, P. G.; Hsiao, Y.; Ikariya, T.; Noyori, R. *J. Am. Chem. Soc.* **1996**, *118*, 344.
(423) Brock, E. E.; Oshima, Y.; Savage, P. E.; Barker, J. R. *J. Phys. Chem.* **1996**, *100*, 15834.
(424) Steeper, R. R.; Rice, S. F.; Kennedy, I. M.; Aiken, J. D. *J. Phys. Chem.* **1996**, *100*, 184.
(425) Johnston, K. P.; Haynes, C. *Am. Inst. Chem. Eng. J.* **1987**, *33*, 2017.
(426) Ji, Q.; Lloyd, C. R.; Eyring, E. M.; van Eldik, R. *J. Phys. Chem. A* **1997**, *101*, 243.
(427) Vidugiris, G. J. A.; Markley, J. L.; Royer, C. A. *Biochemistry* **1995**, *34*, 4909.
(428) Lin, M.-C.; Macgregor, R. B. *Biochemistry* **1996**, *35*, 11846.
(429) Homan, R.; Pownall, H. J. *J. Am. Chem. Soc.* **1987**, *109*, 4759.
(430) Rentzeperis, D.; Kupke, D. W.; Marky, L. A. *Biopolymers* **1993**, *33*, 117.
(431) Leibrock, E.; Bayer, P.; Lüdemann, H.-D. *Biophys. Chem.* **1995**, *54*, 175.
(432) Kunugi, S.; Kawada, T.; Kabata, H.; Nomura, A.; Komiyama, M. *J. Chem. Soc., Perkin Trans. 2* **1991**, 747.
(433) Rau, T.; van Eldik, R. *Metal Ions in Biological Systems*; Sigel, A., Sigel, H., Eds.; Marcel Dekker: New York, 1996; Vol. 32, p 339.
(434) Fauenfelder, H.; Alberding, N. A.; Ansari, A.; Braunstein, D.; Cowen, B. R.; Hong, M. K.; Iben, I. E. T.; Johnson, J. B.; Luck, S.; Marden, M. C.; Mourant, J. R.; Ormos, P.; Reinisch, L.; Scholl, R.; Schulte, A.; Shyamsunder, E.; Sorensen, L. B.; Steinbach, P. J.; Xie, A.; Young, R. D.; Yue, K. T. *J. Phys. Chem.* **1990**, *94*, 1024.
(435) Royer, C. A.; Chakerian, A. E.; Matthews, K. S. *Biochemistry* **1990**, *29*, 4959.
(436) Pande, C.; Wishnia, A. *J. Biol. Chem.* **1986**, *261*, 6272.
(437) Sato, M.; Ozawa, S.; Ogino, Y. *Bull. Chem. Soc. Jpn.* **1991**, *64*, 9.
(438) Makimoto, S.; Nishida, H.; Taniguchi, Y. *Biochim. Biophys. Acta* **1989**, *996*, 233.
(439) Masson, P.; Balny, C. *Biochim. Biophys. Acta* **1990**, *1041*, 223.
(440) Jung, C.; Ristau, O.; Schulze, H.; Sligar, S. G. *Eur. J. Biochem.* **1996**, *235*, 660.
(441) Schulze, H.; Hoa, G. H. B.; Jung, C. *Biochim. Biophys. Acta* **1997**, *1338*, 77.
(442) Kim, J.; Dordick, J. S. *Biotechnol. Bioeng.* **1993**, *42*, 772.
(443) Butz, P.; Greulich, K. O.; Ludwig, H. *Biochemistry* **1988**, *27*, 1556.
(444) Balny, C.; Hooper, A. B. *Eur. J. Biochem.* **1988**, *176*, 273.
(445) Meier, M.; van Eldik, R. *Chem. Eur. J.* **1997**, *3*, 39.
(446) Sugiyama, Y.; Takahashi, S.; Ishimori, K.; Morishima, I. *J. Am. Chem. Soc.* **1997**, *119*, 8592.
(447) (a) Mingos, D. M. P.; Rohl, A. L.; Burgess, J. *J. Chem. Soc., Dalton Trans.* **1993**, 423. (b) Viana, C. A. N.; Reis, J. C. R. *Pure Appl. Chem.* **1996**, *68*, 1541.
(448) Kang, S. K.; Lam, B.; Albright, T. A.; O'Brian, J. F. *New J. Chem.* **1991**, *15*, 757.
(449) Rotzinger, F. P. *J. Am. Chem. Soc.* **1997**, *119*, 5230.
(450) Deeth, R. J.; Elding, L. I. *Inorg. Chem.* **1996**, *35*, 5019.
(451) (a) Kowall, Th.; Foglia, F.; Helm, L.; Merbach, A. E. *J. Am. Chem. Soc.* **1995**, *117*, 3790. (b) Kowall, Th.; Foglia, F.; Helm, L.; Merbach, A. E. *J. Phys. Chem.* **1995**, *99*, 13078. (c) Kowall, Th.; Foglia, F.; Helm, L.; Merbach, A. E. *Chem. Eur. J.* **1996**, *2*, 285.
(452) Bleuzen, A.; Foglia, F.; Furet, E.; Helm, L.; Merbach, A. E.; Weber, J. *J. Am. Chem. Soc.* **1996**, *118*, 12777.
(453) Sueishi, Y.; Kuwata, K. *Chem. Phys. Lett.* **1989**, *160*, 640.
(454) Sueishi, Y.; Kuwata, K. *Chem. Lett.* **1988**, 1651.
(455) Sueishi, Y.; Kuzukawa, M.; Yamamoto, S.; Nishimura, N. *Bull. Chem. Soc. Jpn.* **1992**, *65*, 3118.
(456) Sueishi, Y.; Kuzukawa, M.; Yamamoto, S.; Nishimura, N. *Bull. Chem. Soc. Jpn.* **1991**, *64*, 2188. For spin exchange between di-*tert*-butyl nitroxide radicals in supercritical ethane, see: Randolph, T. W.; Carlier, C. *J. Phys. Chem.* **1992**, *96*, 5146.
(457) Sueishi, Y.; Nishimura, N.; Hirata, K.; Kuwata, K. *Bull. Chem. Soc. Jpn.* **1990**, *63*, 252.
(458) Sueishi, Y.; Nishimura, N.; Hirata, K.; Kuwata, K. *Bull. Chem. Soc. Jpn.* **1988**, *61*, 4253.
(459) Okamoto, M.; Tanaka, F.; Teranishi, H. *J. Phys. Chem.* **1990**, *94*, 669.
(460) Okamoto, M.; Tanaka, F. *J. Phys. Chem.* **1993**, *97*, 177.
(461) Schmidt, R.; Seikel, K.; Brauer, H.-D. *Ber. Bunsen-Ges. Phys. Chem.* **1990**, *94*, 1100.
(462) Seikel, K.; Brauer, H.-D. *Ber. Bunsen-Ges. Phys. Chem.* **1991**, *95*, 900.
(463) Hild, M.; Brauer, H.-D. *Ber. Bunsen-Ges. Phys. Chem.* **1996**, *100*, 1210.
(464) Yasuda, H.; Scully, A. D.; Hirayama, S.; Okamoto, M.; Tanaka, F. *J. Am. Chem. Soc.* **1990**, *112*, 6847.
(465) Schmidt, R.; Janssen, W.; Brauer, H.-D. *J. Phys. Chem.* **1989**, *93*, 466.
(466) Tanaka, F.; Okamoto, M.; Hirayama, S.; *J. Phys. Chem.* **1995**, *99*, 525.
(467) Turro, N, J.; Chung, W.-S.; Okamoto, M. *J. Photochem. Photobiol., A: Chem.* **1988**, *45*, 17.
(468) Nishikawa, M.; Itoh, K.; Holroyd, R. *J. Phys. Chem.* **1988**, *92*, 5262.
(469) Ninomiya, S.; Itoh, K.; Nishikawa, M.; Holroyd, R. *J. Phys. Chem.* **1993**, *97*, 9488.
(470) Holroyd, R. A.; Stradowska, E.; Itoh, K.; Nishikawa, M. *Radiat. Phys. Chem.* **1996**, *47*, 39.
(471) Kobayashi, Y. *Chem. Phys. Lett.* **1990**, *172*, 307.
(472) Gillies, D. G.; Mathews, S. J.; Sutcliffe, L. H. *Magn. Res. Chem.* **1991**, *29*, 823. See also: Brooks, A. A.; Stejskal, E. O.; Weiss, V. W. *J. Chem. Phys.* **1973**, *58*, 4045.
(473) Gillies, D. G.; Mathews, S. J.; Sutcliffe, L. H. *Magn. Res. Chem.* **1991**, *29*, 1221. See also: Jonas, J.; Adamy, S. T.; Grandinetti, P. J.; Masuda, Y.; Morris, S. J.; Campbell, D. M.; Li, Y. *J. Phys. Chem.* **1990**, *94*, 1157. And: Kim, K.; Choi, Y. S.; Yoon, C. J.; Lang, E. *J. Korean Chem. Soc.* **1992**, *36*, 33.
(474) Lilge, D.; Eimer, W.; Dorfmüller, T. *J. Chem. Phys.* **1987**, *86*, 391.
(475) Wakai, C.; Nakahara, M. *J. Chem. Phys.* **1994**, *100*, 8347.
(476) Wakai, C.; Nakahara, M. *J. Chem. Phys.* **1995**, *103*, 2025.
(477) Brower, S. C.; Hayden, L. M. *J. Polym. Sci. B: Polym. Phys.* **1995**, *33*, 2391. See also: Stock-Schweyer, M.; Meurer, B.; Weill, G. *Polymer* **1994**, *35*, 2072.
(478) Bugnon, P.; Lye, P. G.; Abou-Hamdan, A.; Merbach, A. E. *Chem. Commun.* **1996**, 2787.
(479) Bugnon, P.; Lye, P. G.; Abou-Hamdan, A.; Merbach, A. E. *Chimia* **1996**, *50*, 615.
(480) Xie, C.-H.; Campbell, D.; Jonas, J. *J. Chem. Phys.* **1988**, *88*, 3396.
(481) Peng, X.; Jonas, J. *J. Chem. Phys.* **1990**, *93*, 2192. See also: Jonas, J.; Peng, X. *Ber. Bunsen-Ges. Phys. Chem.* **1991**, *95*, 243.
(482) Campbell, D. M.; Mackowiak, M.; Jonas, J. *J. Chem. Phys.* **1992**, *96*, 2717.
(483) Xie, C.-L.; Campbell, D.; Jonas, J. *J. Chem. Phys.* **1990**, *92*, 3736.
(484) Yamada, H.; Mukuno, K.; Umeda, M.; Maeda, T.; Sera, A. *Chem. Lett.* **1996**, 437.
(485) Hara, K.; Yano, H. *J. Phys. Chem.* **1986**, *90*, 4265.
(486) Hara, K.; Akimoto, S.; Suzuki, H. *Chem. Phys. Lett.* **1990**, *175*, 493.
(487) Hara, K.; Yano, H. *J. Am. Chem. Soc.* **1988**, *110*, 1911.
(488) Hara, K.; Suzuki, H. *J. Phys. Chem.* **1990**, *94*, 1079.
(489) Hara, K.; Kiyotani, H.; Kajimoto, O. *J. Chem. Phys.* **1995**, *103*, 5548. See also: Hara, K.; Kiyotani, H.; Bulgarevich, D. S. *Chem. Phys. Lett.* **1995**, *242*, 455.
(490) Bulgarevich, D. S.; Kajimoto, O.; Hara, K. *J. Phys. Chem.* **1995**, *99*, 13356. For a related work on crystal violet, see: Ben-Amotz, D.; Jeanloz, R.; Harris, C. B. *J. Chem. Phys.* **1987**, *86*, 6119.
(491) Hara, K.; Bulgarevich, D. S.; Kajimoto, O. *J. Chem. Phys.* **1996**, *104*, 9431.
(492) Hara, K.; Bulgarevich, D. S.; Kajimoto, O. *Ber. Bunsen-Ges. Phys. Chem.* **1997**, *101*, 1443.
(493) Hara, K.; Akimoto, S. *High Pressure Res.* **1992**, *11*, 55. See also: Hara, K.; Akimoto, S. *J. Phys. Chem.* **1991**, *95*, 5811.
(494) Asano, T.; Okada, T.; Herkstroeter, W. G. *J. Org. Chem.* **1989**, *54*, 379.
(495) Asano, T.; Matsuo, K.; Sumi, H. *Bull. Chem. Soc. Jpn.* **1997**, *70*, 239. See also: Cosstick, K.; Asano, T.; Ohno, N. *High Pressure Res.* **1992**, *11*, 37.
(496) Asano, T.; Furuta, H.; Sumi, H. *J. Am. Chem. Soc.* **1994**, *116*, 5545.
(497) Asano, T.; Cosstick, K.; Furuta, H.; Matsuo, K.; Sumi, H. *Bull. Chem. Soc. Jpn.* **1996**, *69*, 551.
(498) Asano, T.; Furuta, H.; Hofmann, H.-J.; Cimiraglia, R.; Tsuno, Y.; Fujio, M. *J. Org. Chem.* **1993**, *58*, 4418.
(499) Swaddle, T. W.; Doine, H.; Kinrade, S. D.; Sera, A.; Asano, T.; Okada, T. *J. Am. Chem. Soc.* **1990**, *112*, 2378.
(500) Asano, T.; Sumi, H. *High Pressure Science and Technology-1993*; Schmidt, S. C., Shaner, J. W., Samara, G. A., Ross, M., Ed.; AIP Press: New York, NY, 1993; p 1325.
(501) Neuman, R. C.; Berge, C. T.; Binegar, G. A.; Adam, W.; Nishizawa, Y. *J. Org. Chem.* **1990**, *55*, 4564.
(502) Asano, T.; Okada, T. *J. Org. Chem.* **1988**, *53*, 3606.

(503) Okamoto, M. *J. Phys. Chem.* **1990**, *94*, 8182.
(504) Tamura K.; Abe, M.; Terai, M. *J. Chem. Soc., Faraday Trans. 1* **1989**, *85*, 1493.
(505) Chan, I. Y.; Wong, C. M.; Stehlik, D. *Chem. Phys. Lett.* **1994**, *219*, 187.
(506) Bromberg, S. E.; Chan, I. Y.; Schilke, D. E.; Stehlik, D. *J. Chem. Phys.* **1993**, *98*, 6284.
(507) Turro, N. J.; Okamoto, M.; Gould, I. R.; Moss, R. A.; Lawrynowicz, W.; Hadel, L. M. *J. Am. Chem. Soc.* **1987**, *109*, 4973.
(508) Jenner, G. *New J. Chem.* **1991**, *15*, 897.
(509) Isaacs, N. S.; Maksimovic, L.; Laila, A. *J. Chem. Soc., Perkin Trans. 2* **1994**, 495.
(510) Zhulin, V. M.; Kabotyanskaya, E. B.; Kel'tseva, M. V.; Bogdanov, V. S.; Koreshkov, Yu. D. *Izv. Akad. Nauk SSSR, Ser. Khim.* **1990**, 2651.
(511) Zhulin, V. M.; Bogdanov, V. S.; Ostval'd, G. V.; Kabotyanskaya, E. B.; Koreshkov, Yu. D. *Dokl. Akad. Nauk, SSSR* **1989**, *310*, 362. Reaction volumes in benzene and acetonitrile are also reported.
(512) Buback, M.; Tost, W.; Tietze, L. F.; Voss, E. *Chem. Ber.* **1988**, *121*, 781.
(513) Tietze, L. F.; Hübsch, T.; Ott, C.; Kuchta, G.; Buback, M. *Liebigs Ann.* **1995**, 1.
(514) Buback, M.; Kuchta, G.; Niklaus, A.; Henrich, M.; Rothert, I.; Tietze, L. F. *Liebigs Ann.* **1996**, 1151.
(515) Buback, M.; Tost, W.; Hübsch, T.; Voss, E.; Tietze, L. F. *Chem. Ber.* **1989**, *122*, 1179. See also: Tietze, L. F.; Hübsch, T.; Voss, E.; Buback, M.; Tost, W. *J. Am. Chem. Soc.* **1988**, *110*, 4065.
(516) Tietze, L. F.; Hübsch, T.; Oelze, J.; Ott, C.; Tost, W.; Wörner, G.; Buback, M. *Chem. Ber.* **1992**, *125*, 2249.
(517) Buback, M.; Gerke, K.; Ott, C.; Tietze, L. F. *Chem. Ber.* **1994**, *127*, 2241.
(518) Buback, M.; Abeln, J.; Hübsch, T.; Ott, C.; Tietze, L. F. *Liebigs Ann.* **1995**, 9. The pressure effect on the overall rate at 60 °C is also reported.
(519) Klärner, F.-G.; Schröer, D. *Chem. Ber.* **1989**, *122*, 179.
(520) Diedrich, M. K.; Hochstrate, D.; Klärner, F.-G.; Zimny, B. *Angew. Chem., Int. Ed. Engl.* **1994**, *33*, 1079.
(521) Zhulin, V. M.; Ostval'd, G. V.; Bogdanov, V. S.; Kabotyanskaya, E. B.; Koreshkov, Yu. D.; Kondrat'eva, G. Ya. *Dokl. Akad. Nauk SSSR* **1988**, *302*, 1408.
(522) Beck, K.; Hünig, S.; Klärner, F.-G.; Kraft, P.; Artschwager-Perl, U. *Chem. Ber.* **1987**, *120*, 2041.
(523) Zhulin, V. M.; Ostval'd, G. V.; Bogdanov, V. S.; Kondrat'eva, G. Ya.; Zhuravleva, E. B. *Izv. Akad. Nauk SSSR, Ser. Khim.* **1987**, 1678.
(524) Zhulin, V. M.; Kel'tseva, M. V.; Bogdanov, V. S.; Koreshkov, Yu. D.; Kabotyanskaya, E. B. *Izv. Akad. Nauk SSSR, Ser. Khim.* **1990**, 525.
(525) Jenner, G. *New J. Chem.* **1997**, *21*, 1085.
(526) Klärner, F.-G.; Krawczyk, B.; Ruster, V.; Deiters, U. K. *J. Am. Chem. Soc.* **1994**, *116*, 7646. See also, Klärner, F.-G.; Ruster, V.; Zimny, B.; Hochstrate, D. *High Pressure Res.* **1991**, *7*, 133 and Klärner, F.-G.; Krawczyk, B.; Ruster, V.; Deiters, U. K. *High Pressure Res.* **1994**, *13*, 1.
(527) Baran, J.; Mayr, H.; Ruster, V.; Klärner, F.-G. *J. Org. Chem.* **1989**, *54*, 5016.
(528) Isaacs, N. S.; Laila, A. *J. Phys. Org. Chem.* **1994**, *7*, 178.
(529) Isaacs, N. S.; El-Din, G. N. *Tetrahedron* **1989**, *45*, 7083.
(530) Zhulin, V. M.; Zhuravleva, E. B. *Dokl. Akad. Nauk, SSSR* **1986**, *290*, 383.
(531) Zhulin, V. M.; Zhuravleva, E. B.; Makarova, Z. G.; Krayushkin, M. M. *Izv. Akad. Nauk SSSR, Ser. Khim.* **1987**, 1951.
(532) Okamoto, M. *J. Phys. Chem.* **1992**, *96*, 245.
(533) Hild, M.; Brauer, H.-D. *Ber. Bunsen-Ges. Phys. Chem.* **1996**, *100*, 1814.
(534) Jenner, G.; Papadopoulos, M. *Tetrahedron Lett.* **1996**, *37*, 1417.
(535) Doering, W. E.; Birladeanu, L.; Sarma, K.; Teles, J. H.; Klärner, F.-G.; Gehrke, J.-S. *J. Am. Chem. Soc.* **1994**, *116*, 4289.
(536) El'yanov, B.; Gonikberg, E. M.; Jenner, G. *J. Chem. Soc., Perkin Trans. 2* **1992**, 137. New values of the activation volume based on the previously reported kinetic results (Jenner, G.; Papadopoulos, M. *J. Org. Chem.* **1982**, *47*, 4201) are also given. See also: Ben Salem, R.; Jenner, G. *Tetrahedron Lett.* **1986**, *27*, 1575.
(537) Jenner, G.; Ben Salem, R.; El'yanov, B.; Gonikberg, E. M. *J. Chem. Soc., Perkin Trans. 2* **1989**, 1671.
(538) Sugiyama, S.; Mori, A.; Kato, N.; Takeshita, H. *Bull. Chem. Soc. Jpn.* **1989**, *62*, 1143.
(539) Pajak, J.; Brower, K. R. *J. Energy Fuels* **1987**, *1*, 363.
(540) Isaacs, N. S.; van Eldik, R. *J. Chem. Soc., Perkin Trans. 2* **1997**, 1465.
(541) Nishimura, N.; Miyake, J.; Sueishi, Y. *Bull. Chem. Soc. Jpn.* **1989**, *62*, 1777. Pressure effects on the reverse reaction were also measured.
(542) Sueishi, Y.; Sugiyama, Y.; Yamamoto, S.; Nishimura, N. *J. Phys. Org. Chem.* **1993**, *6*, 478.
(543) Sueishi, Y.; Danjo, K.; Yamamoto, S.; Nishimura, N. *Chem. Express* **1991**, *6*, 459.
(544) Sueishi, Y.; Kuwata, K. *Chem. Phys. Lett.* **1988**, *151*, 439.
(545) Yoshimura, Y.; Kimura, Y.; Nakahara, M. *Ber. Bunsen-Ges. Phys. Chem.* **1988**, *92*, 1095.
(546) Yoshimura, Y.; Nakahara, M. *Ber. Bunsen-Ges. Phys. Chem.* **1988**, *92*, 50.
(547) Zhulin, V. M.; Khueidzha, I.; Kabotyanskaya, E. B.; Koreshkov, Yu. D. *Izv. Akad. Nauk SSSR, Ser. Khim.* **1990**, 1911.
(548) Kessler, W.; Luft, G.; Zeiss, W. *Ber. Bunsen-Ges. Phys. Chem.* **1997**, *101*, 698.
(549) Buback, M.; Hinton, C. *Z. Phys. Chem.* **1996**, *193*, 61.
(550) Naud, D. L.; Brower, K. R. *J. Org. Chem.* **1992**, *57*, 3303. Decompositions of cyclohexanol nitrate in toluene, propylene glycol dinitrate in tetralin and toluene, nitroglycerin in toluene, and 1,3,5-cyclohexanetriol trinitrate in toluene were also studied.
(551) Piermarini, G. J.; Block, S.; Miller, P. J. *J. Phys. Chem.* **1987**, *91*, 3872.
(552) Hiskey, M. A.; Brower, K. R.; Oxley, J. C. *J. Phys. Chem.* **1991**, *95*, 3955.
(553) Oxley, J. C.; Hiskey, M.; Naud, D.; Szekeres, R. *J. Phys. Chem.* **1992**, *96*, 2505.
(554) Piermarini, G. J.; Block, S.; Miller, P. J. *J. Phys. Chem.* **1989**, *93*, 457.
(555) Naud, D. L.; Brower, K. R. *High Pressure Res.* **1992**, *11*, 65.
(556) Markaryan, R. E.; Kovarskii, A. L.; Tshetinin, V. G. *J. Solid State Chem.* **1991**, *94*, 1. See also: Szöcs, F.; Klimova, M. *Polymer* **1992**, *33*, 881.
(557) Kishore, K.; Paramasivam, S.; Sandhya, T. E. *Macromolecules* **1996**, *29*, 6973.
(558) Itsuki, H.; Yamamoto, H.; Okazaki, H.; Terasawa, S. *J. Chem. Soc., Perkin Trans. 2* **1990**, 1545.
(559) Itsuki, H.; Kuwabara, M.; Hayase, K.; Terasawa, S. *J. Chem. Soc., Perkin Trans. 2* **1989**, 563.
(560) Kyong, J. B.; Park, B. C.; Kwun, O. C. *J. Korean Chem. Soc.* **1997**, *41*, 443.
(561) Ho, N.; le Noble, W. J. *J. Org. Chem.* **1989**, *54*, 2018.
(562) Kwun, O. C.; Kim, J. R.; Kyong, J. B.; Lee, Y. H.; Kim. J. C. *J. Korean Chem. Soc.* **1996**, *40*, 327.
(563) Kim, J. R.; Kyong, J. B.; Kim, J. C. *J. Basic Sci. (Inst. Basic Sci., Hanyang University)* **1990**, *9*, 121.
(564) Kyong, J. B.; Kevill, D. N.; Kim, J. C. *J. Korean Chem. Soc.* **1993**, *37*, 3.
(565) Chung, W.-S.; Turro, N. J.; Gould, I. R.; Farid, S. *J. Phys. Chem.* **1991**, *95*, 7752.
(566) Yoh, S.-D.; Park, J.-H.; Lee, K.-A.; Han, I.-S. *Bull. Chem. Soc. Jpn.* **1987**, *60*, 1149.
(567) Yoh, S.-D.; Park, K.-H.; Kim, S.-H.; Park, J.-H. *Daehan Hwahak Hwoejee* **1988**, *32*, 48.
(568) Yoh, S.-D.; Kim, S.-H.; Park, J.-H. *J. Chem. Soc., Perkin Trans. 2* **1987**, 1439.
(569) Yoh, S.-D.; Park, K.-H.; Kim, S.-H.; Cheong, D.-Y. *Tetrahedron* **1989**, *45*, 3321.
(570) Choi, K. J.; Lee, Y. H.; Kyong, J. B.; Kim, J. R. *Daehan Hwahak Hwoejee* **1988**, *32*, 291.
(571) Viana, C. A. N.; Calado, A. R. T.; Pinheiro, L. M. V. *J. Phys. Org. Chem.* **1995**, *8*, 63. See also: Viana, C. A. N.; Calado, A. R. T.; Pinheiro, L. M. V. *J. Chem. Res. (S)* **1992**, 6.
(572) Cheung, C. K.; Wedinger, R. S.; le Noble, W. J. *J. Org. Chem.* **1989**, *54*, 570.
(573) Forster, W.; Laird, R. M. *J. Chem. Soc., Perkin Trans. 2* **1991**, 1033.
(574) Kim, Y. C.; Kyong, J. B.; Kim, S. K.; Koo, D. J. *J. Korean Chem. Soc.* **1992**, *36*, 180.
(575) Brower, K. R. *Organic High Pressure Chemistry*; le Noble, W. J., Ed.; Elsevier: Lausanne, Switzerland, 1988; p 213.
(576) Jenner, G. *New J. Chem.* **1995**, *19*, 173.
(577) Klärner, F.-G.; Kalthof, U.; Gante, J. *J. Prakt. Chem.* **1997**, *339*, 359.
(578) Tamura, K.; Yoshinari, M. *Bull. Chem. Soc. Jpn.* **1989**, *62*, 2073.
(579) Isaacs, N. S.; Coulson, M. *J. Phys. Org. Chem.* **1996**, *9*, 639.
(580) Yamamoto, Y.; Saito, K. *J. Chem. Soc., Chem. Commun.* **1989**, 1676.
(581) Kwun, O. C.; Lee, Y. H.; Jeun. I. S. *J. Korean Chem. Soc.* **1995**, *39*, 350.
(582) Kwun, O. C.; Lee, Y. H. *J. Korean Chem. Soc.* **1993**, *37*, 555.
(583) Kwun, O. C.; Kyong, J. B.; Lee, Y. H. *J. Korean Chem. Soc.* **1993**, *37*, 287.
(584) Sueishi, Y.; Mukai, T.; Matsumoto, K.; Yamamoto, S.; Nishimura, N. *Bull. Chem. Soc. Jpn.* **1994**, *67*, 3153.
(585) Gomez, M.; Granell, J.; Martinez, M. *Organometallics* **1997**, *16*, 2539.
(586) Gomez, M.; Granell, J.; Martinez, M. *J. Chem. Soc., Dalton Trans.* **1998**, 37.
(587) Zhulin, V. M.; Makarova, Z. G.; Klimov, E. M.; Malysheva, N. N.; Kochetkov, N. K. *Izv. Akad. Nauk, SSSR, Ser. Khim.* **1989**, 2804.
(588) Sato, M.; Ozawa, S.; Ogino, Y. *J. Phys. Chem.* **1987**, *91*, 5755.
(589) Sato, M.; Nakatani, J.; Ozawa, S.; Ogino, Y. *Nippon Kagaku Kaishi* **1988**, 1794.
(590) Sato, M.; Ozawa, S.; Ogino, Y. *High Pressure Res.* **1990**, *2*, 87.

(591) Mabry, S. A.; Lee, B.-S.; Zheng, T.; Jonas, J. *J. Am. Chem. Soc.* **1996**, *118*, 8887.
(592) Laila, A.; Isaacs, N. S. *J. Prakt. Chem.* **1996**, *338*, 691.
(593) Isaacs, N. S.; Laila, A. H. *J. Phys. Org. Chem.* **1991**, *4*, 639.
(594) Brown, M. C.; Lepree, J. M.; Connors, K. A. *Int. J. Chem. Kinet.* **1996**, *28*, 791.
(595) Coker, A.; Hibbert, F. *J. Chem. Res.* **1994**, 264.
(596) (a) Munoz, R. C.; Holroyd, R. A. *J. Chem. Phys.* **1986**, *84*, 5810. (b) Holroyd, R. A.; Itoh, K.; Nishikawa, M. *Chem. Phys. Lett.* **1997**, *266*, 227.
(597) Munoz, R. C.; Holroyd, R. A.; Itoh, K.; Nakagawa, K.; Nishikawa, M.; Fueki, K. *J. Phys. Chem.* **1987**, *91*, 4639.
(598) Itoh, K.; Holroyd, R. A.; Nishikawa, M. *J. Phys. Chem. B* **1998**, *102*, 3147.
(599) Itoh, K.; Nishikawa, M.; Holroyd, R. A. *J. Chem. Phys.* **1996**, *105*, 5510.
(600) Itoh, K.; Nishikawa, M.; Holroyd, R. A. *J. Chem. Phys.* **1996**, *104*, 1545.
(601) Chen, P.; Holroyd, R. A. *J. Phys. Chem.* **1996**, *100*, 4491.
(602) Holroyd, R. A.; Schwarz, H. A.; Stradowska, E.; Ninomiya, K.; Itoh, M.; Nishikawa, M. *J. Phys. Chem.* **1994**, *98*, 7142.
(603) Itoh, K.; Holroyd, R. A. *J. Phys. Chem.* **1990**, *94*, 8854.
(604) Itoh, K.; Nishikawa, M.; Holroyd, R. A. *J. Phys. Chem.* **1993**, *97*, 503.
(605) Schwartz, H. A. *J. Phys. Chem.* **1993**, *97*, 12954.
(606) Hall, G. E.; Middleton, W. J.; Roberts, J. D. *J. Am. Chem. Soc.* **1971**, *93*, 4778 and other papers cited in ref 498.
(607) Asano, T.; Furuta, H.; Hofmann, H.-J.; Cimiraglia, R.; Tsuno, Y.; Fujio, M. *J. Org. Chem.* **1993**, *58*, 4418. See footnote 8 in ref 498.
(608) Asano, T.; Okada, T. *J. Org. Chem.* **1986**, *51*, 4454. See also earlier papers quoted there and also entries 349−371.
(609) van Eldik, R.; Kelm, H.; Schmittel, M.; Rüchardt, C. *J. Org. Chem.* **1985**, *50*, 2998.
(610) Firestone, R. A.; Smith, G. M. *Chem. Ber.* **1989**, *112*, 1089.
(611) Kim, S.; Johnston, K. P. *Chem. Eng. Commun.* **1988**, *63*, 49.
(612) Chung, W.-S.; Turro, N. J.; Mertes, J.; Mattay, J. *J. Org. Chem.* **1989**, *54*, 4881. Pressure dependence of the total yield of the dimers in the presence of 1,4-dicyanonaphthalene and several triplet sensitizers were also reported.
(613) Dolbier, W. R.; Weaver, S. L. *J. Org. Chem.* **1990**, *55*, 711. See also: Dolbier, W. R.; Seabury, M. J. *J. Am. Chem. Soc.* **1987**, *109*, 4393.
(614) Diedrich, M. K.; Hochstrate, D.; Klärner, F.-G.; Zimny, B. *High Pressure Res.* **1994**, *13*, 7.
(615) Buback, M.; Busch, M.; Lovis, K.; Mähling, F.-O. *Macromol. Chem. Phys.* **1996**, *197*, 303.
(616) Buback, M.; Dröge, T.; van Herk, A.; Mähling, F.-O. *Macromol. Chem. Phys.* **1996**, *197*, 4119.
(617) Sera, A.; Takagi, K.; Katayama, H.; Yamada, H. *J. Org. Chem.* **1988**, *53*, 1157.
(618) Zhulin, V. M.; Makarova, Z. G.; Klimov, E. M.; Malysheva, N. N.; Kochetkov, N. K. *Dolk. Akad. Nauk SSSR* **1989**, *309*, 641. See also: Zhulin, V. M.; Makarova, Z. G.; Malysheva, N. N.; Klimov, E. M.; Kochetkov, N. K. *Izv. Akad. Nauk SSSR, Ser. Khim.* **1988**, 1195. Kochetkov, N. K.; Zhulin, V. M.; Klimov, E. M.; Malysheva, N. N.; Makarova, Z. G.; Ott, A. Ya. *Carbohydr. Res.* **1987**, *164*, 241.
(619) Zhulin, V. M.; Makarova, Z. G.; Klimov, E. M.; Mal'sheva, N. N.; Kochetkov, N. K. *Dokl. Akad. Nauk SSSR* **1987**, *296*, 138.
(620) Conway, B. E.; Ayranci, E. *J. Chem. Thermodyn.* **1988**, *20*, 9.
(621) Sijpkes, A. H.; Van Rossum, P.; Raad, J. S.; Somsen, G. *J. Chem. Thermodyn.* **1989**, *21*, 1061.
(622) Herman, M. S.; Goodman, J. L. *J. Am. Chem. Soc.* **1989**, *111*, 1849.
(623) Hung, R. R.; Grabowski, J. J. *J. Am. Chem. Soc.* **1992**, *114*, 351.
(624) Schmidt, R.; Schütz, M. *Chem. Phys. Lett.* **1996**, *263*, 795.
(625) Terazima, M.; Hara, T.; Hirota, N. *Chem. Phys. Lett.* **1995**, *246*, 577.
(626) Bonetti, G.; Vecli, A.; Viappiani, C. *Chem. Phys. Lett.* **1997**, *269*, 268.
(627) Morais, J.; Ma, J.; Zimmt, M. B. *J. Phys. Chem.* **1991**, *95*, 3885.
(628) Morais, J.; Zimmt, M. B. *J. Phys. Chem.* **1995**, *99*, 8863.
(629) Yamada, H. Kazuoka, T.; Sera, A. *J. Am. Chem. Soc.* **1988**, *110*, 7552.
(630) Tamura, K.; Dan, M.; Moriyoshi, T. *J. Chem. Res. (S)* **1990**, 110.
(631) Nishimura, N.; Danjo, K.; Sueishi, Y.; Yamamoto, S. *Aust. J. Chem.* **1988**, *41*, 863.
(632) Cho, T.; Kida, I.; Ninomiya, J.; Ikawa, S. *J. Chem. Soc., Faraday Trans.* **1994,** *90*, 103.
(633) Schulman, E. M.; Dwyer, D. W.; Doetschman, D. C. *J. Phys. Chem.* **1990**, *94*, 7308.
(634) Sueishi, Y.; Sugiyama, Y.; Yamamoto, S.; Nishimura, N. *Bull. Chem. Soc. Jpn.* **1994**, *67*, 572.
(635) Isaacs, N. S.; Rzepa, H. S.; Sheppard, R. N.; Lobo, A. M.; Prabhakar, S.; Merbach, A. E. *J. Chem. Soc., Perkin Trans. 2* **1987**, 1477.
(636) Yoshimura, Y.; Nakahara, M. *Ber. Bunsen-Ges. Phys. Chem.* **1988**, *92*, 46.
(637) Kwun, O. C.; Kim, M. J. *Daehan Hwahak Hwoejee* **1988**, *32*, 513.
(638) Jee, J.-G. *Bull. Chem. Soc. Jpn.* **1987**, *60*, 4483.
(639) Nishimura, N.; Osawa, Y.; Kuramoto, K.; Sukemichi, K. *Bull. Chem. Soc. Jpn.* **1991**, *64*, 2438.
(640) Nishimura, N.; Iga, S.; Satoh, M.; Yamamoto, S. *Bull. Chem. Soc. Jpn.* **1992**, *65*, 2437.
(641) Letcher, T. M.; Mercer-Chalmers, J. D.; Kay, R. L. *Pure Appl. Chem.* **1994**, *66*, 419.
(642) Yamada, H.; Kazuoka, M.; Moriguchi, N.; Sera, A. *Bull. Chem. Soc. Jpn.* **1993**, *66*, 3528.
(643) Sueishi, Y.; Nishimura, N.; Hirata, K.; Kuwata, K. *Chem. Express* **1989**, *4*, 567.
(644) Kimura, Y.; Yoshimura, Y.; Nakahara, M. *Chem. Lett.* **1988**, 39.
(645) Fulton, J. L.; Yee, G. G.; Smith R. D. *J. Am. Chem. Soc.* **1991**, *113*, 8327.
(646) Peck, D. G.; Mehta, A. J.; Johnston, K. P. *J. Phys. Chem.* **1989**, *93*, 4297.
(647) Archer, D. G.; Majer, V.; Inglese, A.; Wood, R. H. *J. Colloid Interface Sci.* **1988**, *124*, 591.
(648) Hara, K.; Suzuki, H.; Takisawa, N. *J. Phys. Chem.* **1989**, *93*, 3710.
(649) Chung, J.-J.; Lee, S.-W.; Roh, B.-G.; Choi, J.-H. *J. Korean Chem. Soc.* **1992**, *36*, 28.
(650) Moroi, Y.; Kai, Y.; Murata, Y.; Tanaka, M. *J. Jpn. Oil Chem. Soc.* **1996**, *45*, 833.
(651) Ikawa, Y.; Tsuru, S.; Murata, Y.; Okawauchi, M.; Shigematsu, M.; Sugihara, G. *J. Solution Chem.* **1988**, *17*, 125.
(652) Yamanaka, M.; Kaneshina, S. *J. Solution Chem.* **1990**, *19*, 729.
(653) Cruanes, M. T.; Drickamer, H. G.; Faulkner, L. R. *J. Phys. Chem.* **1992**, *96*, 9888.
(654) Chung, K.; Takata, T.; Endo, T. *Macromolecules* **1995**, *28*, 3048.
(655) Eckert, C. A.; Ziger, D. H.; Johnston, K. P.; Kim, S. *J. Phys. Chem.* **1986**, *90*, 2738.
(656) Paulaitis, M. E.; Alexander, G. C. *Pure Appl. Chem.* **1987**, *59*, 61.
(657) Ikushima, Y.; Saito, N.; Arai, M. *J. Phys. Chem.* **1992**, *96*, 2293.
(658) Weinstein, R. D.; Renslo, A. R.; Danheiser, R. L.; Harris, J. G.; Tester, J. W. *J. Phys. Chem.* **1996**, *100*, 12337.
(659) Isaacs, N. S.; Keating, N. *J. Chem. Soc., Chem. Commun.* **1992**, 876.
(660) Johnston, K. P.; Haynes, C. *AIChE J.* **1987**, *33*, 2017.
(661) Srinivas, P.; Mukhopadhyay, M. *Ind. Eng. Chem. Res.* **1994**, *33*, 3118.
(662) Wu, B. C.; Klein, M. T.; Sandler, S. I. *Ind. Eng. Chem. Res.* **1991**, *30*, 822.
(663) Kamat, S. V.; Beckman, E. J.; Russel, A. J. *J. Am. Chem. Soc.* **1993**, *115*, 8845.
(664) Narayan, R.; Antal, M. J. *J. Am. Chem. Soc.* **1990**, *112*, 1927.
(665) Nishikawa, M.; Holroyd, R. A.; Itoh, K. *J. Phys. Chem. B* **1998**, *102*, 4189.
(666) Brower, K. R. *J. Org. Chem.* **1988**, *53*, 3776.
(667) Minier, L. M.; Brower, K. R.; Oxley, J. C. *J. Org. Chem.* **1991**, *56*, 3306.
(668) Hrnjez, B. J.; Mehta, A. J.; Fox, M. A.; Johnston, K. P. *J. Am. Chem. Soc.* **1989**, *111*, 2662.
(669) Randolph, T. W.; Carlier, C. *J. Phys. Chem.* **1992**, *96*, 5146.
(670) Brenneke, J. F.; Tomasko, D. L.; Eckert, C. A. *J. Phys. Chem.* **1990**, *94*, 7692.
(671) Roberts, C. B.; Chateauneuf, J. E.; Brenneke, J. F. *J. Am. Chem. Soc.* **1992**, *114*, 8455.
(672) Roberts, C. B.; Brenneke, J. F.; Chateauneuf, J. E. *AIChE J.* **1995**, *41*, 1306.
(673) Zhang, J.; Connery, K. A.; Brenneke, J. F.; Chateauneuf, J. E. *J. Phys. Chem.* **1996**, *100*, 12394.
(674) le Noble, W. J. *Prog. Phys. Org. Chem.* **1967**, *5*, 207. See p 230 ff.
(675) LeMaster, C. B.; LeMaster, C. L.; Tafazzoli, M.; Suarez, C.; True, N. S. *J. Phys. Chem.* **1988**, *92*, 5933.
(676) Ross, B. D.; True, N. S. *J. Am. Chem. Soc.* **1983**, *105*, 4871.
(677) Chu, P. S.; True, N. S. *J. Phys. Chem.* **1985**, *89*, 2625.
(678) Chu, P. S.; True, N. S. *J. Phys. Chem.* **1985**, *89*, 5613.
(679) LeMaster, C. B.; LeMaster, C. L.; Suarez, C.; Tafazzoli, M.; True, N. S. *J. Phys. Chem.* **1989**, *93*, 3993.
(680) LeMaster, C. B.; LeMaster, C. L.; Tafazzoli, M.; Suarez, C.; True, N. S. *J. Phys. Chem.* **1990**, *94*, 3461.
(681) Shtyrlin, Y. G.; Fedorenko, V. Y.; Iskhakova, G. G.; Kiselev, V. D.; Konovalov, A. I. *Russ. J. Gen. Chem., Engl. Transl.* **1996**, *66*, 484. See also: Kumar, A. *J. Org. Chem.* **1994**, *59*, 4612.
(682) Forman, M. A.; Dailey, W. P. *J. Am. Chem. Soc.* **1991**, *113*, 2761.
(683) Grieco, P.; Nunes, J. J.; Gaul, M. D. *J. Am. Chem. Soc.* **1990**, *112*, 4595.
(684) Hicks, J. M.; Vandersall, M. T.; Sitzmann, E. V.; Eisenthall, K. B. *Chem. Phys. Lett.* **1987**, *135*, 413.
(685) Rettig, W. *Ber. Bunsen-Ges. Phys. Chem.* **1991**, *95*, 259.
(686) Kang, T. J.; Jarzeba, W.; Barbara, P. F.; Fonseca, T. *Chem. Phys.* **1990**, *149*, 81.
(687) Barbara, P. F.; Jarzeba, W. *Acc. Chem. Res.* **1988**, *21*, 195.
(688) Hara, K.; Kometani, N.; Kajimoto, O. *J. Phys. Chem.* **1996**, *100*, 1488.

(689) Hara, K.; Kometani, N.; Kajimoto, O. *Chem. Phys. Lett.* **1994**, *225*, 381.
(690) Schroeder, J.; Schwarzer, D.; Troe, J.; Voss, F. *J. Chem. Phys.* **1990**, *93*, 2393.
(691) Schroeder, J.; Troe, J.; Vöhringer, P. *Chem. Phys. Lett.* **1993**, *203*, 255.
(692) Schroeder, J. *Ber. Bunsen-Ges. Phys. Chem.* **1997**, *101*, 643.
(693) Mohschladt, R.; Schroeder, J.; Schwarzer, D.; Troe, J.; Vöhringer, P. *J. Chem. Phys.* **1994**, *101*, 7566.
(694) Schroeder, J.; Schwarzer, D.; Troe, J.; Vöhringer, P. *Chem. Phys. Lett.* **1994**, *218*, 43.
(695) Gehrke, Ch.; Schroeder, J.; Schwarzer, D.; Troe, J.; Voss, F. *J. Chem. Phys.* **1990**, *92*, 4805.
(696) Gehrke, Ch.; Mohrschladt, P.; Schroeder, J.; Troe, J.; Vöhringer, P. *J. Chem. Phys.* **1991**, *152*, 45.
(697) Nikowa, L.; Schwarzer, D.; Troe, J.; Schroeder, J. *J. Chem. Phys.* **1992**, *97*, 4827.
(698) Rice, J. K.; Baronavski, A. P. *J. Phys. Chem.* **1992**, *96*, 3359.
(699) Hara, K.; Ito, N.; Kajimoto, O. *J. Phys. Chem.* **1997**, *A101*, 2240.
(700) Kang, T. J.; Etherridge, T.; Jarzeba, W.; Barbara, P. F. *J. Phys. Chem.* **1989**, *93*, 1876.
(701) Kim, S. K.; Fleming, G. R. *J. Phys. Chem.* **1988**, *92*, 2168.
(702) Rothenberger, G.; Negus, D. K.; Hochstrasser, R. M. *J. Chem. Phys.* **1983**, *79*, 5360.
(703) Velsko, S. P.; Fleming, G. R. *J. Chem. Phys.* **1982**, *76*, 3553.
(704) Keery, K. M.; Fleming, G. R. *Chem. Phys. Lett.* **1982**, *93*, 323.
(705) Sivakumar, N.; Hoburg, E. A.; Waldeck, D. H. *J. Chem. Phys.* **1989**, *90*, 2305.
(706) Velsko, S. P.; Waldeck, D. H.; Fleming, G. R. *J. Chem. Phys.* **1983**, *78*, 249.
(707) Flom, S. R.; Nagarajan, V.; Barbara, P. F. *J. Phys. Chem.* **1986**, *90*, 2085.
(708) Millar, D. P.; Eisenthal, K. B. *J. Chem. Phys.* **1985**, *83*, 5076.
(709) Browman, R. M.; Eisenthal, K. B.; Miller, D. P. *J. Chem. Phys.* **1988**, *89*, 762.
(710) Kometani, N.; Kajimoto, O.; Hara, K. *J. Phys. Chem.* **1997**, *A101*, 4916.
(711) Salem, L. *Acc. Chem. Res.* **1979**, *12*, 87.
(712) Bonacic-Koutecky, V.; Bruckman, P.; Hiberty, P.; Koutecky, J.; Leforestier, C.; Salem, L. *Angew. Chem., Int. Ed. Engl.* **1975**, *14*, 575.
(713) Bonacic-Koutecky, V. *J. Am. Chem. Soc.* **1978**, *100*, 396.
(714) Bonacic-Koutecky, V.; Michl, J. *J. Am. Chem. Soc.* **1985**, *107*, 1765.
(715) Bonacic-Koutecky, V.; Koutecky, J.; Michl, J. *Angew. Chem., Int. Ed. Engl.* **1987**, *26*, 170.
(716) Salem, L.; Bruckman, P. *J. Am. Chem. Soc.* **1976**, *98*, 5037.
(717) Bruni, M. C.; Daudey, J. P.; Langiet, J.; Malrieu, J. P.; Momic-chioli, F. *J. Am. Chem. Soc.* **1977**, *99*, 3587.
(718) Brooks, B. R.; Schaefer, H. F., III. *J. Am. Chem. Soc.* **1979**, *101*, 307.
(719) Bonacic-Koutecky, V.; Buenker, R.; Peyerimhoff, S. *J. Am. Chem. Soc.* **1979**, *101*, 5917.
(720) Malrieu, J. P.; Trinquier, G. *Theor. Chim. Acta (Berlin)* **1979**, *54*, 59.
(721) Orlandi, G.; Palmiere, P.; Poggi, G. *J. Am. Chem. Soc.* **1979**, *101*, 348.
(722) Olbrich, G. *Ber. Bunsen-Ges. Phys. Chem.* **1982**, *86*, 209.
(723) Orlandi, G.; Zerbetto, F. *J. Mol. Struct.* **1986**, *138*, 185.
(724) Troe, J.; Weitzel, K. M. *J. Chem. Phys.* **1988**, *88*, 7030.
(725) Morais, J.; Ma, J.; Zimmt, M. B. *J. Phys. Chem.* **1991**, *95*, 3885.
(726) Waldeck, D. H. *Chem. Rev.* **1991**, *91*, 415.
(727) Fleming, G. R.; Courtney, S. H.; Balk, M. W. *J. Statistical Phys.* **1986**, *42*, 83.
(728) Sundström, V.; Gilbro, T. *Chem. Phys. Lett.* **1984**, *109*, 538.
(729) Schroeder, J.; Schwarzer, D.; Troe, J. *Ber. Bunsen-Ges. Phys. Chem.* **1990**, *94*, 1249.
(730) Schroeder, J.; Troe, J. *Chem. Phys. Lett.* **1985**, *116*, 453.
(731) Schroeder, J. *Ber. Bunsen-Ges. Phys. Chem.* **1991**, *95*, 233.
(732) Schroeder, J. *J. Phys. Cond. Matter* **1996**, *8*, 9379.
(733) Beutler, T. C.; Beguelin, D. R.; van Gunsteren, W. F. *J. Chem. Phys.* **1995**, *102*, 3787.
(734) Pierotti, R. A. *Chem. Rev.* **1976**, *76*, 717.
(735) Reiss, H. *Adv. Chem. Phys.* **1966**, *9*, 1.
(736) Hofmann, H.-J.; Asano, T.; Cimiraglia, R.; Bonaccorsi, R. *Bull. Chem. Soc. Jpn.* **1993**, *66*, 130.
(737) Cimiraglia, R.; Asano, T.; Hofmann, H.-J. *Gazz. Chim. Ital.* **1996**, *126*, 679.
(738) Jenner, G. Chapter 6 in ref 4.
(739) El'yanov, B. S.; Vasilvitskaya, E. M. *Rev. Phys. Chem. Jpn.* **1980**, *50*, 169.
(740) Schroeder, J.; Troe, J.; Vöhringer, P. *Z. Phys. Chem.* **1995**, *188*, 287.
(741) Waldeck, D. H.; Lothshaw, W. T.; McDonald, D. B.; Fleming, G. R. *Chem. Phys. Lett.* **1982**, *88*, 297.
(742) McCaskill, J. S.; Gilbert, R. G. *Chem. Phys.* **1979**, *44*, 389.
(743) Schroeder, J.; Schwarzer, D.; Troe, J. *Ber. Bunsen-Ges. Phys. Chem.* **1990**, *94*, 1249.
(744) Kang, T. J.; Etheridge, T.; Jarzeba, W.; Barbara, P. F. *J. Phys. Chem.* **1989**, *93*, 1876.
(745) Basilevsky, M. V.; Vener, M. V. *J. Mol. Struct. (Theochem.)* **1997**, *398−399*, 81.
(746) Fröhlich, H. *Theory of Dilelectrics*; Clarendon Press: Oxford, 1958.
(747) Bötcher, C. J. F.; Bordewick, P. *Theory of Electric Polarization*; Elsevier: Amsterdam, 1978; Vol. II.
(748) Zusman, L. D. *Chem. Phys.* **1980**, *49*, 295.
(749) Ovchinnikova, M. Ya. *Khim. Fizika* **1985**, *4*, 3.
(750) Bagchi, B. *Adv. Chem. Phys.* **1991**, *80*, 1.
(751) Maroncelli, M. *J. Mol. Liq.* **1993**, *57*, 1.
(752) Barbara, P. F.; Jarzeba, W. *Adv. Photochem.* **1990**, *15*, 1.
(753) Rips, I. *Ultrafast Reaction Dynamics and Solvent Effects*; Gaudel, Y., Rossky, P. J., Eds.; AIP Press: New York, 1994; p 334.
(754) Smith B. B.; Staib, A.; Hynes, J. T. *Chem. Phys.* **1993**, *176*, 521.
(755) Brooks, A. A.; Steijskal, E. O.; Weiss, V. W. *J. Chem. Phys.* **1973**, *58*, 4045.
(756) Lilge, D.; Eimer, W.; Dorfmüller, T. *J. Chem. Phys.* **1987**, *86*, 391.
(757) Wakai, C.; Nakahara, M. *J. Chem. Phys.* **1995**, *103*, 2025.
(758) Kubo, R.; Toda, M.; Hashitsume, N. *Statistical Physics II, Nonequilibrium Statistical Mechanics*; Springer-Verlag: Berlin, 1985.
(759) Adelman, S. *Adv. Chem. Phys.* **1980**, *44*, 143.
(760) Gertner, B. J.; Wilson, K. R.; Hynes, J. T. *J. Chem. Phys.* **1989**, *90*, 3537.
(761) Carter, E. A.; Hynes, J. T. *J. Chem. Phys.* **1991**, *94*, 5961.
(762) Staib, A.; Borgis, D.; Hynes, J. T. *J. Chem. Phys.* **1995**, *102*, 2487.
(763) Sumi, H.; Asano, T. *J. Chem. Phys.* **1995**, *102*, 9565.
(764) Bagchi, B.; Oxtoby, D. W. *J. Chem. Phys.* **1983**, 78, 2735.
(765) Grote, R. F.; van der Zwan, G.; Hynes, J. T. *J. Phys. Chem.* **1984**, *88*, 4676.
(766) Carmeli, B.; Oxtoby, D. W. *J. Chem. Phys.* **1983**, *78*, 2735.
(767) Hanggi, P.; Talkner, P.; Borkowec, M. *Rev. Mod. Phys.* **1990**, *62*, 251.
(768) Grote, R. F.; Hynes, J. T. *J. Chem. Phys.* **1980**, *73*, 2715.
(769) Staub, J. E.; Borkowec, M.; Berne, B. *J. Chem. Phys.* **1986**, *84*, 1788.
(770) Maneke, G.; Schroeder, J.; Troe, J.; Voss, F. *Ber. Bunsen-Ges. Phys. Chem.* **1985**, *89*, 896.
(771) Troe, J. *Ber. Bunsen-Ges. Phys. Chem.* **1991**, *95*, 228.
(772) Nikowa, L.; Schwarzer, D.; Troe, J.; Schroeder, J. *Ultrafast Phenomena VIII*; Martin, J.-L., Migus, A., Mourou, G. A., Zewail, A. H., Eds.; Springer-Verlag: Berlin, 1993; p 603.
(773) Lee, M.; Holton, G. R.; Hochstrasser, R. M. *Chem. Phys. Lett.* **1985**, *118*, 538.
(774) Frost, W. *Theory of Unimolecular Reactions*; Academic Press: New York, 1973.
(775) Sumi, H.; Asano, T. *Chem. Phys. Lett.* **1995**, *240*, 125.
(776) Saluja, P. P. S.; Whalley, E. *J. Chem. Soc., Chem. Commun.* **1983**, *10*, 552.
(777) Whalley, E.; le Noble, W. J. Chapter 4 in ref 4.
(778) Basilevsky, M. V.; Ryaboy, V. M.; Weinberg, N. N. *J. Phys. Chem.* **1991**, *95*, 5533.
(779) Basilevsky, M. V.; Weinberg, N. N. *Can. J. Phys.* **1995**, *73*, 267.
(780) Sumi, H. *J. Phys. Chem.* **1991**, *95*, 3334.
(781) Sumi, H. *J. Chem. Phys.* **1994**, *100*, 8825.
(782) Sumi, H. *J. Phys. Chem.* **1995**, *100*, 4831.
(783) Sumi, H. *Chem. Phys.* **1996**, *212*, 9.
(784) Berezhkovsky, A. M.; Zitserman, V. Yu. *Physica A* **1990**, *166*, 585.
(785) Berezhkovsky, A. M.; Zitserman, V. Yu.; Yang, D.-Y.; Kuo, J.; Lin, S.-H. *Physica A* **1998**, *251*, 399.
(786) Simon, J. D. *Acc. Chem. Res.* **1988**, *21*, 128.
(787) Barbara, P. F.; Jarzeba, W. *Adv. Photochem.* **1990**, *15*, 1.
(788) Bagchi, B.; Chandra, A. *Adv. Chem. Phys.* **1991**, *80*, 1.
(789) Maroncelli, M. *J. Mol. Liquids* **1993**, *57*, 1.
(790) Jarzeba, W.; Walker, G. C.; Johnson, A. E.; Barbara, P. F. *Chem. Phys.* **1991**, *152*, 57.
(791) Hong, P. F.; Gardecki, J. A.; Papazyan, A.; Maroncelli, M. *J. Phys. Chem.* **1995**, *99*, 17311.
(792) Nagasawa, Y.; Yartsev, A. P.; Tominaga, K.; Johnson, A. E.; Yoshihara, K. *J. Chem. Phys.* **1994**, *101*, 5717.
(793) Nagasawa, Y.; Yartsev, A. P.; Tominaga, K.; Bisht, P. B. Johnson, A. E.; Yoshihara, K. *J. Phys. Chem.* **1995**, *99*, 653.
(794) Yoshihara, K.; Tominaga, K.; Nagasawa, Y. *Bull. Chem. Soc. Jpn.* **1995**, *68*, 696.
(795) Sumi, H.; Marcus, R. A. *J. Chem. Phys.* **1986**, *84*, 4894.
(796) Nadler, W.; Marcus, R. A. *J. Chem. Phys.* **1987**, *86*, 3906.
(797) Berezhkovsky, A. M.; Zitserman, V. Yu.; Polimeno, A. *J. Chem. Phys.* **1996**, *105*, 6342.
(798) Talkner, P.; Braun, H. B. *J. Chem. Phys.* **1988**, *88*, 7538.
(799) Dygas, M. M.; Matkovsky, B. J.; Shuss, Z. *J. Chem. Phys.* **1986**, *84*, 3731.
(800) Langer, J. S. *Ann. Phys.* **1969**, *54*, 258.
(801) Grote, R. F.; Hynes, J. T. *J. Chem. Phys.* **1981**, *74*, 4465.

(802) Grote, R. F.; Hynes, J. T. *J. Chem. Phys.* **1981**, *75*, 2191.
(803) Nitzan, A. *Adv. Chem. Phys.* **1988**, *70*, 489.
(804) Basilevsky, M. V.; Chudinov, G. E. *Chem. Phys.* **1990**, *144*, 155.
(805) Agmon, N.; Hopfield, J. J. *J. Chem. Phys.* **1983**, *78*, 6947.
(806) Agmon, N.; Hopfield, J. J. *J. Chem. Phys.* **1983**, *79*, 2042.
(807) Berezhkovsky, A. M.; Zitserman, V. Yu. *Chem. Phys. Lett.* **1989**, *158*, 369.
(808) Basilevsky, M. V.; Ryaboy, V. M.; Weinberg, N. N. *J. Phys. Chem.* **1990**, *94*, 8734.

CR970461B